

# Open Research Online

---

The Open University's repository of research publications and other research outputs

## Strategies for Devising Automatic Signal Recognition Algorithms in a Shared Radio Environment

### Thesis

#### How to cite:

Wagstaff, Adrian John (2011). Strategies for Devising Automatic Signal Recognition Algorithms in a Shared Radio Environment. PhD thesis The Open University.

For guidance on citations see [FAQs](#).

© 2011 The Author



<https://creativecommons.org/licenses/by-nc-nd/4.0/>

Version: Version of Record

Link(s) to article on publisher's website:

<http://dx.doi.org/doi:10.21954/ou.ro.0000f1ca>

---

Copyright and Moral Rights for the articles on this site are retained by the individual authors and/or other copyright owners. For more information on Open Research Online's data [policy](#) on reuse of materials please consult the policies page.

---

[oro.open.ac.uk](http://oro.open.ac.uk)

**Ph.D. Thesis**

**Strategies for devising automatic signal recognition  
algorithms in a shared radio environment**

**Adrian John Wagstaff**

C.Eng, MSc., BSc(Eng)(Hons), MRAeS, MIET, FVCM

Submitted for the Degree of Doctor of Philosophy

Faculty of Mathematics, Computing and Technology

The Open University

Date of Submission: June 2011

DATE OF SUBMISSION: 1 June 2011

DATE OF AWARD: 18 Nov 2011

---

ProQuest Number: 13837573

All rights reserved

INFORMATION TO ALL USERS

The quality of this reproduction is dependent upon the quality of the copy submitted.

In the unlikely event that the author did not send a complete manuscript and there are missing pages, these will be noted. Also, if material had to be removed, a note will indicate the deletion.



ProQuest 13837573

Published by ProQuest LLC (2019). Copyright of the Dissertation is held by the Author.

All rights reserved.

This work is protected against unauthorized copying under Title 17, United States Code  
Microform Edition © ProQuest LLC.

ProQuest LLC.  
789 East Eisenhower Parkway  
P.O. Box 1346  
Ann Arbor, MI 48106 – 1346

## Abstract

In an increasingly congested and complex radio environment interference is to be expected, which poses problems for Automatic Signal Recognition (ASR) systems. This thesis explores strategies for improving ASR performance in the presence of interference.

The thesis breaks the overall research question down into a number of sub-questions and explores each of these in turn. A *Phase-symmetric Cross Recurrence Plot* is developed and used to show how a radio signal can be manipulated to separate information about the modulation from the information being carried. The *Logarithmic Cyclic frequency Domain Profile* is introduced to illustrate how a logarithmic representation can be used for analysing mixtures of signals with very different cyclic frequencies. After defining a canonical ASR system architecture, the concepts of an *Ideal Feature* and *Interference Selectivity* are introduced and applied to typical features used in ASR processing. Finally it is shown how these algorithmic developments can be combined in a Bayesian chain implementation that can accommodate a wide variety of feature extraction algorithms.

It is concluded that future ASR systems will require features that can handle a wide range of signal types with much higher levels of interference selectivity if they are to achieve acceptable performance in shared spectrum bands. Intelligent segmentation is shown to be a requirement for future ASR systems unless features can be developed that have near ideal performance.

---



**Ph.D. Thesis**

**Strategies for devising automatic signal recognition  
algorithms in a shared radio environment**

**Adrian John Wagstaff**

C.Eng, MSc., BSc(Eng)(Hons), MRAeS, MIET, FVCM

Submitted for the Degree of Doctor of Philosophy  
Faculty of Mathematics, Computing and Technology  
The Open University

Date of Submission: June 2011

## **Acknowledgements**

I am enormously grateful to those who have supported me through this research and the preparation of the thesis. At the Open University my supervisors Adrian Poulton, David Chapman and Mark Woodroffe have provided invaluable advice and moral support, also I am indebted to the directors and my colleagues at Mass Consultants Ltd.

My wife, Sharon and my children, Jennifer and Robert, have tolerated and supported me for the entire duration, providing encouragement without which the work would never have been completed.

## Contents

<b>1</b>	<b>Introduction .....</b>	<b>25</b>
1.1	Motivation .....	26
1.2	Specific research question.....	28
1.3	The work of this Ph.D. ....	28
1.4	Structure of this thesis .....	30
<b>2</b>	<b>Background .....</b>	<b>31</b>
2.1	Applications .....	32
2.1.1	Military applications.....	33
2.1.2	Spectrum enforcement applications.....	33
2.1.3	Cognitive radio applications .....	36
2.2	Radio system architecture .....	37
2.2.1	Information source.....	40
2.2.2	Modulation and coding.....	41
2.2.3	Transmitter.....	43
2.2.4	Phenomenon .....	44
2.2.5	Channel .....	47
2.2.6	Receiver .....	55
2.2.7	Recognition.....	56
2.3	Problems in signal recognition.....	57
2.3.1	Range of bandwidths and time scales.....	58
2.3.2	New signal types.....	63
2.3.3	Noise .....	66

- 2.3.4 Channel effects ..... 66
    - 2.3.5 Interference..... 67
  - 2.4 Review of signal recognition methods..... 67
    - 2.4.1 Segmentation methods ..... 70
    - 2.4.2 Transformation methods..... 75
    - 2.4.3 Features ..... 109
    - 2.4.4 Decision methods ..... 121
    - 2.4.5 Comments on decision methods..... 134
    - 2.4.6 Improving decision processing..... 136
  - 2.5 Summary ..... 137
- 3 Approach ..... 141**
  - 3.1 Sub-questions..... 141
  - 3.2 User survey ..... 144
  - 3.3 Phase-symmetric Cross Recurrence Plot ..... 147
  - 3.4 Logarithmic Cyclic frequency Domain Profile ..... 148
  - 3.5 Canonical ASR architecture..... 149
  - 3.6 Feature performance in the presence of interference..... 150
    - 3.6.1 Ideal Feature and Interference Selectivity..... 150
    - 3.6.2 Interference Selectivity investigation by simulation..... 152
  - 3.7 Combining multiple feature extraction algorithms..... 153
  - 3.8 Summary..... 154
- 4 Results ..... 155**
  - 4.1 Recurrence plots ..... 155
    - 4.1.1 Simulation details..... 156

4.1.2	BPSK symbol rate estimation from Recurrence Plots .....	159
4.1.3	Choice of threshold for BPSK symbol rate estimation from RP ...	166
4.1.4	Phase-symmetric Cross Recurrence Plots .....	168
4.1.5	BPSK symbol rate estimation from PCRP .....	171
4.1.6	Choice of threshold for BPSK symbol rate estimation from PCRP	177
4.1.7	Comparison of RP and PCRP for BPSK symbol rate detection....	179
4.1.8	QPSK symbol rate estimation from RP .....	180
4.1.9	QPSK symbol rate estimation from PCRP .....	183
4.1.10	Choice of threshold for QPSK symbol rate estimation.....	189
4.1.11	Comparison of RP and PCRP for QPSK symbol rate detection	191
4.1.12	Application to other modulation types.....	193
4.1.13	Conclusions .....	200
4.2	Logarithmic Cyclic frequency Domain Profile.....	202
4.2.1	Cyclic frequency.....	203
4.2.2	Cyclostationarity characteristics of communications signals .....	203
4.2.3	Logarithmic axes .....	204
4.2.4	Cyclostationary spectral analysis.....	205
4.2.5	Constant Q transform.....	206
4.2.6	Applying the CQT approach to the CDP .....	206
4.2.7	Implementation of the SCF.....	210
4.2.8	Examples.....	212
4.2.9	Application to spectrum sharing.....	217
4.2.10	Conclusions .....	218
4.3	Canonical ASR architecture .....	219
4.3.1	Top-level package diagram.....	220

4.3.2	Top-level class diagram.....	222
4.3.3	Activity Diagram.....	225
4.3.4	Class hierarchies.....	227
4.3.5	Activities .....	234
4.3.6	Examples .....	244
4.3.7	Summary .....	252
4.4	Feature performance in the presence of interference.....	253
4.4.1	Segmentation .....	254
4.4.2	Detection probability.....	256
4.4.3	The Ideal Feature.....	258
4.4.4	Interference Selectivity of a Feature .....	263
4.4.5	Examples of Feature behaviour.....	265
4.4.6	Interference Selectivity statistics.....	269
4.4.7	Options for handling interference.....	273
4.5	Combining multiple decision-theoretic algorithms .....	277
4.5.1	Bayesian chaining.....	278
4.5.2	Probability density function modelling approach .....	283
4.5.3	Conclusions on combining multiple algorithms.....	287
4.6	Summary.....	288
<b>5</b>	<b>Conclusions.....</b>	<b>291</b>
5.1	Main conclusions .....	291
5.2	Recommendations for further work.....	293
<b>6</b>	<b>References.....</b>	<b>297</b>
<b>7</b>	<b>Bibliography .....</b>	<b>331</b>

**Appendix A User survey .....339**

**Appendix B Simulation details .....353**

**Appendix C Neural network pruning.....357**

**Appendix D Modulation time scales .....363**

**Appendix E Lognormal approximation to a statistical feature .....369**

**Figures**

Figure 1. Conceptual radio system architecture. .... 38

Figure 2. In practice the received signal can be a composite of many signals passing through many channels. .... 39

Figure 3. Many received signals are carrying some form of information, which is modelled as originating in an information source process. .... 41

Figure 4. The modulation and coding block is of particular importance, as signal recognition needs to determine the characteristics of this process. .... 42

Figure 5. The transmitter process is, from the perspective of signal recognition, the simplest part of the signal source..... 43

Figure 6. The phenomenon process models unintentionally-transmitted signals, including natural phenomena and man-made noise..... 44

Figure 7. The channel adversely affects the signal..... 48

Figure 8. Multipath is caused by reflections from nearby structures. .... 50

Figure 9. Doppler shift affects all paths between transmitter and receiver and is caused by the movement of the transmitter or receiver..... 52

Figure 10. In built-up areas obscuration can be a significant factor..... 53

Figure 11. The receiver is often the most complex part of a communications system..... 55

Figure 12. The recognition process attempts to determine the characteristics of the received signal. .... 56

Figure 13. Histogram of time feature lengths in common modulations. .... 60

Figure 14. The number of publications on automatic signal recognition is increasing..... 69

Figure 15. FRESH filter implementation as a bank of time-invariant filters. .... 74

Figure 16. Taxonomy of Transformation methods..... 75



Figure 17. Instantaneous frequency and bandwidth estimation via a single z-domain pole representing the spectral peak. ....	90
Figure 18. SCF estimate of a single complex exponential at a frequency of 0.1. $\Delta f = 1/32$ , $\Delta\alpha = 1/64$ . ....	99
Figure 19. SCF estimate for the sum of two complex exponentials with frequencies of 0.1 and 0.3. $\Delta f = 1/64$ , $\Delta\alpha = 1/128$ . ....	100
Figure 20. SCF estimate for the sum of three complex exponentials with frequencies of 0.1, 0.3 and 0.4. $\Delta f = 1/64$ , $\Delta\alpha = 1/128$ . ....	101
Figure 21. Delay-Multiply Detector.....	103
Figure 22. Squaring detector.....	103
Figure 23. Method of moments analysis of FM signal. ....	106
Figure 24. Taxonomy of decision methods.....	122
Figure 25. Azzouz and Nandi (1996, Fig. 5.16) multi-stage ANN structure.....	132
Figure 26. RP ( $\varepsilon = 0.175$ ) of BPSK, example A1 (alternating symbols).....	160
Figure 27. Fourier transform of first row of Figure 26, BPSK, set A, zero frequency term omitted ( $\varepsilon = 0.175$ ).....	161
Figure 28. RP ( $\varepsilon = 0.175$ ) and Fourier transform of first row for BPSK, example B1.....	161
Figure 29. RP ( $\varepsilon = 0.175$ ) and Fourier transform of first row for BPSK, example B2.....	162
Figure 30. RP ( $\varepsilon = 0.175$ ) and Fourier transform of first row for BPSK, example B3.....	162
Figure 31. RP ( $\varepsilon = 0.175$ ) and Fourier transform of first row for BPSK, example B4.....	162
Figure 32. RP ( $\varepsilon = 0.175$ ) and Fourier transform of first row for BPSK, example B5.....	163
Figure 33. RP ( $\varepsilon = 0.175$ ) and Fourier transform of first row for BPSK, example B6.....	163
Figure 34. RP ( $\varepsilon = 0.175$ ) and Fourier transform of first row for BPSK, example B7.....	163
Figure 35. RP ( $\varepsilon = 0.175$ ) and Fourier transform of first row for BPSK, example B8.....	164

Figure 36. RP ( $\varepsilon = 0.175$ ) and Fourier transform of first row for BPSK, example B9. ...	164
Figure 37. RP ( $\varepsilon = 0.175$ ) and Fourier transform of first row for BPSK, example B10. .	164
Figure 38. Fourier transforms of RP ( $\varepsilon = 0.175$ ) first rows averaged over 10 examples in set B. ....	166
Figure 39. Effect of varying threshold on estimate of power at 1 kHz, averaged over set B symbol sequences and over 50 random symbol sequences .....	167
Figure 40. PCRP ( $D = 1$ , $\varepsilon = 0.175$ ) and Fourier transform of first row for BPSK, example A1 (alternating symols). ....	171
Figure 41. PCRP ( $D = 1$ , $\varepsilon = 0.175$ ) and Fourier transform of first row for BPSK, example B1.....	172
Figure 42. PCRP ( $D = 1$ , $\varepsilon = 0.175$ ) and Fourier transform of first row for BPSK, example B2.....	172
Figure 43. PCRP ( $D = 1$ , $\varepsilon = 0.175$ ) and Fourier transform of first row for BPSK, example B3.....	173
Figure 44. PCRP ( $D = 1$ , $\varepsilon = 0.175$ ) and Fourier transform of first row for BPSK, example B4.....	173
Figure 45. PCRP ( $D = 1$ , $\varepsilon = 0.175$ ) and Fourier transform of first row for BPSK, example B5.....	174
Figure 46. PCRP ( $D = 1$ , $\varepsilon = 0.175$ ) and Fourier transform of first row for BPSK, example B6.....	174
Figure 47. PCRP ( $D = 1$ , $\varepsilon = 0.175$ ) and Fourier transform of first row for BPSK, example B7.....	175
Figure 48. PCRP ( $D = 1$ , $\varepsilon = 0.175$ ) and Fourier transform of first row for BPSK, example B8.....	175

Figure 49. PCRP ( $D = 1$ , $\varepsilon = 0.175$ ) and Fourier transform of first row for BPSK, example B9. ....	176
Figure 50. PCRP ( $D = 1$ , $\varepsilon = 0.175$ ) and Fourier transform of first row for BPSK, example B10. ....	176
Figure 51. Fourier transforms of PCRP ( $D = 1$ , $\varepsilon = 0.175$ ) first rows averaged over 10 examples in set B. ....	177
Figure 52. Effect of varying threshold on estimate of power at 1 kHz, averaged over set B symbol sequences and over 50 random symbol sequences using PCRP ( $D = 1$ ). ....	178
Figure 53. Comparison of 1 kHz peak height for RP and PCRP methods averaged over set B with BPSK modulation. ....	180
Figure 54. RP ( $\varepsilon = 0.175$ ) and Fourier transform of first row for QPSK, example C1. ...	181
Figure 55. RP ( $\varepsilon = 0.175$ ) and Fourier transform of first row for QPSK, example D1. ...	182
Figure 56. RP ( $\varepsilon = 0.175$ ) and Fourier transform of first row for QPSK, example D2. ...	182
Figure 57. RP ( $\varepsilon = 0.175$ ) and Fourier transform of first row for QPSK, example D3. ...	182
Figure 58. Fourier transforms of RP ( $\varepsilon = 0.175$ ) first rows averaged over set D, QPSK. ....	183
Figure 59. PCRP ( $D = 0$ , $\varepsilon = 0.175$ ) and Fourier transform of first row for QPSK, example C1. ....	185
Figure 60. PCRP ( $D = 1$ , $\varepsilon = 0.175$ ) and Fourier transform of first row for QPSK, example C1. ....	185
Figure 61. PCRP ( $D = 2$ , $\varepsilon = 0.175$ ) and Fourier transform of first row for QPSK, example C1. ....	186
Figure 62. PCRP ( $D = 3$ , $\varepsilon = 0.175$ ) and Fourier transform of first row for QPSK, example C1. ....	186

Figure 63. PCR <sub>P</sub> ( $D = 0$ , $\varepsilon = 0.175$ ) and Fourier transform of first row for QPSK, example D1. ....	187
Figure 64. PCR <sub>P</sub> ( $D = 1$ , $\varepsilon = 0.175$ ) and Fourier transform of first row for QPSK, example D1. ....	187
Figure 65. PCR <sub>P</sub> . ( $D = 2$ , $\varepsilon = 0.175$ ) and Fourier transform of first row for QPSK, example D1. ....	188
Figure 66. Fourier transforms of PCR <sub>P</sub> ( $D = 2$ , $\varepsilon = 0.175$ ) first rows averaged over set D, QPSK. ....	188
Figure 67. Effect of varying threshold on estimate of QPSK power at 1 kHz, averaged across set D examples. ....	190
Figure 68. Comparison of 1 kHz peak height for RP and PCR <sub>P</sub> methods averaged over all set D examples, QPSK. ....	192
Figure 69. PCR <sub>P</sub> ( $D = 0$ , $\varepsilon = 0.175$ ) and Fourier transform of first row for PSK8. ....	194
Figure 70. PCR <sub>P</sub> ( $D = 1$ , $\varepsilon = 0.175$ ) and Fourier transform of first row for PSK8. ....	194
Figure 71. PCR <sub>P</sub> ( $D = 2$ , $\varepsilon = 0.175$ ) and Fourier transform of first row for PSK8. ....	194
Figure 72. PCR <sub>P</sub> ( $D = 3$ , $\varepsilon = 0.175$ ) and Fourier transform of first row for PSK8. ....	195
Figure 73. RP ( $\varepsilon = 0.175$ ) and Fourier transform of first row for FSK2, example A1. ....	195
Figure 74. RP ( $\varepsilon = 0.175$ ) and Fourier transform of first row for FSK2, example B1. ....	196
Figure 75. RP ( $\varepsilon = 0.175$ ) and Fourier transform of first row for FSK4, example C1. ....	196
Figure 76. RP ( $\varepsilon = 0.175$ ) and Fourier transform of first row for FSK4, example D1. ....	197
Figure 77. PCR <sub>P</sub> ( $D = 0, 1, 2$ , $\varepsilon = 0.175$ ) for MSK, example A1. ....	197
Figure 78. PCR <sub>P</sub> ( $D = 0, 1, 2$ , $\varepsilon = 0.175$ ) for MSK, example B1. ....	198
Figure 79. PCR <sub>P</sub> ( $D = 0, 1$ , $\varepsilon = 0.175$ ) for PAM2, example A1. ....	198
Figure 80. PCR <sub>P</sub> ( $D = 0, 1$ , $\varepsilon = 0.175$ ) for PAM2, example B1. ....	199

Figure 81. Region of support of the logarithmic SCF, which extends $\pm 1$ in cyclic frequency and $\pm 0.5$ in frequency. The region of support excludes the line of $\alpha=0$ .	209
Figure 82. Implementation of the time-smoothed SCF as a pair of low pass filters.	211
Figure 83. Time-smoothed logarithmic SCF implementation as a cascade of low pass filter pairs.	212
Figure 84. Linear CDP of two tones (256 $\alpha$ points).	213
Figure 85. Logarithmic CDP of two tones (9 $\alpha$ points).	213
Figure 86. PSD of QPSK and BPSK for example 2.	214
Figure 87. Linear CDP of QPSK and BPSK (8192 $\alpha$ points).	215
Figure 88. LCDP of QPSK and BPSK (9 $\alpha$ points).	216
Figure 89. Detection probability versus $E_b/N_0$ for the QPSK example.	217
Figure 90. Detection probability versus $E_b/N_0$ for the BPSK example.	217
Figure 91. Top-level package diagram.	220
Figure 92. Top-level class diagram.	223
Figure 93. Top-level activity diagram.	226
Figure 94. Signal class hierarchy.	228
Figure 95. Segment class hierarchy.	230
Figure 96. Representation class hierarchy.	231
Figure 97. Feature class hierarchy.	233
Figure 98. Pre-processing activities.	235
Figure 99. Segmentation activities.	237
Figure 100. Transformation activities.	239
Figure 101. Feature extraction activities.	241
Figure 102. Decision activities.	243

Figure 103. Ghani and Lamontagne algorithm class diagram. .... 245

Figure 104. Ghani and Lamontagne algorithm activity diagram..... 246

Figure 105. AMRA 1 class diagram. .... 247

Figure 106. AMRA 1 activity diagram..... 248

Figure 107. Hellinger distance method class diagram..... 249

Figure 108. Hellinger distance method activity diagram..... 249

Figure 109. Zero crossing method class diagram. .... 250

Figure 110. Zero crossing method activity diagram..... 251

Figure 111. Example of two interfering Bursts, one narrowband of long duration, the other wideband of short duration. .... 255

Figure 112. Example of simple one-dimensional interference, in which a Burst from Source A is interfered with by a Burst from Source B for part of the observation time. ... 256

Figure 113. Ideal Feature interference selectivity curve. .... 261

Figure 114. Power spectral density for combination (blue) of DSSS+DQPSK 2Mbps WiFi (black) and DPSK8 Bluetooth (red), both at 2412 MHz. .... 266

Figure 115. Interference selectivity of  $\sigma_{ap}$  for DSSS+DQPSK 2Mbps WiFi and DPSK8 Bluetooth, both at 2412 MHz (500 runs per case)..... 267

Figure 116. Interference selectivity curves of  $\sigma_{aa}$  for DSSS+DQPSK 2Mbps WiFi and DPSK8 Bluetooth, both at 2412 MHz (50 runs per case)..... 268

Figure 117. Interference selectivity curves of  $\mu^a_{42}$  for DSSS+DQPSK 2Mbps WiFi and DPSK8 Bluetooth, both at 2412 MHz (50 runs per case)..... 268

Figure 118. Interference Selectivity distributions of Azzouz & Nandi Features. .... 270

Figure 119. Interference Selectivity distributions of delay-multiply features. .... 271

Figure 120. Bayesian chaining of probabilities. .... 279

Figure 121. Schematic illustration of joint probability density function for a single Feature, $y$ , and three Types, $H_1$ , $H_2$ and $H_3$ .....	281
Figure 122. Summary of responses to question 1. ....	341
Figure 123. Histogram summarising responses to question 4.....	347
Figure 124. Perceptron influence diagram. ....	358
Figure 125. Histogram of time feature lengths in common modulations. ....	368
Figure 126. Probability plot of $\gamma_{\max}$ with WGN as an input.....	370
Figure 127. Probability plot of DMD feature with WGN as an input. ....	371
Figure 128. Mean of $\gamma_{\max}$ with FM as input. ....	373
Figure 129. Standard deviation of $\gamma_{\max}$ with FM as input.....	373
Figure 130. Lognormal plot, SNR = 50 dB, $f_d = 0.0001$ .....	374
Figure 131. Lognormal plot, SNR = 50 dB, $f_d = 0.001$ .....	374
Figure 132. Lognormal plot, SNR = 50 dB, $f_d = 0.05$ .....	375

**Tables**

Table 1. Typical Man-Made Noise characteristics..... 46

Table 2. Middleton's classes of impulsive noise..... 47

Table 3. Periodicities in the TETRA protocol..... 59

Table 4. Brief timeline of radio system types (N.B. Not an exhaustive list)..... 65

Table 5. Summary of the types of periodicity introduced by Gardner (1991). ..... 94

Table 6. PCRP symmetry depths for measuring symbol rate in different modulation types.  
..... 200

Table 7. Example Signal classes..... 229

Table 8. Example Segment classes..... 231

Table 9. Example Representation classes..... 232

Table 10. Example Feature classes..... 233

Table 11. Example Type classes..... 234

Table 12. Example Segmentation activities..... 238

Table 13. Example Transformation activities..... 240

Table 14. Example Feature extraction activities..... 242

Table 15. Example Decision activities. .... 244

Table 16. Advantages and disadvantages of different approaches to probability density  
function modelling..... 283

Table 17. Simulated signal types – 2.4 GHz ISM band specific types..... 354

Table 18. Simulated signal types – generic types..... 355



## Notation

$a$	Instantaneous amplitude
$a_{cn}$	Normalised-centred instantaneous amplitude
$a_t$	Amplitude threshold
$b$	Number of bins per decade in constant Q transform
$C$	Number of samples with amplitude greater than a threshold, $a_t$
$c_{11}, c_{12}, c_{21}, c_{22}$	Costs
$d$	Recurrence matrix diagonal index
$D$	Symmetry depth
$F()$	Probability distribution function
$f(.)$	Probability density function
$f_N$	Normalised frequency
$H$	Set of modulation types
$h$	Modulation index
$H_1, H_2$	Hypotheses
$k$	Integer
$L$	Number of detectors in a Bayesian chain
$M$	Number of windows of sample data
$m$	Sample number
$n$	Sample number
$N$	Number of samples in a window of sample data
$N_k$	Length of $k^{\text{th}}$ filter in constant Q transform
$p$	Frequency bin index
$P$	Number of frequency bins

$p()$	Probability of an event
$p(t)$	Time domain signal of interest
$p_1, p_2$	<i>A priori</i> probability of hypothesis 1 or 2 being true
$P_\alpha$	Number of cyclic frequency points on axis of linear SCF
$P_\alpha$	Number of cyclic frequency points on axis of logarithmic SCF
$Q$	Ratio of filter spacing to filter bandwidth in constant Q transform
$q(t)$	Time domain interferer
$R$	Covariance matrix of $x$
$RM$	Recurrence matrix
$R_x$	Autocorrelation of $x$
$R_x^\alpha$	Cyclic autocorrelation of $x$
$t$	Time
$T_0$	Fundamental period of a periodic signal
$t_k$	Time centre of $k^{\text{th}}$ filter in constant Q transform
$X$	DFT of $x$
$x$	Complex, zero-mean, baseband signal
$y$	Detector output , representation or feature
$\Delta_k$	Bandwidth of $k^{\text{th}}$ filter in constant Q transform
$\Gamma_{\max}$	Logarithmic form of $\gamma_{\max}$
$N$	Number of modulation types in the set $H$ .
$\Theta$	Heaviside function
$T$	Transition count
$\alpha$	Cyclic frequency

$\alpha$	Shift parameter
$\varepsilon$	Error or recurrence plot threshold level
$\phi_{NL}$	Non-linear phase
$\phi_{uw}$	Unwrapped phase
$\phi_w$	Wrapped phase
$\gamma_{\max}$	Maximum value of the spectral power density of the normalised-centred instantaneous amplitude
$\eta$	Ratio of amplitude of signal of interest to that of interferer
$\lambda$	Eigenvalue
$\mu^a_{42}$	Kurtosis of amplitude
$\mu^f_{42}$	Kurtosis of frequency
$\sigma$	Standard deviation
$\sigma_a$	Standard deviation of amplitude
$\sigma_{aa}$	Standard deviation of absolute amplitude
$\sigma_{af}$	Standard deviation of absolute frequency
$\sigma_{ap}$	Standard deviation of absolute phase
$\sigma_{dp}$	Standard deviation of direct phase
$\tau$	Time lag
$\omega$	Frequency
$\xi$	Selectivity of a feature

## Abbreviations

ACF	Autocorrelation Function
ADMRA	Analogue and Digital Modulation Recognition Algorithm
AM	Amplitude Modulation
AMR	Automatic Modulation Recognition
AMRA	Analogue Modulation Recognition Algorithm
ANN	Artificial Neural Network
ASK	Amplitude Shift Keying
ASR	Automatic Signal Recognition
AWGN	Additive White Gaussian Noise
BPSK	Binary Phase Shift Keying
CAF	Cyclic Autocorrelation Function
CDMA	Code Division Multiple Access
CDP	Cyclic frequency Domain Profile
CIF	Complete Ideal Feature
COMINT	Communications Intelligence
CQT	Constant Q Transform
CR	Cognitive Radio
CRP	Cross Recurrence Plot
CS	Cyclostationarity
CW	Continuous Wave
DAB	Digital Audio Broadcasting
DBT	Double Bound Test
DFT	Discrete Fourier Transform
DMD	Delay-Multiply Detector
DMRA	Digital Modulation Recognition Algorithm
DOA	Direction Of Arrival
DQPSK	Differential Quadrature Phase Shift Keying
DSB	Double Side Band
DSP	Digital Signal Processor
DSSS	Direct Sequence Spread Spectrum
DTT	Digital Terrestrial Television
DVB	Digital Video Broadcasting

ECM	Electronic Countermeasures
EMI	Electromagnetic Interference
ERP	Event-Related brain Potential
ESM	Electronic Support Measures
EW	Electronic Warfare
FAM	FFT Accumulation Method
FCC	Federal Communications Commission
FDD	Frequency Division Duplexing
FFT	Fast Fourier Transform
FM	Frequency Modulation
FPGA	Field Programmable Gate Array
FSK	Frequency Shift Keying
GFSK	Gaussian Frequency Shift Keying
GIF	Globally Ideal Feature
GMSK	Gaussian Minimum Shift Keying
GSM	Global System for Mobile communications
HF	High Frequency
HMM	Hidden Markov Model
HOS	Higher Order Statistics
HRRP	High Resolution Range Profile
I/Q	In-phase/Quadrature
ICA	Independent Component Analysis
IEEE	Institute of Electrical and Electronics Engineers
IET	Institute of Engineering and Technology
IF	Ideal Feature or Intermediate Frequency
IP	Internet Protocol
ISI	Inter-Symbol Interference
ISM	Industrial, Scientific and Medical
ITU	International Telecommunications Union
LCDP	Logarithmic Cyclic frequency Domain Profile
LE	Licence-Exempt
LPI	Low Probability of Intercept
LSB	Lower Side Band
MAP	Maximum A Posteriori

---

MASS	Mass Consultants Ltd
MCMC	Markov Chain Monte Carlo
MFSK	Multiple Frequency Shift Keying
MIMO	Multiple Input Multiple Output
ML	Maximum Likelihood
NICAM	Near Instantaneous Companded Audio Multiplex
NTIA	National Telecommunications and Information Administration
OBD	Optimal Brain Damage
OCN	One-Class, One-Network
OFDM	Orthogonal Frequency Division Multiplexing
OO	Object Oriented
OU	Open University
PAM	Pulse Amplitude Modulation
PCRP	Phase-symmetric Cross Recurrence Plot
PDF	Probability Density Function
PM	Phase Modulation
PSD	Power Spectral Density
PSK	Phase Shift Keying
PSSTG	Public Spectrum Safety Test Group
QAM	Quadrature Amplitude Modulation
QPSK	Quadrature Phase Shift Keying
RF	Radio Frequency
RFID	Radio Frequency Identification
RM	Recurrence Matrix
RP	Recurrence Plot
RRI	Radio Refractive Index
SA	Sine Anno
SCF	Spectral Correlation Function
SDR	Software Defined Radio
SETI	Search for Extraterrestrial Intelligence
SIGINT	Signals Intelligence
SNR	Signal to Noise Ratio
SUR	Spectrum Usage Rights
SVM	Support Vector Machine

---

TETRA	Terrestrial Trunked Radio
TV	Television
UHF	Ultra High Frequency
UML	Unified Modelling Language
UMTS	Universal Mobile Telecommunications System
USB	Upper Side Band
UWB	Ultra Wide Band
VHF	Very High Frequency
VSB	Vestigial Side Band
WCDMA	Wideband Code Division Multiple Access
WGN	White Gaussian Noise
WLAN	Wireless Local Area Network

This page intentionally blank



# 1 INTRODUCTION

The radio spectrum is becoming ever more complex as it is used for an increasingly diverse range of applications. The advent of personal, mobile communications and home networking has added considerably to the exploitation of the spectrum, which is also used for television and radio broadcasting, industrial and home automation, radar, radio paging and a plethora of other applications. Many electrical and electronic devices also radiate radiowaves which can interfere with the users of the spectrum. There are now areas of the spectrum where interference is the norm rather than the exception. Radio systems working in these bands have to be designed to be robust in the presence of interference.

Automatic Signal Recognition (ASR) algorithms can be used to help people understand the state of the spectrum and can also be built into cognitive radio systems that react intelligently to changes in spectrum occupancy and usage. Such algorithms are typically designed to recognise one signal at a time and the recognition accuracy of such algorithms is adversely affected by interference.

In the context of this thesis interference is considered to be any situation in which two or more signal types are received simultaneously. This is a deliberately wide definition so as to embrace any situation in which, because of the presence of multiple signals, an ASR system is confronted with a non-trivial decision as to the type of signal being received.

This thesis presents the results of an investigation into ASR systems, with a particular emphasis on their behaviour when interference is present. If one wishes to produce ASR algorithms that have good recognition accuracy in shared spectrum bands, then one must find design strategies that can deliver the performance needed by one's application.

The following paragraphs explain the motivation for working in this subject area and the research question itself. In addition the specific contributions of this particular investigation are explained and the main structure of the document is outlined.

## **1.1 Motivation**

ASR is an important field of research and development, with both current and future applications of the technology. It has uses in the defence and civilian worlds, which have some requirements in common but also significant differences. The main emphasis of this project is on non-defence applications as the work has been motivated by various programmes of work carried out for the UK and Dutch spectrum regulators.

One of the main non-defence applications of ASR is in the detecting and investigating of radio spectrum interference, which is a major function carried out by spectrum regulators around the world. Diagnosing interference problems depends on the knowledge of relatively few domain experts who have learnt the readily-observable characteristics of the classic modulation types and have had the experience of identifying many and varied interferers. In the future these tasks

will be complicated further as the trend towards spectrum liberalisation continues. Already the Licence-Exempt (LE) bands are showing a proliferation of complex digital modulations driven by the need to maximise spectrum efficiency and co-existence.

In an increasingly complex radio environment field staff need automated tools to assist them with identifying a plethora of communications and interference signals.

Another major non-defence application of ASR is in cognitive radio (CR) systems. At the moment, ASR algorithms do not have the required level of fidelity and robustness needed to be fully integrated into cognitive radio designs, but this situation is developing rapidly.

Both of these applications of automated signal recognition are driving the research into improved ASR systems. The particular interest for this project has been the former application, with the emphasis on identifying interference signals as well as standard communication signals.

It is recognised that a wealth of existing techniques exists and that these need to be brought together to tackle the complexities of the modern shared spectrum bands. For various reasons then, there is a need to continue to research into the algorithms that can be brought to bear on the ASR task.

## **1.2 Specific research question**

A plethora of algorithmic approaches have been devised for performing the ASR task. In general, however, researchers have concentrated on the performance of algorithms in the presence of simple noise, because interference is immensely complex and the number of possible types of interference is unbounded. Understanding the performance of an algorithm in the presence of all possible interferers requires, therefore, considerably more study than an evaluation against noise alone.

The research question posed by this thesis is: what strategies can be adopted for designing ASR algorithms to deal with modern, complex signal environments? This is a complex question and one that needs to be broken down into a series of smaller questions if one is to make progress in this area. Section 3, therefore, presents an approach to answering this question that relies on investigating a series of sub-questions.

The importance of the answer to this research question is that it will help guide research into and the development of ASR systems that are more robust in the modern radio environment.

## **1.3 The work of this Ph.D.**

The main thread of research has been into the various issues surrounding the design of ASR systems to work in regions of the spectrum where interference can be expected and cannot be ignored.

This research has led to the following outcomes that contribute to the body of knowledge in this area:

1. *Recurrence plots* have, for the first time, been applied to the visualisation of communications signals and show potential as an analysis tool to be used alongside conventional analysis methods. In particular the thesis introduces a modification to the basic recurrence plot called the *Phase-symmetric Cross Recurrence Plot* (PCRP) that shows how it is possible to separate the modulation of a signal from its information content by manipulating a received signal prior to applying a transformation;
2. The recurrence plot method shows the separation of modulation and information, but is not well suited to admixtures of signals with widely different time domain characteristics. It is proposed that one approach to addressing this problem is to use a logarithmic representation. In order to illustrate this approach, a *Logarithmic Cyclic frequency Domain Profile* (LCDP) has been developed. This logarithmic form of the cyclic frequency domain profile promises to be useful in detecting the cyclostationarity signatures of signals of very widely differing bandwidths and therefore handling a wide range of interference conditions;
3. A canonical processing architecture is introduced that is capable of describing ASR systems in an holistic way, thereby facilitating comparison of different architecture designs without being overwhelmed by the details of the differences between them. This architecture sets a framework via which one can reason about the merits of different algorithms;

4. A concept called the *Ideal Feature* is introduced. This is a signal processing function with well-defined characteristics with regards to its behaviour in interfering environments. The Ideal Feature sets a benchmark against which candidate algorithms can be compared;
5. A concept called *Interference Selectivity* is introduced. This concept allows non-ideal features to be compared quantitatively with the Ideal Feature and also with other, non-ideal features.

The work presented in this thesis therefore makes significant contributions to the body of knowledge on the strategies that can be used in devising ASR algorithms for use in shared radio environments. It opens up new avenues for future research in this area and provides a tool whereby progress can be quantitatively assessed.

## 1.4 Structure of this thesis

The remainder of this document presents the findings of this research. Section 2 introduces the subject area, giving the necessary background within which the remainder of the document can be understood. Section 3 describes the approach to the investigation and section 4 presents the results. The overall conclusions of the thesis are given in section 5 along with suggestions for further work in this area. The references and bibliography are given in sections 6 and 7 respectively. Appendices are attached for detailed information that supports and informs the main body of the document.

## 2 BACKGROUND

This section gives the background for the project so that the work can be understood in relation to previous and current research. There are a number of applications of the technology and there is a wide variety of algorithmic techniques for detecting widely differing types of signal.

Section 2.1 looks at applications for this technology, which can be used in commercial and military domains. To some extent ASR functionality is not dependent on the application, but there are some application demands that can influence ASR design. Some applications may, for example, require extremely fast processing and tolerate a lower accuracy, whilst others may not be time critical but demand very high accuracies. Knowledge of the intended application is, therefore, of interest to the designer.

ASR algorithms do not exist in isolation as a purely theoretical concept. They are embedded within radio systems and depend on radio receiver technology to supply them with data on which to act. Section 2.2 discusses the subject area within the context of a generic radio system architecture. It shows where the ASR functionality resides and explains that the recognition process seeks to identify the modulation and coding of intentionally transmitted signals and the characteristics of phenomena that are not intentionally transmitted. This is an important concept, because the information content of signals is not of interest to an ASR algorithm.

Section 2.3 identifies a number of problems that are encountered when designing ASR systems. These problems are at the heart of the motivation for this research and are caused by the changing nature of the radio spectrum. Areas of shared spectrum are home to an increasingly wide variety of signal types that can overlap in time and frequency, making the task of recognising individual signal types ever more complex.

Signal recognition has been an active area of research for several decades. Section 2.4 discusses various approaches to the task that have been developed and classifies the techniques as segmentation, transformation, feature extraction or decision methods. This taxonomy is helpful in navigating through the large body of published literature and is expanded further by the work of this research. The canonical architecture developed in section 4.3 is an evolution of the taxonomy presented in section 2.4 that adds rigour via the use of the Unified Modelling Language (UML). The literature is dominated by the statistical feature methods and cyclostationarity, but section 2.4 endeavours to cover a wider variety of algorithmic approaches and organise them ready for more detailed analysis in section 4.3.

## **2.1 Applications**

There are three primary application areas for ASR, these being the military, spectrum enforcement and cognitive radio applications. The research covered by this project is targeted primarily at non-military applications, with emphasis on spectrum enforcement and cognitive radio.



### **2.1.1 Military applications**

In the military world, ASR forms a small part of the Communications Intelligence (COMINT) function, itself part of the discipline known as Signals Intelligence (SIGINT), which is in turn part of the world of Electronic Warfare (EW) (Rockwell, 2004). By intercepting and recognising communications signals, COMINT systems provide military forces with the ability to control the electromagnetic spectrum and deny its use to their opposition. There are two objectives to this activity. Firstly, by eavesdropping on and geolocating communication links, COMINT activities allow intelligence on enemy operations to be gleaned and exploited for tactical and strategic planning. Secondly, COMINT enables Electronic Counter Measures (ECM), such as jamming, to be carried out. Modern COMINT systems are very sophisticated and often comprise networks of Electronic Support Measures (ESM) sensors that can rapidly detect signals, identify and demodulate them and also geolocate the transmitters (Ferreira, 1996). Moreover, they have to do this in difficult conditions, often with severe interference to the signals of interest (McGehee, 2008).

### **2.1.2 Spectrum enforcement applications**

Non-military applications of ASR are very different in nature, but are growing in importance as the electromagnetic spectrum becomes increasingly important to the daily life of individuals and industry.

A key part of spectrum management in the non-military world is the role performed by the agencies charged with enforcing spectrum usage. Here the emphasis is on reacting to reports of interference from network operators,

broadcasters or members of the public. As Andrews (2008) says "...network operators are waging their own battle with interference..". The operators have to deploy field staff to track down and deal with interference sources in order to meet their targets for service performance (Ofcom, 2009).

The sources of interference are typically many and varied. They include pirate radio stations (Ofcom, 2005), radios that have been imported and are operating on frequencies for which they are not licensed, electromagnetic noise from household, automotive and industrial appliances and many other intentional and unintentional sources (section 2.2.4). By way of example, Wagstaff (2009) describes the interference effects of analogue video senders and microwave ovens on IEEE 802.11 networks.

Typically priority for such investigations is given to cases where safety-of-life is an issue (Ofcom, 2010a) and this may be because the interferer is radiating into a channel that is reserved for emergency calls. In such cases there is pressure to locate and stop the source of interference as quickly as possible. This means getting a team to the site, detecting the signal, identifying it and then carrying out direction finding to locate the source. Prosecution of offenders (Ofcom, 2010b) may be appropriate in some cases, so the information collected during this process must be treated as potential evidence to be used in court.

A new slant to spectrum enforcement is appearing in the UK as spectrum licence costs have soared. In March 2000 the UK government auctioned five licences for the 3G phone bands and received £22bn from the companies that won the bidding

process (Radiocommunications Agency, 2000). Each of the companies involved had invested over £4bn for exclusive usage of these frequency bands. Clearly they have a right to expect that interference within these bands would be dealt with severely. To do this effectively relies on accurate signal recognition and facilities for geolocating interferers.

Ofcom, the body that replaced the Radiocommunications Agency in 2003, is now pursuing more advanced spectrum management methods. Spectrum Usage Rights (SUR) are proposed as the way ahead for many future licences (Ofcom, 2006) and are intended to control the spectrum by stipulating to what degree a licence holder may interfere in neighbouring frequency bands or geographic locations (Aegis, 2006). In concept this approach will allow licence holders more freedom to choose the modulations, protocols, number of transmitters and radiated powers that they deploy around the country. SUR therefore will help to remove the barriers that currently exist on modulation types in use in the licensed bands. This is seen as being good for business, but it does mean that spectrum enforcement is likely to become more complex (Davies, 2008). The responsibility for maintaining quality of service under the SUR scheme will, however, be largely the responsibility of the licensee (Ganley, 2006).

To support spectrum enforcement effectively, ASR needs to provide emitter identification at a level that is appropriate. In a military role the ASR may need to provide information that is detailed enough to allow jamming to be carried out and such information might, for example, include the mode of transmission. In the spectrum enforcement role such detailed information would be superfluous

and the ASR only needs to try to indicate what kind of device is involved. The operators need to know, for example, whether they are looking for a mobile handset or a mast-mounted transmitter. It is also desirable to know whether the emitter is radiating intentionally or not, since many causes of interference are from machinery and electronics that are not properly suppressed.

### **2.1.3 Cognitive radio applications**

The concept of Cognitive Radio (CR) was proposed as a means of adding intelligent processing to software defined radio to deliver personalised services (Mitola III and Maguire Jr, 1999, p.18). It can also be thought of in terms of improving utilisation of the spectrum (Haykin, 2005, p. 201). The case for this technology appears to be gaining ground, with increasing research activity at the time of writing (Steenkiste *et al*, 2009) (Poole, 2010).

The Wireless Innovation Forum (formerly the Software Defined Radio Forum) acts as the main focus for these activities with various universities and companies developing new concepts, techniques and tools. This work has led to rapid development of CR architectures and expected to continue to evolve to provide greater quality of service and quality of information for lower cost (Mitola III, 2009, p. 639).

In LE bands, such as the 2.4 GHz Industrial, Scientific and Medical (ISM) band, there are already a number of radio systems that co-exist, e.g. Bluetooth and WiFi, without any significant cognitive radio functionality being implemented.

The pressure on some parts of the spectrum is such that cognitive radio may become economically viable and perhaps necessary (Steenkiste *et al*, 2009). A significant example of this is in the USA, where the FCC has recently released the TV "whitespace" regions for use by secondary, unlicensed services (Ghasemi and Sousa, 2008) (Reardon, 2008) and Ofcom in the UK is expected to follow suit (Chacksfield, 2009). These are regions that lie between the existing analogue TV regions and are only currently used for wireless microphones. The wide bandwidths and favourable propagation available at these frequencies mean that some researchers see a business case for running data access in these bands (Martin *et al*, 2008).

In the USA spectrum sensing is required in the TV whitespace bands (Sherman, 2009). To be effective, such functionality will require the rapid detection of primary signals (Wang and Gaddam, 2009) and the accurate and robust identification of modulation type (Kim *et al*, 2008).

It is likely that more such applications of cognitive radio functions will appear in the coming years. Cognitive radio depends on a radio being aware of its environment, which includes recognising the various signal types present (Le *et al*, 2006). Accurate and robust ASR will be, therefore, one component in achieving success in these business areas.

## **2.2 Radio system architecture**

Before examining the analysis methods used for ASR itself, this section presents a conceptual radio system architecture. This makes it clear that ASR does not exist

in isolation, but is part of a processing chain and that some assumptions have to be made about the processes surrounding the ASR itself.

Figure 1 shows the conceptual radio system architecture assumed in this thesis. It is not dissimilar to a conventional block diagram of a communication system (Ziemer and Tranter, 1995, p. 4) but has been modified to better suit the study of the signal recognition process.

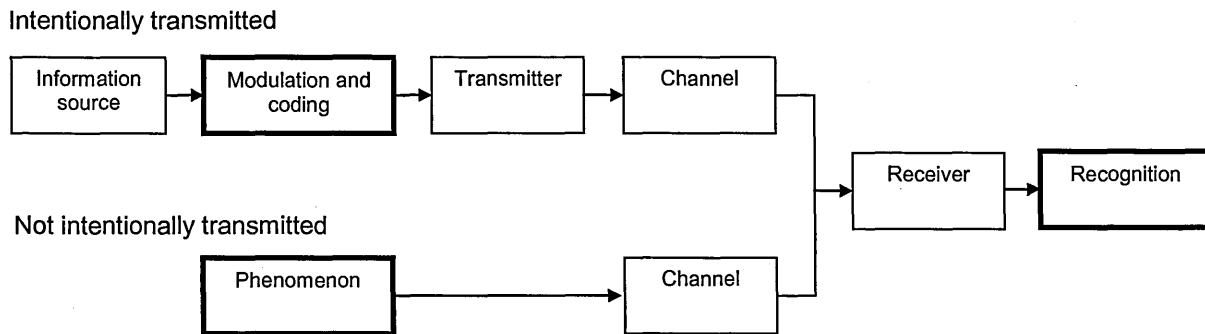


**Figure 1. Conceptual radio system architecture.**

Each of the components of this processing chain are described below and it is generally assumed that most, but not always all, of these processing blocks exist in practical systems.

There are two branches on the left hand side of Figure 1. The upper branch represents intentionally transmitted signals, typically carrying some sort of information. The lower branch represents other phenomena which may be natural or man-made, but are not intentionally transmitted.

There are three blocks in Figure 1 that are of particular interest for this thesis. These are the Modulation and Coding block and the Phenomenon block, which are the processes whose characteristics are to be estimated and the Recognition block, which is the process that performs the estimation. Each block in the chain is now described and this discussion leads towards the proposal of a standard model for the Recognition block in Section 4.3.

In a real world situation there may be many upper branches and many lower branches as illustrated in Figure 2. A receiver could intercept many modulated signals from transmitters and also many phenomena. All these signals pass through channels, which can distort the signals, and are summed at the receiver. The goal of recognition can be to determine the type of one or all of these incoming signals. Different applications may require different behaviour from the ASR system.

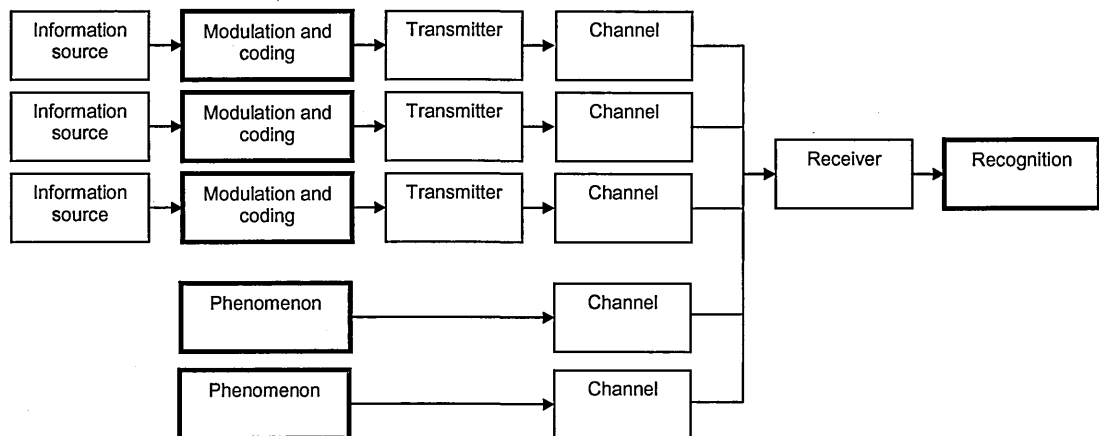


**Figure 2. In practice the received signal can be a composite of many signals passing through many channels.**

Noise, in this model, is always unwanted and originates in all the boxes to the left of (and including) the receiver. Noise aggregates throughout the processing

chain. Whilst noise can be suppressed through some kinds of processing, it can never be entirely eliminated (Krauss *et al*, 1980, p. 9) and the Recognition process will always have to deal with some amount of noise at its input.

In this model, interference is defined as any signal present at the input to the receiver that is unwanted. Thus interference can be a modulated signal, a phenomenon, or a channel effect. Common terms for modelling interference are Adjacent Channel Interference (ACI) and Co-Channel Interference (CCI). Wagstaff (2007) discusses these terms in relation to other metrics used for measuring interference.

### **2.2.1 Information source**

The first block in Figure 3 is the *information source* process. Many intercepted signals are carrying some form of information and this can be represented as a single information source. In signal recognition we are not generally interested in the information content. Indeed it may be that, by suppressing the information content, the performance of the signal recognition can be improved. One such technique (see section 4.1) is proposed as part of this thesis.



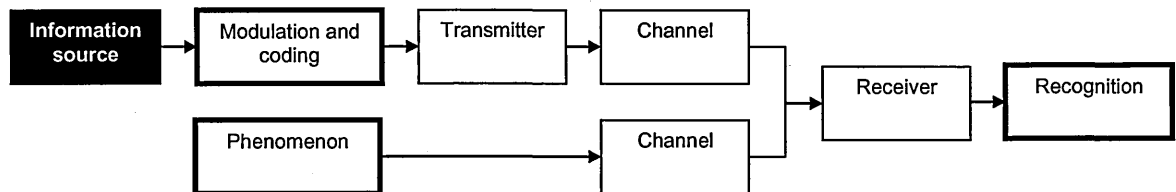


**Figure 3. Many received signals are carrying some form of information, which is modelled as originating in an information source process.**

Not all signals carry information, however. These are typically noise and interference sources, but there are also some man-made emitters that do not carry information. Continuous Wave (CW) emitters are used in a number of applications, including RFID tag stimulation (Oduncu, 2008) and as Doppler sensors for intruder detection (Singapore Technologies, 2005). In such cases the information comes from analysing the response to stimulation from another object rather than the signal itself.

### **2.2.2 Modulation and coding**

The *modulation and coding* block, highlighted in Figure 4, is of importance to this thesis. For intentionally-transmitted signals, it is the set of characteristics of the modulation and coding process that is to be estimated by the signal recognition process.

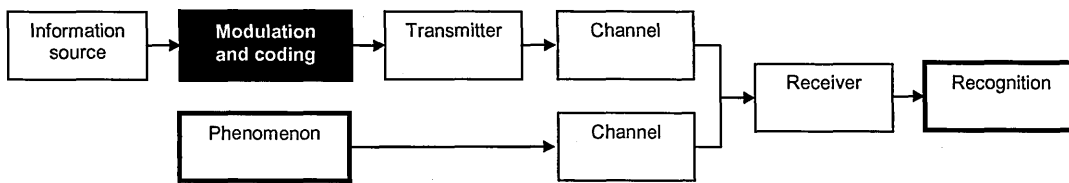


**Figure 4. The modulation and coding block is of particular importance, as signal recognition needs to determine the characteristics of this process.**

The goal of an ASR system is to describe the modulation and coding in use. One way of doing this would be to report the standard where this is applicable (e.g. IEEE 802.11n, POCSAG, NICAM, GSM), which is the approach typically used by proprietary ASR products (Agilent, 2005), (Tadiran, 2011), (Wavecom, 2007). A different way of describing a communications signal would be to denote the modulation parameters using a coding scheme such as that used in SM.1138 (ITU-R, 1995). Whichever type of description is used, identification typically depends on estimating features of a received signal and these features range from very simple to very complex.

Early analogue modulations, such as Frequency Modulation (FM), were very simple in that they could be characterised by just one or two parameters (e.g. FM deviation). Early digital modulations, such as Frequency Shift Keying (FSK), were still relatively simple to characterise using parameters such as number of tones, frequency spacing and symbol rate.

Modern communications protocols can be far more complex and cannot easily be described by a few numbers. A modern protocol stack, such as IEEE 802.11n, has complex, time-varying physical layers that require many parameters for complete

characterisation, e.g. spatial multiplexing scheme, modulation type and mode, symbol rate, number of subcarriers, etc. Furthermore, modern modulation schemes treat the modulation and coding as a single entity (Burr, 2001, p. 208). These complexities make the task for the ASR system more difficult than it was, say, thirty years ago.

### 2.2.3 Transmitter

The highlighted block in Figure 5 is the *Transmitter* which may, for the purposes of this thesis, be regarded as perhaps the simplest of the processing blocks.

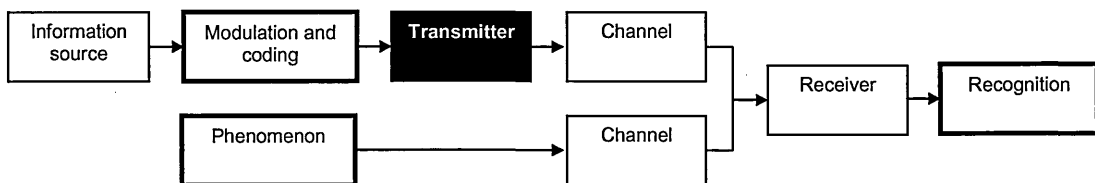


**Figure 5. The transmitter process is, from the perspective of signal recognition, the simplest part of the signal source.**

A reasonable model is to consider the functions of the transmitter to be some or all of the following:

- Conversion to radio frequency from the frequency band at which the modulation and coding have been performed (usually real or complex baseband);
- Filtering to suppress any unwanted frequencies;
- Power control;
- Radiation into the environment via one or more antennas;

- Anomalous transmitter characteristics such as overmodulation and non-linearities.

Where there are multiple antennas being used in combination (e.g. Multiple Input Multiple Output (MIMO) technologies) then we shall consider the processing required to be part of the modulation and coding rather than the transmitter.

#### 2.2.4 Phenomenon

The *Phenomenon* block is emphasised in Figure 6. It has been included in this processing model to highlight the fact that many of the signals received in a real-world situation are not intentionally transmitted and are not always well structured in that they cannot be decomposed into Information source, Modulation and coding followed by a Transmitter. Such signals include natural phenomena and electromagnetic radiation emitted unintentionally by man-made devices that were not designed to transmit.

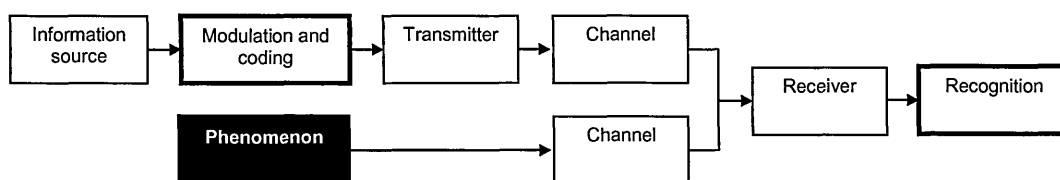


**Figure 6. The phenomenon process models unintentionally-transmitted signals, including natural phenomena and man-made noise.**

Ordinarily such phenomena are treated as part of the noise or interference added as part of the channel process, but the model used here treats them separately. When these signals are interfering with desired communications they can also become the subject of the recognition process. In this event the recognition process is not looking to identify the modulation and coding, rather it is seeking to identify the type of phenomenon.

A complete list of phenomena is not practical, but the following sections give indications of the types of signals that may be encountered and may, depending on the application, need to be recognised.

#### **2.2.4.1 Natural phenomena**

The major types of natural phenomena of concern to ASR systems are the electromagnetic emissions from lightning and the sun.

Lightning emissions (also known as 'sferics' or 'spherics') tend to be impulsive in nature, with several different physical mechanisms producing them (Uman, 1994)(Le Vine and Krider, 1977)(Thomas *et al*, 2001)(Shao and Jacobson, 2002). Lightning discharges are routinely monitored by large-scale monitoring systems (Fedoseev and Fedoseev, 2001) and many of the effects of lightning on electrical equipment and structures are well-understood (Rakov and Rachidi, 2009).

Solar radiation is noise-like with variations over time and location (Ward and Golley, 1991) and the expected levels are currently recorded in ITU-R P.372.

#### **2.2.4.2 Non-natural phenomena**

Non-natural phenomena include both interference and noise sources and are typically covered within the spectrum monitoring literature under the general title of Man-Made Noise (MMN), some examples of which are listed in Table 1, which is not an exhaustive list.

Phenomenon	Characteristics
Microwave oven	2.4 GHz band, short pulses with fast frequency modulation
Automotive ignition	Impulsive
Switches	Impulsive
Electronic devices	Harmonics of clock frequencies
Mains electricity	50 Hz and harmonics thereof
Neon lighting	Impulsive
Fluorescent lighting start up	Impulsive

**Table 1. Typical Man-Made Noise characteristics.**

The most comprehensive model of Man-Made Noise is the Middleton noise model (1973, 1975, 1976, 1978a, 1978b). This work uses a mathematical description of the underlying physical processes involved in noise generation to aggregate the total noise environment present at a particular location. Although attractive due to its description of a noise environment in terms of physically significant parameters (such as emitter density), the model is very complex and this limits its usefulness in practical applications

Middleton's model considers electromagnetic noise as comprised of two main components: White Gaussian Noise (WGN) and Impulsive Noise (IN). WGN levels for MMN are measured internationally and recorded in ITU-R P.372.

The IN component of MMN is further classified by Middleton as comprising that which could interfere with typical receiver systems in different ways, as listed in Table 2 (Wagstaff and Merricks, 2003, p. 12).

Class A	Interference is spectrally comparable to, or less than, the measurement bandwidth of the receiver.
Class B	Interference is broadband compared to the measurement bandwidth. Class B noise is typically made up of very short impulses that are very wideband and are frequently man-made in origin. The class includes impulses from automotive ignition circuits, thermostats, lighting, etc.
Class C	This is the sum of class A and class B interference.

**Table 2. Middleton's classes of impulsive noise.**

Many other papers have been published casting varying degrees of light on the analytical study of man-made noise, some addressing quite specific aspects of the analysis. Particularly relevant are Spaulding's paper on bandwidth scaling (Spaulding, 1962) and an investigation into frequency dependence of man-made noise in urban environments (Sheikh and Parsons, 1983).

Middleton's model is rather unwieldy for many purposes, so simpler statistical models are also in use (Wagstaff and Merricks, 2005). Examples of other models are by Parsons, (1992), Jeruchim *et al* (1992), Achatz *et al* (1998) and Shukla (2001).

**2.2.5 Channel**

Figure 7 highlights the *channel* block. The channel through which the signal propagates will adversely affect the signal in several ways. Typically the signal itself will be altered by the medium in which it is propagating. Also, noise will be

added to the signal and interference may be introduced. Generally, one can expect the signal to degrade more as the distance between the transmitter and the receiver is increased.

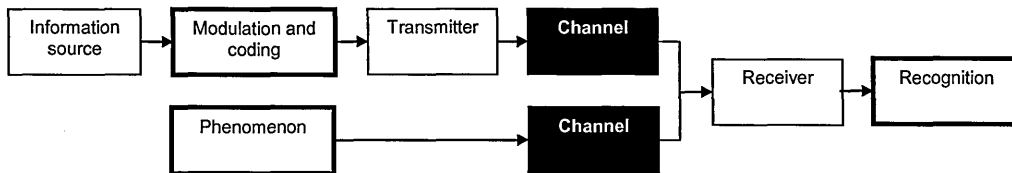


**Figure 7. The channel adversely affects the signal.**

This section describes some of the most important channel effects that are encountered. Section 2.2.5.1 introduces the concepts of radio propagation through the atmosphere. Section 2.2.5.2 considers multipath and section 2.2.5.3 looks at non-multipath effects. Fading models are discussed in section 2.2.5.4.

#### **2.2.5.1 Effects of propagation through the atmosphere**

As radio waves pass through the earth's atmosphere a number of effects are encountered. The first of these to comment on is the Radio Refractive Index (RRI), which is not constant, but varies with height (Doble, 1996, pp. 7-8), time and location (Winder and Carr, 2002, p.8). This is mainly because of the varying amount of water vapour, but atmospheric pressure and temperature also affect the RRI. This variation in RRI causes radio waves to bend and enables very long range communications at lower frequencies.

Propagation through the atmosphere also leads to attenuation and this can be simply modelled via the free-space transmission loss formula, which is an expression of the inverse square law for the propagation of electromagnetic radiation. The received power,  $P_r$ , is a function of the wavelength,  $\lambda$ , transmitted



power,  $P_t$ , distance between the transmitter and receiver,  $D$ , and the gains of the antennas at each of the link,  $G_t$  and  $G_r$ . It is given by the following equation, which assumes that there is no obstruction between the transmitter and receiver (Ziemer and Tranter, 1995, p. 766):

$$P_r = P_t G_t G_r \left( \frac{\lambda}{4\pi D} \right)^2 \quad (1)$$

Equation (1) is convenient for some applications but is often too simplistic, because it assumes lossless propagation in free space. Also the assumption of free-space propagation is only valid over short distances or when well above the earth's surface.

When a more accurate model of the propagation characteristics is required then one has to consider several factors. These include the centre frequency and bandwidth of the channel, diffraction over terrain, reflections, the relative speed of the transmitter and receiver, weather conditions, etc. The net effect of all of these at the receiver is a variation in the amount of attenuation. This variation is commonly referred to as fading when viewed from the receiver's perspective.

The different causes of fading are commonly grouped into two main types. These are multipath effects and non-multipath effects.

#### **2.2.5.2 Multipath Effects**

A key concept is that of multipath which is the effect seen when a signal is combined with one or more versions of itself reflected in some way (Figure 8).

Such reflections can be from obstacles reflection from nearby structures (Ranade, 1989) or caused by atmospheric refraction effects.

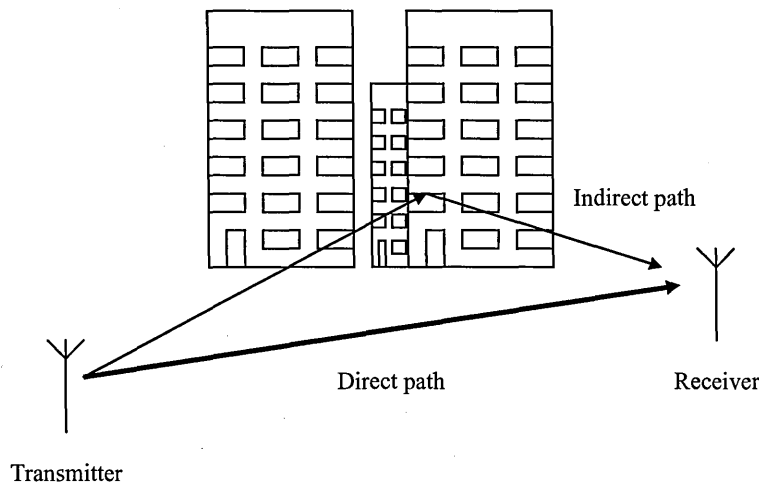


**Figure 8. Multipath is caused by reflections from nearby structures.**

When a signal is combined with a time-delayed copy of itself, the phase shift between them is important, because the two signals combine as a phasor sum. This combination can be constructive or destructive so the amplitude can be increased or decreased in multipath conditions, leading to a form of fading (see section 2.2.5.4). In addition to fading the time shift between multiple copies of a signal can lead to dispersion in time sufficient to cause Inter-Symbol Interference (ISI) (Burr, 2001, p. 243).

In a real world situation, there are usually numerous reflection paths and these will vary over time, so the effect on the signal changes over time (Hall *et al*, 1996, pp. 199-200). Pätzold (2002, p. 4) describes the effect of multipath on a digital impulse as the impulse dispersion, which can be modelled in the frequency domain as a transfer function representing the characteristics of the radio channel.

The channel in modern radio communication frequently contains many structures that generate multipath effects. The movement of these reflectors, transmitter or receiver will additionally apply Doppler shifts to the components arriving at the receiver. It is important to note that, if the transmitter or receiver is moving, then all the signal components will be affected by Doppler shift, not just the direct path (Figure 9).

Pätzold (2002, p. 5) describes the frequency dispersion of a channel, which depends mainly on the maximum Doppler shift component. The existence of frequency dispersion implies that the impulse dispersion is time varying. Pätzold goes on to state that mobile radio channels are linear, time-variant systems, which is an important concept for the basis on which such systems are modelled. That they are linear systems means they obey the principles of superposition (Ifeachor and Jervis, 2002, pp. 173), which enables the signal components to be summed using phasor representation. However, as the impulse response of such channels is time varying, it is not possible to apply the superposition integral (Ziemer and Tranter, 1995, pp. 66-68) approach to obtaining the output in response to an arbitrary input and numerical methods of performance prediction become necessary.

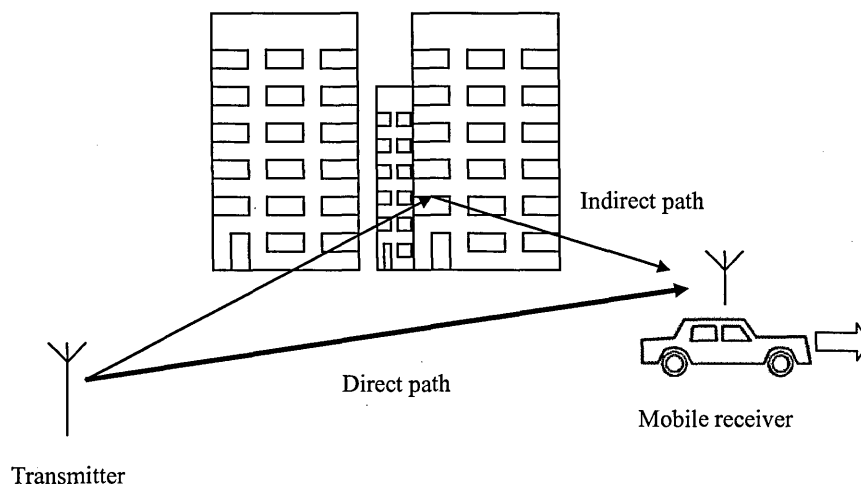


**Figure 9. Doppler shift affects all paths between transmitter and receiver and is caused by the movement of the transmitter or receiver.**

### 2.2.5.3 Non-Multipath Effects

The non-multipath effects generally affect the signal over a slower time scale than the multipath effects and result in a mean-depression of the received signal strength (Doble, 1996, p. 22).

There is a simplified view of long-distance propagation which assumes that a transmitted ray will, because of the normal variation of the RRI with height, follow a path that has a radius of curvature that is approximately  $4/3$  times that of the earth. The figure of  $4/3$  is a median value normally used for communication design purposes, but the true value at any particular location will differ from this (Samson, 1975). The nominal curvature of the ray will be affected by any changes in the RRI profile. This includes refraction through the atmosphere and weather.

Other effects include diffraction around terrain and, in built-up areas, attenuation caused by obscuration by walls and other obstructions (Figure 10).

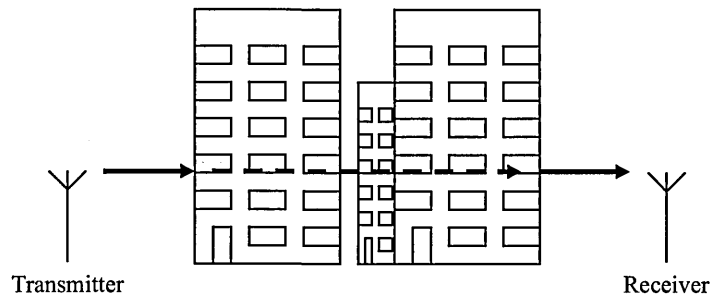


**Figure 10. In built-up areas obscuration can be a significant factor.**

#### 2.2.5.4 Fading

The free-space model given in equation (1) is frequently not adequate to describe the attenuation and phase modification that a signal undergoes as it passes from the transmitter to the receiver. For a more complete model one has to consider other factors affecting the radio system in addition to the free space loss including the impact of multipath effects and non-multipath effects.

As the impact of these various channel effects is to cause the received signal strength to vary, the term fading is applied. Fading is typically classified as slow fading or fast fading (Hall *et al*, 1996, pp. 153-155). These terms express how the signal strength varies:

- **Slow fading** (also known as frequency-flat, or large-scale fading) is the slow variation in signal attenuation due to non-multipath effects (Tse and Viswanath, 2005, p. 10). The signal is assumed to be relatively narrow band and so the attenuation affects the whole signal equally. This effect is common

in mobile communications when the transmitter and receiver are passing through built-up areas. Very much slower fading results from variations in the RRI (Doble, 1996, p. 17) associated with changes of the water content in the atmosphere.

- **Fast fading** (also known as frequency-selective or small-scale fading) is a reduction in the signal strength in part of its spectrum due to multipath effects (Tse and Viswanath, 2005, p.10). It results in a variation in signal strength that is faster than that observed with frequency-flat fading. With a wideband signal there are many frequency components, so there is likely to be phase cancellation within a portion of the signal's bandwidth. If the distance between the transmitter and receiver is changing then the Doppler shift will cause the affected frequency band(s) within the signal to move.

The difference between slow and fast fading can be described in terms of the coherence time of the channel. In slow fading, the channel, the attenuation and phase shift of the channel are assumed to be constant during each symbol (Ziemer and Tranter, 1995, p. 637) which is not the case for fast fading.

Fading is normally modelled by multiplying the transmitted signal with a stochastic process (Pätzold, 2002, p. 33). In the case of slow fading a lognormal process is commonly used. Fast fading channels are modelled using either a Rayleigh or Rician process. The Rician process is applicable when the direct path from the transmitter can be seen at the receiver together with reflected paths, whereas the Rayleigh process is used when the direct path cannot be seen and

only reflected paths are received. The Rayleigh process is, therefore, a limiting case of the Rician process.

### 2.2.6 Receiver

The *Receiver* is the penultimate processing element in Figure 11. Modern radio receivers are complicated devices, often supporting multiple modes of operation and often configurable in real-time.

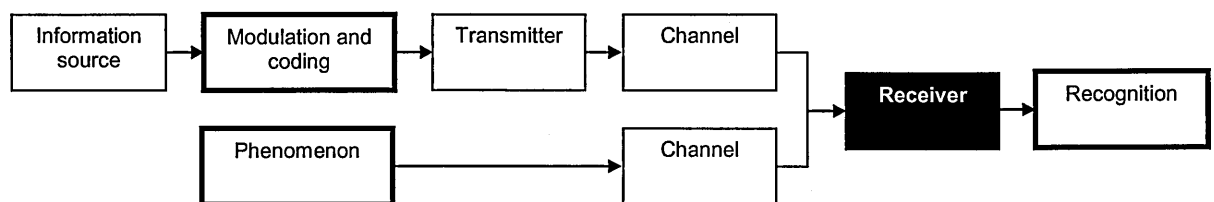


**Figure 11. The receiver is often the most complex part of a communications system.**

The main functions of the receiver, from the point of view of signal recognition, are:

- Capture of the signal via one or more antennas;
- Conversion from radio frequency to real or complex baseband;
- Gain control, which can be adaptive;
- Real-time demodulation of the signal to recover the original information content.

Whilst the receiver provides the demodulated output, it has to also provide access to the real or complex baseband signal for most signal recognition schemes to work. For the purposes of signal recognition design, it is a convenient assumption that the receiver is specified with sufficient performance that it does not significantly impair the signal further. For this to be the case the receiver

bandwidth must exceed that of the signal of interest and the dynamic range must be sufficient to allow the signal to be captured without incurring any non-linear effects due to saturation. The noise figure of the receiver must also be low enough so that the signal is not adversely affected by noise due to the receiver itself.

Achieving satisfactory performance in a dynamic spectrum may be helped by use of adaptive narrowing of the receiver bandwidth to match the signals of interest. This subject is considered later in this thesis in terms of the segmentation process for ASR.

### 2.2.7 Recognition

The *Recognition* process in Figure 12 is the main focus of this thesis and is the last block in the processing chain.

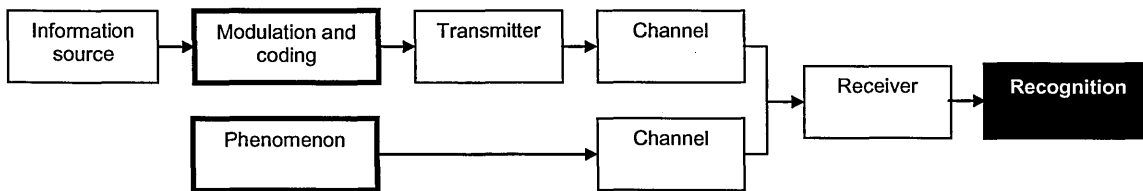


**Figure 12. The recognition process attempts to determine the characteristics of the received signal.**

In order to perform recognition automatically, it is frequently assumed that the Modulation and Coding process in Figure 12 exists and has characteristics that can be estimated by the Recognition process. It is important to note that the Information Source is not of particular interest and the Recognition process is



normally only interested in determining the type of signal being used to carry the information.

Not all signals intercepted by a receiver will have clearly identifiable modulation and coding processes. Natural processes (e.g. lightning), in particular, carry no information and do not have any deliberate modulation and coding process. There may still, however be a need to recognise such phenomena. In this case the Recognition process has to estimate the characteristics of the Phenomenon process in Figure 12.

## **2.3 Problems in signal recognition**

This section describes some of the major problems encountered in ASR. In particular these are:

- Range of bandwidths and time scales;
- New signal types;
- Noise;
- Channel effects;
- Interference.

In addition to these problems there will be time and processing constraints that depend a great deal on the application. Such limitations make it harder to deal with the problems as they limit the complexity of algorithmic solutions that can be used.

### 2.3.1 Range of bandwidths and time scales

As wider bandwidth signals are used, either to increase the information bandwidth, or to decrease the probability of intercept, the chance of a wideband receiver encountering a relatively narrow band signal increases. Also, the chance of intercepting more than one signal increases and this is further increased in the shared spectrum bands where different modulation types have to co-exist.

A modern signal recognition system therefore has to contend with detecting a range of signal bandwidths and has to look for features over a correspondingly wide range of time scales. This can place a high load on the available processing resources.

By way of an example, modern spectrum analysers can provide a wide range of resolution bandwidths to match the bandwidths of the signals of interest. A typical example is the Rohde & Schwarz FSQ26 which has six resolution bandwidths ranging from 300 kHz to 50 MHz. Furthermore, that particular product includes a resampling capability that allows the user to specify any integer sampling rate from 20 kSamples/s up to 50 MSamples/s. The samples are in I/Q form. The term I/Q data is used throughout this thesis as a shorthand for the analytic signal or complex baseband representation. Any band-limited signal can be represented as the product of a sinusoidal complex exponential carrier and a complex baseband signal (Burr, 2001, pp. 16-19).

The specification of such instruments has been driven, to a very large extent, by the need to test communications equipment. Thus the wide range of measurement

bandwidths available reflects the range of signal bandwidths that are encountered in development and test situations. Modern commercial products, such as the "WiFi" equipment conforming to IEEE 802.11 Wireless Local Area Network standards, have signal bandwidths over 20 MHz. At the same time there are still many narrow band signals, often based on 12.5 kHz bandwidths.

It is not just the signal bandwidth that varies widely, however; it is also the time scales over which features of communications protocols are to be seen. As an example, consider the time structures of the Terrestrial Trunked Radio (TETRA) standard shown in the table below (Stavroulakis, 2007, p. 192). This protocol exhibits structures at five main levels over six orders of magnitude. These levels of complexity are seen in many other modern protocols.

Hyperframe duration = 61.2s	Hyperframe rate = 0.0163 Hz
Multiframe duration = 1.02 s	Multiframe rate = 0.98 Hz
Frame duration = 56.67 ms	Frame rate = 17.65 Hz
Slot duration = 14.17 ms	Slot rate = 70.59 Hz
Symbol duration = 55.56 $\mu$ s	Symbol rate = 18 kHz

**Table 3. Periodicities in the TETRA protocol.**

The equipment exists to allow very accurate measurements to be made of any one of the parameters and this is indeed done as part of development and test by the product manufacturers. Such measurements are, in a spectrum monitoring application, affected by many factors including channel effects and component ageing. The accuracy achievable in practice outside the laboratory can therefore often be limited by factors outside the control of the receiver designer.

A practical ASR system should be able to recognise any signal type in a robust manner. When considering the sample rate of the receiver and taking into account the issues of large time scales, this leads to a problem of representation.

In order to bound the problem further we can consider the timescale parameters of typical modulation schemes. Figure 13 is a histogram of the lengths of time domain features compiled from modulations in use today (see Appendix E for source data). It clearly shows the spread of timescales that occur in real world signals.

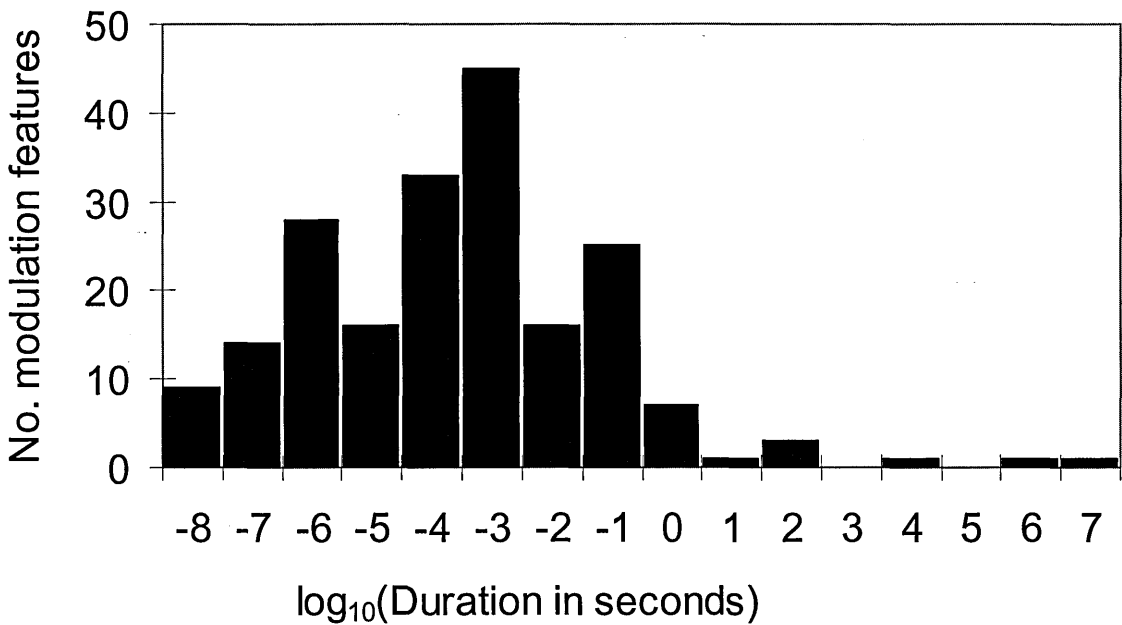


**Figure 13. Histogram of time feature lengths in common modulations.**

Returning to the capabilities of the Rohde & Schwarz FSQ26 spectrum analyser mentioned above, the shortest feature in time to be analysed, dictated by the 50 MSamples/s rate will be in the order of 20 ns. Using a single I/Q buffer of 512 kSamples and the slowest sample rate of 20 kSamples/s leads to an upper limit on

the feature time scale of 26.2 s. This receiver can measure nearly all the time scales of interest, but would not be able to measure the longest intervals.

Processing such a wide range of parameters within a single algorithm leads to excessive demands on memory and processor resources. As an example consider the calculation of a Spectral Correlation Function (SCF) for ten orders of magnitude. This would imply a matrix with  $10^{20}$  elements, which would be impractical to create, manipulate and store with current computing technology (Wagstaff, 2008).

There are three main approaches one can follow to avoid this problem:

- a) Use a set of sample rate bands, which is a pragmatic solution. It does however mean that the ASR system has to be separately trained for all possible modulations in all the bands. The inherent weakness of this approach can be seen by considering how a wide bandwidth signal might appear when viewed in a narrow band width analysis band. One such example is given by Wagstaff and Merricks (2006) in which an Ultra Wide Band (UWB) source was analysed with relatively narrow bandwidths and the suppression of significant features was clearly demonstrated. In general it will be difficult to train an ASR system to recognise signals when the receiver bandwidth is not well matched to the signal bandwidth as features will not be clearly visible;
- b) Identify the signal bandwidth and reduce the capture bandwidth down to that of the signal. This is the approach adopted by Hachemani *et al* (2007), who use an iterative reduction of the captured bandwidth down to the

bandwidth of the signal of interest. This approach will work well when the signal bandwidth can be measured easily and when there are no complications due to the presence of interferers;

- c) Use a representation that is non-linear so that the time resolution varies at different time scales. An algorithm that handles such a representation would be attractive as it would easily scale to different bandwidths.

The first two approaches assume that the received signal can be well-matched to the receiver in all cases. It is further assumed that some sort of segmentation process will ensure that this is the case. Segmentation is introduced here as a conceptual processing stage in which the centre frequency and bandwidth of the receiver and the time duration of the signal capture are arranged such that just one signal type enters the rest of the identification chain. This is a non-trivial problem, especially where interference is unavoidable. If one has no control over the interference (the usual case) then the design of signal separation algorithms appears to be a formidable obstacle.

Given that perfect segmentation may not be achievable in all cases and that devising suitable algorithms is non-trivial, it is worth considering alternative representations that are less reliant on perfect signal isolation by the segmentation process. There is a motivation, therefore, for trying to find a non-linear time representation that solves some of the problems encountered with linear representations.

One approach to dealing with the problem has been proposed by the author by means of a logarithmic form of the cyclic frequency domain profile as part of this Ph.D. work (Wagstaff, 2008). This technique was devised to allow narrow band signals to be analysed for cyclostationary features without unduly increasing the processing required. The alternative would be to employ a segmentation function and resample narrow band signals prior to cyclostationary processing. The advantage of the proposed technique is that it does not require the signal to be centred in frequency as part of segmentation. As the cyclostationary processing removes much of the additive noise, the proposed technique offers the potential for improving the feature detection performance at low signal to noise ratios. More detail on this specific algorithm is given in section 4.2.

### **2.3.2 New signal types**

The world of radio communications has been changing rapidly over the last few decades. New signal types continually appear and this trend does not seem to be abating.

Table 4 below lists various radio system types ordered by the decade in which they were first introduced. It is not an exhaustive list, but does serve to illustrate the rate at which new systems have been developed. It is clear that there has been a rapid development of new systems that started in the 1980s and has continued ever since. What is not clear, however, is whether this trend will continue and for how long.

What the list below does not show, however, is that many of the systems are now obsolete, so that there are not as many systems deployed at any one time as it would appear. It also does not show the many proprietary radio systems that have been deployed and continue to be developed. It is highly likely that a large number of systems have been developed and used but not well advertised, either for commercial or defence security reasons.

The main problem for recognition systems is that they have to be updated as new systems appear and old ones become obsolete. There has to be a mechanism for propagating the knowledge about new technologies to devices already in use. It is natural to think in terms of upgrading via the Internet in the same way that software such as anti-virus programs and operating systems are kept current via periodic updates.

On the reasonable assumption that new signal types will continue to appear for some years to come and that no one system can ever be completely up-to-date, then there is always some probability that a signal will be seen that must be classified as unknown. This particular facet of the signal recognition problem is not well addressed in the literature. The processing architecture should incorporate the possibility of encountering an unknown signal type, for not to do so would inevitably lead to misclassification.



Decade	Systems introduced		
1930 - 39	AM broadcast	FM broadcast	Walkie-Talkie
1940 - 49	Citizens' Band	MTS	NTSC
1950 - 59	NTSC RS-170a		
1960 - 69	ARP	IMTS	OLT
	PAL	SECAM	
1970 - 79	Golay pager	MTD	NMT
1980 - 89	AMTS	AMPS	DAB
	DECT	GSM	Jaguar V
	Mobitex	NICAM	PAS
	POCSAG	PRC-117	SINGGARS
1990 - 99	APOC	CDPD	DataTAC
	DVB-S	DVB-T	ERMES
	Flex	GPRS	iDEN
	inFlexion	IS-54	IS-95
	IS-136	pACT	PCS
	PDC	PHS	ReFLEX
	TETRA	WiFi 802.11a/b	Z-Wave
2000 - 2009	6loWPAN	ATSC	Bluetooth
	DVB-H	DVB-SH	DVB-T2
	EDGE	E-UTRA	FOMA
	GAN (UMA)	HSPA+	iBurst
	Insteon	LTE	TD-CDMA
	Wibree	WiBro	WiDEN
	WiFi 802.11g/n	WiMAX	Zigbee

**Table 4. Brief timeline of radio system types (N.B. Not an exhaustive list)**

### 2.3.3 Noise

As discussed in section 2.2.4, there are many phenomena that introduce noise into the received signal, including lightning, solar radiation and man-made noise. As the received signal strength drops compared to the background noise level the probability of misrecognition increases. Researchers understand this and are always looking for improvements to recognition algorithms that improve the performance (i.e. reduce the number of misrecognitions) at low Signal to Noise Ratio (SNR).

### 2.3.4 Channel effects

As well as additive noise, the received signal will also suffer the effects of the channel through which it passes (section 2.2.5). When a receiver knows what signal to expect it can perform equalisation and matched filtering to counter the effects of the channel. A recognition system may not have such *a priori* knowledge and so may have to interpret a received signal's characteristics without, in the first instance, being able to compensate for channel impairments. Alternatively, blind estimation of the channel characteristics can be carried out to perform equalisation within the ASR processing.

Lay and Polydoros (1995) evaluated an algorithm called Per-Survivor Processing for blind channel estimation to handle the ISI due to a band-limited channel. The algorithm was successfully combined with two modulation classification tests. Boutte and Santhanam (2008) also considered the effects of ISI and showed that it skewed feature statistics and increased the effective noise power seen by the recognition system.

### **2.3.5 Interference**

When two or more signals overlap in time and/or frequency then they are interfering with each other. The recognition system has to deal with this and still provide accurate recognition wherever possible. It is the nature of many real-world problems that automatic recognition is most needed when interference conditions exist, as human operators find it difficult to separate the signals by eye, but need assistance in resolving the interference problem.

Interference in some bands is now rife and should be considered as unavoidable in the Licence-Exempt bands. A study for Ofcom by the author showed clearly that interference in the 2.4 GHz ISM band is widespread and worsens dramatically in urban areas (Wagstaff, 2009).

Dealing with the effects of interference on ASR systems is an emerging area for research. Zaerin *et al* (2009) proposed a feature based on cumulants that would be more robust in the presence of interference between different modulation types.

Currently there is no generally accepted approach to handling interference in ASR systems. This thesis deals with some of the issues concerned with evolving a suitable approach.

## **2.4 Review of signal recognition methods**

The last few decades have seen considerable research into ASR. By identifying the modulation types of communications signals it is possible to provide much of

the functionality needed by field staff when trying to interpret the outputs of radio receivers used in signal interception.

This section reviews some of the methods that have been applied to the ASR task. The emphasis is on recognising the modulation characteristics of communication signals, as that is where the bulk of the research has concentrated. Other signals, such as impulsive noise and other interferers, have not been addressed at length in the published literature.

When discussing ASR it is difficult to be exhaustive as it is such a wide ranging discipline. ASR as a research discipline can be traced back to about 1980 and particularly the work on cyclostationarity by Gardner (1986a). This coincided with the introduction of the first modern digital communications systems using modulations such as FSK and Pulse Amplitude Modulation (PAM).

Work has progressed rapidly with an increasing number of journal articles and conference papers. Figure 14 shows a graph of the number of articles and papers published each year, based on a survey by the author of 300 publications in the IEEE Xplore and Science Direct databases. This rise has coincided with development of software defined radio and cognitive radio technologies and does not currently shown any sign of abating.

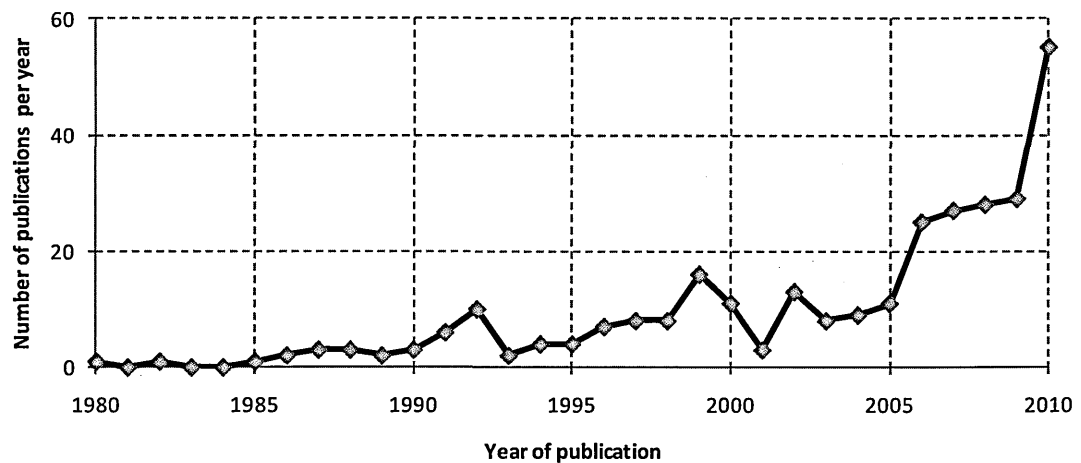


**Figure 14. The number of publications on automatic signal recognition is increasing.**

There are a great many types of algorithm in the literature, but it is possible to group them broadly by type. Section 4.3 proposes a detailed taxonomy for these algorithms, but at this stage it is sufficient to group them as follows:

- Segmentation methods (section 2.4.1);
- Transformation methods (section 2.4.2);
- Feature extraction methods (section 2.4.3);
- Decision methods (section 2.4.4).

This discussion concentrates on feature-based methods, as this is by far the most researched class of methods. Recognition can, in principle at least, be accomplished by other approaches. In a limited environment, for example, it is possible to apply all known demodulation and decoding algorithms and inspect the outputs to identify the communication system type. Another example is that of preparing a library of all possible signals against which the received signal samples can be compared. Such alternative approaches are conceptually possible but are not discussed in the research literature as they are seen as generally

impractical. The feature-based methods are widely applicable and practical to implement in real ASR systems.

#### **2.4.1 Segmentation methods**

In manually operated systems, the segmentation can be performed wholly by the user or can be semi-automated. As a minimum, the segmentation must provide a series of waveform samples, either by buffering the input signal or continuously feeding samples to other activities. It may, additionally, apply filtering in order to restrict the bandwidth of the signal to be analysed and resampling in order to match the sample rate to the signal bandwidth.

There are three problems to be solved by any segmentation system:

1. What are the constituent signals that need to be separated?
2. What algorithm should be used to separate them?
3. Has the segmentation been successful?

To date the author has not found any research results that deal with all of these questions, but elements are there, particularly with regard to the second question.

In automated systems, segmentation can be performed in the time domain, frequency domain or both. For example, analysis of a power spectral density plot could allow the segmentation process to select a signal based on its centre frequency and bandwidth.

The major functional groups within the segmentation processing are:

1. Time domain segmentation to isolate one or more bursts of signal corresponding to a single emitter;
2. Frequency domain segmentation (filtering) to remove any artefacts of the analogue receiver processing and to isolate a single emitter for analysis;
3. Code domain segmentation is appropriate for those signals that are coded;
4. Resampling to match the sample rate to the bandwidth of the received signal or to align the sample rate with a multiple of the symbol rate of the received signal. Resampling is a well-documented application of multirate digital signal processing (Ifeachor and Jervis, 2002, pp. 579-640);
5. Removing any centre frequency offset caused by mistuning of the receiver. This process is often referred to as 'despinning', because it removes the rotation over time of the I/Q constellation which is caused by the centre frequency offset.

Automatic segmentation could depend on information from the other activities. To do this may require more advanced techniques than time/frequency segmentation.

More complex methods, such as FREquency Shift (FRESH) filtering may be necessary when multiple signals are overlapped in time and/or frequency. FRESH filtering requires an adaptive process and can be used for single receiver or multiple receiver systems.

If more than one receiver is available then there are techniques (such as Independent Component Analysis and Principal Component Analysis) available to separate the signal(s) of interest. These are not expanded on here.

### **Time domain segmentation**

Splitting received signals into time domain bursts can be performed simply by thresholding the instantaneous amplitude. More complex signal detection techniques could be used for this task, such as cross-correlation (Ifeachor and Jervis, 2002, pp. 242-273), the Wigner-Ville distribution (Pace, 2004, pp. 222-235) and subspace methods (Wagstaff, 2007, Appendix A, pp.14-32). This is a very diverse and extensive area with many techniques optimised for detecting specific types of signal. This subject area is not expanded further here.

### **Frequency domain segmentation**

When it is clear that the signal of interest can be separated from others in the frequency domain, then it is a straightforward process to produce a filter that can isolate the signal of interest. The design of filters is covered extensively in the signal processing literature (Lynn, 1984, pp. 173-216), (Ifeachor and Jervis, 2002, pp. 317-341) and so is not addressed further here.

### **FRESH filtering**

Time domain segmentation and frequency domain filtering are useful when the signal of interest is not overlapped by another signal in time or frequency respectively. When the signals are overlapped then it becomes necessary to look for other ways of performing the segmentation.



One such approach is FREquency SHift (FRESH) filtering, which was introduced by Gardner as part of his work on cyclostationarity (Gardner, 1993). The FRESH filter is one that exploits the cyclostationarity characteristics of a signal to remove unwanted interference and noise (Adlard, 2000) and does so by varying the filter definition in a periodic manner.

The specific form of FRESH filtering introduced by Gardner for complex signals is called Linear-Conjugate-Linear (LCL) filtering, the general form of which is to apply time-invariant filters to a number of frequency shifted versions of the input signal and then combine the outputs of the filters to arrive at the estimate of the signal of interest.

The form of the filter obtained for an estimate of a desired signal,  $\hat{d}(t)$ , with an input signal,  $x(t)$ , is:

$$\hat{d}(t) = \sum_{m=1}^M a_m(t) \otimes x(t) e^{i2\pi\alpha_m t} + \sum_{n=1}^N b_n(t) \otimes x(t) e^{i2\pi\beta_n t} \quad (2)$$

This implementation is illustrated in Figure 15 which shows two sets of time-invariant filters. The upper set of filters operates on the non-conjugated, frequency-shifted version of the input signal. The lower set of filters operates on the conjugated, frequency-shifted version. The outputs of all the filters are then summed to create the estimate of the signal of interest.

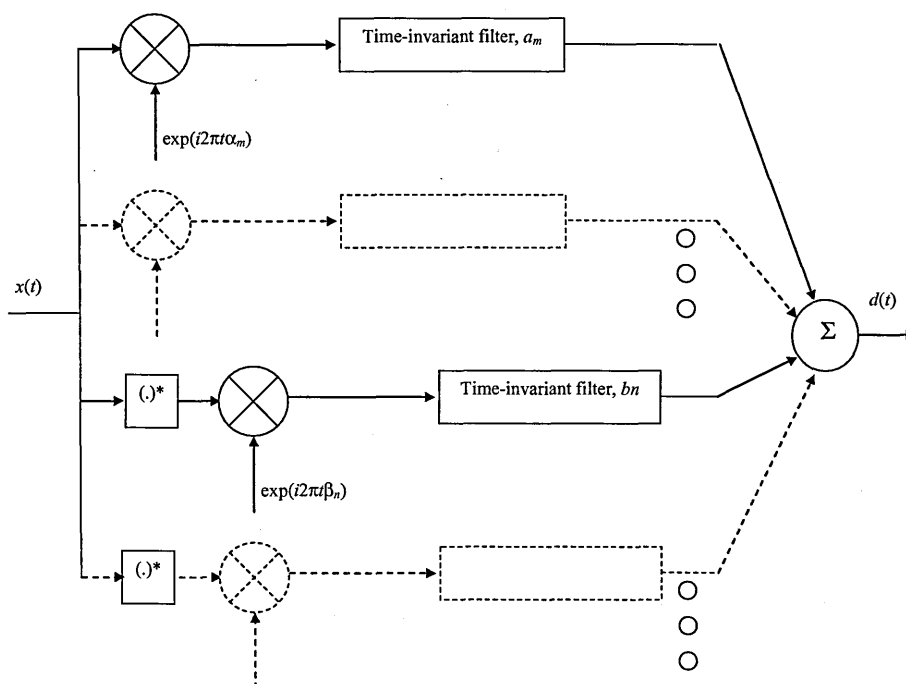


**Figure 15. FRESH filter implementation as a bank of time-invariant filters.**

The numbers of filters,  $M$  and  $N$ , depend on the number of cyclic frequencies,  $\alpha_m$  and  $\beta_n$ , present in the signal of interest. To arrive at the filters themselves,  $a_m(t)$  and  $b_m(t)$ , it is necessary to use an optimisation procedure, which is closely related to Wiener filtering (Lynn, 1984, pp. 224-228). Gardner (1993) achieves this by minimising the time-averaged squared error between the estimate of the desired signal of interest and the actual signal of interest. The adaptation can be carried out using methods such as the least mean squares algorithm or recursive least squares algorithm (Ifeachor and Jervis, 2002, pp.654-665). The resulting process is called cyclic Wiener filtering and is equivalent to processing the signal with a series of time-variant filters whose characteristics vary periodically with periods based on the cyclic frequencies of the signal of interest.

The segmentation methods described here are relatively simple in the sense that they do not include sophisticated adaptation processes to handle rapidly changing,

interfering radio environments. This is an area that will need more research to handle the challenges of the current and future radio spectrum.

**2.4.2 Transformation methods**

It is common for received signal data to be transformed into one or more different representations in an ASR system before features are extracted that can be used for identification. This is because many features are not readily identifiable from the raw time domain data. A common example is frequency, which can be calculated from time domain data but is more easily extracted once converted into a representation such as the power spectral density estimate.

It is possible to group the many techniques available into either demodulation methods or periodicity transform methods. Figure 16 shows this taxonomy of the types of transformation processing.

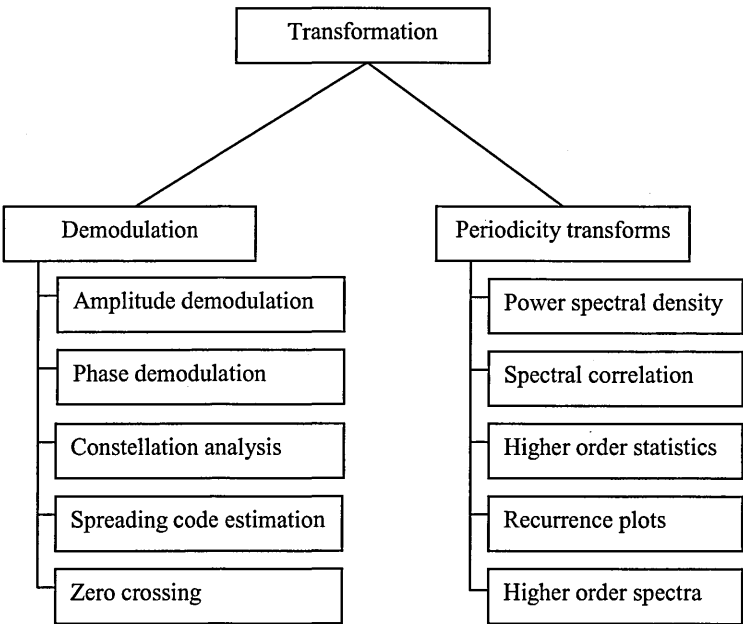


**Figure 16. Taxonomy of Transformation methods.**

There are very many ways of looking for periodicity and they tend to be generic, so such techniques can be applied in a wide variety of circumstances. Listed in Figure 16 are power spectral density, spectral correlation, higher order statistics, recurrence plots and higher order spectra.

More specialised than periodicity detectors are the demodulation methods, such as the amplitude, frequency and phase demodulators, constellation analysis, spreading code estimation and zero crossing methods.

#### **2.4.2.1 Demodulation**

Demodulation methods are the 'brute force' approach to ASR. Working on the assumption that an information source has been deliberately modulated before transmission, one can attempt to perform the demodulation and recover the original information. When the spectrum has only a small number of simple modulations present then it is a viable approach. As the spectrum becomes more complex it becomes more difficult to implement. Without *a priori* knowledge of how an information source has been modulated, one is forced to resort to brute force search to find the correct demodulator. This approach also assumes that one can recognise that demodulation has been successful, which may not always be the case.

Even without knowledge of the modulation scheme it can be useful to attempt a demodulation. Some of the simple demodulators, such as amplitude, phase and frequency demodulation (described in the following sections), reveal useful information about many signal types in a generic way. It is therefore practical to

use these techniques to reduce the search space. Demodulators used in this way are transforming the original signal into a form in which feature extraction is more effective.

### **Amplitude demodulation**

A signal can have intentional amplitude modulation, in which case amplitude demodulation will reveal the information content. In ASR the information content is not of particular interest, rather one wants to find features of the signal that can lead to identification.

In ASR amplitude demodulation can reveal the start and end of signal bursts and also allow the detection layer to examine how flat the signal is in the time domain. Signals with first order cyclostationarity, in particular, will exhibit periodicity in their amplitude so obtaining their amplitude envelopes will allow the periodicity to be measured.

Amplitude demodulation is a straightforward operation, especially in modern receivers that output signals directly in their complex (I/Q) representation. Given a complex, baseband, signal sample,  $x(i)$ , its instantaneous amplitude,  $a(i)$ , is given by:

$$a(i) = |x(i)| \quad (3)$$

It is also convenient to define an average of this parameter. Azzouz and Nandi (1996, p. 46) defined the normalised, centred, instantaneous amplitude as:

$$a_{cn}(i) = \frac{a(i)}{m_a} \quad (4)$$

where  $m_a$  is the average of  $a$  over an analysis segment of length,  $N_s$ .

$$m_a = \frac{1}{N_s} \sum_{i=1}^{N_s} a(i) \quad (5)$$

### **Phase demodulation**

Phase demodulation is particularly germane to those signal types in which some, or all, of the information is encoded in the phase domain.

As with amplitude demodulation, phase demodulation is relatively straightforward if the received signal is in complex baseband representation. The instantaneous phase,  $\phi_n$ , of a signal sample,  $x_n$ , is given by:

$$\phi_n = \tan^{-1} \left( \frac{\text{Re}(x_n)}{\text{Im}(x_n)} \right) \quad (6)$$

It is normally assumed that the arctangent operation produces a wrapped phase variable,  $\phi_w$ .

### **Frequency demodulation**

Instantaneous frequency,  $\omega(t)$ , is defined as the differential of phase with respect to time (Cohen, 1993), i.e.:

$$\omega(t) = \frac{d}{dt} \phi_{uw}(t) \quad (7)$$

where  $\phi_{uw}$  is the unwrapped instantaneous phase.

For modulations that encode information in the frequency domain, i.e. FM and FSK, the demodulation process is an estimation of the instantaneous frequency.

### **Constellation analysis**

Constellation analysis is an important subclass of signal recognition methods. This section looks at various types of constellation analysis used by different researchers. It will be seen that different representations have been investigated with advantages being claimed for each type of representation.

Digital transmission techniques are now commonplace and many techniques have been developed to classify the various modulation types in terms of their constellation type and size. Such algorithms will typically facilitate the recognition of a number of constellation types such as BPSK, QPSK and QAM. As an example, the algorithms considered by Edinger *et al* (2007) sought to classify 4-QAM, 16-QAM and 64-QAM.

Constellation analysis algorithms usually assume that symbol timing has already been achieved, so that an estimate of the constellation is already available. A cyclostationary technique can be used to extract the periodicity corresponding to the symbol rate. Synchronising to the symbol rate, removing the centre frequency offset and aligning the sample time to the signal phase produces a Coherent Synchronous Environment (CSE) (Donoho and Huo, 1997, p.133). Achieving a CSE allows a constellation diagram to be drawn, which, in the absence of noise and/or interference, would clearly show the structure of the modulation. Equally,

failure to achieve a perfect CSE is highly likely to adversely impact the performance of an ASR technique that depends on that assumption.

There is a wide variety of algorithms used for constellation analysis. These can be broadly grouped by the different representations used:

- Constellation diagram representation;
- Radial probability density representation;
- Radon transform representation;
- Power moment matrix representation;
- Hellinger distance representation.

Each of these representations assumes that a constellation diagram representation exists, but transformations are applied to improve the analysis in some way (e.g. increasing robustness, decreasing processing time).

### ***Constellation Diagram Representation***

Digital modulations, such as BPSK and QPSK can be conveniently represented for many purposes via a constellation diagram. This is a plot of the complex part of the I/Q signal versus the real part (Burr, 2001, p.19). If it is known that a signal can be compactly represented in this way, then analysis of the constellation diagram can reveal information about the modulation type.

The constellation diagram conveniently removes the information in the signal by integrating the amplitudes and phases at each of the symbol periods over multiple symbols. Hence, if one is interested purely in determining the type of modulation being used, then the constellation diagram is a natural choice of representation.



Analysis methods using this representation tend to be based on either decision-theory or clustering.

A two-dimensional histogram of samples on the I/Q plane can be treated as a joint probability density function (PDF). With a model of the PDFs of typical modulation types, the Bayesian detector methods can be used to determine when a modulation is present. This is the basis of a large family of techniques that includes the following algorithms, all of which can be considered statistically optimal in some sense:

- quasi Log-Likelihood Ratio (qLLR) (Kim and Polydoros, 1988);
- Sequential Probability Ratio Test (SPRT) (Lin and Kuo, 1996);
- Average Likelihood Ratio Test (ALRT) (Lay and Polydoros, 1995);
- Generalised Likelihood Ratio Test (GLRT) (Lay and Polydoros, 1995);
- Hybrid Likelihood Ratio Test (HLRT) (Tadaion *et al*, 2005);
- Differential processing (Shi and Karasawa, 2008).

The identification of groups of samples on the I/Q plane can be thought of as a clustering problem. Each point of a noisy constellation diagram has a degree of membership to each cluster. In this view the clusters are the areas on the constellation diagram corresponding to each of the main constellation vertices. So, for example, a QPSK signal would have four vertices on the constellation diagram, which, after WGN has been added, become four clusters. As the SNR decreases the clusters grow larger and start to merge.

Mobasser (1999) treated the constellation diagram as the result of a binomial probability distribution contaminated by WGN and then defined a fuzzy-c means classifier to group the points. That algorithm then used a Maximum Likelihood (ML) detector following the clustering process.

The constellation diagram representation is also affected by ISI due to multipath or band-limited channels. Such effects are more easily visualised in terms of the eye diagram (Mathworks, 2011) rather than the constellation diagram. If the channel generates ISI as well as noise, then ASR is at a disadvantage compared to communications receivers, because, without prior knowledge of the modulation type or blind channel estimation, it is not possible to use an equalisation filter (Ziemer and Tranter, 1995, p. 503) to remove the ISI effects.

### ***Radial probability density representation***

Wood *et al* (1990) sought to remove dependency on knowledge of the carrier frequency by looking only at the distance of each sample from the origin of the I/Q plane. This approach leads to a radial PDF which can be compared against the PDFs of candidate modulation types.

A similar approach was used by Soliman and Hsue (1992), who generalised the method by considering moments up to the eighth order. They concluded that using higher order moments improved the performance of such schemes, but that there is an optimum order beyond which performance will start to degrade.

### *Radon transform representation*

The Radon transform (van Ginkel et al, 2004) is a mathematical technique typically applied as a method for searching for lines in digital images. The transform converts a line in an image into a peak at a single point on a two-dimensional histogram. Detecting a peak in the Radon transform output is therefore equivalent to, but simpler than, looking for a line in the image.

Whilst constellations are not made up of lines, they are typically composed of a number of points arranged in a regular grid pattern. The Radon transform treats the grid pattern as a series of parallel and orthogonal lines, then represents those lines in terms of their angles and distances from the origin of the I/Q plane. There is a simplification here, as the lines are parallel and are therefore at one of two orthogonal angles. The Radon transform, therefore, projects the constellation from I/Q space into a simpler Cartesian plane.

Wood *et al* (1988) applied the Radon transform to the task of constellation analysis. This initial analysis showed the technique to be robust for a range of QAM constellations in the presence of WGN, incomplete equalisation and carrier removal.

Wood *et al* (1990) then compared this method to a method based on the radial probability density function. They concluded that the Radon transform method is the more effective method at low SNRs when the carrier frequency is well known. This caveat is important, as the Radon transform method depends on detecting

points in the I/Q plane. Any error in the carrier frequency causes the constellation to rotate and severely limits the effectiveness of any method that depends on finding the individual points.

Wood and Treichler (1994) revisited the Radon transform method with a view to improving its performance in the presence of large carrier frequency uncertainties. Their approach was to sweep a range of carrier frequency offsets and search for that which gave the best fit. Their conclusion highlights the main problem of constellation-based recognition algorithms, which is that they need *a priori* knowledge of key parameters. Without that knowledge, one is forced to use search algorithms to explore the parameter space looking for parameters that will allow the constellation diagram to be constructed correctly.

### ***Power Moment Matrix Representation***

Hero *et al* (1997) presented the power moment method, which was an image analysis technique for problems such as character recognition. This method was similar to the invariant moments approach (Li, 1992), but more suited to I/Q plane constellations. The power moment method relied on forming a matrix from higher order moments of the image and performing subspace decomposition.

Hero III and Hadinejad-Mahram (1998) took the constellation analysis method of Soliman and Hsue (1992) and generalised it using the power moment method. Soliman and Hsue's algorithm for classifying PSK modulated signals had relied on forming histograms of the phases plotted on the constellation diagram and then calculating moments of those histograms, but only up to the eighth order moment.

The new method of Hero III and Hadinejad-Mahram (1998) relied on computing a large matrix containing more than 100 joint phase and magnitude moments. The resulting matrix could be denoised by eigenanalysis and was invariant to amplitude changes and phase rotations.

### ***Hellinger Distance Representation***

The Hellinger distance (Beran, 1977)(Gibbs and Su, 2002) is a statistical measure of the difference between probability distributions that has shown to be both robust and efficient (Lindsay, 1994).

Donoho and Huo (1997) proposed using the Hellinger distance in constellation recognition because it would be more robust than ML methods but would achieve very nearly the same classification performance. The method assumes a Coherent Synchronous Environment (CSE) and treats histograms on the I/Q plane as PDFs. The PDF of a received signal is compared with the PDFs of candidate constellations using a norm, which is the Hellinger distance. Thus the comparison with candidates is reduced to a simple comparison of distances.

Huo and Donoho (1998) developed the Hellinger distance method further. Their method was about ten times faster than a comparable ML approach and was particularly suitable when there were two candidate digital modulations. To extend the method to more than two modulations a hierarchical classification scheme was employed.

In this section it has been shown that constellation analysis has been a major research area with many varied algorithmic approaches being investigated. Some of the methods require very accurate removal of frequency and phase errors, so that the constellation diagram is very clear before analysis commences. Other techniques, such as the power moment matrix method, have been designed to tolerate errors in the frequency and phase estimation. The constellation diagram is such an important means of portraying digital modulations that the author anticipates this representation to continue to play a major role in future automatic signal recognition systems.

### **Spreading code estimation**

Spread spectrum modulations originated in military communications where they offer reduced probability of interception by hostile forces. Any technique that makes a radio signal difficult to detect is likely to make the ASR task more difficult. These spread spectrum modulations are now very widely used in non-defence applications, as they allow multiple radios to transmit at relatively low power and without interfering with each other. By allocating different spreading codes to different transmitters, several users can effectively share the same frequency band and not jam each others' communications.

The military need for demodulating low probability of intercept communications has driven the technology for detecting spread spectrum radio links and also for recovering the spreading code (or 'chip code'). Once the chip rate and spreading code are known, it is possible to recover the unspread signal and hence demodulate it for interception and intelligence extraction.

Bouder and Burel (2000) presented a technique that used a neural network to estimate a spreading code. They tested this method on a signal that had been spread with a Gold code, which is a spreading code with good autocorrelation properties (Gold, 1967). They successfully recovered the code at a signal to noise ratio of -5 dB. Their method relied on a pre-processing stage in which it was assumed that the symbol rate was already known and they asserted that this could be achieved via cyclostationarity analysis.

### **Zero crossing sampling**

Zero crossing sampling was a popular technique in earlier systems as it required less processing than, for example, I/Q demodulation. A detector circuit simply records the time at which an input (real) signal crosses the zero line. Despite being a relatively simple sampling method, it can provide very useful statistics for signal recognition. If a signal has already been sampled using amplitude digitisation, then the zero crossing version can be recreated if needed.

Hsue and Soliman (1989) proposed and investigated a relatively sophisticated modulation classification system using the output of a zero crossing sampler. Their system was tested at 15 dB SNR and successfully discriminated a range of PSK and FSK modulations. Furthermore they described how their system could be implemented in a parallel processor to further speed up the process of analysing a signal. The method consists of calculating a number of statistical features from the intervals between zero crossings and estimates of the symbol transition times. This technique is covered in more detail in section 4.3.6.

#### 2.4.2.2 Periodicity transforms

Many of the representations available are based on trying to reveal periodicity in the received signal. This section describes power spectral density, spectral correlation, higher order statistics, recurrence plots and higher order spectra. These techniques all look for periodicity, but in very different ways and with different definitions of what periodicity is.

##### Power spectral density

The Power Spectral Density (PSD) reveals the frequency domain structure of a signal. Measurements that can be made in the frequency domain include estimates of a signal's:

- centre frequency (or frequencies);
- bandwidth;
- number of peaks.

The centre frequency can be a good indicator of a signal's type, as many signals are transmitted on known frequencies in defined geographical areas. Similarly the bandwidth is useful as it is possible to eliminate many possible alternatives early in the decision process by knowing the bandwidth. The number of peaks is relevant to FSK signals that exhibit clear peaks in the PSD. Frequency hopping signals also result in multiple peaks, but these are usually clearly separated in time and result in quite different PSD patterns from FSK signals.

It is straightforward to estimate the PSD in a practical receiver using any of the FFT-based nonparametric techniques (Ifeachor and Jervis, 2002, p. 687-707) or



by storing the amplitude demodulated output of a scanning receiver (which is the principle used by the spectrum analyser).

As well as nonparametric PSD estimation via FFT-based methods, parametric estimation is also an option. Typically parametric methods provide better resolution than nonparametric methods but depend on having an accurate model of the process creating the signal (Ifeachor and Jervis, 2002, p. 682). Both approaches have their advantages and disadvantages and the system designer needs to understand these in order to obtain satisfactory estimates of the PSD.

Ghani and Lamontagne (1993) compared the periodogram with the Welch periodogram. Their analysis also compared recognition performance using PSD estimators to that with a bispectrum estimator, but the Welch PSD estimator was the best performing algorithm.

Ghani and Lamontagne concluded that the Welch periodogram was the better approach when trying to discriminate between AM, FM, ASK, QPSK, SSB-USB, SSB-LSB, two types of FSK, BPSK and CW. The reason for preferring the Welch periodogram was that it gives less variability in the PSD estimates compared to the periodogram without averaging. Interestingly they observed that the sidelobes of the PSD were important in classifying signal type correctly. In order to make the classification decision these researchers compared a k-Nearest Neighbour classifier with an Artificial Neural Network (ANN). They concluded that, although it was slow to train, the ANN gave lower error rates and was faster in operation than the k-Nearest Neighbour method.

Rather than calculating the PSD, Assaleh *et al* (1992) modelled the signal as an autoregressive sequence. A second order model allowed them to estimate the instantaneous frequency and bandwidth of the signal. The mean and standard deviation of these parameters were then used for recognition using a decision tree.

These authors modelled the signal using a z-domain polynomial of the form:

$$1 - a_1 z^{-1} - a_2 z^{-2} - \dots - a_N z^{-N} \quad (8)$$

The poles of this polynomial were then used to estimate the instantaneous frequency and bandwidth. In their case, Assaleh *et al* (1992, p.713) chose to assume that there was only one signal present and that a second order polynomial was therefore appropriate. With such a simplification, there is one pair of complex poles in the z-domain and just one of these is illustrated in Figure 17.

The pole,  $Z$ , can be described in polar form by its magnitude,  $M$  and angle,  $\theta$ .

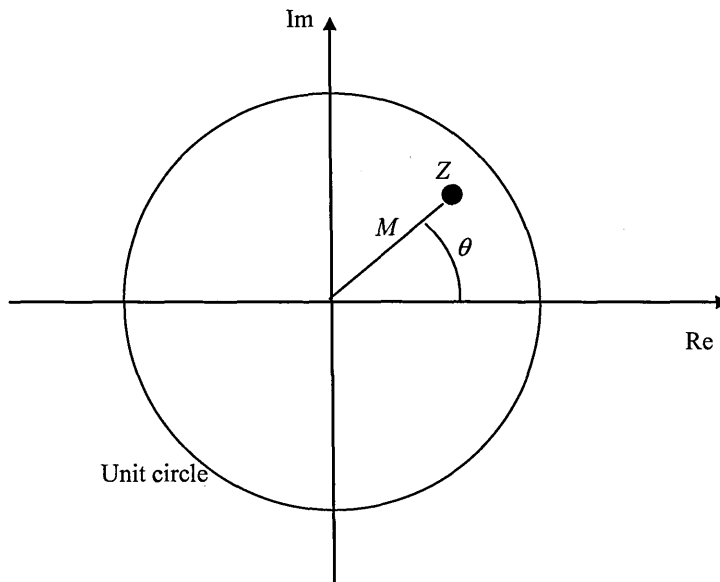


**Figure 17. Instantaneous frequency and bandwidth estimation via a single z-domain pole representing the spectral peak.**

Given the above description of the spectral peak by a pole in the z-domain and a sampling frequency of  $f_s$ , the instantaneous frequency,  $f$ , and bandwidth,  $b$ , are given by:

$$f = \frac{f_s}{2\pi} \theta = \frac{f_s}{2\pi} \tan^{-1} \left( \frac{\text{Im}(Z)}{\text{Re}(Z)} \right) \quad (9)$$

$$b = -\frac{f_s}{\pi} 10 \log_{10} \left( \frac{1}{\text{Im}(Z)^2 + \text{Re}(Z)^2} \right) \quad (10)$$

Assaleh *et al* (1992) used the time-averaged statistics of these two parameters as inputs to a decision tree.

Hachemani *et al* (2007) also used the bandwidth of a signal as one of the recognition discriminators. To do this, they first calculated the PSD. The bandwidth was then determined using an artificial neural network trained directly on PSD examples; there was no intermediate step at which the bandwidth was explicitly measured.

### **Spectral correlation**

Spectral correlation is typically measured using the techniques of cyclostationarity. It is a very significant property as many man-made signals display some form of repetition that can be seen as spectral correlations.

Two particular forms of detector are then considered, firstly the SCF, which is a generic detector of second-order cyclostationary features. Then, the Delay-

Multiply Detector (DMD) is described, which is a simpler mechanism for finding second-order cyclostationary features.

### ***Cyclostationarity***

The work of Gardner is particularly relevant to ASR, as he worked extensively on the application of cyclostationarity (CS) theory to the processing of communication signals and developed the theory necessary for applying cyclostationarity techniques to ASR (Gardner, 1986a), (Gardner, 1991). The cyclostationarity approach relies on detecting periodic features in the time domain structure of signals. Gardner formalised the concept of cyclostationarity by introducing the Cyclic Autocorrelation Function (CAF) and SCF. Gardner (1991) gives a good introduction to the concepts of cyclostationarity and describes the CAF and SCF in detail.

Cyclostationarity techniques have been applied widely to the problem of recognising communication modulation schemes. These techniques enable hidden periodicities in man-made and natural signals to be detected and quantified (Gardner *et al*, 1987), (Giannakis, 1999). They have therefore been applied to diverse problems, not only in communications, but also in radar (Gini and Greco, 2002), (Huang and Zhou, 2006), (Pourrostam *et al*, 2007), marine acoustics (Hinich, 2000), (Amindavar and Moghaddam, 2000), mechanical engineering (Antoni *et al*, 2004), (Sabri *et al* 2006), (Antoni, 2007), medical science (Knaflitz and Bonato, 1999), (Girault *et al*, 2006), etc. A wide body of research has grown up to exploit these cyclostationarity techniques (Serpedin *et al*, 2005), (Gardner *et al*, 2006). Much of the theory has been developed with communications in mind,

because such signals are man-made and frequently exhibit very strong cyclostationarity characteristics.

The essence of this approach is that telecommunications signals nearly always have an element of periodicity and frequently, have several different periods due to the different layers of the protocol stack (modulation, coding, access control, etc.). Sometimes these periodicities manifest themselves as discrete lines in the PSD, but it is frequently the case that there are no lines in the PSD, rather there are symmetries in the frequency domain. These symmetries can be detected by a number of related methods, principally:

- Lines in the Autocorrelation Function (ACF);
- Spectral lines in the spectrum of some non-linear transform of the signal (e.g. squaring);
- Spectral lines in the cross-spectrum of the signal and a time-delayed version of itself.

In cyclostationarity theory the CAF and SCF are the most general-purpose of the algorithms that can be employed. They give complementary ways of analysing received signals and can be considered analogous to the ACF and PSD.

Gardner (1991) defined the types of periodicity listed in Table 5, namely first-order, hidden and second-order periodicities. Subjectively one can think of first-order periodicity as being more obvious or 'stronger' than the hidden periodicities. It is the periodicity we are used to encountering in a wide variety of physical, oscillatory systems.

Gardner's approach was to say that there are other forms of periodicity and that these are 'hidden' in the sense that they are not revealed by the techniques normally used for finding periodicity. Hidden periodicity does not produce discrete lines in the PSD.

Gardner went further than this and defined a specific type of hidden periodicity, which he called second-order periodicity. Second-order periodicity is only revealed when the signal is subject to a quadratic manipulation, such as a squaring function. Second order periodicity can also be thought of in terms of symmetries in the PSD (even though the symmetry may be difficult to see by eye).

First-order periodicity	Discrete lines in the PSD estimate.
Hidden periodicity	No discrete lines in the PSD estimate, but periodicity can be revealed by some other function.
Second-order periodicity	A specific class of possible hidden periodicities.  Second-order periodicity produces discrete lines in the cross-spectral density estimate of the signal and some time-delayed version of it.

**Table 5. Summary of the types of periodicity introduced by Gardner (1991).**

Gardner (1986a) based his approach to analysing second-order periodicity on the definition of two functions – the CAF and the SCF. These are essentially the cross-spectral density estimates of the signal for a range of values of the time delay.

The CAF and SCF can be defined in various ways. The approach used here is based on Gardner's work as this is the form most suitable for analysing communications signals.

The definitions start with an autocorrelation estimate for the signal,  $x$ , with a period  $T_0$ . Given a time lag,  $\tau$ , the autocorrelation estimate at time,  $t$ , for a finite number of samples,  $N$ , is given by:

$$\hat{R}_x(t, \tau) = \lim_{N \rightarrow \infty} \frac{1}{2N+1} \sum_{n=-N}^N x(t + nT_0 + \tau/2) x^*(t + nT_0 - \tau/2) \quad (11)$$

The CAF is then given by a Fourier series expansion of the autocorrelation estimate. The term  $\alpha$  is introduced here and is referred to as the cyclic frequency.

$$\hat{R}_x^\alpha(\tau) = \frac{1}{T_0} \int_0^{T_0} \hat{R}_x(t, \tau) e^{-i2\pi\alpha t} dt \quad (12)$$

Gardner then took the Fourier transform of this to obtain the SCF:

$$\hat{S}_x^\alpha(f) = \int_{-\infty}^{\infty} \hat{R}_x^\alpha(t, \tau) e^{-i2\pi f t} d\tau \quad (13)$$

The CAF and SCF can also be defined without the complex conjugate operation in (11). There are, therefore, two different CAFs and SCFs for any complex signal. The CAFs and SCFs were applied by Gardner to a range of analogue and digital modulations to show how different features are revealed.

The calculation of these functions is processing-intensive, so different researchers have investigated fast implementations. Brown and Loomis (1993) gave a

summary of two common methods of calculating the SCF, namely the FFT Accumulation Method (FAM) and Strip Spectral Correlation Algorithm (SSCA).

Cyclostationarity is, essentially, a second order statistical method and can be thought of as an extension of the power spectral density estimate. It is reasonable to consider the application of higher order statistical methods, such as the bispectrum and trispectrum. This avenue may need to be explored for some signal types if it is necessary to look for periodicities that cannot be revealed by the cyclostationarity approach.

Cyclostationarity is now the dominant method in cognitive radio development. A number of authors (Öner and Jondral, 2007), (Sutton *et al*, 2007) are developing cyclostationary detectors for use in practical cognitive radio systems.

Currently much of the research emphasis is in using cyclostationarity methods as reliable modulation detectors for software-defined and cognitive radio (Öner and Jondral, 2004a), (Öner and Jondral, 2004b), (Le *et al*, 2005), (Kim *et al* 2007), (Maeda *et al*, 2007). The future success of these particular technologies depends on being able to design reliable wireless systems that can operate in areas of shared spectrum.

In many applications the cyclostationarity approach can be seen as a complement to statistical feature-based approaches to ASR (Le *et al*, 2005), (Azzouz and Nandi, 1996), (Lopatka and Pedzisz, 2000), (Dobre *et al*, 2007), (Grimaldi *et al*, 2007). The cyclostationarity approach is particularly suited to the identification of



commercial communications (in which relatively few standard protocols dominate) via recognition of well-documented time domain characteristics. The feature-based approaches, on the other hand, yield information on the type of modulation itself, thereby facilitating fully non-cooperative interception and demodulation.

Communications signals are, in many cases, designed for ease of detection and demodulation in conditions of time-varying interference and disturbance due to propagation. The features that assist with reception of such signals frequently lead to cyclostationarity. This has facilitated the development of detectors that exploit the cyclostationarity properties in order to achieve robust detection in unpredictable environments. Detectors based on cyclostationarity techniques have been designed for software-defined radio (Öner and Jondral, 2003), (Öner and Jondral, 2007), and also cognitive radio (Kim *et al*, 2007).

It has been demonstrated (Öner and Jondral, 2003, 2005 and 2007), (Kim *et al*, 2007) that cyclostationarity detection can be used for older types of modulation, such as Gaussian Minimum Shift Keying (GMSK) and Phase Shift Keying (PSK) and also newer types, such as Code Division Multiple Access (CDMA) and Orthogonal Frequency Division Multiplexing (OFDM).

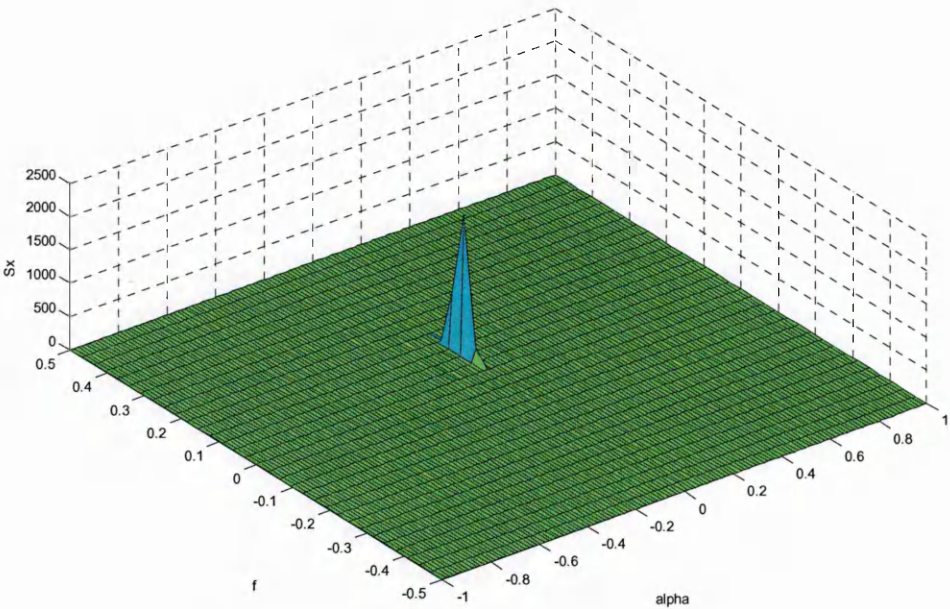
A recent proposal (Maeda *et al*, 2007) has been for a spectrum sharing scheme for systems using OFDM modulations based on deliberately injecting cyclostationarity to facilitate modulation recognition.

***Form of the SCF***

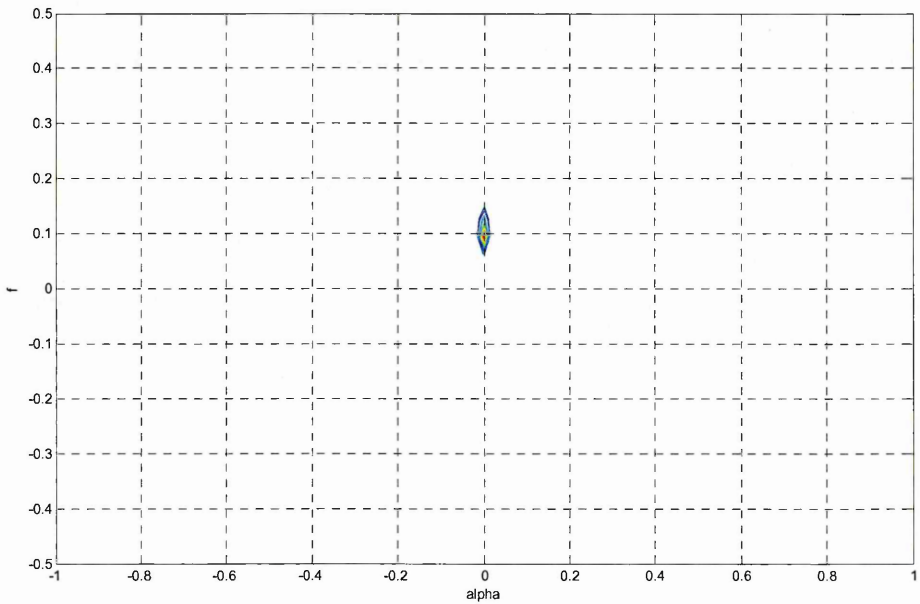
Various authors present the theoretical SCF for basic modulation types. Rather than repeat this work here, the general form of the SCF is explained here by way of simple examples. Using an implementation of the FAM in Matlab based on that by da Costa (1996) we can readily study the form of the SCF for different types of signal.

Starting with a single complex exponential at a relative frequency of 0.1, the SCF will have a single peak at that frequency and at zero  $\alpha$ . This is shown as a surface plot in Figure 18(a).

In general it is easier to work with a contour plot than a surface plot. This is shown in Figure 18(b) for the same signal.



(a) Surface plot



(b) Contour plot

**Figure 18. SCF estimate of a single complex exponential at a frequency of 0.1.**  
 **$\Delta f = 1/32, \Delta \alpha = 1/64$ .**

Adding a second complex exponential, this time at a frequency of 0.3 reveals the basic relationships of the SCF. The contour plot for this situation is shown in Figure 19.

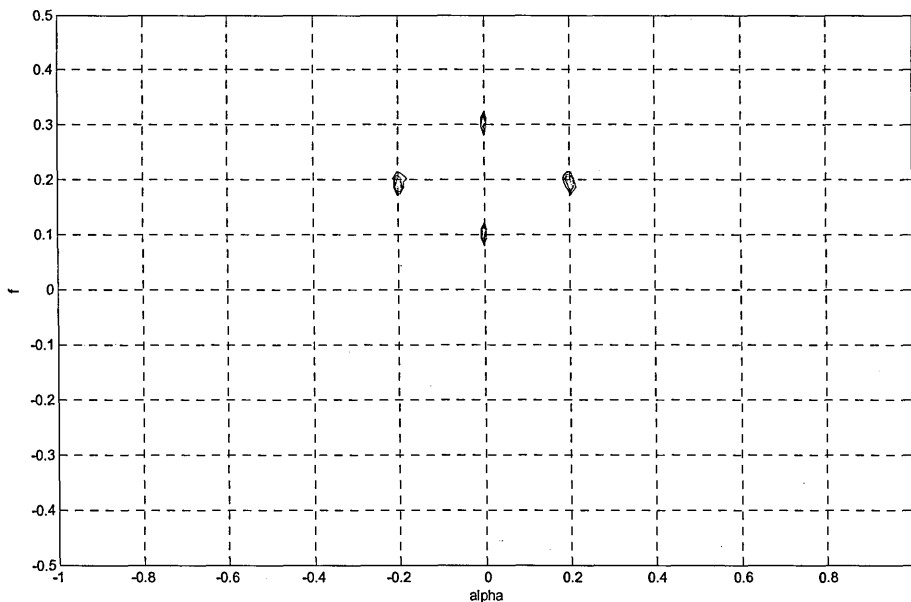


**Figure 19. SCF estimate for the sum of two complex exponentials with frequencies of 0.1 and 0.3.  $\Delta f = 1/64$ ,  $\Delta\alpha = 1/128$ .**

Here we can see that both frequencies are visible as points on the frequency axis. In addition to these, two new points are created, which are symmetrical about the frequency axis and at coordinates  $(\pm|f_2 - f_1|, (f_1 + f_2)/2)$  where  $f_1$  and  $f_2$  are the two frequencies (0.1 and 0.3 in this example).

If we now add a third complex exponential, this time with a frequency of 0.4, then we get the contour plot shown in Figure 20. This has generated three points on the frequency axis plus three points on each side.



frequencies. All other properties of the SCF can be visualised in terms of these simple relationships.

Some important observations can be made at this point:

- Each off-axis peak corresponds to a pair of peaks on the frequency axis. Since the frequency axis is an estimate of the PSD, then we see that the off-axis points each correspond to a pair of peaks in the PSD;
- The two axes are not orthogonal, since the  $\alpha$  coordinates are functions of points on the frequency axis. One may wish to perform image processing on the SCF contour plot, but one should recognise that, because the axes are not orthogonal, the image processing algorithm will be processing a lot of redundant data and may therefore be inefficient;
- Any real signal will have an SCF that is symmetrical about the  $\alpha$  axis;
- Adjusting the centre frequency offset will not affect the shape of the SCF for a complex signal. Rather it will simply move the SCF up or down the frequency axis.

The SCF is a general-purpose transform that can be applied to any signal to search for cyclostationary features.

### ***Squaring and delay-multiply detectors***

The SCF introduced above can be used as a generic detector of cyclostationary features. It is, however, a processing-intensive task to calculate the full SCF. Fast algorithms have been devised for this (Simić and Simić, 1999), (Roberts *et al*, 1991), but it may not be necessary if a receiver is searching for known cyclostationary features of a signal. An alternative approach is to use a delay-

multiply detector (DMD, also known as a Pre-Filter Delay-Multiply detector) which can be used when a cyclic frequency is known *a priori*.

The basic structure of the delay-multiply detector is shown in Figure 21. An input signal,  $x(t)$ , is multiplied by a time-delayed version of itself. Optionally, the delayed signal can be conjugated. Typically the delay is made equal to the reciprocal of a cyclic frequency that is a known characteristic of the modulation, such as its symbol rate or chip rate. The multiplication is a non-linear operation which generates one or more spectral lines in the output,  $y(t)$ . The presence of the given type of signal is then detected by measuring the height of the spectral line(s) of interest. The specification of the prefilter typically depends on the pulse shape of the signal to be detected.

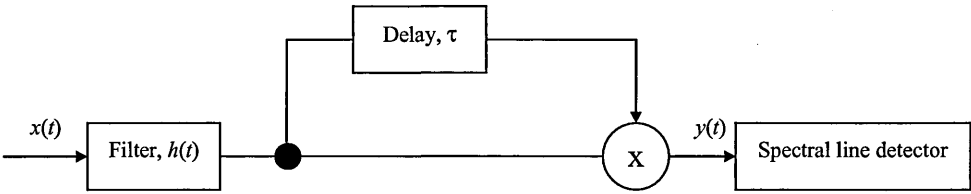


**Figure 21. Delay-Multiply Detector.**

The delay is not always required, as some signal types display amplitude modulation at a rate related to the symbol rate. If there is no delay, then the DMD becomes the squaring detector shown in Figure 22. A squaring detector is simply a DMD with zero delay. This is the technique employed by, for example, Shi and Karasawa (2008) for QAM modulated signals.

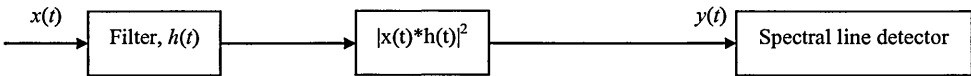


**Figure 22. Squaring detector.**

A non-zero delay is needed, however, for constant amplitude signals which do not exhibit periodicity when passed through a simple squarer.

The DMD can be used to look for the presence of signals in a shared spectrum environment. Kuehls and Geraniotis (1990) applied the technique to the detection of BPSK and BPSK DSSS signals and compared several possible architectures, including the case of a simple squarer (i.e. zero delay) with optimal prefiltering. They concluded that, if the symbol rate were known *a priori*, then the optimal delay-multiply detector would have very similar performance to, and no better than, that of the optimal simple squarer.

More recently, Öner and Jondral (2003) applied this technique to a case in which a GSM signal was to be detected in the presence of an OFDM signal. By a suitable linearisation of the GMSK modulation used in GSM, the authors demonstrated the generation of spectral lines in the DMD output when the delay was set equal to half the reciprocal of the GSM symbol rate.

### **Higher Order Statistics (HOS)**

It is possible to define a range of statistics that describe a signal by making use of higher order moments and cumulants. Each of these is a measure of (odd or even) symmetry in the power spectral density function and therefore indicates something about a signal's periodicity.

The HOS methods differ from the spectral correlation approach in that there is no direct reference to the autocorrelation function. Spectral correlation is based on



the principle that the autocorrelation function is periodic and can be approximated by a Fourier series. The HOS methods do not make such an assertion, so are more general in their application.

Typical examples of 'lower order statistics' would be the instantaneous frequency and bandwidth of a signal (Cohen, 2003). Examples of 'higher order statistics' would then be the instantaneous skew and kurtosis. It is possible to define signals that have identical frequency and bandwidth but different skew and kurtosis (Loughlin and Davidson, 2000). A corollary of this line of reasoning is that that there may be signal types, either extant or in the future, that can only be differentiated by comparing their higher order moments.

A fourth order method of moments estimator for measuring the Carrier to Interference Ratio (CIR) was developed by Kozono (1987). This algorithm has been extensively tested by the author of this thesis (Wagstaff and Merricks, 2006, p.21-25) and found to be effective for FM, AM, FSK and GMSK. An example from Wagstaff and Merricks (2006) is given in Figure 23, which shows a noisy FM signal amplitude (green trace) and the successful measurement of both the signal amplitude level (blue trace) and the underlying noise level (red trace).

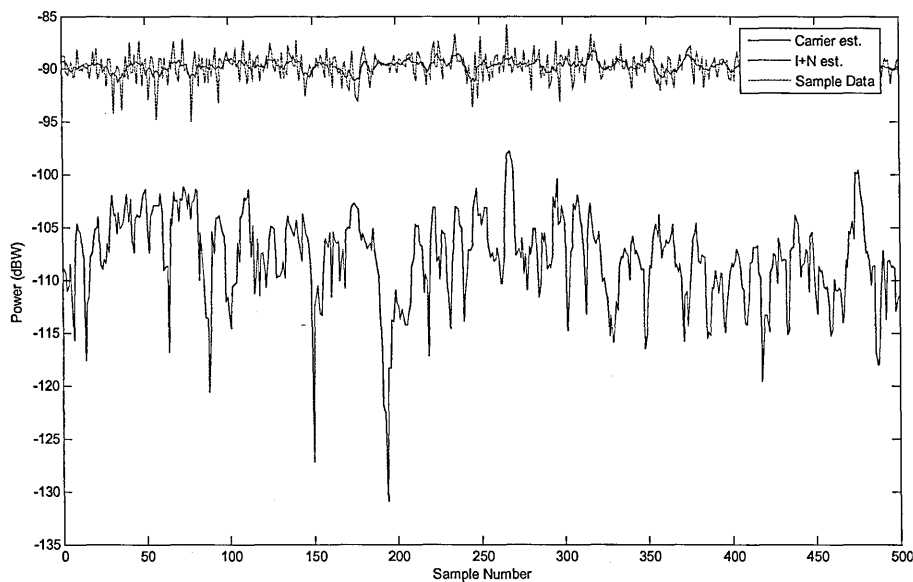


**Figure 23. Method of moments analysis of FM signal.**

The technique only works where the signal amplitude can be assumed to be constant, so does not work for the majority of modern digital modulations. The success of the algorithm does, however, demonstrate the ability to detect and measure signal characteristics from higher order statistics in a real world application.

The identification of OFDM signals was approached by Akmouche (1999) on the basis that OFDM is asymptotically Gaussian, unlike single carrier modulations. His approach uses fourth order cumulants and is very similar to the Kozono (1987) method.

### **Recurrence plots**

The Recurrence Plot (RP) method has been developed for analysing the behaviour of dynamical systems (Eckmann *et al*, 1987). It is particularly suited for revealing behaviour that is only partly periodic, such as that exhibited by chaotic systems.

The development of recurrence plots has allowed a wide variety of time domain behaviours to be studied. They have been applied in the analysis of muscle flexure (Ahmad and Chappell, 2008), heart rates (Mewett *et al*, 1999) (Cimponeriu and Bezerianos, 1999), neural modelling (Marwan and Meinke, 2002) and molecular dynamics (Manetti *et al*, 1999). They have also been used for noise reduction of audio signals (Matassini *et al*, 2002) and for analysing the synchronisation between speakers' and listeners' eye movements (Richardson and Dale, 2005). In communications the recurrence plot has been applied to the analysis of Internet Protocol (IP) network traffic (Masugi, 2006).

The basic concept of drawing an RP is simple and is typically expressed via the following definition of a recurrence matrix (e.g. Marwan *et al*, 2007):

$$RM_{m,n}(\varepsilon) = \Theta\left(\varepsilon - \left\| \vec{x}_m - \vec{x}_n \right\| \right) \quad (14)$$

The variable of interest,  $x$ , is represented in an appropriate phase space and sampled at two points in time,  $m$  and  $n$ . The 'distance' between these points is compared against a threshold,  $\varepsilon$ . The Heaviside function,  $\Theta$ , is then applied purely to facilitate plotting as a series of points.

An unthresholded form of this expression can be obtained by removing the Heaviside function. The resulting form of recurrence matrix must then be plotted as a grey scale or colour scale image rather than a monochrome image.

The concept of distance between points in equation (14) can be calculated by any suitable norm for the data of interest. Whichever norm is used, the effect is to produce an image that illustrates when the variable of interest returns to a point in phase space that it has nearly passed through at an earlier point in time. This is a convenient way of illustrating a trajectory in two dimensions when the variable of interest has more than two dimensions. Equation (14) can, therefore, be thought of as a projection onto a two dimensional plane from a phase space with a higher number of dimensions.

Recurrence plots have not been applied to the signal recognition problem before, but they may be of use in some circumstances. As part of this investigation the use of recurrence plots has been examined. See sections 3.3 and 4.1.

### **Higher order spectra**

Dandawaté and Giannakis (1994) gave examples of how polyspectra (e.g. bispectrum, trispectrum) methods could be applied to the detection of higher order cyclostationarities in signals. In particular they discussed the detection of cyclic-varying channel characteristics for a QAM system and made the point that the second-order spectral correlation cannot be used to estimate the channel parameters. An application of the polyspectral approach is in the estimation of the channel for MIMO communications systems (Tugnait and Zhou, 2002).

Gökmen and Ertüzün (1998) wrote that the polyspectral methods required significantly more processing than cyclostationary methods and were therefore unsuitable for real-time applications. Le *et al* (2005) again wrote that such methods are processing-intensive and therefore unsuitable for real-time processing.

Progress has, however, been made in improving the processing efficiency of these methods, driven by applications such as image processing (Dianat and Raghuveer, 1990), radar (Du *et al*, 2005), astronomy (Tyler and Schulze, 2004) and communications (Kachenoura *et al*, 2006). It is therefore reasonable to expect these methods to be deployed in the future if they confer advantages over other techniques.

### **2.4.3 Features**

Many ASR systems look for features in the signals they receive. The features described in the literature can be grouped into two main types. In this thesis they are termed statistical and parametric, although there is no precedent for this in the literature.

Parametric features are those that try to detect or estimate a parameter, such as symbol rate, chip rate constellation size, number of subcarriers, etc. Such parameters are typically (but not necessarily) discrete values and the features reflect the fact that the observed value of these parameters will converge on the discrete values. Unlike statistical features, parametric features do not look at short

term variations in observation data, but are based on the long term averaged values.

Broadly speaking there are two types of parametric feature processing algorithm: detectors and estimators. Detectors assume that a value exists and look for its presence in the observed data, whereas estimators try to work out what the value of the parameter is from the observed data.

Statistical features depend on estimates of various statistical properties of a signal. They are typically moments of some observable representation of the signal, such as the instantaneous amplitude. These features recognise that parameters of interest (e.g. instantaneous amplitude) will often be observed with values that are given by probability distributions and that those distributions can be estimated by observing the parameter variations over a period of time.

A wide range of statistical measurements can be calculated from received signals. Typically these can be calculated quickly and efficiently and so are suitable for real-time processing. There is a large body of literature using this approach, much of it dominated by work carried out by Azzouz and Nandi (1996).

#### **2.4.3.1 Statistical features**

Azzouz and Nandi published a number of papers on ASR starting in 1995. The publication of these and their book (Azzouz and Nandi, 1996), which summarises their work, has clearly had a major impact on ASR research and development. Many authors refer to the book and journal papers by Azzouz and Nandi and the

same techniques appear with minor refinements in many places (Kremer and Shiels, 1997), (Arulampalam *et al*, 1999), (Dubuc *et al*, 1999), (Lopatka and Pedzisz, 2000), (Chin Tan *et al*, 2001), (Le Guen and Mansour, 2002), (Matsuzaki *et al*, 2003), (Iversen, 2003), (Iversen, 2004). Other authors use significantly different statistical features to the Azzouz and Nandi set, but the overall approach is similar (e.g. Beidas and Weber, 1998).

A series of ASR algorithms for both analogue and digital communications signals was developed by Azzouz and Nandi. Their work included the use of decision trees and artificial neural networks to determine the modulation type from a number of statistical features.

What is immediately apparent about this body of work is that it was largely written before the advent of modulations such as OFDM and CDMA and at a time when spread spectrum techniques were still largely confined to military applications. This is a very important point to note when considering applying these techniques in a modern spectrum monitoring environment.

The recognisers proposed by Azzouz and Nandi (1996) were classified according to the types of signals they were intended for:

- Analogue Modulated signal Recognition Algorithms (AMRA);
- Digitally Modulated signal Recognition Algorithms (DMRA);
- Analogue & Digitally Modulated signal Recognition Algorithms (ADMRA).

It is apparent that the authors found it difficult to devise a single decision tree to handle all possible modulation types and therefore resorted to artificial neural networks to try to alleviate these problems.

All three types of recogniser relied on the same basic feature recognition approach with either decision trees or artificial neural networks as the classifiers and were designed to use as little processing power as possible to give real-time operation.

It is readily apparent that the situation has now changed quite markedly. In the last decade there has been a huge increase in computing power, with technologies such as Field Programmable Gate Arrays (FPGA) and Digital Signal Processors (DSP) now being extensively used in software radio applications.

Azzouz and Nandi (1996) recommended that the received signal be split into frames of 2048 samples and the key features calculated from these. Overall recognition is decided by choosing the most prevalent modulation type across all the frames. This approach has an inherent weakness in that it cannot look for structure across longer periods of time that may provide important discriminators between modulations.

The Azzouz and Nandi approach makes the assumption that the sample rate of the receiving system can be set to a value considerably higher than that of the carrier frequency of the signal. In the examples given they assume a carrier frequency of 150 kHz and a sample rate of 1200 kSamples/s. This will work for narrowband signals that are either sampled directly or at an intermediate frequency. This is not, however, a practical approach for many modern communications systems, in



which the carrier frequency can be several GHz and the bandwidth is often several MHz. In practice, the modern approach to signal acquisition is very often likely to be based on downconversion to a complex baseband representation. The ASR subsystem therefore needs to be flexible enough to accommodate different sampling architectures and particularly those that produce I/Q outputs.

A general class of ASR methods rely on the calculation of a number of key features based on various statistical moments and the subsequent use of a classifier, such as a decision tree or an ANN.

A number of features have appeared over the past few decades, notably those introduced in Azzouz and Nandi (1996). These authors defined the following statistical features:

- Constant envelope parameter,  $\gamma_{\max}$
- Standard deviation of the absolute phase,  $\sigma_{ap}$
- Standard deviation of the direct phase,  $\sigma_{dp}$
- Spectrum symmetry parameter,  $P$
- Standard deviation of amplitude,  $\sigma_a$
- Standard deviation of absolute amplitude,  $\sigma_{aa}$
- Standard deviation of absolute frequency,  $\sigma_{af}$
- Kurtosis of amplitude,  $\mu^f_{42}$
- Kurtosis of frequency,  $\mu^f_{42}$

These features were designed to differentiate between a range of digital and analogue modulations. There has been a trend for modulations to become more

complex and spectrally efficient since Azzouz and Nandi's work. Many modern signals resemble noise when considered from a statistical distribution point of view, making the ASR task harder. This does not invalidate their work, but does mean that statistical methods have to be revisited over time to ensure their performance still meets the requirements of the application.

The following sections consider some of the statistical features defined by Azzouz and Nandi (1996) to highlight the main concepts. It should be borne in mind, however, that many more statistical features could be proposed and there is nothing intrinsically unique about these particular features.

**Constant envelope parameter,  $\gamma_{\max}$**

This parameter is the maximum value of the spectral power density of the normalised-centred instantaneous amplitude. It is used mainly for recognising a constant envelope signal - typically FM, FSK and CW:

$$\gamma_{\max} = \frac{\max |DFT(a_{cn})|^2}{N} \quad (15)$$

where  $N$  is the number of samples in a window of sample data and  $a_{cn}$  is the normalised-centred instantaneous amplitude.

Note that the discrete Fourier transform is being taken of the signal's amplitude rather than the signal itself. This means that the parameter will be useful in distinguishing signals that exhibit amplitude periodicity from those that have no amplitude variation.

The definition of  $\gamma_{\max}$  is such that it cannot be less than zero, which leads to a skewed distribution. Further investigation as part of the background work to this thesis suggests that it can be approximated to a lognormal distribution, but this must be done with caution (see Appendix E).

### **Standard deviations of phase, $\sigma_{ap}$ , $\sigma_{dp}$**

These are two very similar parameters. The first,  $\sigma_{ap}$ , is the standard deviation of the absolute value of the centred, non-linear component of the instantaneous phase,  $\phi_{NL}$ . By 'non-linear' it is implied that we are only interested in the residual phase after any frequency offset has been removed.

For robustness it is calculated using only samples that have amplitudes higher than a threshold,  $a_t$ . For  $C$  samples above the threshold, the  $\sigma_{ap}$  parameter is given by:

$$\sigma_{ap} = \sqrt{\frac{1}{C} \left( \sum_{a_n(i) > a_t} \phi_{NL}^2(i) \right) - \left( \frac{1}{C} \sum_{a_n(i) > a_t} |\phi_{NL}(i)| \right)^2} \quad (16)$$

Any parameter that measures the phase deviation of a signal will be affected by the relative sampling rate, so one must be careful of this when using  $\sigma_{ap}$ .

The other, closely related, statistical feature is defined as follows and differs only in the absence of the absolute operator:

$$\sigma_{dp} = \sqrt{\frac{1}{C} \left( \sum_{a_n(i) > a_l} \phi_{NL}^2(i) \right) - \left( \frac{1}{C} \sum_{a_n(i) > a_l} \phi_{NL}(i) \right)^2}$$
(17)

### **Spectrum symmetry parameter, $P$**

This parameter is defined as:

$$P = \frac{P_L - P_U}{P_L + P_U}$$
(18)

where  $P_L$  and  $P_U$  are the powers in the lower and upper sidebands respectively.

It is used to identify any asymmetry in the PSD of the signal and so is mainly of use in distinguishing the various forms of amplitude modulation, particularly LSB, USB and VSB.

Such modulations are not of particular interest in the VHF and UHF bands nowadays. The signals of this type are the VSB modulation that is used to carry the analogue television video signals and the AM air traffic control air-to-ground communications. Such signals are not spectrally efficient (Burr, 2001, p. 5) compared to "digital" signals and are therefore being phased out. In the UK the PAL-I system is currently being replaced by Digital Terrestrial Television (DTT).

Digital modulation schemes rely on complex baseband representations that are inherently asymmetrical (Burr, 2001, p21). However, the averaged PSD needs to

be symmetrical in order to make efficient use of the available spectrum. From this line of reasoning it is concluded that the spectrum symmetry parameter will only be of very limited use in the frequency bands of interest.

#### **Standard deviations of amplitude, $\sigma_a$ , $\sigma_{aa}$**

These parameters are defined as:

$$\sigma_a = \sqrt{\frac{1}{C} \left( \sum_{i=1}^{N_s} a_{cn}^2 \right) - \left( \frac{1}{C} \sum_{i=1}^{N_s} a_{cn}(i) \right)^2} \quad (19)$$

$$\sigma_{aa} = \sqrt{\frac{1}{N_s} \left( \sum_{i=1}^{N_s} a_{cn}^2 \right) - \left( \frac{1}{N_s} \sum_{i=1}^{N_s} |a_{cn}(i)| \right)^2} \quad (20)$$

Azzouz and Nandi used the  $\sigma_a$  parameter for differentiating between DSB and PSK2 and also between AM or FM and PSK4. They used the  $\sigma_{aa}$  parameter for differentiating between ASK2 and ASK4.

#### **Standard deviation of absolute frequency, $\sigma_{af}$**

The standard deviation of the absolute frequency is used for discriminating between FSK2 and FSK4, which are commonly used by pager systems, such as POCSAG and FLEX.

$$\sigma_{af} = \sqrt{\frac{1}{C} \left( \sum_{a_n(i) > a_t} f_N^2(i) \right) - \left( \frac{1}{C} \sum_{a_n(i) > a_t} |f_N(i)| \right)^2} \quad (21)$$

The  $f_N$  term is a normalised frequency. Azzouz and Nandi chose to normalise this with respect to the symbol rate, which can be done only if one is certain that a symbol rate can be clearly observed.

### **Kurtosis of amplitude and frequency**

Azzouz and Nandi also define two kurtosis parameters. The first is based on the instantaneous amplitude and is used to discriminate between AM and the ASK signal types (ASK 2 and ASK4).

$$\mu_{42}^a = \frac{E\{a_{cn}^4(t)\}}{\{E\{a_{cn}^2(t)\}\}^2} \quad (22)$$

where  $E\{\}$  denotes the expectation operator.

The second kurtosis parameter is based on the instantaneous frequency and is used to discriminate between FM and the FSK signal types (FSK2 and FSK4).

$$\mu_{42}^f = \frac{E\{f_N^4(t)\}}{\{E\{f_N^2(t)\}\}^2} \quad (23)$$

Other statistical parameters defined by other authors following similar approaches to the above definitions. Each takes some representation of the received signal and applies a statistical moment to a set of samples of that signal. The range of possible representations and variety of statistical moments means that it is not practical to produce an exhaustive list of these statistical parameters. The main conclusion to draw is that feature extraction can be based on transforming a signal into a suitable representation and then calculating a statistical moment.

### **Carrier frequency estimation**

Azzouz and Nandi (1996) devote an appendix of their book to this subject as it is critical for obtaining reliable statistics of the type they propose. They put forward three main techniques for this:

1. **Peak of the periodogram.** This method is only appropriate for those modulations that have a carrier frequency that can be clearly detected. In practice this is not the case for many modulations and is only suitable for relatively simple ones.
2. **Frequency-centred method.** This is recommended for symmetric signals. As many modern signals are symmetric (because such modulations are spectrally efficient), it is worth considering for general-purpose use.
3. **Zero-crossing method.** This is based on counting the zero-crossings of the RF signal and is the method recommended by Azzouz and Nandi (1996). In their investigations it was found to be accurate, but only if the weak segments of a signal were removed.

In addition to these methods, the carrier frequency can also be calculated from the rate of change of the unwrapped phase. This approach is more suitable for signals obtained in complex baseband form. The issue of noise is still very important however.

#### **2.4.3.2 Relationships between cyclostationarity and statistical moments**

All the key features proposed by Azzouz and Nandi (1996) look at the signal itself and do not consider multiplying the signal by a time-delayed version of itself.

The authors were aware of cyclostationarity and higher order methods, but only mentioned these at the very end of their book when considering future research directions. Nevertheless, three of the features ( $\sigma_{ap}$ ,  $\sigma_{aa}$ ,  $\sigma_{af}$ ) contain nonlinear functions that will act in a similar way to the quadratic transformations described in Gardner (1991) and act to reveal hidden periodicities in input signals.

Whilst this would seem to imply that the Azzouz and Nandi approach is weaker than Gardner's method, there is an important observation to be made. Gardner started the development of the cyclostationarity theory and based it heavily on the CAF and SCF. These exploit only one type of non-linearity. Azzouz and Nandi's second order statistics suggest considering also nonlinear functions of the phase and instantaneous frequency. Searching the literature has not revealed any research looking at any such alternatives.

Summarising the main characteristics of statistical feature methods:

1. Such methods are appealing because they do not require large amounts of processing and are therefore suitable for use in real-time applications.
2. Determination of the centre frequency is critical to the performance of any statistical feature that incorporates phase or rate of change of phase in its calculation. In practice there are many factors that limit the ability to measure the centre frequency correctly. Such factors include the signal to noise ratio, multipath effects and relative motion of the transmitter and receiver.
3. Experiments with the various features show that they are typically very dependent on, not only the centre frequency offset, but also the number of



samples used and synchronisation. It appears that the many of the results claimed for these techniques are based on the analysis of simulated signals only. It is very hard to remove completely all synchronisation from a simulation and this can mean the difference between a technique working in the field or not.

4. Unlike research into cyclostationarity, the statistical feature methods are not, in general, derived from theoretical representations of the signals concerned. This is a weakness, since features are contrived on the basis of what can be calculated easily rather than what acts as a good discriminator between modulation types.

#### **2.4.4 Decision methods**

The previous sections have looked at different ways of obtaining features that can be used to distinguish different types of signal. This section goes on to consider the ways in which decisions can be made automatically about the type of signal that has been observed.

Hachemani *et al* (2007) called this processing the 'fusion layer' and propose logical rules, neural networks or Bayesian networks for this task. Their interest was in developing the technology for cognitive radio applications and they identified a number of standard detectors as suitable inputs for decision processing.

Decision algorithms are, in this thesis, organised into the groups shown in Figure 24.

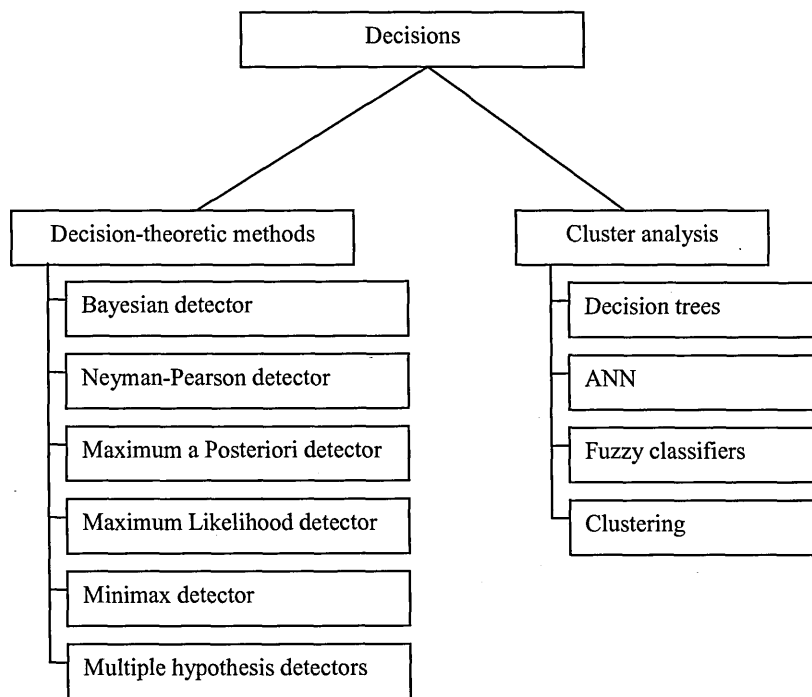


**Figure 24. Taxonomy of decision methods.**

The first group of algorithms in Figure 24 is the decision-theoretic group. The algorithms in this group consist of those algorithms that are conventionally called 'detectors'. This is because they are usually employed for finding the presence of a signal in a noisy environment.

The second group of algorithms shown in Figure 24 is the cluster analysis group containing those algorithms that seek to find regions of similarity in a given representation. These regions are the clusters which relate to the identification of the emitter being received. The algorithms that work in this way include decision trees, Artificial Neural Network algorithms, fuzzy classifiers and clustering algorithms.

#### 2.4.4.1 Decision-theoretic methods

This section considers the decision problem from the probabilistic point of view. The decision as to whether a signal is present in a noisy environment is conventionally performed by 'detectors', of which a number are listed in Figure 24.

The Bayes detector is introduced first, as this is a generic model that can be applied to any situation in which the *a priori* statistics of the signal and channel are known. Common variations on the Bayes detector are the Neyman-Pearson detector, the Maximum A Posteriori (MAP) detector, the Maximum Likelihood Detector, the Minimax detector and multiple hypothesis detectors.

Each of these basic detector types is now introduced. In addition a practical approach to employing Bayesian detection in an ASR context is proposed in section 4.4.2.

##### **Bayes Detector**

The derivation of the Bayes detector is given in Ziemer and Tranter (1995, pp. 604-608). This is a useful starting point for looking at probabilistic decisions, as it forms the basis of many signal detection algorithms.

The derivation starts from the premise that there is a single measurement,  $z$ , and there are two hypotheses,  $H_1$  and  $H_2$ , one of which must be selected by the decision algorithm. A decision is needed that the measurement belongs to one of these two hypotheses. Some *a priori* information is needed in order to make the

decision and this information is assumed to be available in the form of a number of costs and probabilities.

Four costs are defined *a priori*. These are:  $c_{11}$ , which is the cost of selecting  $H_1$  when it is true;  $c_{12}$ , the cost of selecting  $H_1$  when  $H_2$  is true;  $c_{21}$ , the cost of selecting  $H_2$  when  $H_1$  is true and, finally,  $c_{22}$ , the cost of selecting  $H_2$  when it is true. No particular criteria are specified for these costs, so they have to be tailored to the required application.

Also assumed to be known *a priori* are the probabilities of  $H_1$  being true ( $p_1$ ) and  $H_2$  being true ( $p_2$ ).

Ziemer and Tranter (1995, pp. 604-607) then showed that the minimum average cost decision criteria is given by:

$$\frac{f(z|H_2)}{f(z|H_1)} \underset{H_1}{\overset{H_2}{>}} \frac{p_1(c_{21}-c_{11})}{p_2(c_{12}-c_{22})} \quad (24)$$

The left hand side of equation (24) is called the likelihood ratio, commonly denoted as  $\Lambda$ , and the right hand side of the equation is the decision threshold.

Ziemer and Tranter (1995, pp. 604-607) also give the following derivation of the Bayes detector for the simple case of a constant with additive WGN, which is summarised here in order to help explain this general class of methods.

The first hypothesis,  $H_1$ , corresponds to the case of just WGN. The second hypothesis,  $H_2$  is the case of WGN plus a constant,  $k$ . It is assumed that the observation,  $z$ , is a random variable with a probability distribution that depends on whether or not  $k$  is present.

If the signal,  $k$ , is not present then the (conditional) probability distribution for a WGN variance of  $\sigma_n^2$  is:

$$f_z(z | H_1) = \frac{1}{\sqrt{2\pi\sigma_n^2}} e^{-z^2/2\sigma_n^2} \quad (25)$$

If the signal,  $k$ , is present, then the distribution is:

$$f_z(z | H_2) = \frac{1}{\sqrt{2\pi\sigma_n^2}} e^{-(z-k)^2/2\sigma_n^2} \quad (26)$$

The corresponding likelihood ratio is then:

$$\Lambda = \frac{e^{-(z-k)^2/2\sigma_n^2}}{e^{-z^2/2\sigma_n^2}} = e^{2kz-k^2/2\sigma_n^2} \quad (27)$$

This can be used in equation (24) to perform optimal detection, in the sense of minimising average cost. In the example of Ziemer and Tranter (1995, pp. 608-609) the probabilities are assumed to be  $p_1 = p_2 = 0.5$  and the costs are  $c_{11} = c_{22} = 0$  and  $c_{21} = c_{12}$ . This leads to a simplification of equation (24) which is:

$$\exp\left(\frac{2kz-k^2}{2\sigma_n^2}\right) \underset{H_1}{\overset{H_2}{>}} 1 \quad (28)$$

The natural logarithm can be taken of both sides of this expression, which leads to:

$$\begin{array}{c} H_2 \\ z > \frac{k}{2} \\ H_1 \end{array} \quad (29)$$

Using the above probabilities and costs therefore results in a threshold which equals  $k/2$ , so the Bayes detector, in this particular case, will choose  $H_1$  if the measurement is below half the constant,  $k$ , and  $H_2$  if it is above that value. Thus it is seen that the Bayes detector yields a "common sense" result in this simple example. Note, however, that a simplification has been used and this leads to result identical to that for the MAP detector.

It should be emphasised that the full Bayes detector needs values to be specified for the four *a priori* costs and two *a priori* probabilities. It also requires knowledge of the two probability density functions that make up the likelihood ratio. Whether all these are available will depend on the application.

### **Neyman-Pearson Detector**

The Neyman-Pearson detector is a simplification of the Bayes detector that can be used when not all the *a priori* costs and probabilities are known. It relies on fixing the maximum probability of obtaining a 'false alarm' at an acceptable level and then optimising the probability of obtaining a correct decision (Ziemer and Tranter, 1995, p. 613), or, equivalently, minimising the probability of a 'miss' (Bar-Shalom, 1993, p. 66).

**Maximum A Posteriori Detector**

This is another variant of the Bayes detector and is obtained by setting the costs  $c_{11} = c_{22} = 0$  and  $c_{21} = c_{12}$  (Ziemer and Tranter, 1995, pp. 613-614). With this simplification, equation (24) becomes the following equation, which only involves *a posteriori* probabilities:

$$p(H_2 | z) \underset{H_1}{\overset{H_2}{>}} p(H_1 | z) \quad (30)$$

**Maximum Likelihood Detector**

The ML detector has already been mentioned in section 2.4.2, in which it was stated that Mobasseri (1999) used the technique for comparing constellation diagrams.

The ML detector (Lathi, 1983, pp. 595-596) is a variant on the Bayes detector, but makes the assumption that the hypotheses are equally likely. Under that assumption the PDFs are symmetrical and the decision can be represented as follows:

$$p(z | H_2) \underset{H_1}{\overset{H_2}{>}} p(z | H_1) \quad (31)$$

This simply says that the ML detector will choose the hypothesis to which the observation,  $z$ , is closest.

The ML detector is equivalent to the Bayes detector if all the *a priori* probabilities are equal. It is simpler than the MAP detector as the *a posteriori* probabilities do not need to be calculated.

There are numerous examples in the literature of ML detection applied to the signal recognition problem. Shi and Karasawa (2008), for example, used ML detection to select from a set of constellations as part of their constellation analysis.

### **Minimax Detector**

The minimax detector is another variant of the Bayes detector which involves choosing the *a priori* probabilities such that the Bayes risk is maximised (Ziemer and Tranter, 1995, p. 614). Lathi (1983, pp. 596-598) explained that the minimax detector is equal to the maximum likelihood detector when the *a priori* probabilities are equal.

### **Multiple Hypothesis Detectors**

Ziemer and Tranter (1995, p. 614) stated that the Bayes detector can be generalised to handle multiple hypotheses. They then went on to explain that the MAP form is easier to visualise. The MAP version calculates  $p(H_i|z)$  for each of the  $i$  hypotheses and the one with the highest probability is selected.

#### **2.4.4.2 Cluster analysis**

This section considers the decision problem from a clustering point of view in which a signal is represented by a number of features which are treated as a



multidimensional space. Decision trees and artificial neural networks are the most prevalent of such techniques in the literature.

### **Decision trees**

Decision trees have been used widely and are relatively easy to construct. They do not, however, scale well as the number of possible signal types increases.

Assaleh *et al* (1992) used a decision tree to classify a signal as CW, FSK2, FSK4, BPSK or QPSK. Their approach achieved a success rate of 99% at 15 dB SNR. The inputs to their decision tree were the statistics of the instantaneous frequency and bandwidth which were estimated by autoregressive spectrum analysis (section 2.4.2).

Azzouz and Nandi (1996) investigated a number of different decision trees for a variety of statistical features. They documented the results of optimising decision trees for analogue modulations, digital modulations and combinations of analogue and digital modulations. None of the trees performed perfectly in all cases and the authors moved on to investigate artificial neural networks as a way of trying to get around the limitations of decision trees. The results of Azzouz and Nandi's work suggested that decision trees are easy to construct when the number of signal types is relatively small. As the number of signal types is increased, however, it becomes harder to design a decision tree that can achieve satisfactory performance.

It is noticeable in the literature that the decision tree approach (Dubuc *et al*, 1999), (Ramakonar *et al*, 1999), (Boudreau *et al*, 2000), (Matsuzaki *et al*, 2003), (Grimaldi *et al*, 2007) is more often used than artificial neural networks (Kremer and Shiels, 1997), (Arulampalam *et al*, 1999), (Yaqin *et al*, 2003).

The automatic construction of decision trees is discussed by Callan (2003, pp. 241-252) who quoted the ID3 algorithm as an example of an algorithm suitable for trees where each node can be represented as a simple binary decision. The Iterative Dichotomiser 3 (ID3) algorithm is one of a family of algorithms designed to automatically generate a decision tree from a set of examples (Quinlan, 1986).

One can envisage similar algorithms being employed to automate the design of decision trees where the binary decisions have to be made on the basis of the statistics typically used in signal recognition. Callan (2003, p. 248) went on to present some of the problems with automatic decision tree construction. These are very similar to those found in artificial neural network design, namely under-learning, over-learning and the selection of good training data. Just as with artificial neural network design, it is recommended that some of the available data is excluded from the training set and used for testing the performance of a decision tree. Callan also refers to a process he calls 'post pruning' whereby some decision nodes are removed after over-fitting a decision tree. This is similar in concept to the artificial neural network pruning proposed in Appendix C.

### **Artificial neural networks**

Ghani and Lamontagne (1993) used a Welch periodogram to estimate the PSD of a signal and then compared the performance of a k-Nearest Neighbour classifier with a perceptron artificial neural network (that is they used a combination of back propagation and supervised learning as the basic structure). They concluded that the ANN approach was the better of the two methods.

Louis and Sehier (1994) used the means and first three moments of the signal phase, modulus and frequency as inputs to a perceptron ANN. This approach was based on earlier work, with Louis and Sehier's research concentrating on the design of the ANN. They found that a hierarchical ANN was a better solution than a single, global network.

Azzouz and Nandi (1996) used a perceptron approach to build their ANN algorithms. They explored how this could be applied to their statistical features and, when looking at both analogue and digital modulations, achieved a success rate of better than 96% when the SNR was 15 dB or higher. Richterova (2005) repeated their work using a similar two stage ANN but used real signals rather than simulated ones. The success rate was 75% in this study.

An important outcome from these investigations was that a multi-stage ANN was preferred when classifying digital and analogue modulations. This structure is shown in Figure 25. Richterova's (2005) structure was virtually identical.

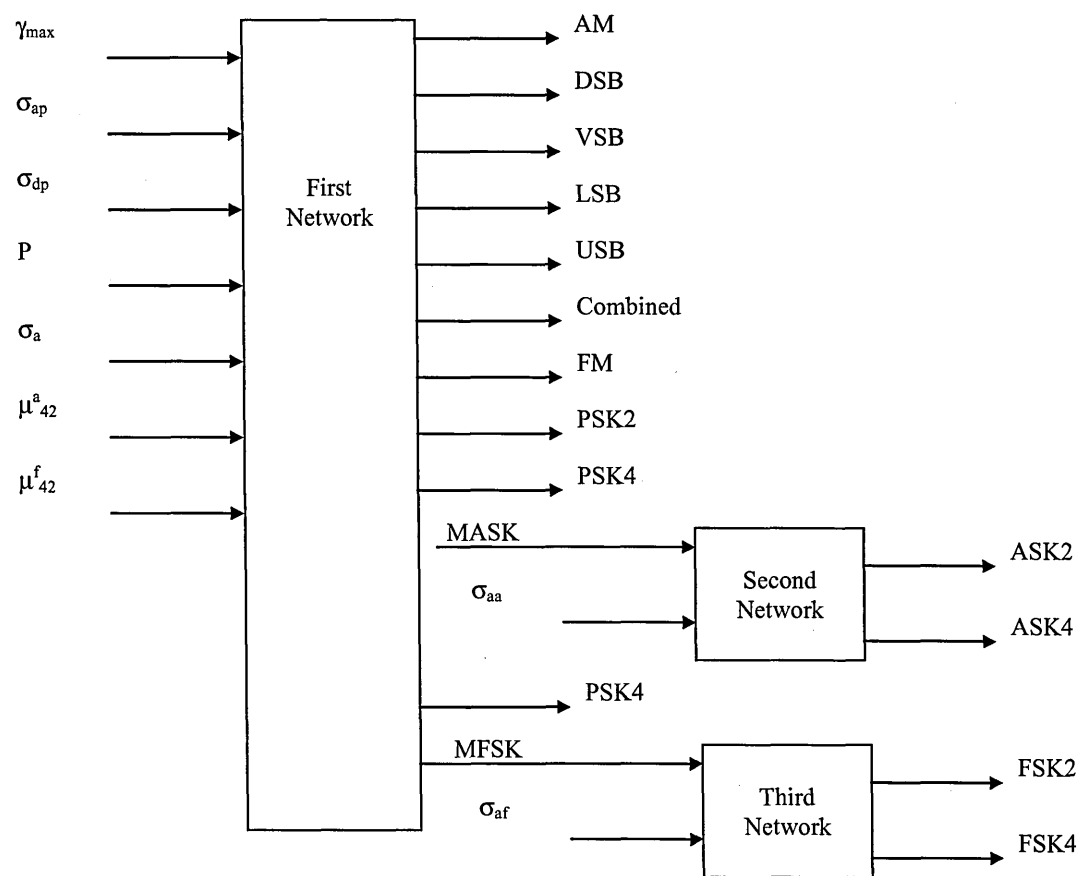


Figure 25. Azzouz and Nandi (1996, Fig. 5.16) multi-stage ANN structure.

Iversen (2004) also used a perceptron and applied it to a similar set of statistical features. The target set of modulations was ASK2, ASK4, PSK4, FSK2, FSK4 and QAM8 and the results were similar to those of the other researchers mentioned above.

Le *et al* (2005) modified this approach by using a One-Class, One-Network (OCON) architecture, which is essentially a series of perceptrons, one for each modulation type. They applied this to AM, FM, BPSK, QPSK, QAM8 and QAM16. It is interesting that the emphasis in 2005 had shifted towards the PSK and QAM modulations, which was driven by the change in radio systems. These researchers reported a success probability of over 80% at an SNR of 20 dB and

produced diagrams illustrating the clusters of the statistical features that could be recognised by their ANN architecture. As with the previous investigations, they observed the reduction in classification success rate as the SNR dropped. They also observed that, by increasing the dimensionality of each classifier, the discrimination between modulations was improved.

Le *et al* (2005) stated that they were interested in finding the minimum number of features needed to identify each type of modulation. One way of achieving this is via the 'pruning' method which is introduced in Appendix C. Pruning allows the least significant inputs to an ANN to be removed, which reduces the processing required when the ANN is deployed in a real-time system.

Thus it is seen that there is a history of applying perceptron ANN architectures to statistical features. Such schemes typically produce good results when the SNR is higher than 15 dB. It should be noted that these investigations have all concentrated on relatively narrow band signals by modern standards. Iversen (2004), for instance, used a sampling rate of 1200 kSamples/s and symbol rates of 12.5 kBaud, which are much lower than the high data rates currently in use in many applications.

None of these investigations considered the effect of interference apart from WGN. When looking at narrowband signals, there is less opportunity for interference, so this is reasonable. This is not a reasonable assumption when moving to wider, shared bands.

### **Other approaches**

Mention must also be made of clustering (Druckmann *et al* 1998), Hidden Markov Models (HMM) (Schreyögg *et al*, 1997) and fuzzy classification (Lopatka and Pedzisz, 2000), (Sengr and Gldemir, 2005), although these appear less frequently in the literature. To date no research has been found that compares these various methods, so it is not possible to state whether or not they offer significant benefits over the other decision methods discussed above.

#### **2.4.5 Comments on decision methods**

Based on the findings of the literature search, the following observations are made about the existing decision processing approaches:

1. All the decision methods encountered to date have operated on a closed domain with a finite number of signal types. In reality the number of possible signal types is not known and new types appear regularly. By assuming a closed domain, the decision logic cannot inherently handle the fact that it may not be able to recognise a signal. Practical systems therefore have to be programmed to classify signals as 'unknown' based on some appropriate criterion;
2. There is typically very little discussion in the literature of how signals that overlap in time and frequency can be handled;
3. The decision methods do not feed back their results to the segmentation function, which must, necessarily, precede the ASR function;

4. There is usually a probabilistic element to the decision function. This will assume typically that the signal is the only one present, so only one probability needs to be assigned;
5. Where multiple features are calculated, they are normally treated in the literature as statistically independent. This is a simplification that is unreasonable, because a change in a signal characteristic may affect many features. For example, consider Azzouz and Nandi's standard deviations of phase,  $\sigma_{ap}$  and  $\sigma_{dp}$  (section 2.4.3). These two features are both functions of the instantaneous phase, so will have some form of correlation between them. In general, one cannot assume that features are not statistically independent unless it is known that they are functions of statistically independent signal parameters;
6. *A priori* information about the presence of known emitters in the environment is not discussed in the literature.

#### 2.4.5.1 *A priori* knowledge

No literature has been found that has considered the use of *a priori* knowledge about the likely distribution of emitter types. In practice there is considerable knowledge available that could be drawn upon in order to improve the performance of an ASR system. In particular the following are especially significant:

- Location of signal in the spectrum;
- Geographical constraints;
- Direction of arrival of the emitter;
- Spectrum occupancy;

- Transmitter locations.

However the system designer must always be aware that interference incidents can be due to such factors as imported equipment and out-of-band transmissions from faulty equipment. Any system that includes *a priori* knowledge to bias recognition decisions must still allow such interferers to be identified.

The Bayesian chain method, described in section 4.5.1 is one approach that is suitable for incorporating *a priori* information into a recognition process.

#### 2.4.6 Improving decision processing

It is interesting to postulate that improved decision processing would incorporate the following three aspects:

- Probabilistic identification;
- An open domain of signal types;
- Multiple hypotheses to cater for the overlapping of signals in time and frequency.

An interesting parallel can be drawn between the techniques applied to multisensor data fusion and the single sensor ASR problem. If one applied more than one technique to the received data and the results were independently derived, then the single sensor problem would be directly analogous to the multisensor problem.

Techniques such as Bayesian, Dempster-Shafer (Leung and Wu, 2000), Multiple Hypothesis Testing (Blackman, 2004) and the Double Bound Test (Wang *et al*,



1998) have been applied in the multisensor case so it is interesting to look for similar approaches that can extend the capability of ASR processing.

## 2.5 Summary

This section has reviewed the background literature on the subject of ASR so that the work of this thesis can be understood in terms of previous and current research. It is a relatively new subject area, having started about thirty years ago, but a very large body of literature has accrued in that time and it has proved necessary to structure the literature review to make it manageable.

It has been seen that there are commercial and military applications of ASR technology. In the military world the interest is in communications intelligence (COMINT) and the use of ASR to determine the type of signal intercepted by a passive receiver. In the commercial markets the main interests are in terms of use by the spectrum regulators for identifying signals in the field and also by the designers of cognitive radio systems, for which ASR is a link in the chain of processing that allows a radio to adapt to its environment. In all these applications there is a common theme that the modern radio environment is becoming ever more complex with unintentional interference and intentional band sharing making it harder to separate and identify different signals.

A generic radio system architecture has been introduced as a model whereby the role and context of ASR processing can be understood. ASR is one link in a chain of information processing that starts with an information source and ends with an identification of the type of signal used to carry that information.

A number of problems in ASR have been identified, the main ones being the range of bandwidths and time scales, the introduction of new signal types and the corruption of the signal by noise and interference. These problems are the main themes of the research carried out for this thesis.

There is a wealth of literature concerning techniques applied to different aspects of the ASR problems, although there is a distinct bias towards some problem areas. This section classified the methods as segmentation, transformation, feature extraction and decision methods. The literature tends to concentrate on the feature extraction methods. Transformation methods tend to be those used in other kinds of signal analysis work, although there are some novel methods used for analysing constellations (e.g. power moment matrix). The decision methods are, without exception, taken from general purpose decision theory in other domains. Segmentation is a much less studied area and one that this author feels will need considerably more research for ASR to handle the challenges of the future.

After surveying the available literature it is clear that the focus to date has been on developing low-level techniques that can discriminate individual signal types presented to the recognition process in isolation. Where signal corruption has been considered it has been confined largely to simple noise and channel propagation models. Rarely has interference been considered in the research to date and rarely have researchers considered the high-level ASR system design.

It is felt that these issues need to be addressed in order to devise ASR systems that can handle the problems encountered in a shared, interfering radio spectrum. Accordingly the research documented by this thesis has concentrated on addressing the issues of how to design an ASR system that can handle multiple, interfering signals.

It has largely been assumed that it is possible to devise feature extraction methods that can be optimised for single signal types and there is a wealth of existing literature that can be consulted when one wishes to delve into the feature identification for any specific modulation type. The research approach has therefore been tailored to branch away from the existing research themes and tackle the wider problems facing ASR in the 21<sup>st</sup> century. This means considering the implications of wider bandwidth communications in shared spectrum bands.

This page intentionally blank

### **3 APPROACH**

This section of the thesis explains how the project was approached. The main research question was split into five more manageable sub-questions, each of which gave rise to a specific research activity, the results of which fed into the overall conclusions of the thesis.

The development of the approach was iterative. As understanding of the problem domain grew it was possible to elaborate the sub-questions more clearly and thereby research more effectively in each area. This approach was successful in that it led to useful conclusions and a number of significant contributions to the subject area.

#### **3.1 Sub-questions**

The research question posed in section 1.2 was what strategies can be adopted for designing ASR algorithms to deal with modern, complex signal environments? This overall research question was too complex to solve in one project, so a series of sub-questions were posed and answers investigated for each in turn. These sub-questions promoted several strands of enquiry which were linked such that a logical path could be followed in explaining the conclusions.

The investigation started broadly and then concentrated on the more detailed aspects of the problem. The following series of sub-questions guided the research:

- **Sub-question 1: To what extent do the users' problems accord with the understanding of the author?**

As part of the preliminary work, it was felt to be important to gain an understanding of the users' problems so that the research would be appropriate and relevant. In addition to literature search (section 2), a short user survey was carried out (section 3.2) to test the author's assumptions about user problems.

- **Sub-question 2: The information content of a signal is not of interest for solving the recognition problem, so to what extent can the signal type be separated from the information content?**

The research applied the recurrence plot method to communications signals and then modified the method to show how it is possible to enhance the modulation type of a communications signal at the expense of information content (section 3.3). The degree to which it can be achieved was investigated by considering the relative enhancement of an estimate of the symbol rate.

- **Sub-question 3: In situations where interferers have very different time scales to those of the the signal of interest, to what extent is it possible to use a logarithmic cyclic frequency representation as a basis for easing the processing demands of cyclostationarity estimators?**

Handling signals with very different bandwidths, symbol rates, etc. is one of the issues that ASR algorithms have to deal with in shared spectrum bands. An algorithm called the Logarithmic Cyclic frequency Domain Profile was devised to show that a logarithmic cyclic frequency representation is

possible whilst retaining a linear frequency domain representation (section 3.4).

- **Sub-question 4: Given that it is possible to design algorithms with specific capabilities, such as modulation separation and logarithmic representation, to what extent can different algorithms be assessed in terms of their relative performance in the presence of interference?**

A strategy for developing improved algorithms depends on the ability to compare them quantitatively. This question was addressed in three main steps. First, a canonical model of ASR processing was designed and shown to support all the different types of ASR system found in the literature (section 3.5). Then, theoretical concepts were proposed that would facilitate the quantitative comparison required (section 3.6.1). Finally, in order to demonstrate the quantitative comparison of representative feature extraction algorithms, a lengthy series of simulations was executed to the point where distinct trends could be identified with a high degree of confidence (section 3.6.2).

- **Sub-question 5: Multiple algorithms can be applied to the ASR problem, each with its own strengths and weaknesses. To what extent can these algorithms be brought together to produce an accurate result?**

No single algorithm was found that could recognise all features of all signals in all environments. Until such an algorithm is found multiple algorithms will be needed to meet the users' need for accuracy in the presence of interference.

A decision-theoretic approach was proposed for combining multiple algorithms based on a Bayesian chain (section 3.7).

This series of questions led to results that showed that interference is and will continue to be a problem and that ASR algorithms can be developed that exhibit specific desirable behaviours in the presence of interference. It then led to a means of comparing algorithm performance so that better feature extraction algorithms can be developed and to an architecture that can combine multiple algorithms.

The following paragraphs describe each of the research methods in more detail before the results are presented in section 4.

## **3.2 User survey**

This project stemmed from discussions with various people within the spectrum monitoring industry and, in particular, from research projects carried out for the UK and Dutch spectrum regulators. It was apparent that there were a number of problems with the existing state of the art in ASR and some of these have been described in section 2.3.

Understanding the problem domain was essential before commencing the research. There is an extensive body of academic literature in this area and this represented a major background to the work. It was felt, however, that it was important to confirm with the user community that this was a problem worth



studying and that the specific area of investigation is relevant to current and future applications of the technology.

Whilst it was clear to the author that a number of technical problems existed, it was not clear how these related to the user experience. The literature search did not reveal sufficient information on user experience at the level required. A survey was therefore carried out, which took the form of an online questionnaire. The online questionnaire was implemented using the service available from [www.surveymonkey.com](http://www.surveymonkey.com).

The questionnaire was piloted with a few colleagues at first in order to identify poorly worded questions and improve the structure. The questionnaire was then sent to 62 colleagues in the industry. 16 people responded to this questionnaire, which gave a small, but helpful, indication of the relative importance of different issues. The details of the questionnaire responses are given in Appendix A.

The following questions were asked of the users:

- Which RF bands do you believe are the most difficult for a human operator to analyse?
- Which automated signal recognition systems do you use?
- Do you think that, as more services move towards digital communications, signal recognition will become easier or harder for the human operator?
- The fourth question gave a list of features that might be desirable in an ASR system and asked the users to rate them by importance for their needs.

- The last question was an open one, asking the users for any comments they would like to make.

These questions struck a reasonable balance between closed and open forms. The closed questions allowed a small amount of statistical analysis to be performed. The open question at the end allowed the users to express ideas that the author may not have considered. In hindsight it may have been possible to extract more useful information from the survey by improving the survey method. Should the survey be revisited, it is recommended that methods other than online questionnaire, such as structured interviews, be considered. With a relatively small community of people expert in a specialist area it is probably better to carry out more detailed, face-to-face or telephone interviews with individuals to extract more information from each participant.

To summarise the detailed results of the survey:

- **Spectrum Usage:** The author's own work in the 2.4 GHz ISM band suggested very strongly that usage of licence-exempt spectrum is becoming very complex, with interference conditions highly likely to be encountered in urban areas (Wagstaff, 2008). The survey results supported this with licence-exempt bands being areas for concern in the user community and a belief that signal recognition will get harder as more digital services are deployed.
- **Need for ASR tools:** The results of the survey suggested that ASR tools are not in common usage and that there are few such tools that are readily obtainable by field staff. Lack of tool availability and high price are hampering interference investigations and this situation is expected to worsen.

- **Performance requirements:** It was clear that recognition accuracy is the most important requirement for an ASR tool. Speed, display of identification confidence and display of signal parameters were given as the next most important requirements.

The main outcome of the user survey was that it influenced the remainder of the research, with an emphasis on the importance of achieving accurate identification in the presence of interference. It also reinforced the author's belief that interference will continue to be a facet of the world of communications in the future.

### **3.3 Phase-symmetric Cross Recurrence Plot**

Many methods exist for processing radio signals for the purpose of signal visualisation and recognition and some of these have been described in section 2.4. The recurrence plot method has not been applied to communications signals previously, but it provides a visualisation of various phenomena in other domains (as described in section 2.4.2) and offers promise for application in ASR.

Initial investigations concentrated on how different signal types appear when analysed with the recurrence plot. It was clear, at a subjective level, that repetitive structures could be visualised with this method and that it offered the potential of being a novel representation from which useful measurements could be obtained. This line of enquiry led to a search for ways of making qualitative measurements that could be useful as part of an ASR system.

Experimentation with different modifications to the recurrence plot led to a variant that could be used to process communication signals in such a way that a modulation's characteristics could be emphasised at the same time as the information content was suppressed. This variant has been given the name of Phase-symmetric Cross Recurrence Plot and has proved to be a useful mechanism by which feature enhancement can be demonstrated.

The recurrence plot and the PCRP were tested with simulated sets of known symbol patterns, starting with BPSK modulation and then examining QPSK and other modulation types. The results of these investigations are presented in section 4.1.

### **3.4 Logarithmic Cyclic frequency Domain Profile**

In an interfering environment there is the potential to encounter multiple signals with a wide range of time scales and bandwidths. This is exacerbated by the move towards shared, licence-exempt spectrum bands and wider bandwidth signals.

With a wide range of signal properties existing in the time domain, a recognition algorithm should be capable of discriminating signals with widely differing characteristics. It was postulated that a logarithmic representation would help with handling interfering signals.

The literature search did not reveal any algorithms that are couched in terms of logarithmic representation. The cyclostationarity methods, however, are widely

used in signal recognition and attention was therefore drawn to these. Would it be possible to modify a cyclostationarity method to operate with a logarithmic representation?

It was found that it was possible to combine the cyclostationary representation called the Cyclic frequency Domain Profile (CDP), which operates in a linear cyclic frequency domain, with ideas taken from the constant Q transform, which operates in terms of logarithmic frequency. This led to the development of a variant of the CDP that has a logarithmic cyclic frequency, thereby showing that it is possible to produce such an algorithm and that such a representation is suitable for the ASR task. This algorithm is presented in section 4.2. The LCDP algorithm was published in the IET Communications journal (Wagstaff, 2008).

### **3.5 Canonical ASR architecture**

In the absence of a generic model of ASR processing, this line of enquiry started by designing a generic processing model based on the methods found via the literature search. The model developed is asserted to be a canonical model, in that it is the simplest model that fits every ASR system found in the literature to date. The usefulness of this model lies in standardising terminology and facilitating reasoning about ASR systems at a high level.

The ASR model is presented in section 4.3 in the form of Unified Modelling Language diagrams. UML has become an industry standard method for describing software systems and is widely understood across industry. The emphasis here is on producing the class and activity diagrams that describe the

main data structures involved, the relationships between those structures and the processing to be performed on them.

The model was developed by applying it to all the types of ASR algorithm that were found in the literature. Each ASR algorithm was compared to the model and adjustments were made to the model to ensure that all the algorithms were accommodated.

It was found that all the algorithms could be represented using a few classes and activity diagrams, even though the mathematical details of those algorithms varied widely. After only a few updates to the UML model it was possible to draw all the algorithms using the notation introduced in section 4.3.

### **3.6 Feature performance in the presence of interference**

In order to understand how feature extraction algorithms perform when a signal is interfered with, it was necessary to deal with a wide variety of signal types and combinations of types with varying frequency offsets, amplitudes, etc. The approach to this involved defining new theoretical concepts and then building a simulation to investigate those concepts.

#### **3.6.1 Ideal Feature and Interference Selectivity**

One of the barriers to understanding the performance of ASR systems in the presence of interference is the absence of suitable terminology. Terms such as Co-Channel Interference (CCI) and Adjacent Channel Interference (ACI) are widely used within the Electromagnetic Compatibility (EMC) testing community, but are relatively simple measures of interference (Wagstaff, 2007, Appendix C,

p.17). In order to improve this situation, a new way of thinking about interference was needed, one that could indicate, quantitatively, how severe the impact of interference would be on an ASR system.

It was conjectured that if an Ideal Feature exists, it would function correctly under all interference conditions. The performance of real features could then be evaluated by comparing their characteristics with that of the Ideal Feature. A performance metric was proposed called Interference Selectivity to allow quantitative assessment of the real features.

Given this performance metric, it was then necessary to know how existing, typical features might behave. Only then would it become clear whether or not improvements were needed. Simulation was used to produce statistics on the Interference Selectivity metric, the results of which could inform the design process.

The proposal for a method of evaluating the performance of recognition features in the presence of interference led to the need to understand the performance of existing features.

What is the Interference Selectivity achieved by typical features? Is this performance sufficient to allow interference to be effectively ignored, or is it necessary to look for improvements? If improvements are needed, then what Interference Selectivity is required?

### 3.6.2 Interference Selectivity investigation by simulation

To answer these questions a Matlab simulation was constructed based on the canonical architecture defined previously. The alternative approach would be to obtain mathematical definitions of the interference selectivity for a very wide range of interference events. The simulation approach was considered to be more likely to produce results within the timescales of the project and, if necessary, could be readily extended to include other signal types and different recognition algorithms.

By simulating the interference between a wide variety of signals and a number of different recognition algorithms, it was possible to explore the concept of interference selectivity. The simulation was based on the types of signal to be found in the 2.4 GHz ISM band, which is a licence-exempt band commonly used for wireless networking and also used by microwave ovens, wireless video senders and other consumer technology.

A total of 63 signal types were simulated with bandwidths ranging from zero (i.e. Continuous Wave) to 22 MHz. These were paired in different combinations and analysed using 13 features. A total of 1,339 signal pairings were evaluated, requiring the simulation of over 5 million interference events. This gave confidence in the statistics of the Interference Selectivity estimates. The details of the simulation parameters are given in Appendix B and the results are described in section 4.4.



This simulation gave valuable insights into the ability of existing features to handle interference. Studying the results led to useful observations on the possible ways forward for handling interference in future ASR systems.

### **3.7 Combining multiple feature extraction algorithms**

One of the main items of feedback from the user survey was that identification accuracy is the most important characteristic of an ASR system. This must be achieved in an increasingly complex, interfering environment.

The subsequent work led to results that showed that:

- feature extraction algorithms can be developed which remove information content from signals to highlight the modulation and the PCRP was developed as an example;
- certain desirable behaviours can be built into a feature extraction algorithm, with the LCDP being developed as an example of such an algorithm;
- it is possible to reason about ASR systems at a high-level by considering the required functionality in the form of a canonical architecture;
- feature extraction algorithms can be compared quantitatively in terms of their performance in interference.

The last stage in the research considered how these threads might be pulled together by devising an architecture for combining the outputs of the best feature extraction algorithms. There are many ways in which this might be done. Rather than consider all possible methods, the rationale adopted here was to consider one approach in particular and recommend further work where necessary.

Section 4.5 presents the results of this work, which concentrated on proposing a decision-theoretic method based on a Bayesian chain. This method is proposed as a means of showing how the earlier strands of research can be brought together. It does not claim to be optimal in any particular sense, but would form a useful basis for work in this area.

### **3.8 Summary**

Potential users of ASR systems were surveyed and, in combination with the results of the literature search, this provided the motivation for the main direction of the research.

The overall approach to the research was to break the overall research question (section 1.2) down into a series of more manageable sub-questions (section 3.1), each of which was investigated in some detail. The majority of the research was algorithmic, with simulation used to provide evidence of performance where needed.

This approach to the research was successful in that it led to useful contributions and insights that will help to guide future algorithm development.

## 4 RESULTS

This section presents the detailed results of the investigation. The appendices are referred to, where appropriate, in order to present more detail than is appropriate here.

Section 4.1 presents the PCR method and its application to communications signals of various types. Section 4.2 describes the results of the investigation into the LCDP algorithm. Section 4.3 presents the proposed canonical architecture for describing ASR systems and section 4.4 gives the findings of the investigation into ASR performance in the presence of interference. Section 4.5 brings the various strands of research together by presenting a way of combining the outputs of multiple feature extraction algorithms.

### 4.1 Recurrence plots

In section 3.1 the second sub-question that was posed was:

**To what extent can the type of modulation be separated from the information content of a signal?**

This sub-question was addressed by considering the visualisation and analysis of signals via the Recurrence Plot method. The concept of the RP was introduced briefly in section 2.4.2.

This part of the research concentrated on investigating an effect that had been observed by the author when a Cross Recurrence Plot (CRP) was constructed from a signal and a phase-rotated version of that signal. This investigation aimed

to understand and quantify key aspects of the behaviour of RP methods insofar as they can help answer the research sub-question.

The investigation starts by examining the determination of symbol rate of a set of BPSK signals using the two different types of recurrence plot. It then extends this same analysis to a set of QPSK signals and finally looks at some other modulations of interest.

By these investigations it is shown how deliberately removing information from a communications signal, in this case information encoded in the phase, it is possible to construct a representation that enhances a particular aspect that is useful for recognition purposes. In these examples it is the symbol rate that is the parameter to be enhanced.

#### **4.1.1 Simulation details**

The following sequences of 24 symbols are used to illustrate the behaviour of the algorithms for different modulations. In all cases the symbol rate is 1 kBaud giving a time series 24 ms in duration. The signals are simulated at a sample rate of 10 kSamples/s, so there are 10 samples per symbol.

Each simulation is created by concatenating three copies of the symbol sequence, then modulating the longer sequence with the required modulation scheme. The bandwidth is then increased by a factor of 10 by resampling in order to facilitate visualisation as recurrence plot images. Finally the leading and trailing samples are rejected leaving the centre third to be used in the analysis. This procedure

eliminates any effects the resampling filter may have had at the start or end of the simulated sequence. The result is a series of 240 complex baseband (I/Q) samples (Burr, 2001, pp. 16-18) starting at the centre of the first symbol in the sequence.

**4.1.1.1 Set A**

Set A is a single sequence of alternating zeroes and ones.

Example	Symbol Sequence
A1	0 1 0 1 0 1 0 1 0 1 0 1 0 1 0 1 0 1 0 1 0 1

**4.1.1.2 Set B**

Set B comprises 10 sequences of the symbols zero and one. Each sequence has been taken from a random series but selected such that it has an equal number of ones and zeroes.

Using the same number of ones and zeroes reflects the use of line codes such as Manchester and return-to-zero (RZ) (Ziemer and Tranter, 1995, p. 557). These are used in radio communications systems to aid clock recovery by ensuring there are no long periods without a symbol transition and also to remove the DC component from the transmitted spectrum (Burr, 2001, p. 112).

Example	Symbol Sequence
B1	000110100000111010110111
B2	010100011110011100001101
B3	010110101001100110110010
B4	000101010110101011111000
B5	010000011101011110001110
B6	101011001000001101111010
B7	000011101100001111110001
B8	010101111000011001100110
B9	001110111010010110100010
B10	001011010100001111110100

#### 4.1.1.3 Set C

Set C is a single sequence comprising the symbols 0 to 3 in ascending order and repeating.

Example	Symbol Sequence
C1	012301230123012301230123

#### 4.1.1.4 Set D

Set D comprises 10 sequences of the symbols 0 to 3. Each sequence has been taken from a random series but selected such that it has an equal number of each symbol.

As with set B the equal number of symbols reflects the use of line coding to aid timing recovery and remove the DC component from the transmitted spectrum.

Example	Symbol Sequence
D1	1 2 1 1 2 3 3 1 3 3 2 3 2 0 0 1 0 0 0 2 1 0 3 2
D2	2 1 1 0 2 0 3 3 1 2 3 3 0 3 2 1 0 0 1 3 0 2 1 2
D3	0 0 3 2 1 1 3 3 2 2 3 3 1 2 0 2 3 1 1 0 1 0 0 2
D4	2 0 0 0 3 3 2 0 1 1 1 3 2 0 3 0 2 2 1 3 1 2 1 3
D5	1 3 1 1 1 1 2 3 2 1 2 0 2 3 2 0 0 3 0 2 3 3 0 0
D6	0 1 2 0 3 3 1 0 3 1 1 0 0 2 2 0 2 3 2 1 1 3 3 2
D7	2 1 0 0 2 1 3 2 0 0 3 2 1 1 3 2 1 3 0 3 3 0 1 2
D8	2 1 2 2 2 1 0 3 0 3 0 3 3 3 0 1 1 2 0 2 0 3 1 1
D9	1 0 0 2 1 0 2 1 1 3 1 3 3 0 2 3 3 1 3 2 2 2 0 0
D10	1 0 2 0 3 1 1 2 3 2 3 2 1 1 2 0 3 1 2 3 0 3 0 0

#### 4.1.2 BPSK symbol rate estimation from Recurrence Plots

The first step in this investigation is to demonstrate the estimation of BPSK symbol rate from an RP. This could be done in many ways, but a straightforward method is to take the Fourier transform of a single row from one side of the RP and look for a peak corresponding to the symbol rate.

As an example consider the series of 24 alternating symbols in example A1. The RP for this sequence is shown in Figure 26.

It will be recalled that the RP, as defined in (14) take a threshold,  $\varepsilon$ , as a parameter. The choice of threshold affects the appearance of the RP and it must be set to reveal the characteristics of interest. For the purpose of the current investigation the threshold has been set at 0.175 (see section 4.1.3 for the rationale behind this choice) which allows the the symbol transitions to be seen clearly in Figure 26.

Looking along the leading diagonal, known as the Line Of Identity (LOI), there are 23 crossings corresponding to the locations of the symbols. At each end of the LOI there are two 'half symbols' so there are 24 symbols in total.

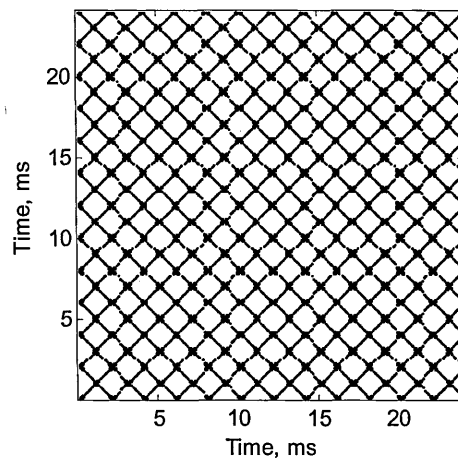


**Figure 26.** RP ( $\varepsilon = 0.175$ ) of BPSK, example A1 (alternating symbols).

The Fourier transform is now calculated of just the first row using a 256 point Fast Fourier Transform and this results in the power spectral density plot of Figure 27. The symbol rate of 1 kBaud is seen but is the first harmonic at 1 kHz and not the dominant peak. The fundamental frequency is 0.5 kHz, which can be understood by remembering that the input sequence consisted of alternating



symbols and so the first row of the RP only reveals 12 symbols similar to the first on that row rather than 24.

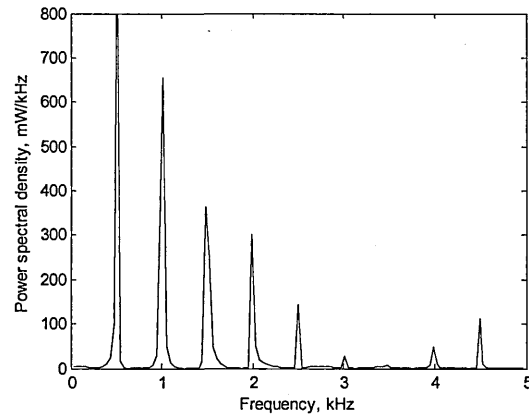


**Figure 27.** Fourier transform of first row of Figure 26, BPSK, set A, zero frequency term omitted ( $\varepsilon = 0.175$ ).

Further examples are shown below for the symbol patterns in set B listed in section 4.1.1. In each case there is a peak at 1 kHz, but there are other peaks that are frequently stronger. These peaks represent the information carried by each symbol sequence and so are different for every example.

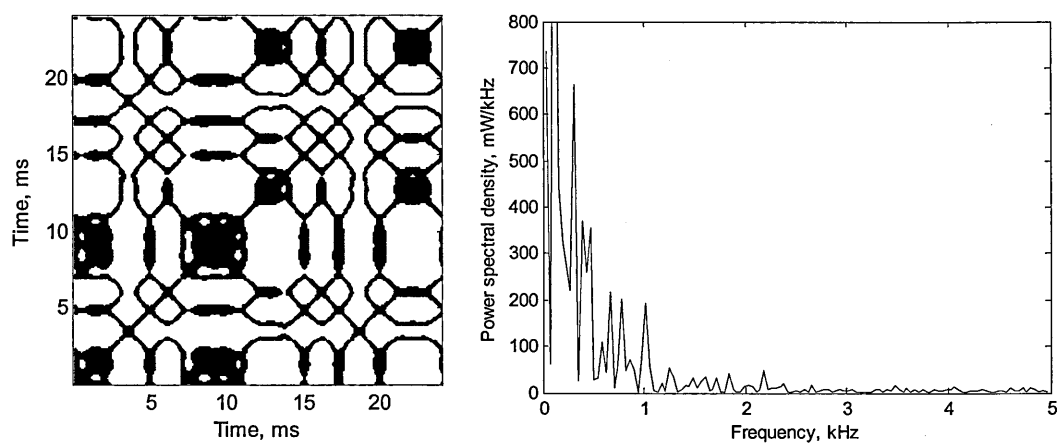


**Figure 28.** RP ( $\varepsilon = 0.175$ ) and Fourier transform of first row for BPSK, example B1.

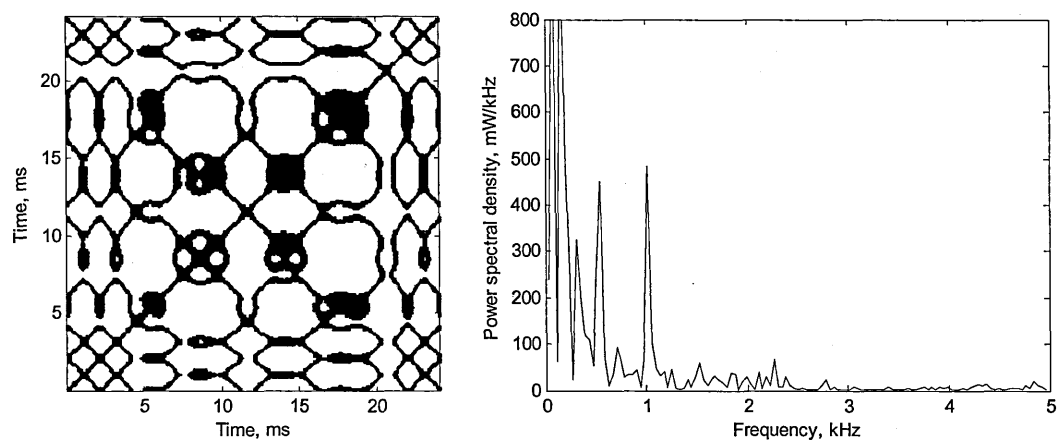


Figure 29. RP ( $\epsilon = 0.175$ ) and Fourier transform of first row for BPSK, example B2.

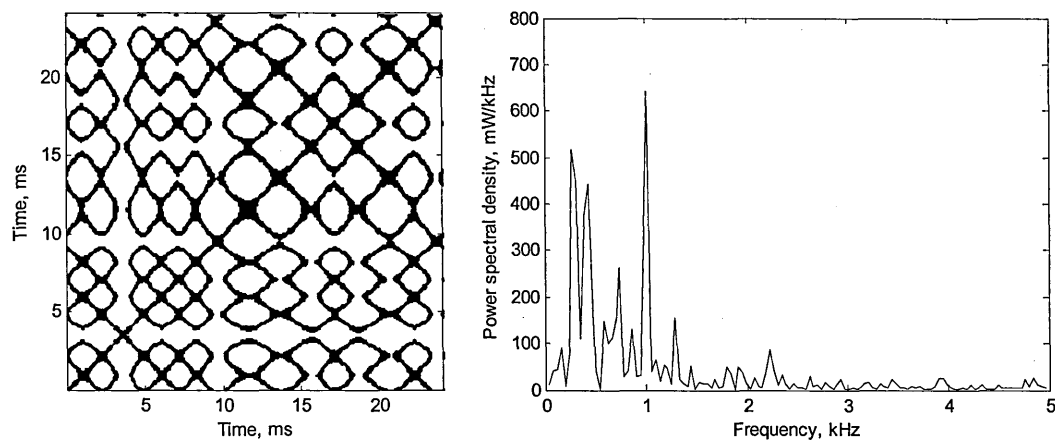


Figure 30. RP ( $\epsilon = 0.175$ ) and Fourier transform of first row for BPSK, example B3.

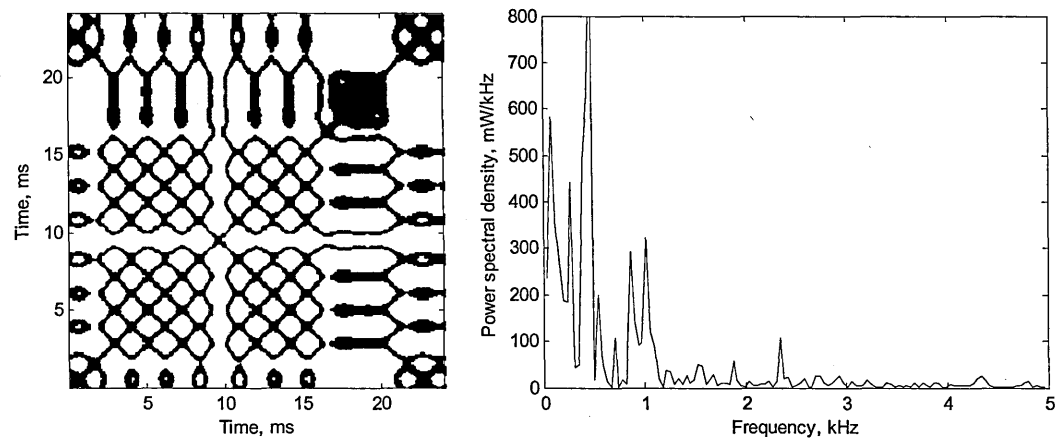


Figure 31. RP ( $\epsilon = 0.175$ ) and Fourier transform of first row for BPSK, example B4.

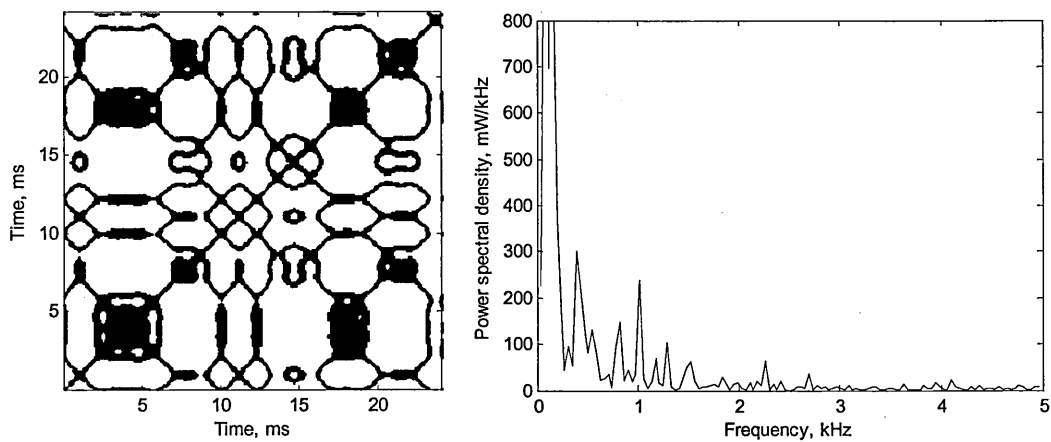


Figure 32. RP ( $\varepsilon=0.175$ ) and Fourier transform of first row for BPSK, example B5.

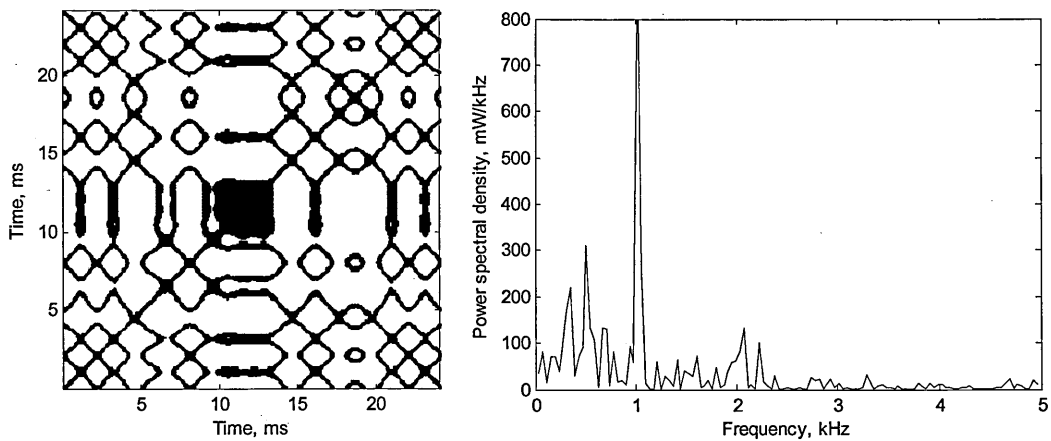


Figure 33. RP ( $\varepsilon=0.175$ ) and Fourier transform of first row for BPSK, example B6.

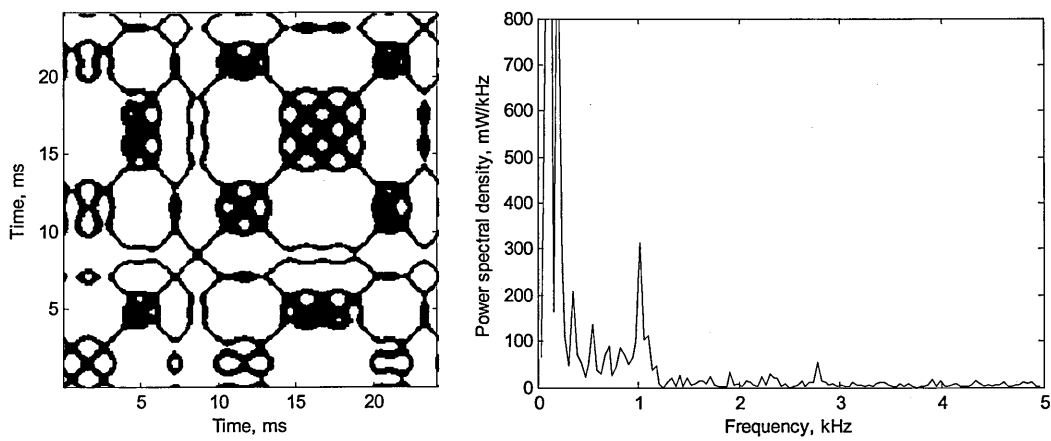


Figure 34. RP ( $\varepsilon=0.175$ ) and Fourier transform of first row for BPSK, example B7.

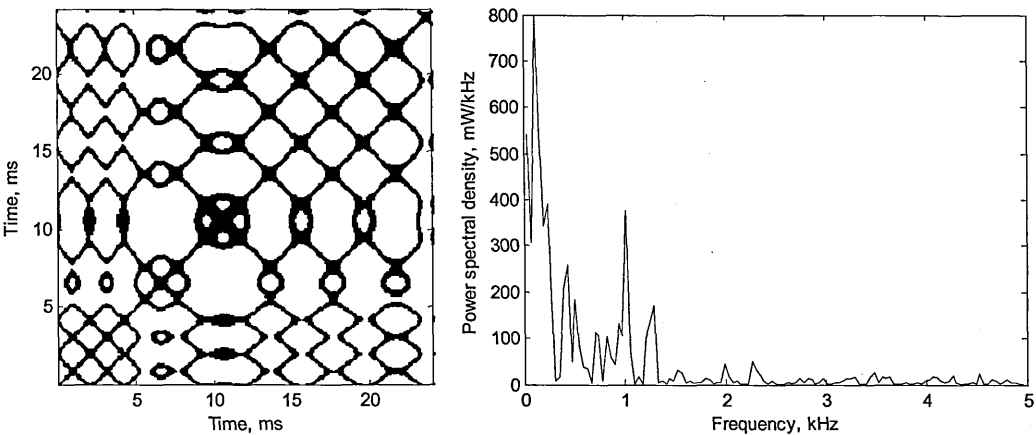


Figure 35. RP ( $\varepsilon = 0.175$ ) and Fourier transform of first row for BPSK, example B8.

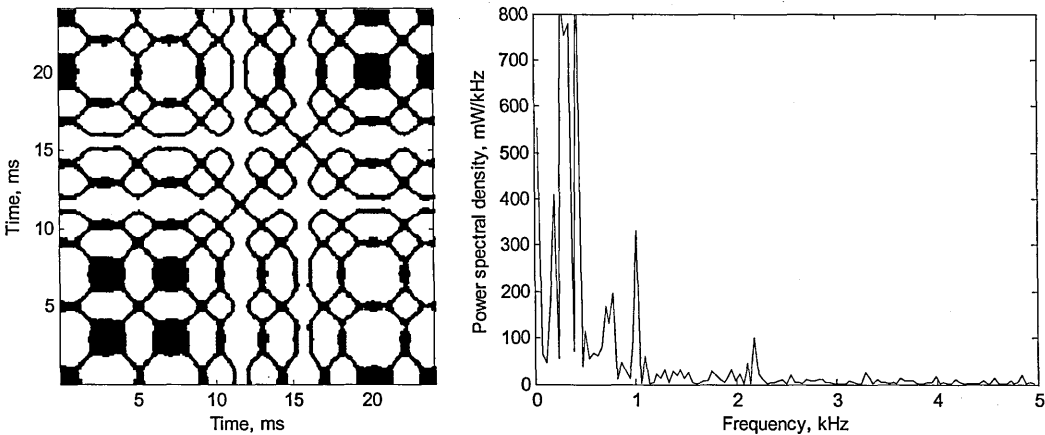


Figure 36. RP ( $\varepsilon = 0.175$ ) and Fourier transform of first row for BPSK, example B9.

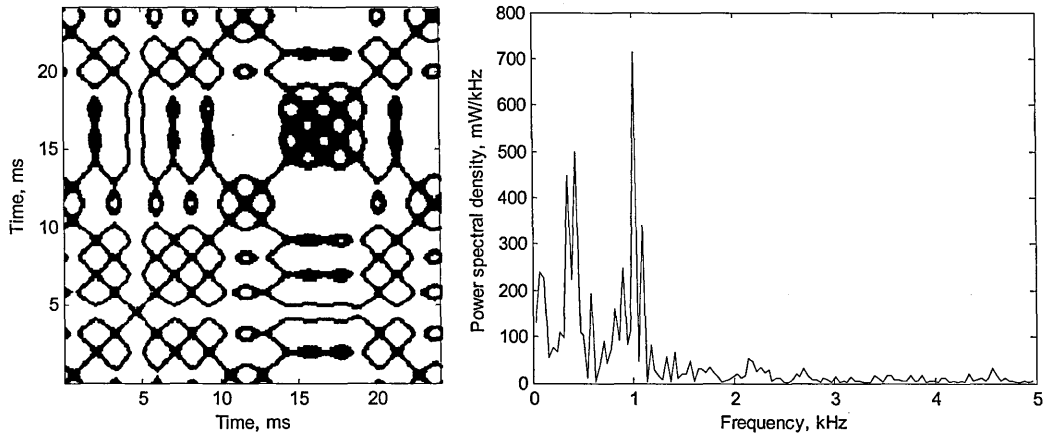
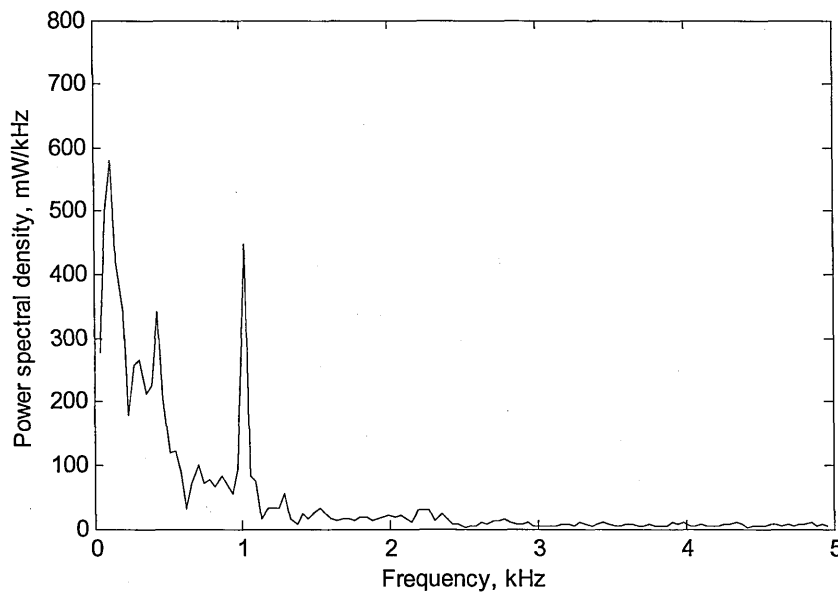


Figure 37. RP ( $\varepsilon = 0.175$ ) and Fourier transform of first row for BPSK, example B10.

A Fourier analysis of one row of the RP can be used to identify the symbol rate. One has to be careful, however, to distinguish between the spectral peaks since the pattern of symbols directly influences the position and relative strength of the peaks. In seven of the ten cases shown above the 1 kHz peak corresponding to the symbol rate was not the dominant peak.

One way of emphasising the spectral peak corresponding to the symbol rate is to average the power spectral density estimate over multiple sequences, which rejects user data in favour of information about the modulation.

The result of doing this for all ten example symbol sequences in set B is shown in Figure 38. The peak at 1 kHz is clearly visible and the averaging process has suppressed some of the information content of the symbol sequences in favour of the peak due to the symbol rate, which is the modulation characteristic of interest. It is important to note though, that the 1 kHz peak is not the dominant peak, so further work is still needed to suppress the user information.



**Figure 38. Fourier transforms of RP ( $\epsilon = 0.175$ ) first rows averaged over 10 examples in set B.**

This section has demonstrated a means of determining the symbol rate from the RP and considered the use of averaging to emphasise the power spectral density peak corresponding to the symbol rate. The averaging method, however, still left a number of strong peaks on the power spectral density estimate so the 1 kHz peak was not an unambiguous indicator of the symbol rate.

#### **4.1.3 Choice of threshold for BPSK symbol rate estimation from RP**

In the previous section the RP threshold,  $\epsilon$ , was set at 0.175 without justification. This section explains the choice of threshold.

Figure 39 shows a plot of the power spectral density at the 1 kHz peak for a range of thresholds.

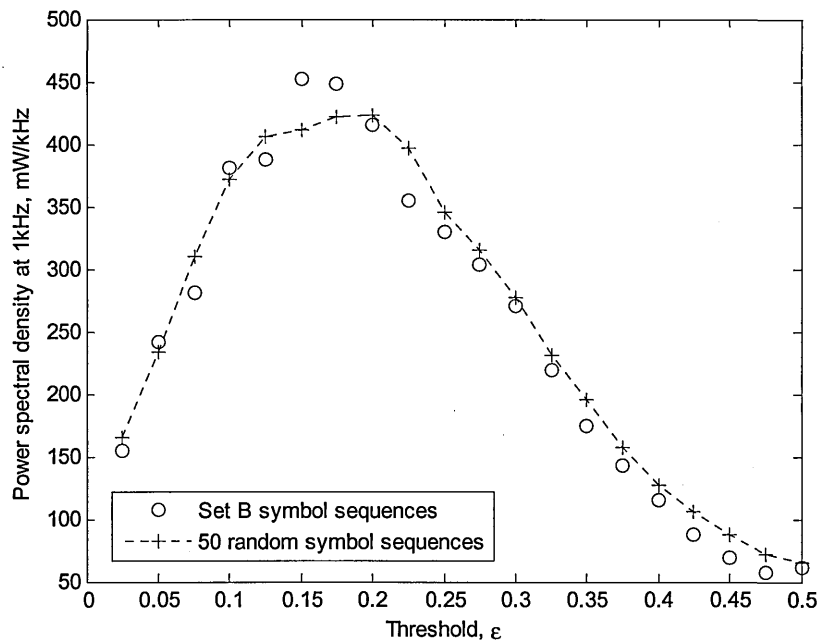


**Figure 39. Effect of varying threshold on estimate of power at 1 kHz, averaged over set B symbol sequences and over 50 random symbol sequences**

The results have been averaged over all ten set B symbol sequences from section 4.1.1 and also for 50 random symbol sequences in order to indicate the average performance more clearly. All sequences used had an equal number of ones and zeroes, reflecting the use of line codes in practical communications systems.

The difference between the data sets was not great when it came to optimising the threshold setting. The ten set B symbol sequences resulted in a peak threshold at 0.15 and the 50 random symbol sequences peak at 0.2. The maximum value appeared to be somewhere between these two, so a threshold 0.175 was chosen for the tests in section 4.1.2.

#### 4.1.4 Phase-symmetric Cross Recurrence Plots

In the form of equation (14) the RP does not take advantage of the inherent phase symmetry of PSK signals. As part of this Ph.D. the RP concept has been modified to exploit the phase symmetry that exists in many digital modulations.

This technique enhances the modulation component of a received signal at the expense of the information contained in its phase. The approach taken was to devise a variant of the CRP (Marwan *et al*, 2007) in which the received signal is compared with phase-rotated versions of itself.

The proposed phase-modified variant of the recurrence matrix is defined as:

$$RM_{m,n}(\varepsilon, D) = \bigcup_{k=0}^{2^D-1} \Theta\left(\varepsilon - \left\|x_m - x_n e^{ik\pi 2^{(1-D)}}\right\|\right) \quad (32)$$

where the signal,  $x$ , is compared with a phase-rotated version of itself. The Euclidean norm has been used here, but other norms could be explored as further research.

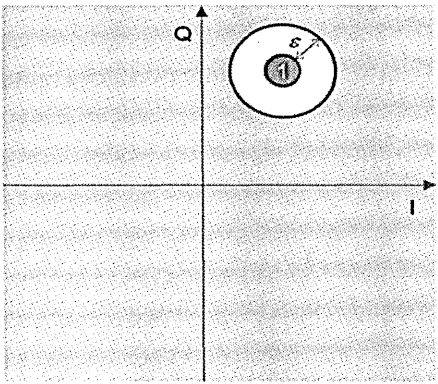
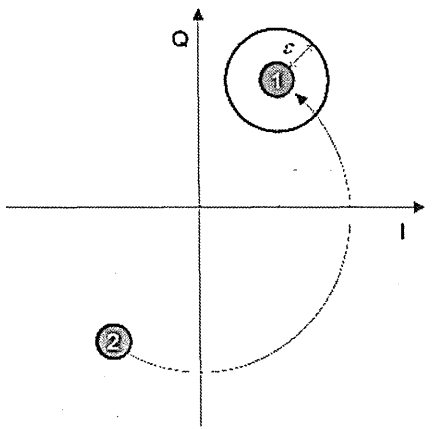
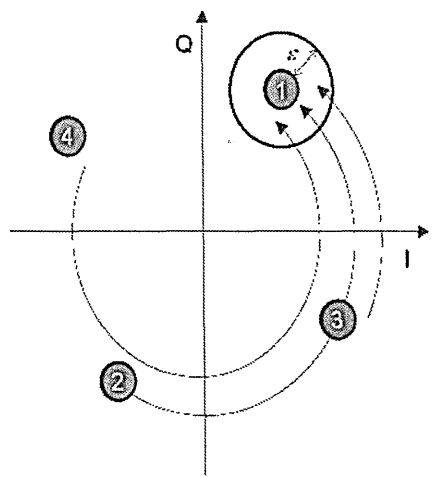
The parameter  $D$  is introduced here as an integer parameter called the 'symmetry depth'. When the symmetry depth is zero then equation (32) reduces to the conventional recurrence matrix (without embedding). Higher values of  $D$  allow this recurrence matrix to take advantage of the symmetries in phase modulated signals.



The plots from this equation will be called PCR<sub>P</sub> to distinguish them from conventional forms RP and CRP in the literature. The aim has been to manipulate the signal prior to analysis such that modulation features can be emphasised, which will be explained in the following paragraphs.

Note that it is common in recurrence plot work to use embedding, which is the practice of reconstructing the phase space from a series of samples. Embedding has not been included in the above definition, which simplifies the notation a little, as there is no need to consider the vector form. The application of embedding will be dealt with as further research, as it has not been found necessary to use it in the work to date.

The PCR<sub>P</sub> has been designed to remove some of the phase information in the signal. This can be demonstrated pictorially by considering the meaning of equation (32) in I/Q space.

	<p>In the PCR with <math>D = 0</math> any point in I/Q space that comes within the threshold Euclidean distance, <math>\epsilon</math>, of a starting point, 1, will appear as a dot on the PCR. All other points in I/Q space will not be shown on the PCR.</p>
	<p>With <math>D = 1</math> any point, such as point 2 shown here, that can be shifted by a rotation of <math>\pi</math> into the threshold region around point 1 will also appear as a dot on the PCR.</p>
	<p>At higher symmetry depths more points in I/Q space will be shifted into the error region around point 1. Here <math>D = 2</math> and points 2, 3 and 4 are all shifted into the threshold region. In the limit, as <math>D</math> approaches infinity, all samples in the signal that lie on the circle passing through point 1 would appear as dots on the PCR. Hence, as <math>D</math> increases, less phase information is preserved.</p>

It is clear that phase information is lost by this transformation, because it would not be possible to examine a dot on the PCRCP and work out unambiguously where it originated in I/Q space. In the last diagram of the series above a point within the error region around point 1 could have originated at any of points 1, 2, 3 or 4.

#### 4.1.5 BPSK symbol rate estimation from PCRCP

This section repeats the investigation of section 4.1.2 replacing the RP with the PCRCP. The figures below use a symmetry depth,  $D$ , of one and a threshold,  $\varepsilon$ , of 0.175 (section 4.1.6) and can be compared directly with those in section 4.1.2.

In Figure 40, which is obtained from example symbol sequence A1, it is clear that the spectral peak at 1 kHz corresponding to the symbol rate is the dominant peak. Comparing this PCRCP with the RP in Figure 26 it will be seen how the PCRCP has 'filled in' the plot with more points. Examining the Line Of Identity (LOI) the number of crossing points has doubled and also the number of points on the first row has doubled, which is why the peak at 0.5 kHz has been lost.

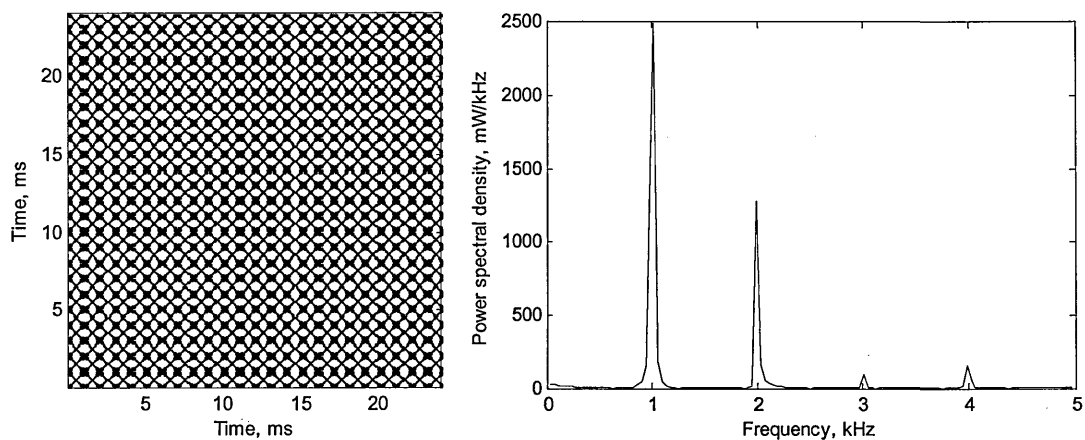


**Figure 40. PCRCP ( $D = 1$ ,  $\varepsilon = 0.175$ ) and Fourier transform of first row for BPSK, example A1 (alternating symols).**

This 'filling in' behaviour is seen in all the other examples below. Comparison with the previous graphs shows how the PCRp creates points that lie in the gaps on the original RP. Also it is clear that the 1 kHz spectral peak has, in all cases, been emphasised compared to the set of graphs in section 4.1.2.

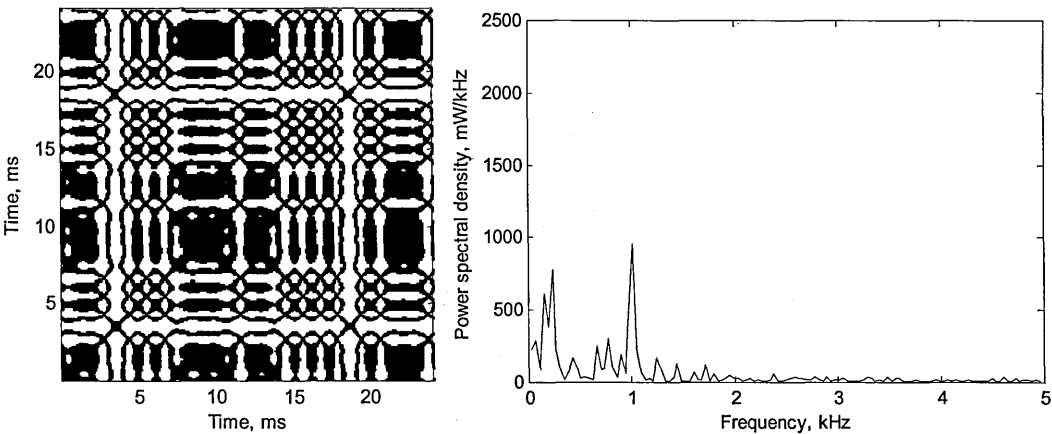


**Figure 41.** PCRp ( $D = 1$ ,  $\varepsilon = 0.175$ ) and Fourier transform of first row for BPSK, example B1.

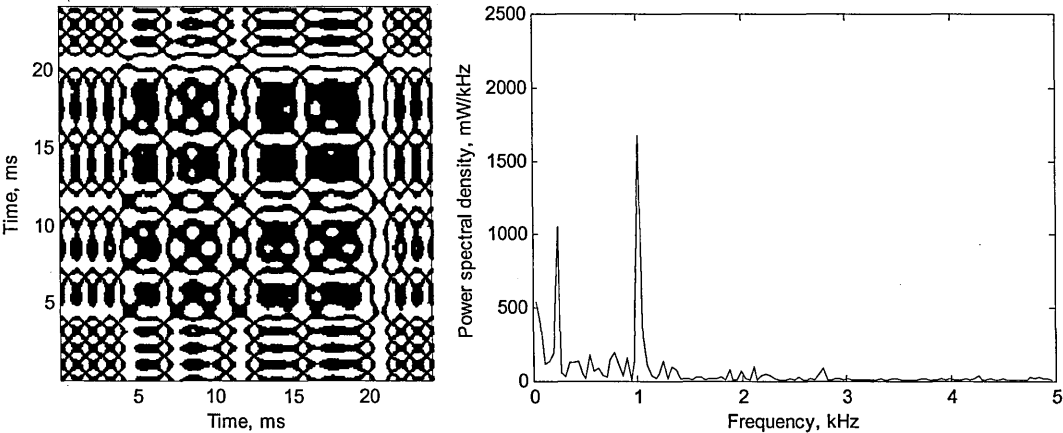


**Figure 42.** PCRp ( $D = 1$ ,  $\varepsilon = 0.175$ ) and Fourier transform of first row for BPSK, example B2.

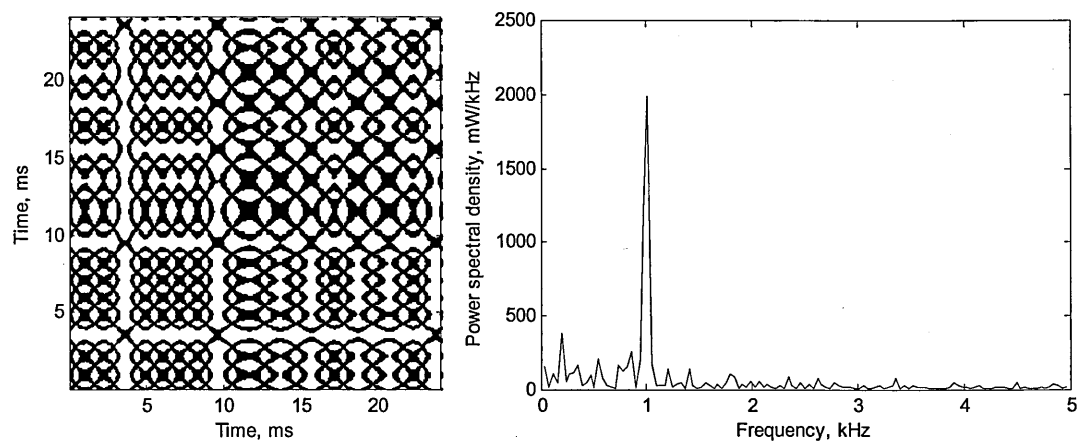


Figure 43. PCRP ( $D = 1$ ,  $\varepsilon = 0.175$ ) and Fourier transform of first row for BPSK, example B3.

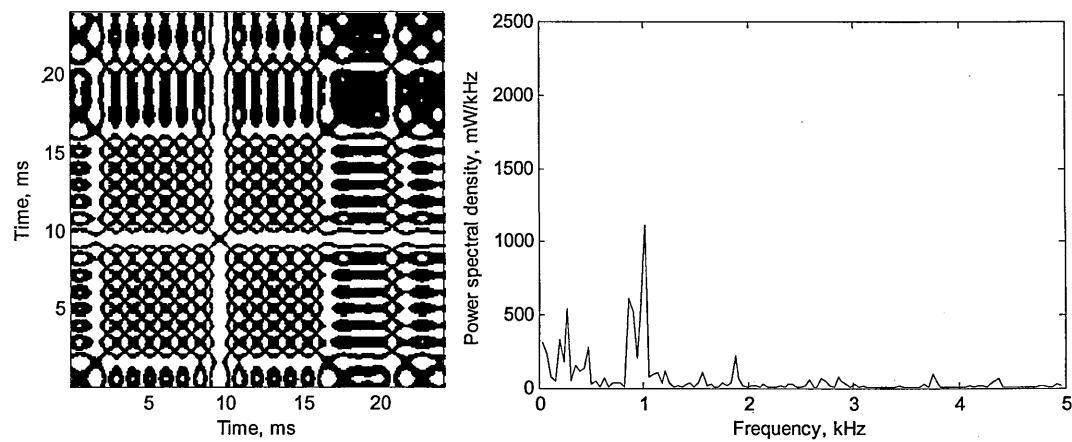


Figure 44. PCRP ( $D = 1$ ,  $\varepsilon = 0.175$ ) and Fourier transform of first row for BPSK, example B4.

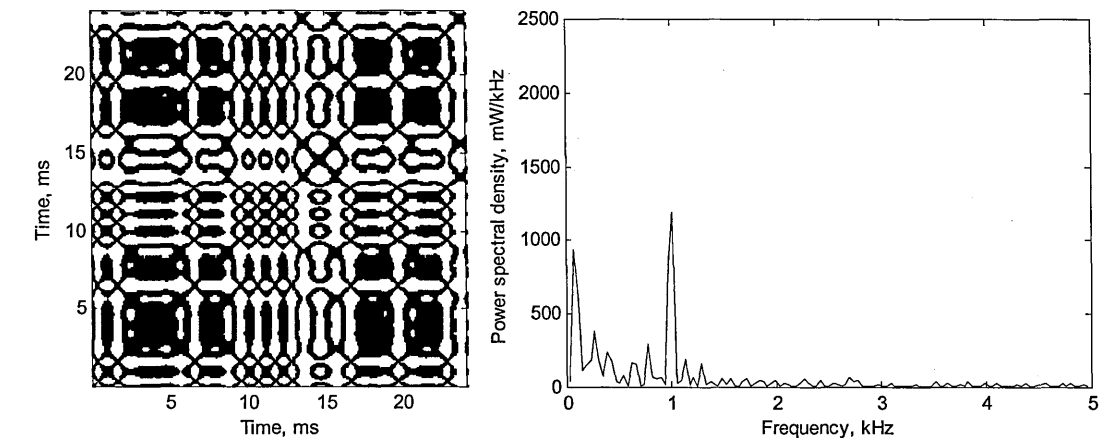


Figure 45. PCRCP ( $D = 1$ ,  $\varepsilon = 0.175$ ) and Fourier transform of first row for BPSK, example B5.

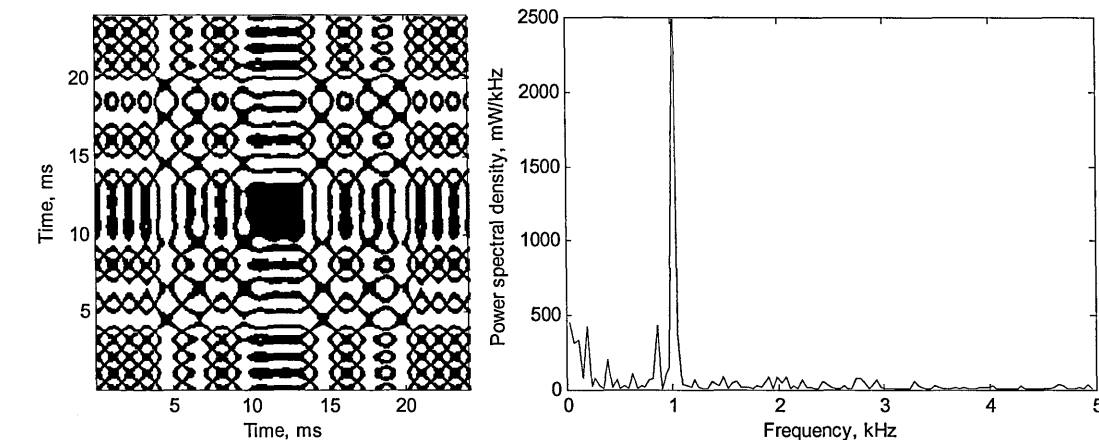


Figure 46. PCRCP ( $D = 1$ ,  $\varepsilon = 0.175$ ) and Fourier transform of first row for BPSK, example B6.

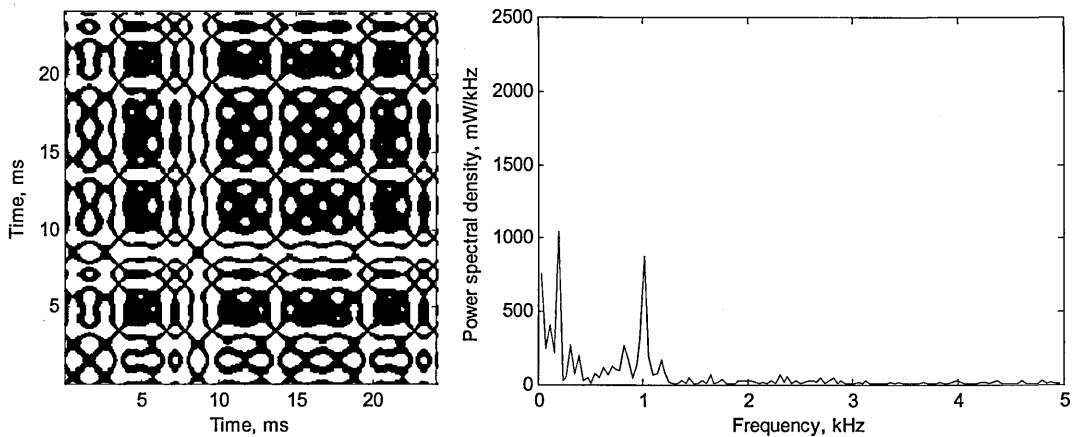


Figure 47. PCRCP ( $D = 1$ ,  $\varepsilon = 0.175$ ) and Fourier transform of first row for BPSK, example B7.

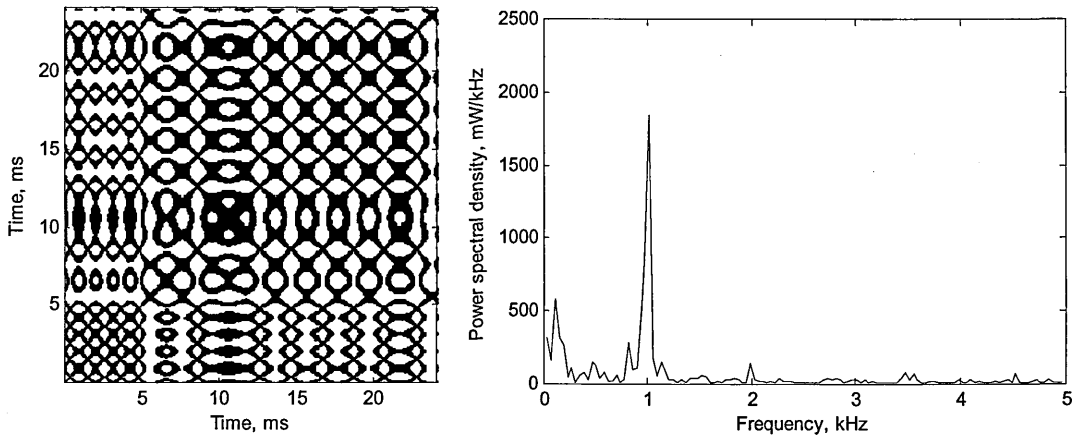
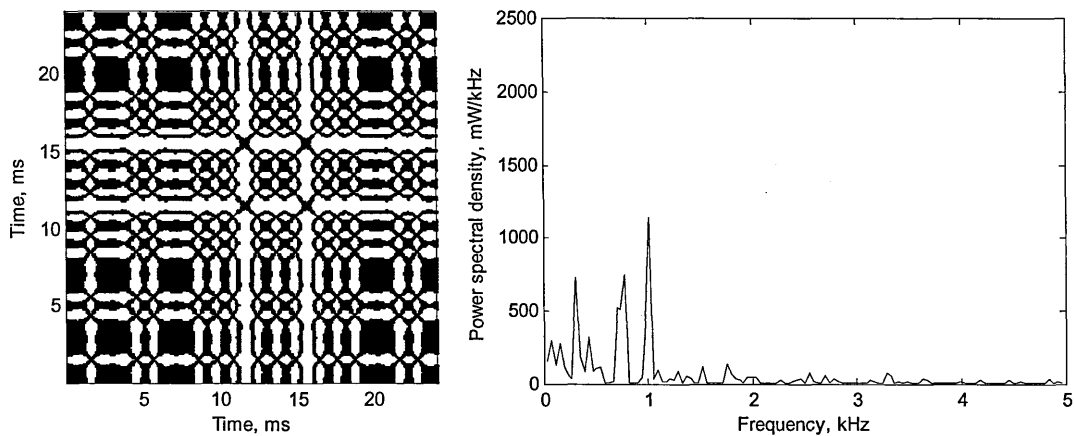
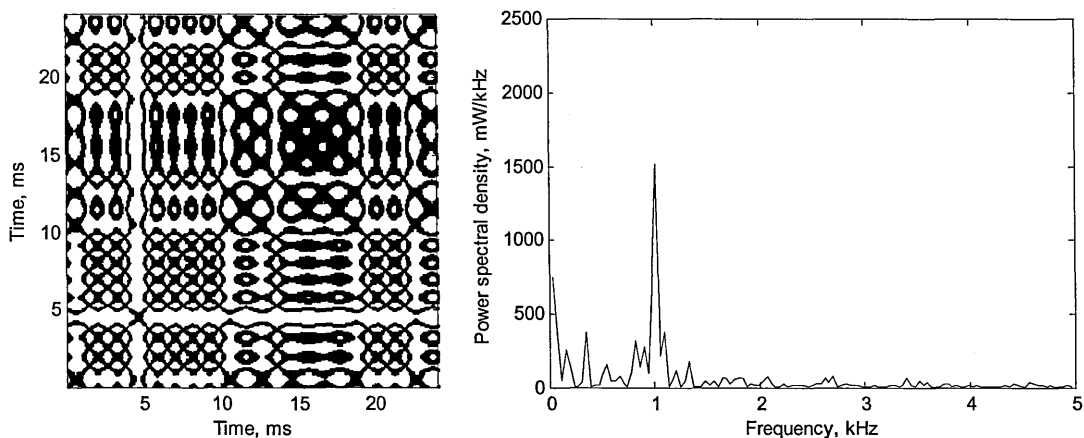


Figure 48. PCRCP ( $D = 1$ ,  $\varepsilon = 0.175$ ) and Fourier transform of first row for BPSK, example B8.



**Figure 49. PCRCP ( $D = 1$ ,  $\varepsilon = 0.175$ ) and Fourier transform of first row for BPSK, example B9.**



**Figure 50. PCRCP ( $D = 1$ ,  $\varepsilon = 0.175$ ) and Fourier transform of first row for BPSK, example B10.**

In section 4.1.2 averaging was performed to produce a combined power spectral density plot (Figure 38). Repeating this averaging, but this time using the spectra from the PCRCP results in Figure 51. Again the averaging emphasises the 1 kHz spectral peak and suppresses the other spectral components, but there has been further improvement in the clarity of the peak compared to the other spectral components because of the PCRCP processing.



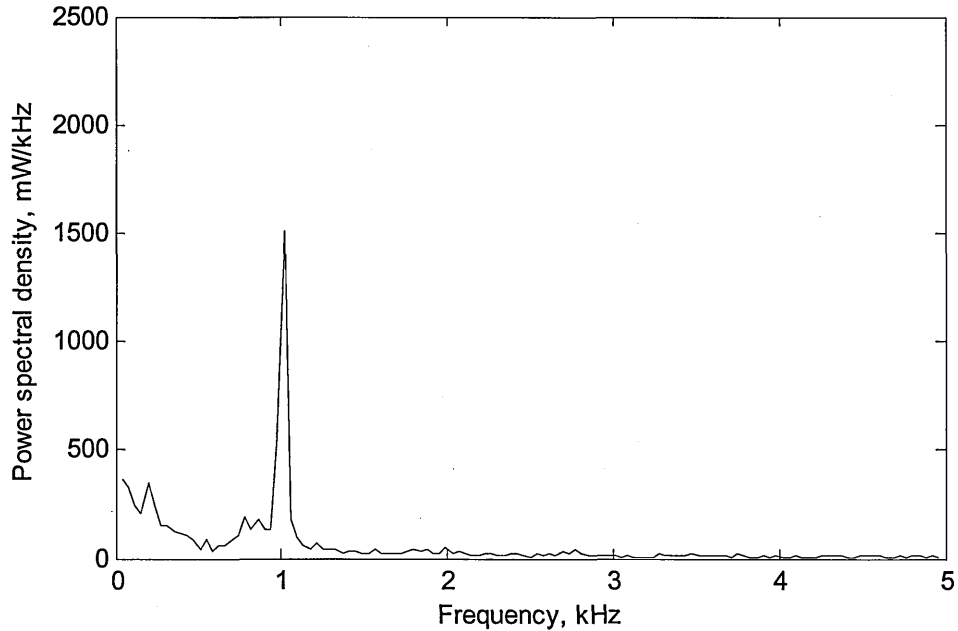


**Figure 51. Fourier transforms of PCR<sub>P</sub> ( $D = 1$ ,  $\varepsilon = 0.175$ ) first rows averaged over 10 examples in set B.**

This section has demonstrated a means of determining the symbol rate from the PCR<sub>P</sub> which produces results that are better than those from the RP, because the PCR<sub>P</sub> removes some of the information in the time domain leading to greater emphasis on the symbol rate. In particular it suppresses the spectral peak at half the symbol rate allowing the peak at the symbol rate to be the dominant peak.

#### **4.1.6 Choice of threshold for BPSK symbol rate estimation from PCR<sub>P</sub>**

The above examples of the PCR<sub>P</sub> method assumed a threshold,  $\varepsilon$ , of 0.175, which was also the value chosen for the RP method. It is reasonable to question whether the same threshold should be used for both methods.

Figure 52 can be compared with Figure 39 and shows the average height of the 1 kHz spectral peak for a range of thresholds.

Results are given for both the ten set B symbol sequences and 50 random symbol sequences in order to indicate the average performance more clearly. A value of 0.175 was clearly close to the maximal value overall and was chosen for the examples given here.

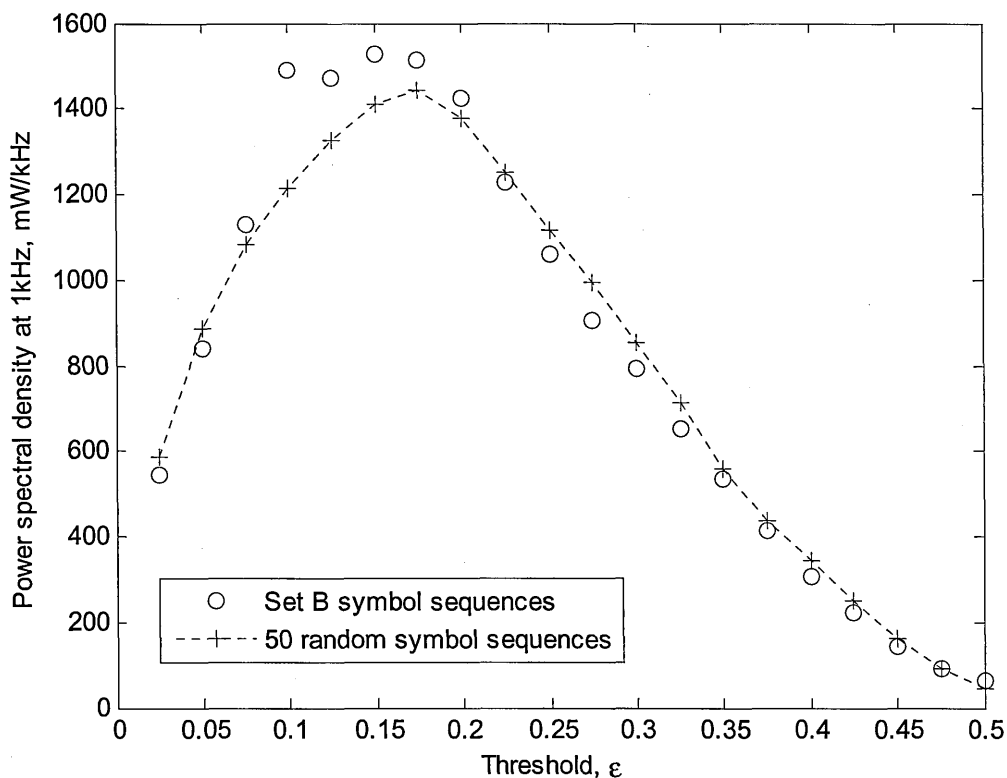


**Figure 52.** Effect of varying threshold on estimate of power at 1 kHz, averaged over set B symbol sequences and over 50 random symbol sequences using PCRP ( $D = 1$ ).

#### 4.1.7 Comparison of RP and PCRP for BPSK symbol rate detection

The relative heights of the 1 kHz peaks in the power spectral density graphs have been calculated for all examples in set B using BPSK modulation. It was found that using the conventional RP ( $\varepsilon = 0.175$ ) led to an average peak that is 7% of the total power.

Note that, in order to make the RP and PCRP comparable in this way, the 'DC' terms must be removed which is achieved by subtracting the mean of the RP or PCRP before calculating the power spectral density.

Analysing the same ten cases using the PCRP approach ( $D = 1$ ,  $\varepsilon = 0.175$ ) led to the average 1 kHz peak height increasing to 16% of the total power. This is a significant result as it suggests that the symbol rate detection capability has been more than doubled by deliberately removing phase information via the PCRP method.

Figure 53 illustrates this result further by showing how the relative 1 kHz peak height varies with the threshold parameter,  $\varepsilon$ . The PCRP ( $D = 1$ ) demonstrates an improvement in peak height across all thresholds examined.

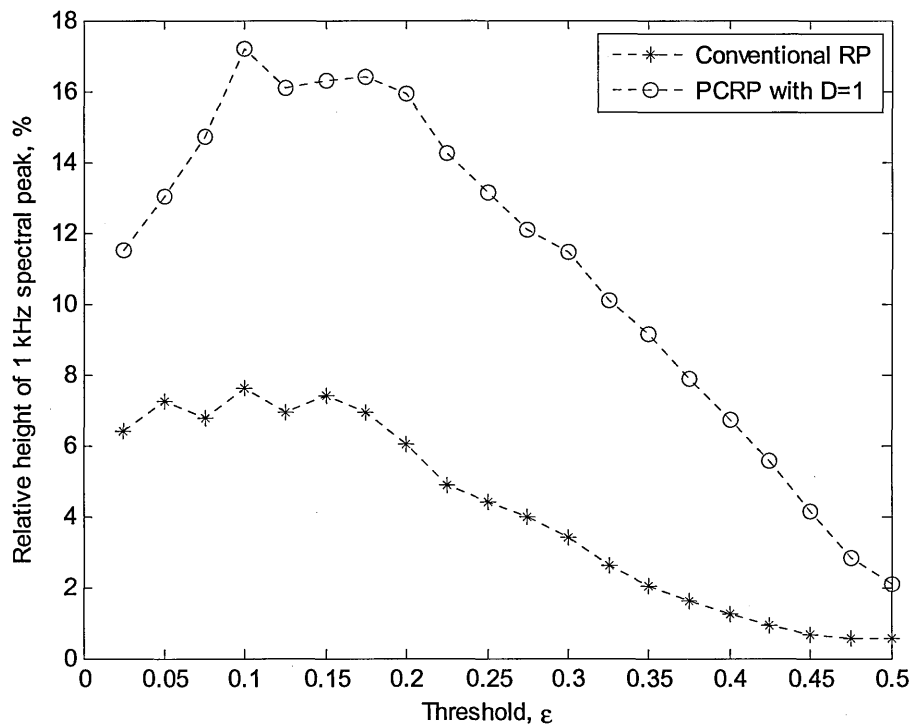


**Figure 53. Comparison of 1 kHz peak height for RP and PCR methods averaged over set B with BPSK modulation.**

These results have helped to show how, for BPSK, information can be suppressed in favour of the modulation parameter of interest, in this case the symbol rate. The next paragraphs go on to extend this analysis to QPSK and show how the same principle also applies to that type of modulation.

**4.1.8 QPSK symbol rate estimation from RP**

This section considers QPSK, which is approached in a similar way to BPSK in section 4.1.2. Detecting the symbol rate is used to show how the RP and PCR can be analysed.

The symbol rate can be detected via a 1 kHz peak in the power spectral density estimate obtained via a Fourier transform of the first row of the RP. In this case the threshold used for the RP was again 0.175, as explained in section 4.1.10

Figure 54 shows the RP and power spectral density plots for the C1 example. The first observation to make is that, because this example sequence progresses around an I/Q circle there are no sudden phase shifts and the RP in Figure 54 comprises only lines parallel to the LOI. Another observation is that, in the corresponding Fourier Transform plot, the 1 kHz peak now has three lower subharmonics which is a result of there being four phases in the constellation rather than two.

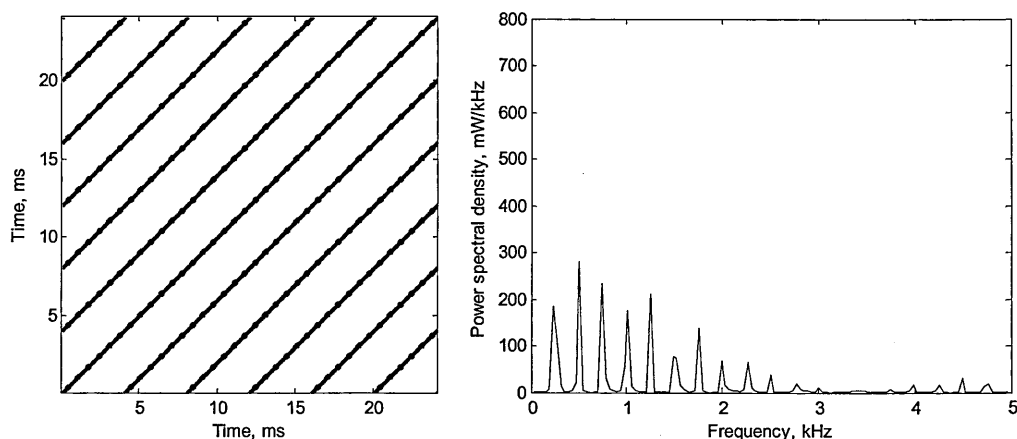


**Figure 54. RP ( $\epsilon=0.175$ ) and Fourier transform of first row for QPSK, example C1.**

The following plots show the results obtained for the first three example sequences in set D. At a subjective level the RPs do not reveal the symbol boundaries as clearly in the QPSK examples as they did in the BPSK examples of section 4.1.2.

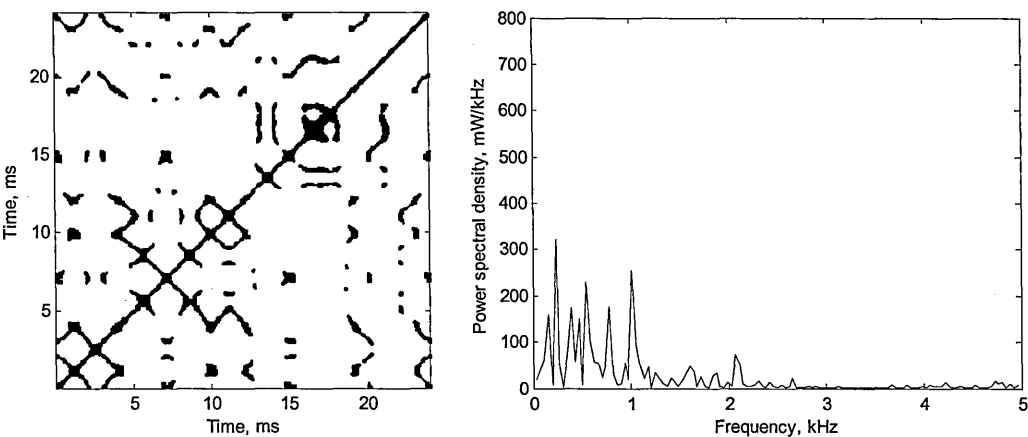


Figure 55. RP ( $\varepsilon=0.175$ ) and Fourier transform of first row for QPSK, example D1.

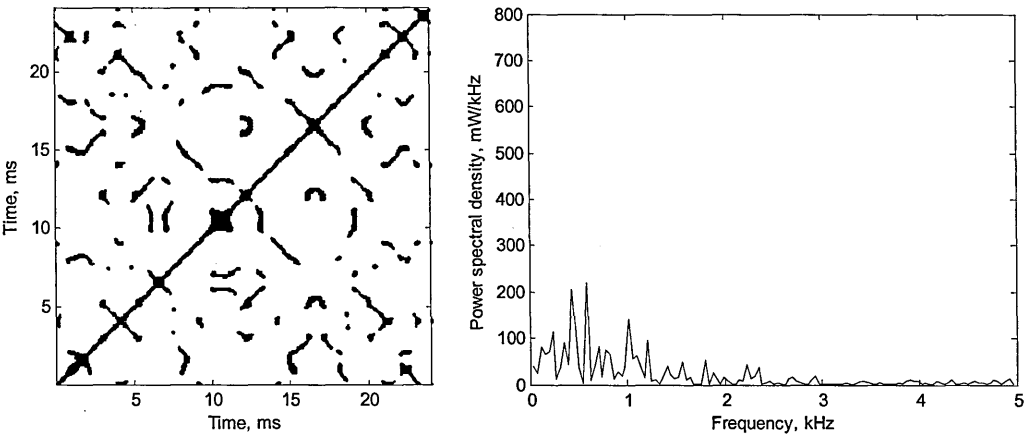


Figure 56. RP ( $\varepsilon=0.175$ ) and Fourier transform of first row for QPSK, example D2.

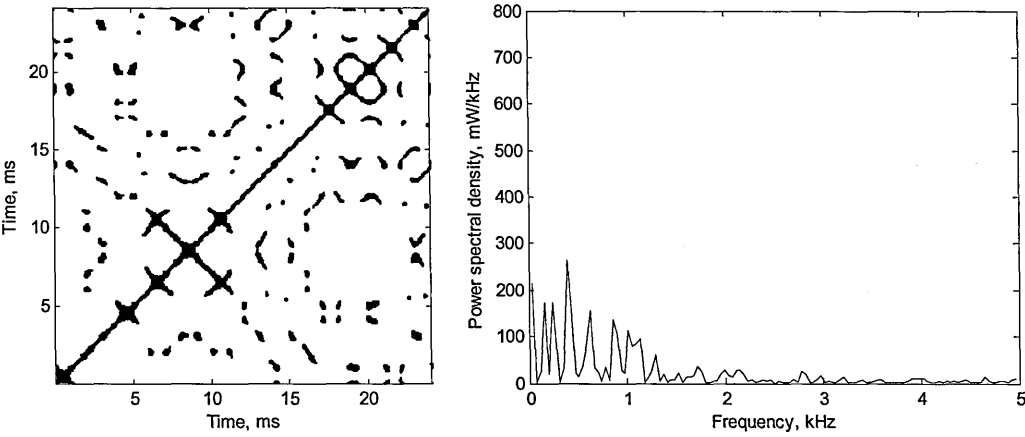
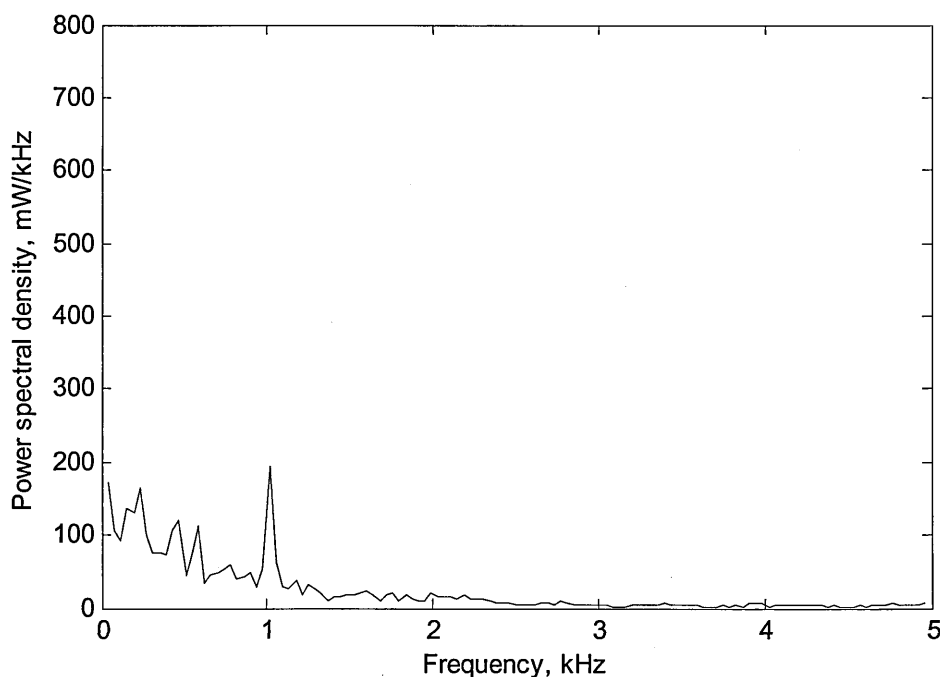


Figure 57. RP ( $\varepsilon=0.175$ ) and Fourier transform of first row for QPSK, example D3.

As with the discussion on BPSK in section 4.1.2 the 1 kHz spectral peaks can be aggregated by averaging over multiple symbol sequences. Figure 58 is obtained by averaging over the 10 set D examples.



**Figure 58. Fourier transforms of RP ( $\varepsilon = 0.175$ ) first rows averaged over set D, QPSK**

Some suppression of the other peaks has occurred but more suppression would be needed to make the 1 kHz peak an unambiguous indicator of the symbol rate.

#### **4.1.9 QPSK symbol rate estimation from PCRP**

The PCRP can be applied to the problem of QPSK symbol rate estimation in the same way it was applied in section 4.1.5 for BPSK. The PCRP has been designed with a symmetry depth parameter that can be increased to remove more phase information. This section presents some examples that illustrate the effect of increasing the symmetry depth and concludes with using this mechanism prior to performing averaging of the spectra.

Consider the first QPSK example, which has already been looked at in the previous section in terms of applying the conventional RP. In the PCRP the conventional RP is obtained by setting  $D = 0$ . The analysis of BPSK above used  $D = 1$ . The symmetry depth is now increased further in Figure 59 to Figure 62.

When  $D = 0$  and  $D = 1$  the 1 kHz peak has three subharmonics and one subharmonic respectively. However, when  $D = 2$  the 1 kHz peak is dominant and there are no significant subharmonics, which indicates that the PCRP is now matched to the modulation type. There are four constellation points in QPSK and the PCRP with  $D = 2$  maps the four constellation points into the threshold region.

Also shown (Figure 62) is the case where  $D = 3$ . There is no 1 kHz peak showing that the PCRP is no longer matched to the QPSK modulation. It has been found that increasing the symmetry depth beyond the value at which the PCRP is matched to the modulation produces no further improvement in the height of the symbol rate peak and will not be considered further in this thesis as it is not a useful mode of operation.



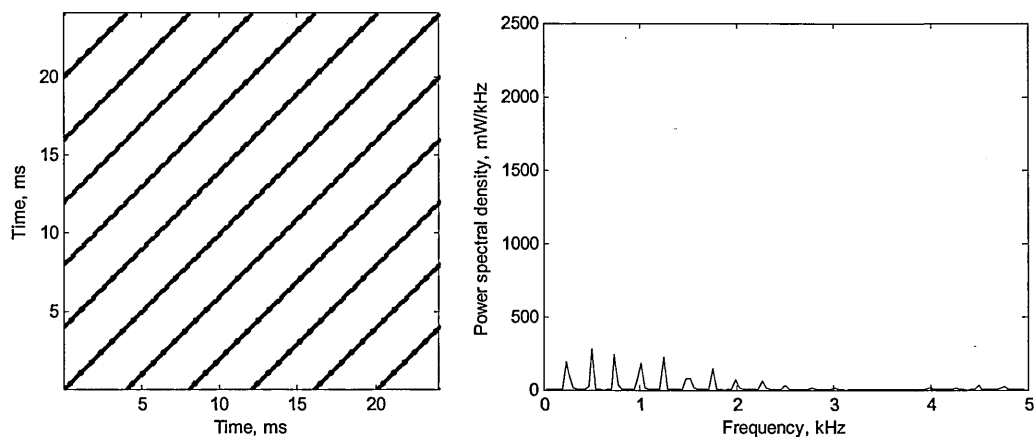


**Figure 59. PCRP ( $D = 0$ ,  $\varepsilon = 0.175$ ) and Fourier transform of first row for QPSK, example C1.**

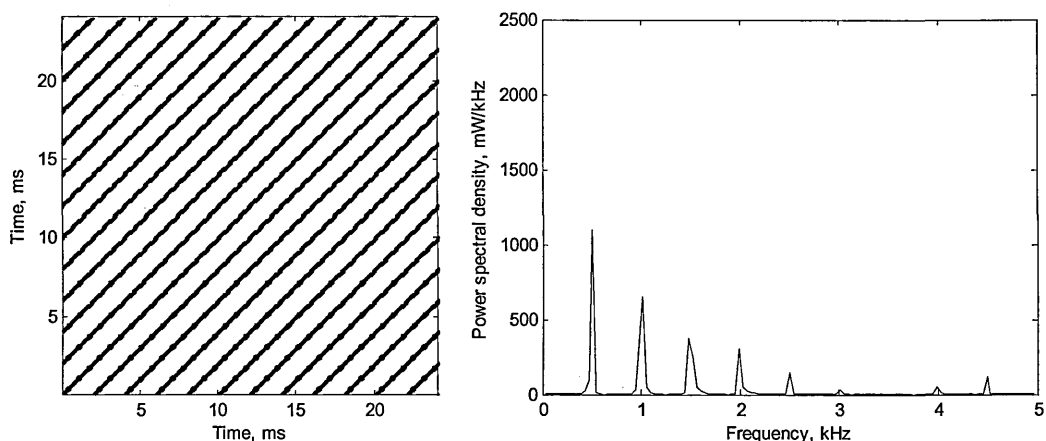


**Figure 60. PCRP ( $D = 1$ ,  $\varepsilon = 0.175$ ) and Fourier transform of first row for QPSK, example C1.**

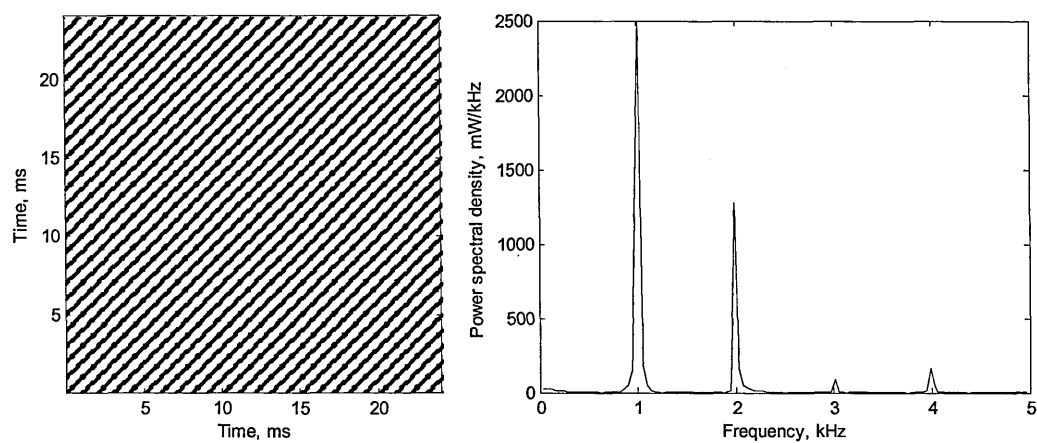


Figure 61. PCRCP ( $D = 2$ ,  $\varepsilon = 0.175$ ) and Fourier transform of first row for QPSK, example C1.

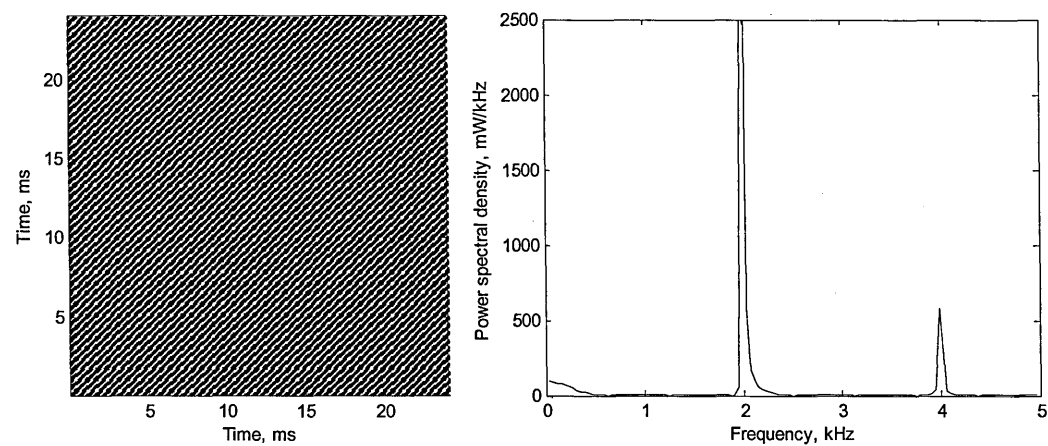
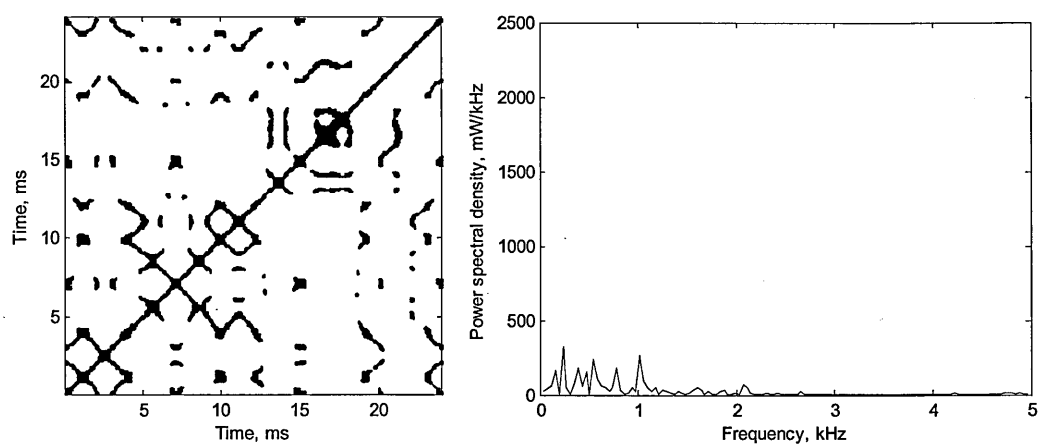
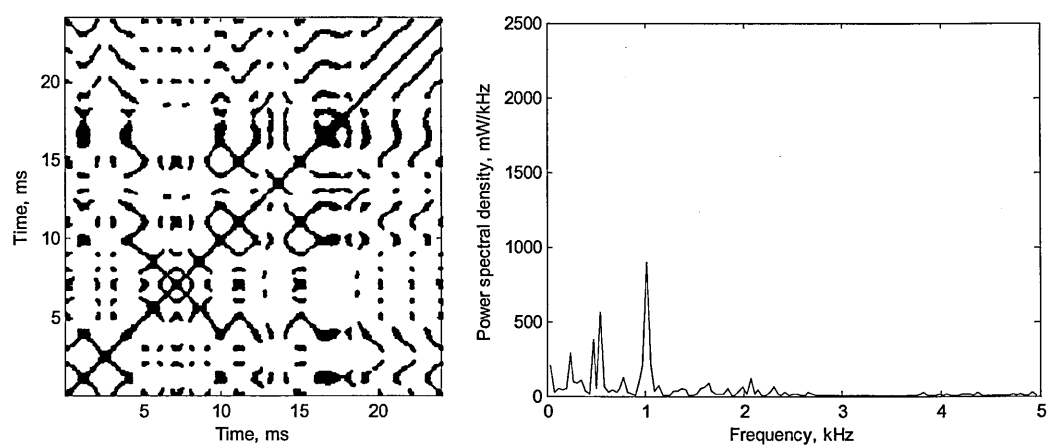


Figure 62. PCRCP ( $D = 3$ ,  $\varepsilon = 0.175$ ) and Fourier transform of first row for QPSK, example C1.

Now consider the PCRPs of the first example from set D in the following three figures. It will be seen how increasing the symmetry depth from zero to two 'fills in' in the recurrence plots and also how the 1 kHz spectral peak is emphasised when the symmetry depth equals two. These same behaviours are seen in all the set D examples.



**Figure 63.** PCRP ( $D = 0$ ,  $\varepsilon = 0.175$ ) and Fourier transform of first row for QPSK, example D1.



**Figure 64.** PCRP ( $D = 1$ ,  $\varepsilon = 0.175$ ) and Fourier transform of first row for QPSK, example D1.

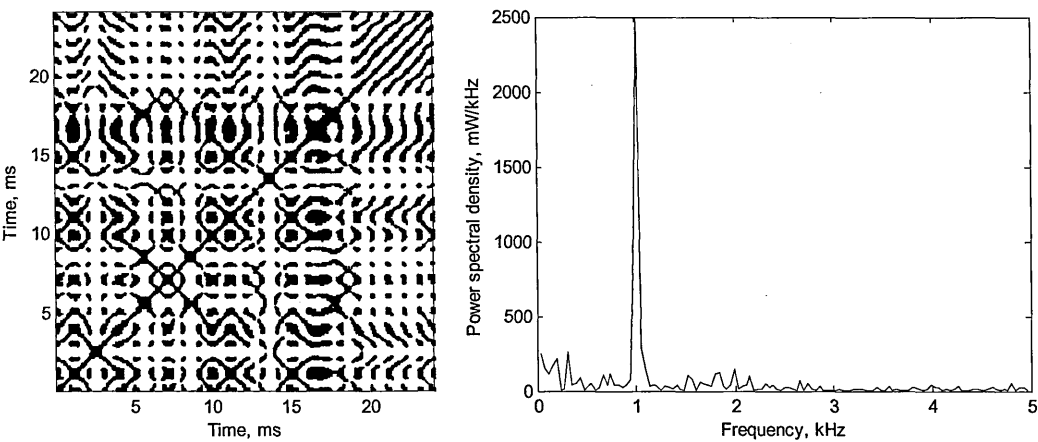


Figure 65. PCR P. ( $D = 2$ ,  $\varepsilon = 0.175$ ) and Fourier transform of first row for QPSK, example D1.

As with the previous examples the power spectral density plots can be averaged and this suppresses the frequency components that are not present in all the examples. The result is shown in Figure 66 which is directly comparable with Figure 58. It can be seen that using the PCR P with  $D = 2$  has resulted in emphasis of the 1 kHz spectral peak corresponding to the 1 kBaud QPSK symbol rate.

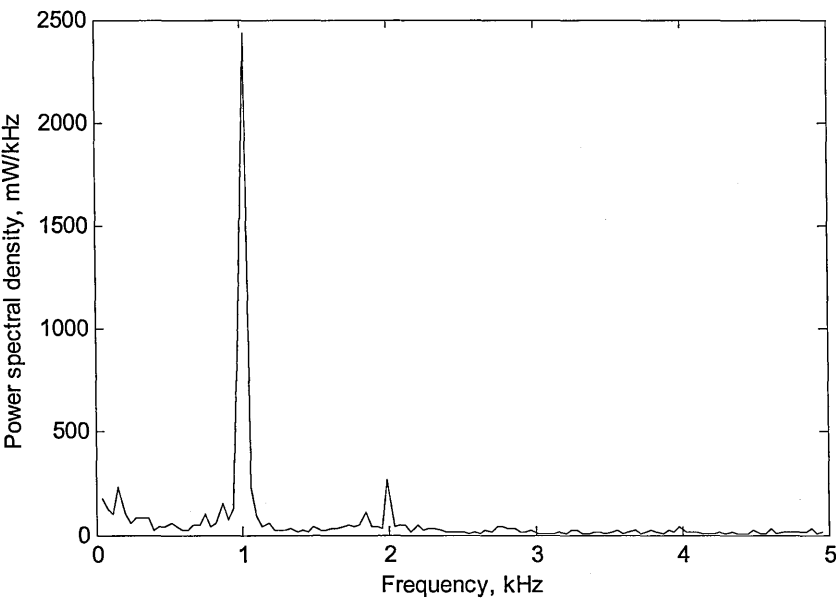


Figure 66. Fourier transforms of PCR P ( $D = 2$ ,  $\varepsilon = 0.175$ ) first rows averaged over set D, QPSK.

#### 4.1.10 Choice of threshold for QPSK symbol rate estimation

As with the BPSK analysis the choice of threshold for the RP and PCRP representations for QPSK analysis needs to be justified. Figure 67 shows the height of the 1 kHz spectral peak for a range of thresholds and for three different representations: the conventional RP and the PCRP with  $D=1$  and  $D=2$ . Inspection of Figure 67 suggests that some performance advantages would be gained by determining the best threshold for each representation individually.

It was decided, for the purposes of this exploration of the technique, to use a fixed threshold of 0.175 for two main reasons:

1. To retain commonality with the BPSK investigation.
2. Practical implementations will either have to use fixed thresholds or adapt their thresholds to the received signal. Whichever design were used it would be necessary to gain an understanding of performance with a fixed threshold.

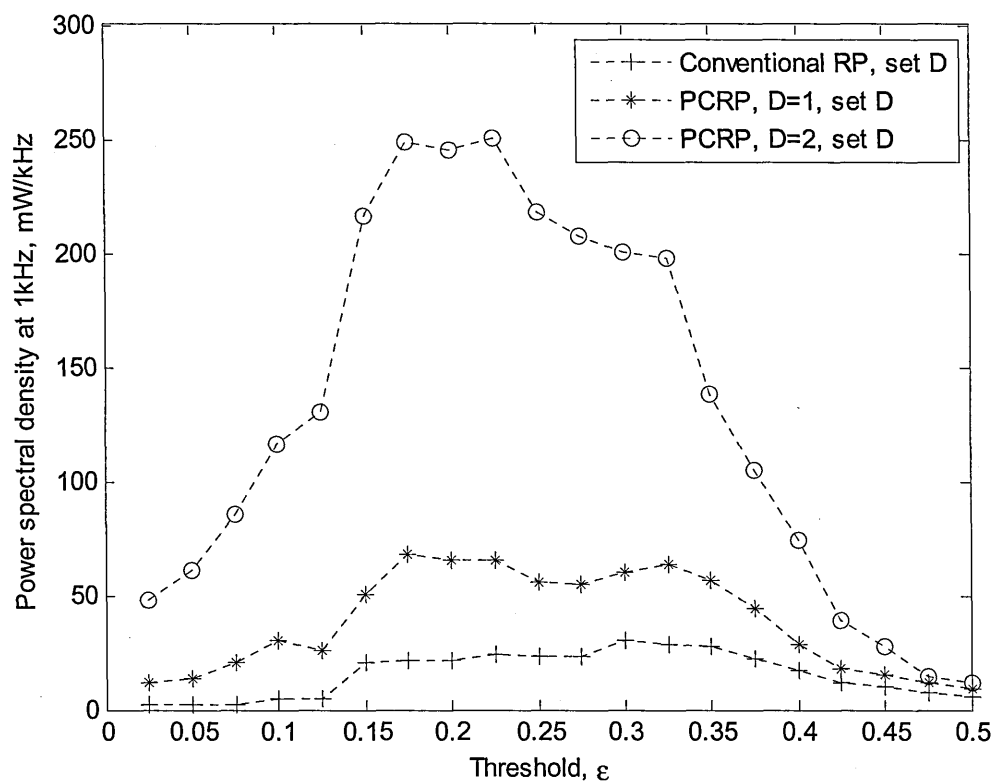


**Figure 67. Effect of varying threshold on estimate of QPSK power at 1 kHz, averaged across set D examples.**

The research to date has not investigated the choice of thresholds for these representations in depth. It is felt that improved understanding will come from developing optimisation criteria, so further research is needed in this area. For the purposes of this thesis it is sufficient to recognise that the thresholds have to be optimised in order to obtain the best performance from RP-based methods.

#### 4.1.11 Comparison of RP and PCRP for QPSK symbol rate detection

Section 4.1.7 compared the RP and PCRP methods for measuring the symbol rate in BPSK. This section carries out a similar analysis for QPSK.

The relative heights of the 1 kHz peaks in the power spectral density graphs have been calculated for all 10 examples in set D with QPSK modulation. It was found that using the conventional RP ( $\epsilon=0.175$ ) led to an average peak that is 6% of the total power. Analysing the same ten cases using the PCRP approach ( $\epsilon = 0.175$ ) led to the average 1 kHz peak height increasing to 12% of the total power when  $D = 1$  and 24% when  $D = 2$ . Thus, as with BPSK, the symbol rate peak can be significantly enhanced when the PCRP method is used. If the symmetry depth is increased further to  $D = 3$  the 1 kHz peak height reduces to 15% of the total power.

Figure 68 shows the results for QPSK and is directly comparable with Figure 53 which showed the results for BPSK. The figure shows how the relative 1 kHz peak height varies with the threshold parameter,  $\epsilon$ , and symmetry depth,  $D$ . The PCRP ( $D = 1$  and  $D = 2$ ) demonstrates an improvement in peak height across all thresholds examined but especially so when  $D = 2$ .

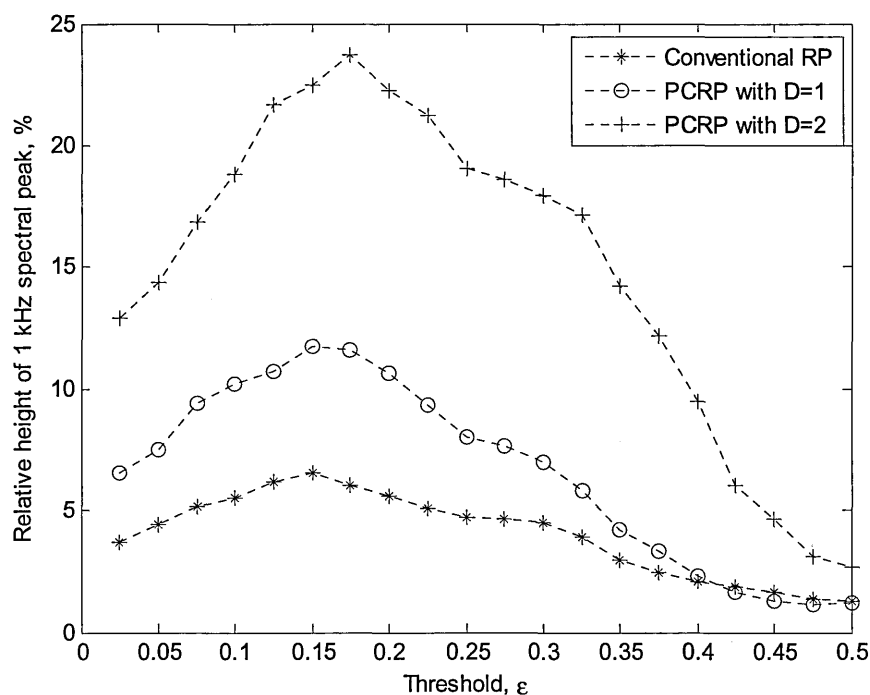


**Figure 68. Comparison of 1 kHz peak height for RP and PCRP methods averaged over all set D examples, QPSK.**

It must be emphasised that, in order to get the best performance from the PCRP, the symmetry depth parameter,  $D$ , must be matched to the modulation type. This is not ideal from an ASR point of view, so further work is needed to determine whether other modifications to the PCRP could remove this dependence on *a priori* knowledge of modulation type.

These results have showed how information may be removed from a representation by manipulating that representation deliberately in such a way that a modulation characteristic of interest is emphasised over the information content. In the case of both BPSK and QPSK modulation it has been possible to modify the RP representation such that the information content is suppressed and the symbol rate is emphasised.



#### 4.1.12 Application to other modulation types

The detection of symbol rate via the RP and PCRP methods has been described in the above paragraphs. The method can be applied to other modulation types, but is most suited to digital modulations where the information is encoded in the phase of the signal. This section lists some examples to illustrate this.

In this section the threshold has been set to 0.175 throughout without considering the optimisation in detail. This approach allows the plots to be compared with those in the BPSK and QPSK investigation.

##### 4.1.12.1 PSK8

BPSK and QPSK were used to explain the PCRP method and these required symmetry depths of one and two respectively to enhance the symbol rate. PSK8 is the next modulation in this series and, as expected, it requires a symmetry depth of three for symbol rate enhancement by the PCRP. The example shown in Figure 69 to Figure 72 is for a single sequence of 24 symbols (2 3 1 7 4 5 4 2 3 5 7 4 5 3 6 0 1 6 1 0 0 7 2 6) with a symbol rate of 1 kBaud and a sample rate of 10 kSamples/s. It will be seen that the 1 kHz spectral peak is enhanced significantly when the symmetry depth,  $D = 3$ .

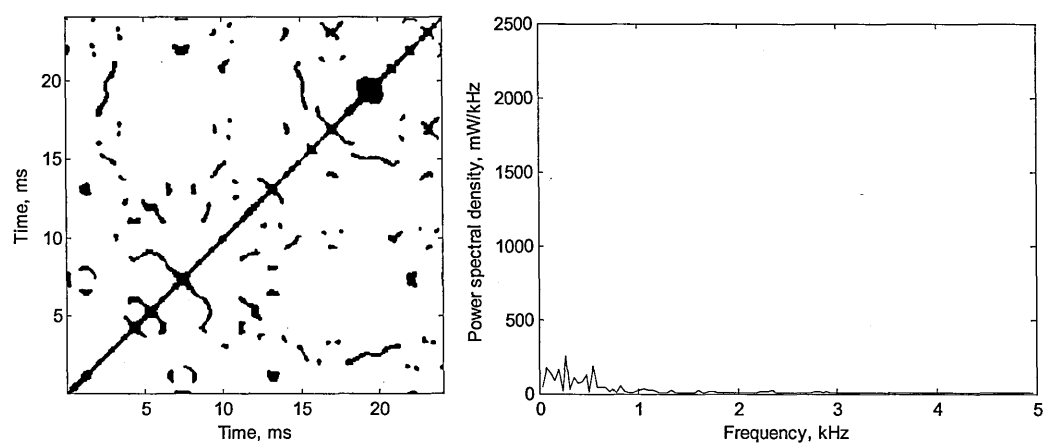


Figure 69. PCRCP ( $D = 0$ ,  $\varepsilon = 0.175$ ) and Fourier transform of first row for PSK8.

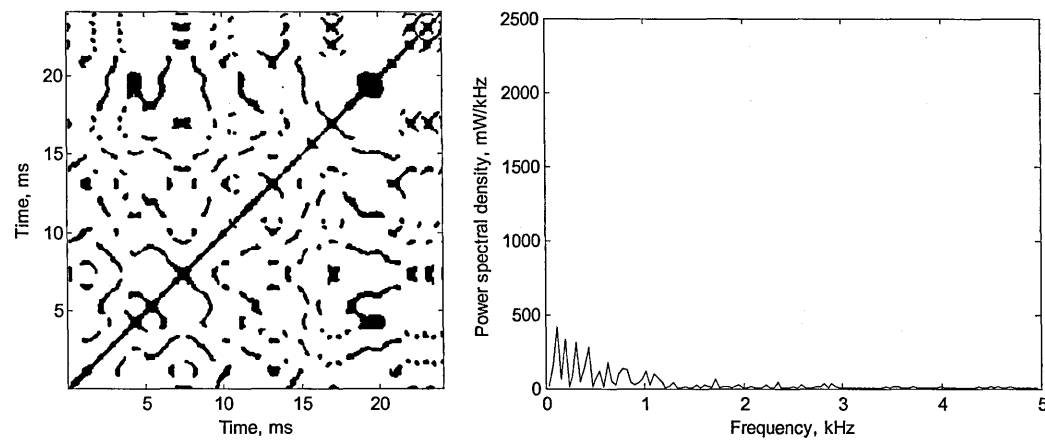


Figure 70. PCRCP ( $D = 1$ ,  $\varepsilon = 0.175$ ) and Fourier transform of first row for PSK8.

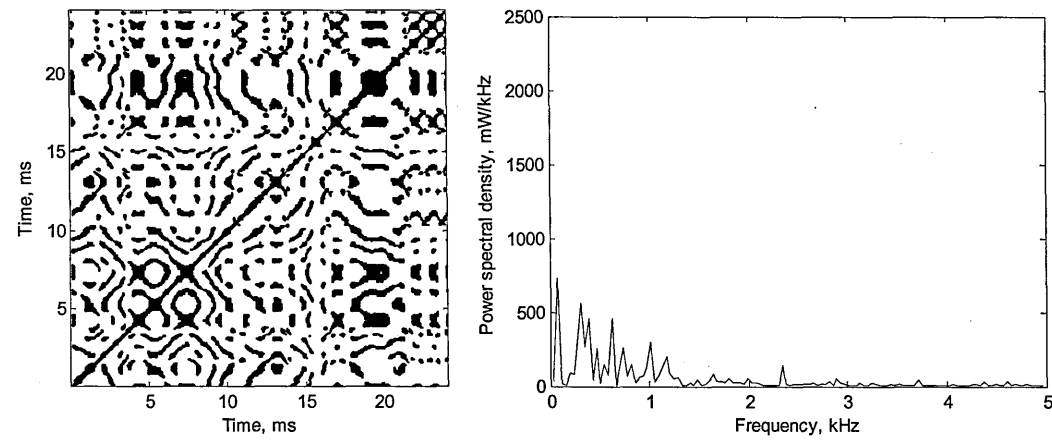


Figure 71. PCRCP ( $D = 2$ ,  $\varepsilon = 0.175$ ) and Fourier transform of first row for PSK8.

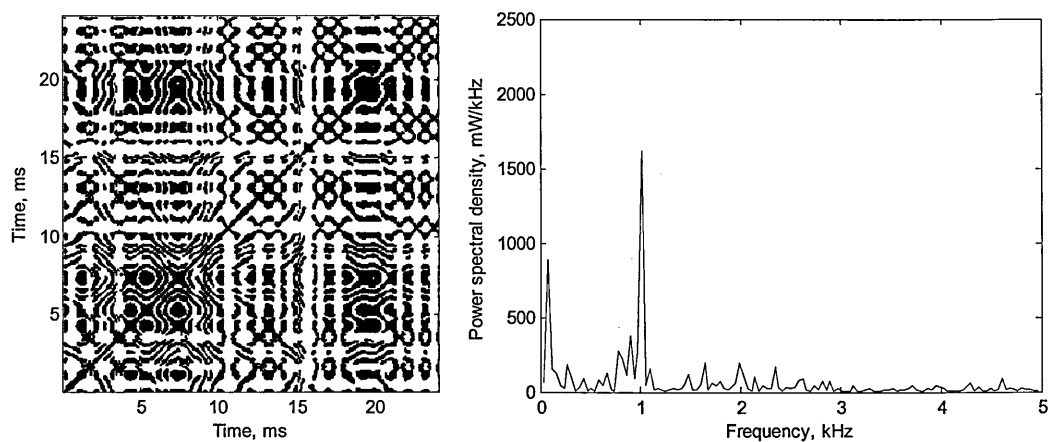


Figure 72. PCRP ( $D = 3$ ,  $\varepsilon = 0.175$ ) and Fourier transform of first row for PSK8.

#### 4.1.12.2 Frequency Shift Keying

FSK is shown in the following two figures which use FSK2 and symbol sequence A1 with a frequency separation of 2 kHz, a symbol rate of 1 kBaud and a sample rate of 10 kSamples/s. The 1 kHz peak (and harmonics thereof) is clearly visible with no need to use the PCRP. Further investigation shows that the symmetry depth needs to be increased to one if the frequency separation is close to, or less than, the symbol rate.

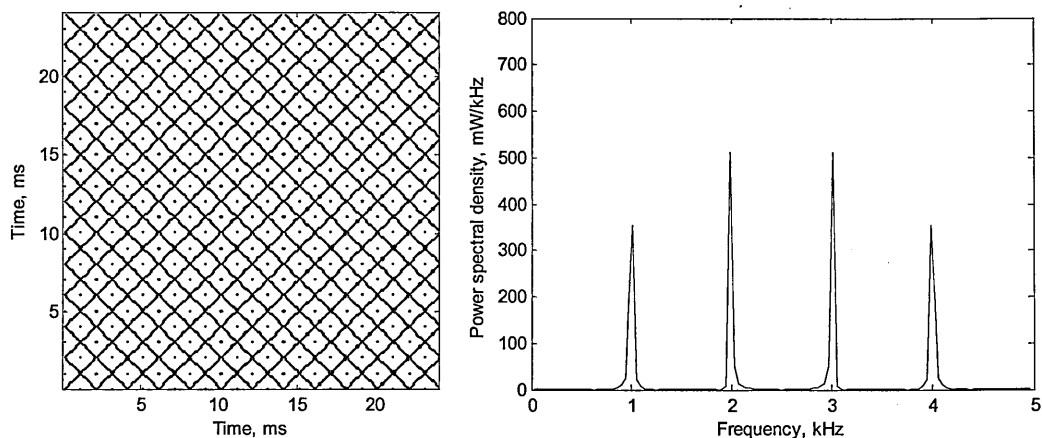


Figure 73. RP ( $\varepsilon = 0.175$ ) and Fourier transform of first row for FSK2, example A1.

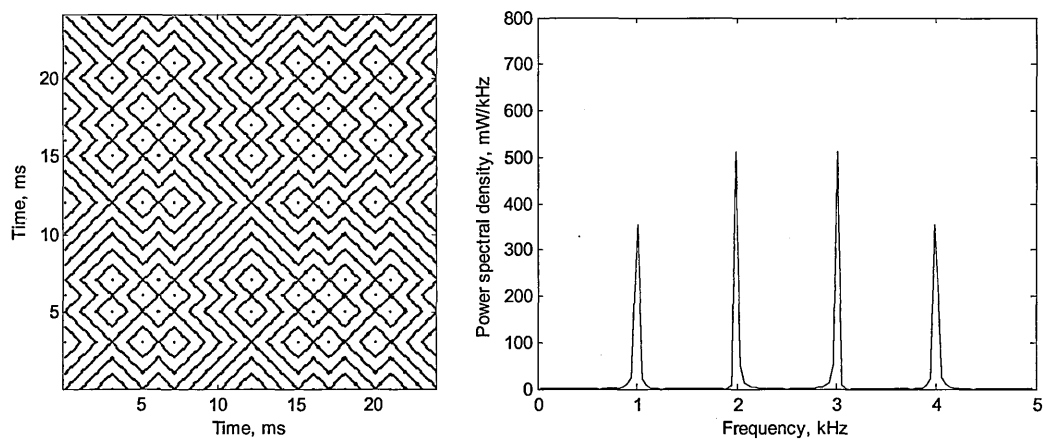


Figure 74. RP ( $\epsilon = 0.175$ ) and Fourier transform of first row for FSK2, example B1.

FSK4 is similar to FSK2 but there is a subjective difference in the RP. The two examples below use the QPSK example symbol sequences as inputs and have the same parameters as the FSK2 above.

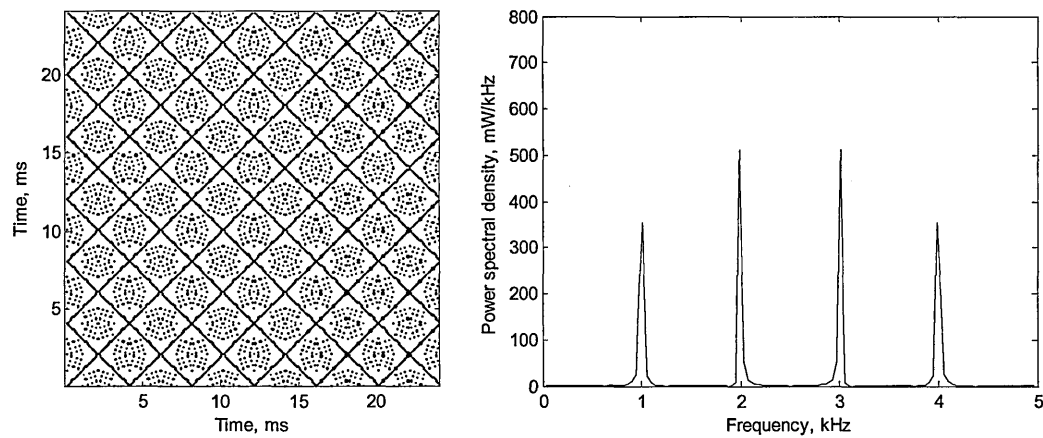
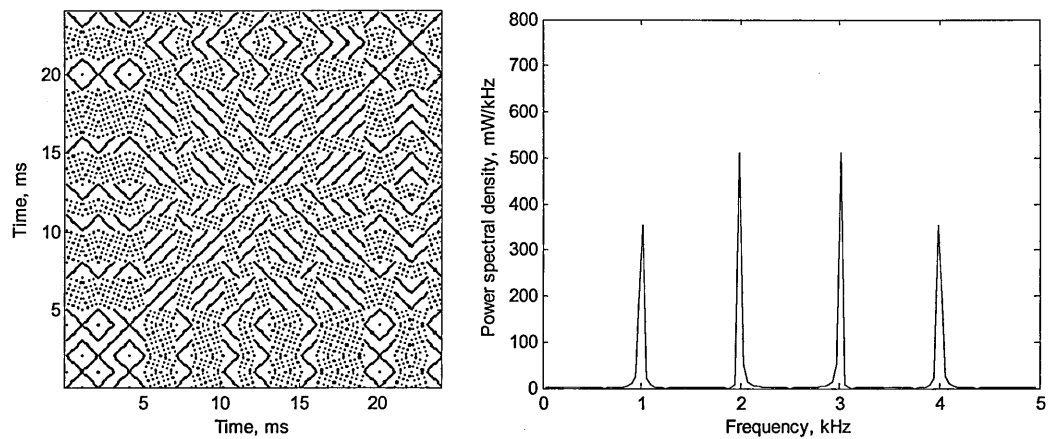


Figure 75. RP ( $\epsilon = 0.175$ ) and Fourier transform of first row for FSK4, example C1.



**Figure 76.** RP ( $\varepsilon=0.175$ ) and Fourier transform of first row for FSK4, example D1.

**4.1.12.3 Minimum Shift Keying**

Minimum Shift Keying (MSK) requires a symmetry depth of two for correct analysis with the PCR method. Figure 77 and Figure 78 show two examples of MSK PCRPs with  $D = 0, 1$  and  $2$ . The symbol rate is 1 kBaud and the sample rate is 10 kSamples/s. It can be seen how the 'filling in' of points is not complete until the symmetry depth has been increased to two.

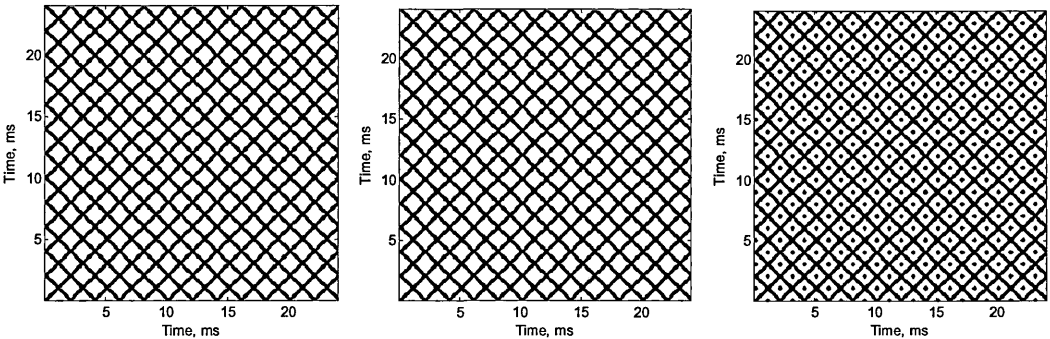


**Figure 77.** PCRPs ( $D = 0, 1, 2$ ,  $\varepsilon = 0.175$ ) for MSK, example A1.

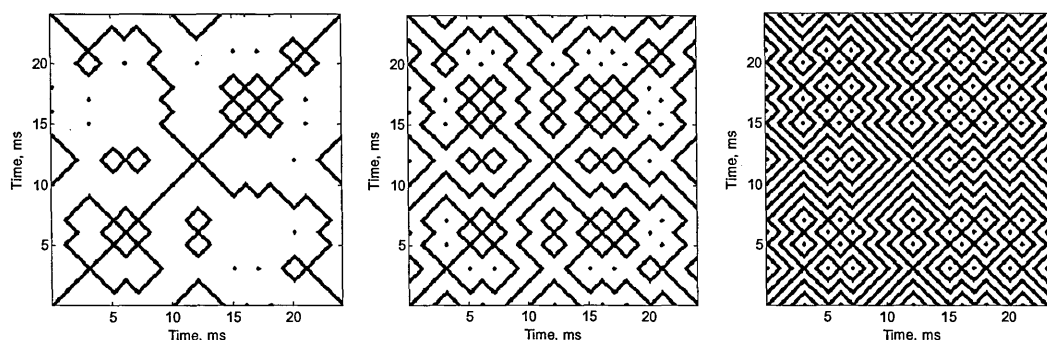


**Figure 78. PCRPs ( $D = 0, 1, 2$ ,  $\varepsilon = 0.175$ ) for MSK, example B1.**

#### 4.1.12.4 Pulse Amplitude Modulation

Two level Pulse Amplitude Modulation (PAM2) can be analysed with a symmetry depth of one. The following figures show examples of the PCRPs for PAM2. The symbol rate is 1 kBaud and the sample rate is 10 kSamples/s. Complete 'filling in' of the PCRPs is achieved when  $D = 1$ . This works for PAM2 but not for PAM4, for which no combinations of  $D$  and  $\varepsilon$  have been found that produce meaningful estimates of symbol rate. The PAM modulation schemes do not encode the information in phase so the PCRPs is not expected to work.

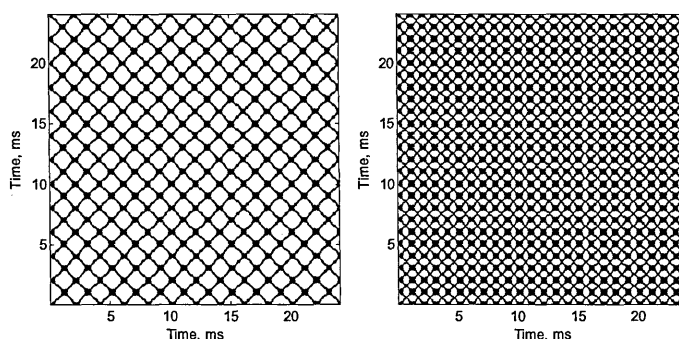


**Figure 79. PCRPs ( $D = 0, 1$ ,  $\varepsilon = 0.175$ ) for PAM2, example A1.**

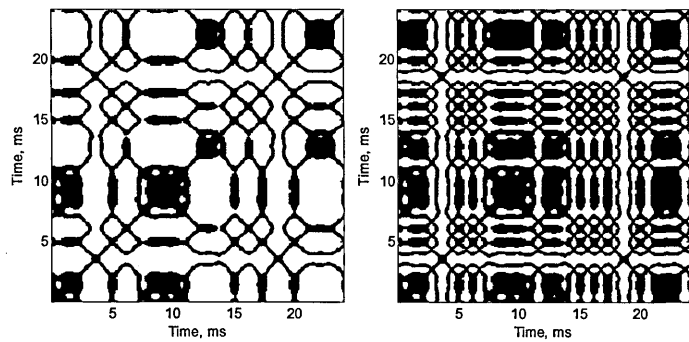


**Figure 80.** PCRP ( $D = 0, 1, \varepsilon = 0.175$ ) for PAM2, example B1.

**4.1.12.5 Quadrature Amplitude Modulation**

Quadrature Amplitude Modulation (QAM) does not lend itself to symbol rate analysis by PCRP. This is because information is encoded in amplitude as well as in phase.

**4.1.12.6 Summary of modulation types**

In summary, the following table lists the modulations examined and the symmetry depth that should be used to analyse them for the purposes of enhancing the symbol rate.

Symmetry Depth	Modulation Types
0	FSK2, FSK4 (frequency separation > symbol rate)
1	FSK2, FSK4 (frequency separation $\leq$ symbol rate)  PAM2  BPSK
2	MSK  QPSK
3	PSK8
Not suitable	PAM4, QAM

**Table 6. PCRП symmetry depths for measuring symbol rate in different modulation types.**

**4.1.13 Conclusions**

This section has presented the results of an investigation into the use of recurrence plots for analysing the time domain structures within a communications signal.

A modified version of the recurrence has been devised that allowed information to be suppressed in favour of the symbol rate and this was shown to be effective for a number of modulation types that encode information in phase. This result went a long way towards answering the question posed at the start of this section, which was to what degree the information about the type of a modulation can be separated from the information content?



The PCRП was shown to behave differently for different modulation types, but significantly increased symbol rate peak height for both BPSK and QPSK. For other modulation types this technique offers little or no improvement, but the principle has successfully been demonstrated that it is possible to suppress information in favour of modulation characteristics.

One approach to using recurrence plot methods has been presented in this section with the intention of using it to explore the research question. It is a novel application of such methods and there may be some merit in investigating such methods further. Generally the recurrence plot methods have been applied to natural phenomena rather than man-made phenomena, but this may prove to be a useful cross-fertilisation of ideas from other areas of science into the field of ASR research, especially when dealing with natural sources of electromagnetic radiation.

At a technical level, further work will be required to determine optimisation criteria and find ways of handling modulations that the PCRП cannot cope with. Further work is also needed to evaluate the performance of the PCRП algorithm in the presence of noise, interference and centre frequency offset. In addition to the technical investigations there is also considerable work to be done in engaging with other researchers in the recurrence plot research community in order to bring their ideas to bear on the problems of ASR.

## 4.2 Logarithmic Cyclic frequency Domain Profile

In section 3.1 the third sub-question was given as:

**To what extent can a logarithmic representation be used to handle interferers whose modulation may have very different time scales to those of the signal of interest?**

This has been investigated by developing a logarithmic form of one of the representations from the family of cyclostationary techniques, which have been applied widely to the problem of recognising communication modulation schemes. This section describes the transform developed as part of this research and illustrates its application to communication signals with widely different time domain characteristics.

Cyclostationarity techniques are processing-intensive, so much effort has been invested in researching algorithms that can reduce the number of computational steps required, with Fast Fourier Transform (FFT) approaches predominating. In this work a novel approach to improving the extent of the cyclic frequency ( $\alpha$ ) is proposed. By using the Constant Q Transform (CQT) a logarithmic form of the SCF has been produced. This allows the cyclic frequency,  $\alpha$ , axis to be drawn in logarithmic form.

Such a representation can be advantageous when the receiver bandwidth cannot be well matched to the signal frequency and bandwidth using *a priori* knowledge of spectrum allocation. This is typically the case with interferers, as the receiver will be matched to the signal of interest rather than the interferer. At least one of

the signals received will not, in general, be well matched to the receiver centre frequency and bandwidth.

It is shown that a CQT-based SCF can form the basis of a Logarithmic Cyclic frequency Domain Profile algorithm without loss of sensitivity compared to the conventional, linear form.

#### **4.2.1 Cyclic frequency**

A concept fundamental to cyclostationarity analysis is that of cyclic frequency,  $\alpha$ . A cyclostationary signal is one that contains a hidden periodicity and  $\alpha$  is the measure of the frequency of this periodicity. The definition (Gardner, 1986a), (Gardner, 1986b) is that a time-series,  $x(t)$ , contains second-order periodicity with cyclic frequency,  $\alpha$ , if and only if there exists some stable Quadratic Time Invariant (QTI) transformation of  $x(t)$  into  $y(t)$  such that  $y(t)$  contains first-order periodicity with frequency  $\alpha$ .

The cyclostationarity methods seek to estimate the cyclic frequency in much the same way that Fourier methods seek to estimate frequency. The processing required is not inconsiderable and, as with Fourier processing, fast processing algorithms have been developed to speed up the time taken to analyse a buffer of data.

#### **4.2.2 Cyclostationarity characteristics of communications signals**

The prime objective of using cyclostationarity analysis when considering communications signals is the determination of the various periodicities present,

including symbol rates, frame rates, multiframe rates, etc. When more than one signal is present then these periodicities may have to be estimated for all the signals, which raises the problem explained in section 2.3.1 of the range of bandwidths and time scales.

The SCF is the main cyclostationarity tool used for identifying such periodicities (Antoni, 2007). If used in a brute-force way to cover up to 15 orders of magnitude in both frequency and cyclic frequency, it would lead to a matrix with  $10^{30}$  elements. Such an array would be impractical to create, manipulate and store with current computing technology. A wide bandwidth SCF is therefore difficult to use in spectral bands in which wide and narrow band emitters coexist.

#### **4.2.3 Logarithmic axes**

One way of circumventing the problem of dealing with a large SCF matrix would be to use logarithmic axes for the SCF estimate. The maximum compression would be achieved if both the frequency and cyclic frequency axes were logarithmic. This can only be achieved if the signal is in a complex baseband representation and is centred at zero frequency. In many applications one cannot guarantee perfect frequency centring of the signal. A more practical approach is therefore to assume a complex baseband signal and allow the signal to be centred at any frequency. In this case it is only the cyclic frequency axis that can be logarithmic, but this still achieves dramatic reductions in the size of the SCF array required.

The Logarithmic Cyclic frequency Domain Profile is the name given here to the representation obtained by applying a logarithmic transform to the cyclic frequency axis. The LCDP is a very compact representation of the cyclostationarity characteristics of a signal and is therefore suitable for ASR processing as well as a wide range of other scientific applications.

#### 4.2.4 Cyclostationary spectral analysis

Gardner (1986b) defined the CAF for a cyclostationary process,  $x(t)$ , as a function of cyclic frequency,  $\alpha$ . This was given in section 2.4.2 as:

$$\hat{R}_x^\alpha(t) = \frac{1}{T_0} \int_0^{T_0} \hat{R}_x(t, \tau) e^{-i2\pi\alpha\tau} d\tau \quad (33)$$

The SCF is then the Fourier transform of the CAF:

$$\hat{S}_x^\alpha(f) = \int_{-\infty}^{\infty} \hat{R}_x^\alpha(t) e^{-i2\pi ft} dt \quad (34)$$

The SCF can be normalised, which yields the spectral coherence,  $C_x^\alpha(f)$ :

$$C_x^\alpha(f) = \frac{S_x^\alpha(f)}{[S(f + \alpha/2)S(f - \alpha/2)]^{1/2}} \quad (35)$$

The CAF, SCF and spectral coherence are useful depictions of the hidden periodicities in the signal (Gardner *et al*, 1987) (Asai *et al*, 2005), but they yield large arrays that require significant post-processing in order to extract the features of interest. A simpler representation is the CDP which is simply the largest SCF component at each value of  $\alpha$  and this can be represented in the computer as a one-dimensional vector rather than a two-dimensional array.

Kim *et al* (2007) give a good illustration of how the CDP can be applied to ASR in cognitive radio applications. They define the CDP as:

$$I(\alpha) = \max_f |C_x^\alpha(f)| \quad (36)$$

The CDP is not sensitive to tuning offsets, because it is a projection of the SCF onto the cyclic frequency axis. This property is useful as the CDP will be largely invariant to tuning errors, providing the error is not large compared to the bandwidth of the signal of interest. The CDP is, therefore, relatively straightforward to apply in non-cooperative communications applications such as signal interception.

#### 4.2.5 Constant Q transform

The CQT was introduced by Brown (1991) with the main objective of aligning an analysis frequency scale with that used in western music. It is essentially a filter bank, whose centre frequencies follow a logarithmic sequence. The non-linearity means that it is difficult to design an inverse CQT (Fitzgerald *et al*, 2006), but its use in the forward sense is well-established for music analysis. Various fast implementations based on Fast Fourier Transforms and filter banks have been developed (Brown and Puckette, 1992), (dos Santos *et al*, 2004), (Wang and Tong, 2004).

#### 4.2.6 Applying the CQT approach to the CDP

In section 4.2.3 the author proposed the concept of an LCDP. In order to achieve this, the author took the concept of the CQT approach and applied it as a modification to conventional linear cyclostationarity analysis. This modification

involved redefining the  $\alpha$  axis to be a logarithmic quantity rather than a linear one.

The required  $\alpha$  axis is defined by the following sequence. Note that base 2 is used purely because it is thought to be a convenient form from which to derive a digital implementation. Other bases might be appropriate and should be considered for further work in this area.

$$\alpha_k = \alpha_0 2^{k/b} \quad (37)$$

where  $\alpha_0$  is the minimum value of  $\alpha$  required and  $k$  is an index defining the position in the filter bank. The parameter  $b$  is the number of filters per decade and so dictates the resolution of the  $\alpha$  axis.

The  $Q$  factor gives the widths of the filters, which increase as  $k$  increases. A suitable value for  $Q$  is obtained from:

$$Q = \left. \frac{\alpha_0}{d\alpha/dk} \right|_{k \rightarrow 0} = \frac{b}{\ln 2} \quad (38)$$

The length of each filter is then given by:

$$N_k = \left\lceil Q \frac{f_s}{\alpha_k} \right\rceil \quad (39)$$

With the addition of a window function,  $W$ , (e.g. Hamming) to reduce spectral leakage, the form of the CQT required can be written as:

$$\hat{X}(x_n) = \frac{1}{N_k} \sum_{n=0}^{N_k-1} W(k, n) x_n e^{-i2\pi Qn/N_k} \quad (40)$$

This estimate can be used in the calculation of a time-averaged logarithmic SCF and hence a Logarithmic Cyclic frequency Domain Profile.

The region of support of the logarithmic SCF is modified as a result of using the CQT. This is shown in Figure 81, in which the main features to observe are the linear scaling of the frequency axis and the logarithmic scaling of the cyclic frequency axis. The power spectral density (i.e. at  $\alpha = 0$ ) cannot be represented on this form of the SCF and must be calculated separately.



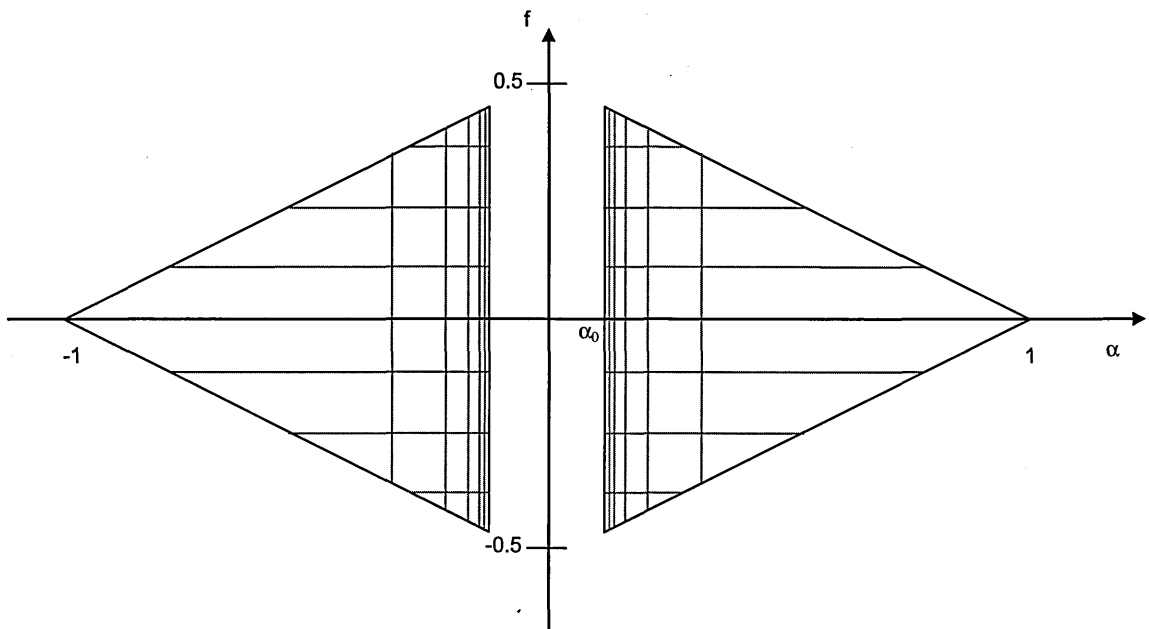


**Figure 81. Region of support of the logarithmic SCF, which extends  $\pm 1$  in cyclic frequency and  $\pm 0.5$  in frequency. The region of support excludes the line of  $\alpha=0$ .**

The logarithmic SCF is a smaller data structure than the linear SCF covering the same range of frequencies and cyclic frequencies. This leads to a corresponding reduction in the amount of memory needed to hold the SCF and a reduction in the amount of processing needed for its calculation.

Both forms of the SCF have the same resolution and range of frequencies and the same range of cyclic frequencies; they differ only in the resolution of the cyclic frequency axis. The size of the SCF will be linearly related to the product of the number of frequency points and the number of cyclic frequency points. As the number of frequency points is the same for both forms of SCF, the maximum memory requirement of the SCF depends only on the ratio of the numbers of cyclic frequency points. This ratio is given by:

$$\frac{P_{\alpha}}{P_{\alpha'}} = \frac{\lceil 10^G + 1 \rceil}{\lceil \log_{base}(10^G) + 1 \rceil} \quad (41)$$

Where  $P_{\alpha}$  and  $P_{\alpha'}$  are the numbers of cyclic frequency points in the linear and logarithmic SCFs respectively.  $G$  is the orders of magnitude to be covered by the cyclic frequency axis and  $base$  is the logarithmic base.

For values of  $base$  between 2 and 9 and orders of magnitude,  $G$ , between 2 and 9, equation (41) can be simplified to:

$$\frac{P_{\alpha}}{P_{\alpha'}} \approx 10^{G-1} \quad (42)$$

As an example, consider an LCDP that is to cover eight orders of magnitude in cyclic frequency. This would require the computation and storage of a logarithmic SCF that has  $O(10^{-7})$  times fewer elements than the comparable linear SCF, where the  $O(.)$  notation indicates the upper bound on the processing requirements (Cormen *et al*, 1999, p. 26).

#### 4.2.7 Implementation of the SCF

The implementation of cyclostationarity techniques is a significant research area in its own right. A well-established body of papers considers the implementation of the SCF, which can be estimated in different ways, with time-smoothing and frequency-smoothing being the two main approaches. The time-smoothing approach (Gardner, 1986c), (Roberts *et al*, 1991) is illustrated in Figure 82 which assumes time averaging over a period  $\Delta t$  and a frequency step size of  $\Delta f$ .

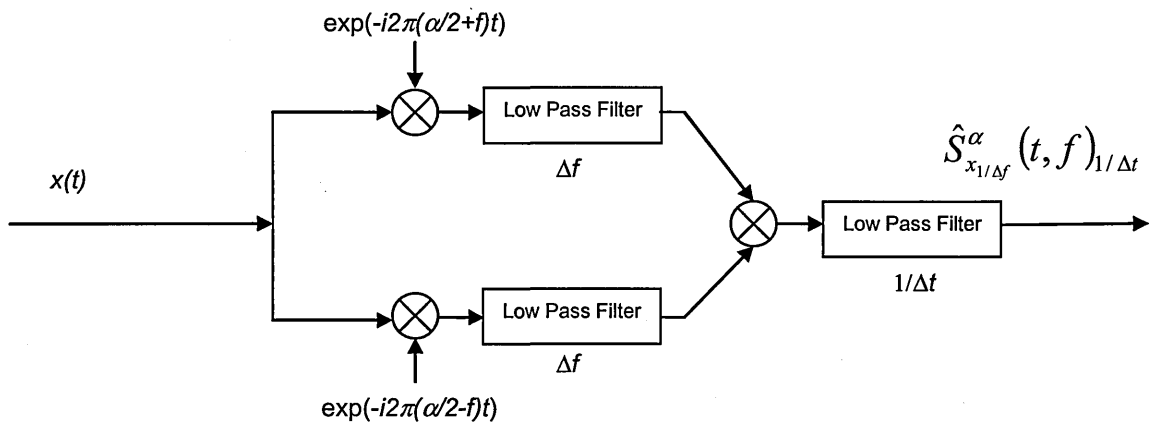


**Figure 82. Implementation of the time-smoothed SCF as a pair of low pass filters.**

This is not the only method of realising a consistent estimator of the SCF. Antoni (2007) has proposed a general quadratic form that allows cyclic spectral estimation to be viewed in terms of other conventional spectrum estimation techniques, such as the multitaper periodogram.

The first step towards a logarithmic implementation is proposed in this thesis based on modifying the time smoothed estimator of Figure 82 and is shown in Figure 83. It will be seen that this implementation relies on a cascade of filters whose bandwidths halve at each successive division of the input signal. Halving of the bandwidth comes from assuming a base 2 logarithmic series. Other logarithmic bases may result in more convenient representations. This is an area for further research.

Figure 83 illustrates the first two stages of this implementation, together with the mapping onto the left hand side of the SCF region of support (see Figure 81)

The logarithmic CDP estimate is obtained by finding the maxima of the computed SCF points at each stage, according to equation (36).

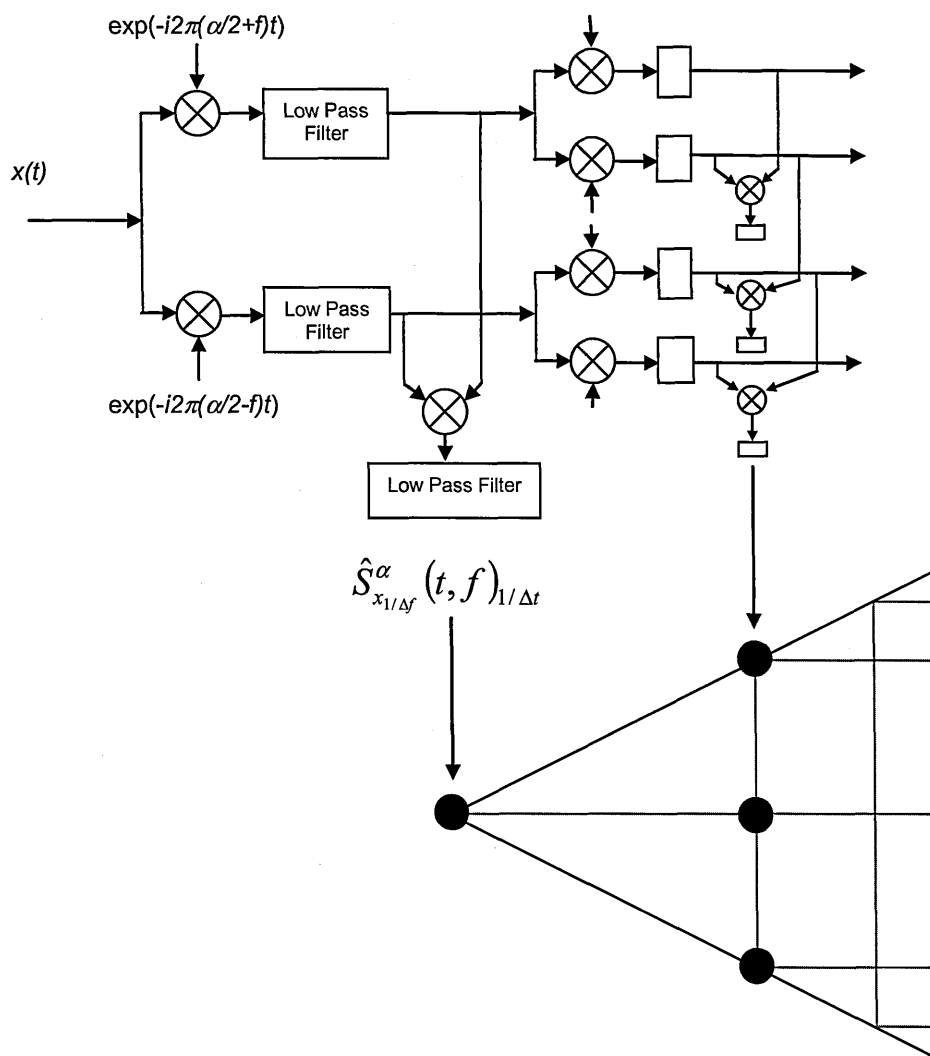


**Figure 83. Time-smoothed logarithmic SCF implementation as a cascade of low pass filter pairs.**

### 4.2.8 Examples

The above implementation has been prototyped in the Matlab computing environment so the concept can be explored. In this section, two examples are given to compare the LCDP with the linear CDP defined by Kim *et al* (2007).

### Example 1 - Simple tones

The first example is of two simple tones added together. They have the same amplitude and frequencies of 0.05 and 0.0578 relative to the sample rate. The difference in frequency is therefore 0.0078.

The CDP with a resolution of 256 points is shown in Figure 84 and the LCDP with a resolution of 9 points is shown in Figure 85. Note that the magnitudes of these plots have been normalised by dividing through by their maximum values. It will be seen that the peak in the LCDP is wider than those in the CDP, but this is simply because of the reduction in resolution.

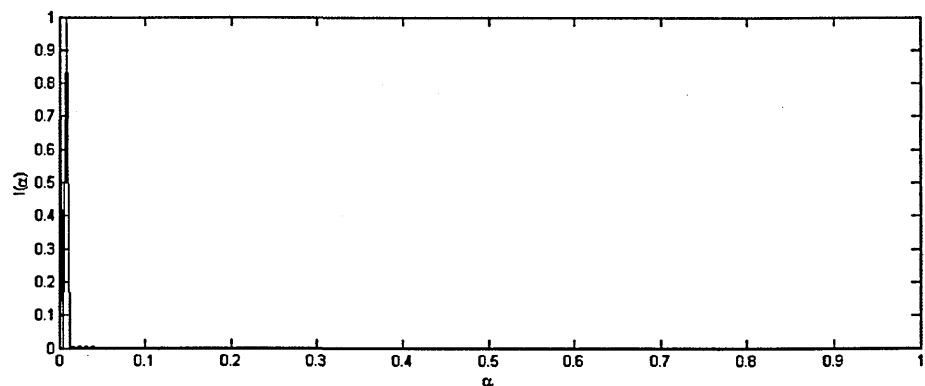


Figure 84. Linear CDP of two tones (256  $\alpha$  points).

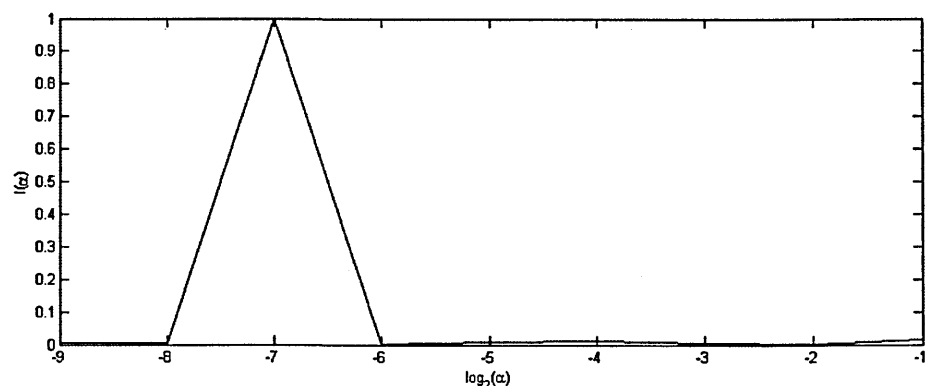
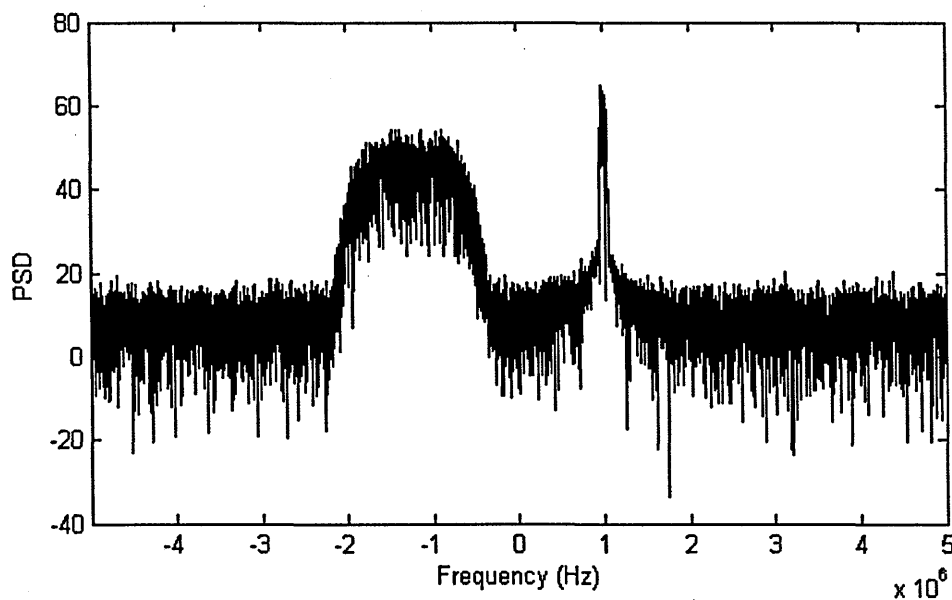


Figure 85. Logarithmic CDP of two tones (9  $\alpha$  points).

### Example 2 - QPSK and BPSK

As a more practical example, consider the combination of two signals, such as might appear within the bandwidth of a receiver operating in a region of the spectrum that can be shared by different kinds of service. The receiver has no knowledge of the types of signal it will encounter and has been set to its default bandwidth of 10 MHz.

The first signal is QPSK modulated with a symbol rate of 1.25 Mbaud and the second signal is a BPSK with a symbol rate of 78 kBaud. The BPSK therefore has a significantly narrower bandwidth than the QPSK. The PSD that would be seen by a receiver with 10 MHz input bandwidth is shown in Figure 86.



**Figure 86. PSD of QPSK and BPSK for example 2.**

The linear CDP for this scenario, with a resolution of 8192 points, is shown in Figure 87. Both symbol rates can be detected, but the lower symbol rate is hard to

discern visually on the left hand side of the graph. Additional smoothing would remove more noise and expose the symbol rate peaks more clearly.

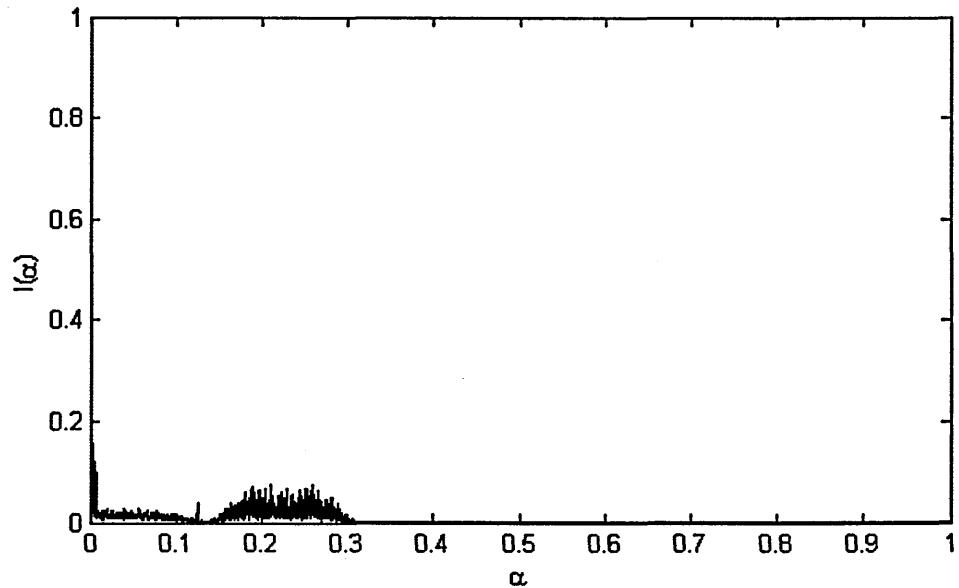


**Figure 87. Linear CDP of QPSK and BPSK (8192  $\alpha$  points).**

If the LCDP method is applied to this scenario using nine points along the logarithmic cyclic frequency axis then Figure 88 is obtained. The two symbol rates can clearly be seen at approximately  $2^{-3}$  (QPSK) and  $2^{-7}$  (BPSK), demonstrating that a single cyclostationarity detector can be used in cases where the signals in the environment have very different symbol rates. Note that approximately the same number of sample points has been used for the two algorithms. For the linear algorithm 8288 samples were used and 8192 samples were analysed using the logarithmic version. Comparison of Figure 87 and Figure 88 shows that the LCDP can lead to significant reductions in the resolution of the alpha axis.

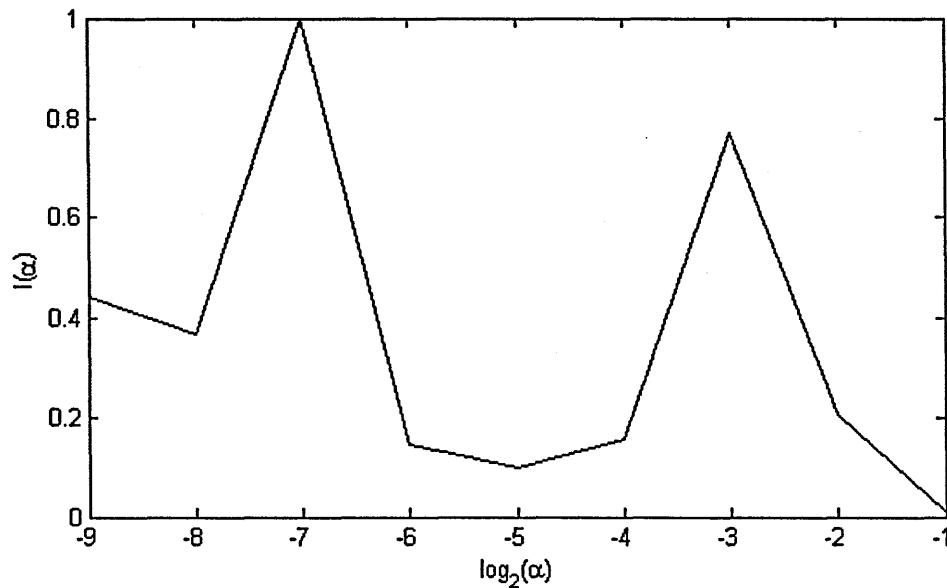


Figure 88. LCDP of QPSK and BPSK (9  $\alpha$  points).

#### 4.2.8.1 Detection probability

Using this same example, the detection probabilities,  $P_d$ , of the linear and logarithmic algorithms are now compared. In these examples  $P_d$  is the probability that a signal can be discerned from additive WGN using a MAP detector (section 2.4.4). The probability has been estimated by simulation of the signals in varying levels of WGN.

Figure 89 shows the value of  $P_d$  versus  $E_b/N_0$  (Evans, 1999, p.161) for the QPSK signal and Figure 90 shows the same relationship for the BPSK signal. In both cases there is no significant difference between the two algorithms. There is, therefore, no loss of sensitivity incurred by the use of the lower resolution logarithmic algorithm. The implication of this result is that the system designer can look for an optimal configuration in a specific application by considering only the trade-off between processing overhead and cyclic frequency resolution.



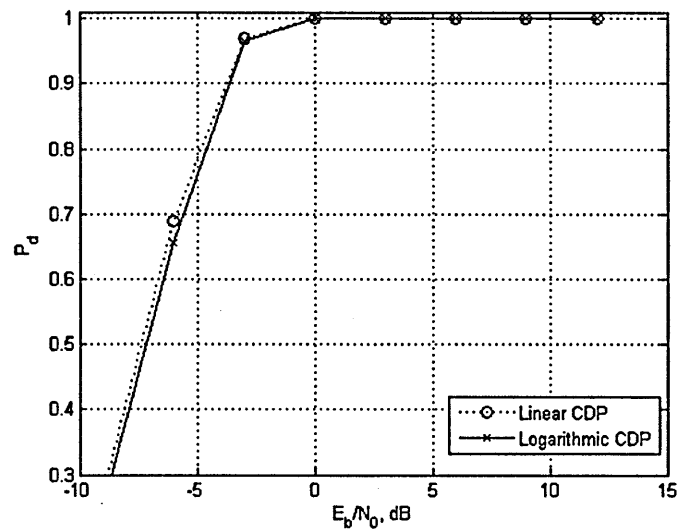


Figure 89. Detection probability versus  $E_b/N_0$  for the QPSK example.

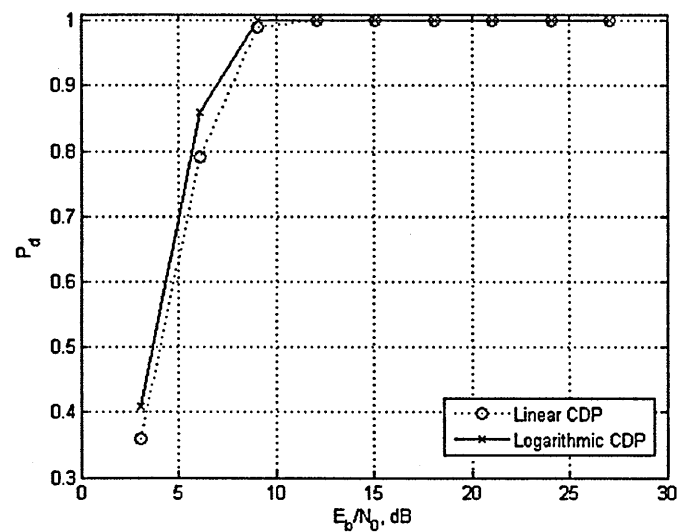


Figure 90. Detection probability versus  $E_b/N_0$  for the BPSK example.

#### 4.2.9 Application to spectrum sharing

A recent proposal (Maeda *et al*, 2007) has been for a spectrum sharing scheme for systems using OFDM modulations based on deliberately injecting cyclostationarity to facilitate modulation recognition. Based on the concept introduced in this paper, it is proposed that such a scheme could be extended such

that the cyclostationarity features are visible across a logarithmic range of cyclic frequencies. This would allow narrow band systems to operate in the same area of shared spectrum as wide band systems.

#### **4.2.10 Conclusions**

This section has outlined a method for compressing the SCF and CDP estimates that are commonly used in the analysis of cyclostationary signals. The use of a technique based on the Constant Q Transform allows the cyclic frequency axis to be compressed logarithmically. This significantly reduces the amount of memory needed for processing the signature data. It has been demonstrated, via simulation, that there would be no loss of sensitivity if a logarithmic algorithm were used instead of a linear one.

Work is now needed to produce efficient implementations tailored for use in specific real-time applications. These would have widespread application in communication signals analysis for cognitive radio and automatic modulation recognition.

A logarithmic CDP algorithm would facilitate non-cooperative identification of spectral redundancies over many orders of magnitude. This would help communication systems of widely varying types to co-exist in areas of shared spectrum. Such a capability would be particularly relevant to the sharing of wireless systems with widely differing bandwidths.

### 4.3 Canonical ASR architecture

In section 3.1 the following sub-question was posed:

**Given that it is possible to design algorithms with specific capabilities (e.g. modulation separation and logarithmic representation) it is reasonable to conclude that algorithms can be devised that possess one or more behaviours appropriate for recognising signals in the presence of interference. To what extent, then, can different algorithms be assessed in terms of their relative performance in the presence of interference?**

This section addresses the first part of the answer to this question, which is to develop a generic architecture for ASR systems to enable all such algorithms to be considered from a high-level perspective. Section 4.4 then continues the answer by looking at the performance of feature extraction algorithms in the presence of interference.

It is useful to divide the ASR methods in the literature (section 2.4) into identifiable groups and organise them according to a taxonomy that can help with understanding the domain. In this section a taxonomy is introduced that can assist with this understanding. This draws partly on the work of other authors (e.g. Dobre *et al*, 2007) but is a more rigorous and abstract framework than other work and is therefore more useful for describing the salient aspects of different approaches to recognition processing.

The taxonomy of signal recognition methods has been developed using an object-oriented approach. The object-orientated approach to analysis allows a single, self-consistent model to be created that combines functionality and data structure. Older methods of analysis that were based on separate functional and data decomposition lacked the richness of description that is possible with UML. It is assumed that the reader is familiar with object-oriented analysis in general and with the UML in particular. Fowler and Scott (2000) offer a good summary of the UML at the level required here.

#### 4.3.1 Top-level package diagram

Figure 91 shows the package diagram used here for describing the major components of the problem. There are two packages, one representing the sources of the signals to be identified and the other representing the recognition processing.

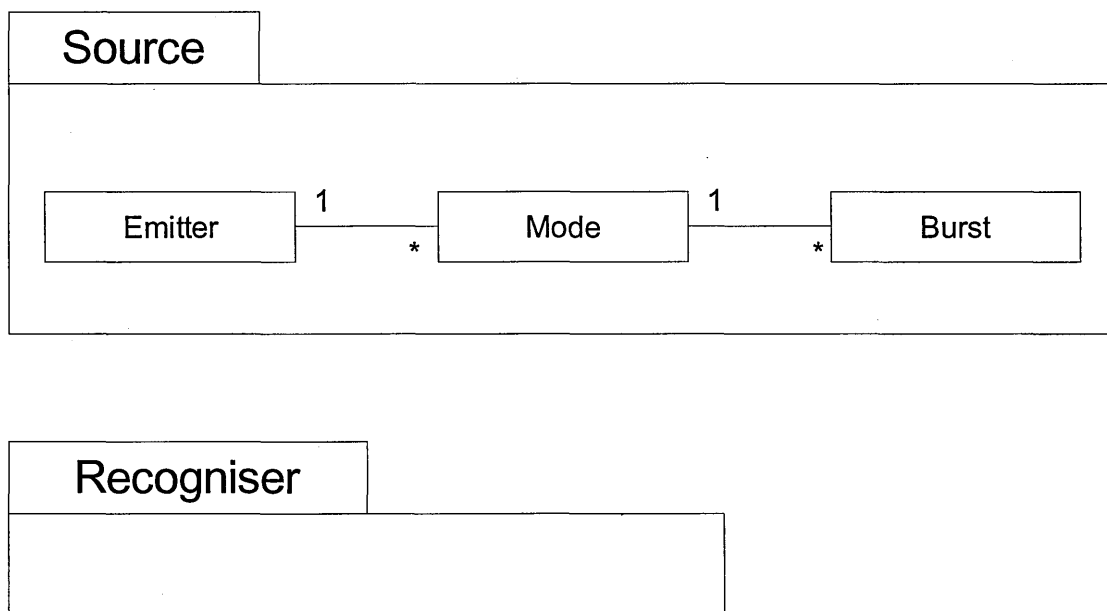


Figure 91. Top-level package diagram.

A relatively simple model is used in order to avoid the complexity of describing all possible sources of radio waves. The justification for this is that this model is sufficient for operational purposes and any more complexity is probably superfluous. Furthermore, the model fits the types of processing encountered in the literature search (section 2.4).

The Source package is a simplified representation of a source of radio waves, which may be natural or man-made. It is a simpler model than that described in section 2.2, but is more appropriate when the source of the radiation is not yet known.

There are three classes in the Source package, which are:

- **Emitter.** This class acts as the root class for defining a source of radio waves. The assumption is that there is a single entity that may be considered to be the Emitter. In the case of a device such as a mobile phone it is clear that the Emitter will model the entire phone. Other cases are not so straightforward. Lightning, for example, is a distributed phenomenon, but in most practical applications it is sufficient to model the whole lightning phenomenon as a single Emitter object;
- **Mode.** Many modern radio sources can operate in more than one mode. A multimode handset is an excellent example. The Mode class allows such behaviour to be modelled;
- **Burst.** No practical radio system will radiate continuously for an infinite time. Radio waves are emitted in a particular mode for a period of time. The

Burst class allows each transmission to be represented by a different instantiation.

The Source package allows radio sources to be modelled in a compact way. It does not contain an explicit description of the physical architecture of the source. The number of antennas, for example, is not modelled. It is with this simplification in mind that the development of a signal recognition system is carried out.

A decision has to be made by the designer as to the level at which the recognition system is going to attempt to identify the Source. It can attempt to identify it at the Emitter, Mode or Burst level. The simplest approach is to identify at the Burst level and the most complex approach is to identify at the Emitter level. The relationship between the Recogniser and the Source therefore depends on the level at which recognition is to be attempted.

The Source package will not be considered further. For the purpose of this thesis the structure of this package has been elaborated only to the level of detail needed to guide the investigation of the Recogniser package structure.

#### **4.3.2 Top-level class diagram**

Concentrating now on the Recogniser package, the top-level class diagram for that package is introduced.

From an object-oriented analysis point of view, there are a number of object types that can be manipulated by a signal recognition process. These are shown in Figure 92, which has classes corresponding to each object type of interest.

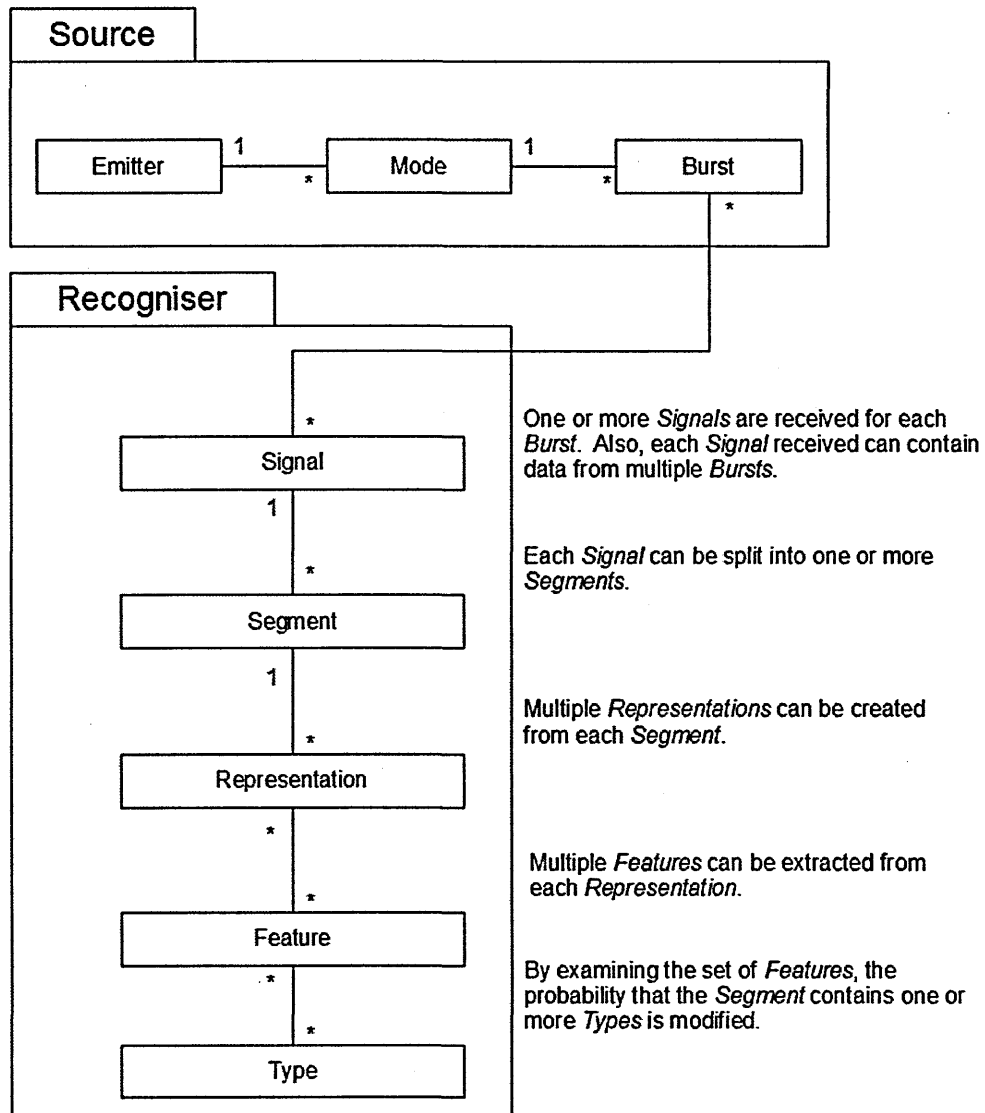


**Figure 92. Top-level class diagram.**

The following classes are identified in the top-level class diagram:

- **Signal.** This is the class for objects holding signals, where a signal is defined as a set of data received over a given period of time from one or more

antennas. In this model the Signal class is shown with a relationship to the Burst class in the Source package, which is the main relationship between the two packages. In general this is a many-to-many relationship;

- **Segment.** Each Signal object can be split up into one or more segments. In this model there is no constraint on how this segmentation is to be done. One approach, however, is to assert that a Segment should ideally correspond to a Burst of a single type. It is this assertion that is made in this thesis, i.e. that the recognition system must seek to achieve a segmentation such that each Segment relates to one Burst only. If this is achieved then there is a direct relationship between Signal and Burst and the Segment class becomes redundant. If, on the other hand, perfect segmentation cannot be achieved, then the relationships between the Source and Recogniser packages are more complex, leading to uncertainty in the recognition results;
- **Representation.** Virtually all recognition techniques rely on transforming a Segment into one or more Representations in order to emphasise particular characteristics. Examples of algorithms suitable for producing typical Representations were introduced in section 2.4.2;
- **Feature.** By analysing the Representations it is possible to identify Features that allow different Sources to be distinguished from each other. Section 2.4.3 introduced typical Features encountered in the literature;
- **Type.** Ultimately the goal of signal recognition is give a decision on the Source at an appropriate level. The modelling of the Type class should therefore correspond to the Emitter, Mode or Burst class as required by the application. The simplest model would equate the Type class with the Burst



class, ignoring the higher complexities of the Source. Section 2.4.4 described typical decision methods that can be used in the decision processing.

A top-level class diagram has been proposed in this section. This has been derived by inspecting the data processing used in a wide range of signal recognition systems. The proposed model asserts that all practical signal recognisers can be regarded as manipulators of information that can be modelled using the classes Signal, Segment, Representation, Feature and Type.

This is similar to, but more formally specified than, the statistical pattern recognition model in Soliman and Hsue (1992, p. 908) in which the concepts of signal, observation, feature and decision space are used. The same model can encompass the decision-theoretic approaches (Soliman and Hsue, 1992, p. 908) by recognising that the likelihood ratio typically used in such methods can be regarded as a form of feature derived from some representation of the input signal.

The evidence to support this model is given in section 4.3.6, which gives examples of typical ASR architectures taken from the open literature and represented in the form of this model.

### **4.3.3 Activity Diagram**

Sections 4.3.2 presented the generic top-level class diagram of the UML model. This section describes the functionality at a similarly generic level.

Figure 93 shows a generic top-level activity diagram that captures the main processing required.

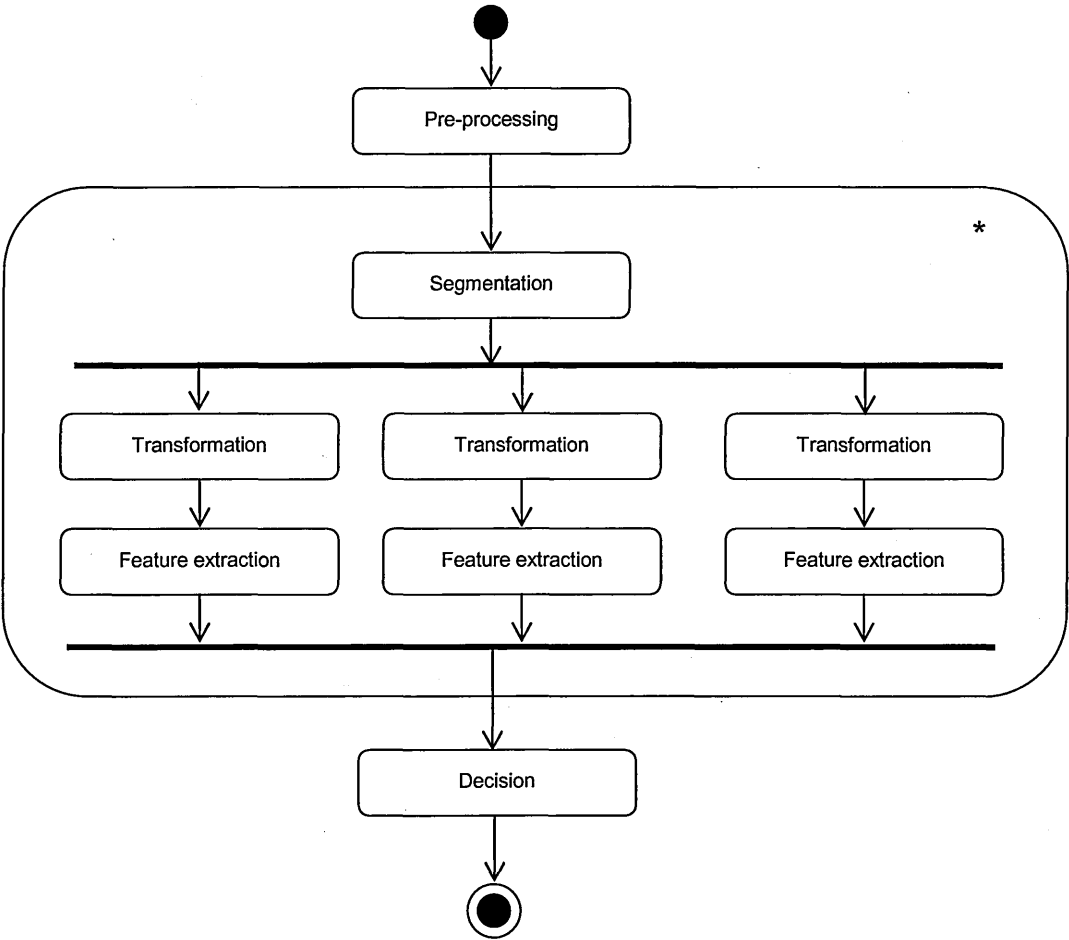


**Figure 93. Top-level activity diagram.**

Once the Signal has been collected and split into Segments, each Segment can then be processed in parallel, transformed into multiple Representations and multiple Features. Once all the Features have been calculated the last activity in the diagram is the Decision activity which determines the Type.

Figure 93 supports dynamic concurrency, as indicated by the asterisk in the box surrounding most of the activities. The implication here is that the system can search for the best identification by repeatedly segmenting and attempting identification again. This extension to the model allows multiple hypothesis

systems to be included to take account of the complexities of the modern signal environment.

#### **4.3.4 Class hierarchies**

The top-level classes were described in section 4.3.2. This section expands on each of these top-level classes by adding class hierarchies to support specific types of information that are handled by typical ASR systems. The various classes listed here are grouped into the major types: Signals, Segments, Representations, Features and Types.

Using the concept of inheritance allows class hierarchies to be constructed in object-oriented analysis and design. The concept of inheritance can be applied to the classes proposed here by recognising that the various top-level classes given in section 4.3.2 are generic. Each class in the top-level class diagram forms the basis of a class hierarchy. These hierarchies are now described.

##### **4.3.4.1 Signal class hierarchy**

At the start of the processing chain there are various representations of Signals and these share some general characteristics. Typically in a digital computer they will be stored as finite length arrays of either integer or real numbers.

One possible representation of a hierarchy based on the Signal class is shown in the class diagram of Figure 94. Here the Signal class is shown at the top of the diagram with various other classes derived from it.

There are three main variants of the Signal class. These are the Signal\_real class for real sample data, the Signal\_iq class for complex baseband (I/Q) data and the Signal\_zc for zero crossing sample data.

It is possible to identify variants of these classes. Shown in the figure are the Signal\_iq\_centred class for I/Q data that is frequency centred and the Signal\_iq\_coherent class for I/Q data that is frequency centred and also time synchronised such that it is coherent with the symbol rate of the emitter.

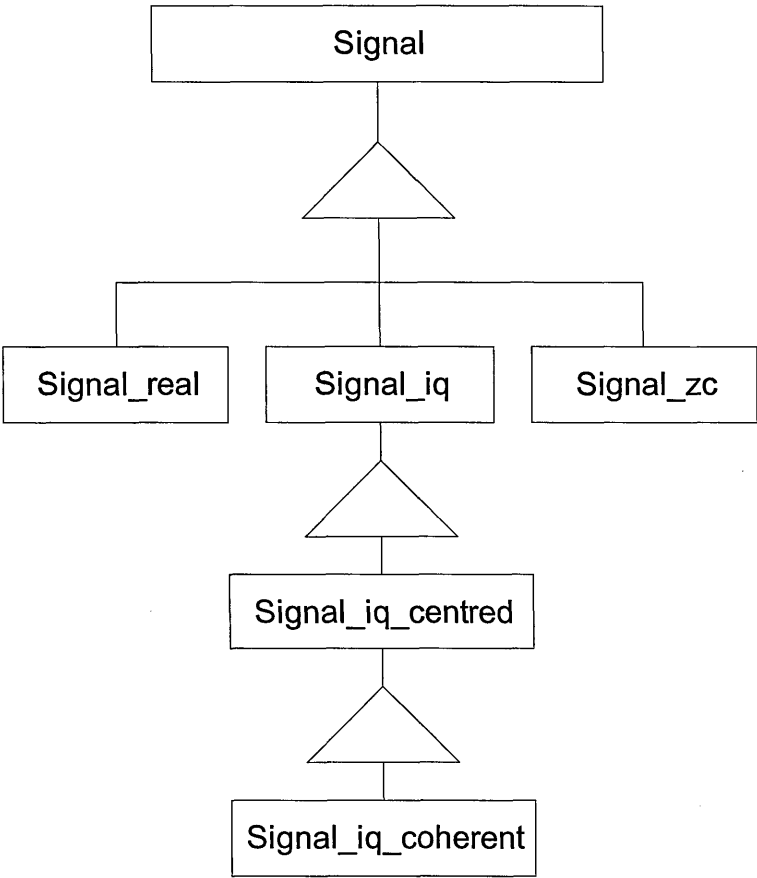


**Figure 94. Signal class hierarchy.**

Further variants of this class hierarchy are conceivable, but Figure 94 is sufficient to illustrate the approach to modelling variants of the Signal class as a class hierarchy.

The following classes are derived from the Signal base class. The last column of the table indicates where there is an example of the given class later in this section.

Class	Description	Example
Signal_iq	Class for the storage of sampled, complex, baseband data, also known as I/Q data.	4.3.6.2, 4.3.6.3
Signal_iq_centred	Class for the storage of frequency-centred, sampled, complex, baseband data, also known as I/Q data.	
Signal_iq_coherent	Class for the storage of I/Q data that has been synchronised to the symbol rate and is therefore coherent with the symbol data.	4.3.6.3
Signal_real	Class for the storage of real (i.e. not complex) sampled signal data.	
Signal_zc	Class for the storage of zero crossing sampled data.	4.3.6.4

**Table 7. Example Signal classes.**

4.3.4.2 Segment class hierarchy

The Segment class hierarchy is shown in Figure 95 and is virtually identical to that of the Signal class. For each type of signal there is a corresponding segment.

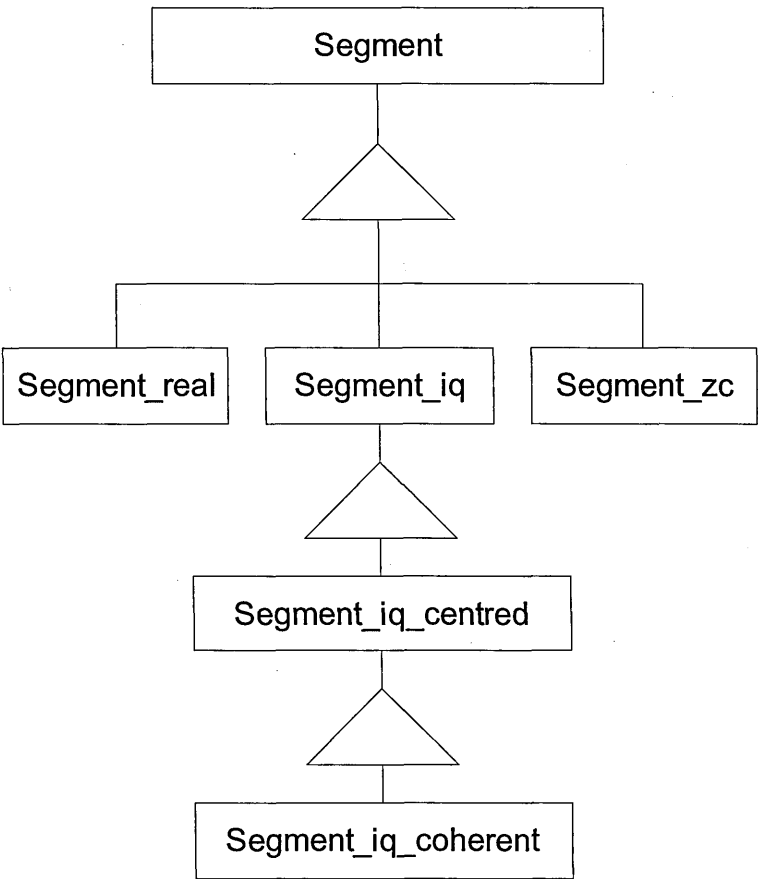


Figure 95. Segment class hierarchy.

The following classes are derived from the Segment base class. References are given to examples later in this section.

Class	Description	Example
Segment_iq	Class for the storage of sampled, complex, baseband data, also known as I/Q data.	4.3.6.1, 4.3.6.2
Segment_iq_centred	Class for the storage of frequency-centred, sampled, complex, baseband data, also known as I/Q data.	

Class	Description	Example
Segment_iq_coherent	Class for the storage of I/Q data that has been synchronised to the symbol rate and is therefore coherent with the symbol data.	4.3.6.3
Segment_real	Class for the storage of real (i.e. not complex) sampled signal data.	
Segment_zc	Class for the storage of zero crossing sampled data.	4.3.6.4

**Table 8. Example Segment classes.**

**4.3.4.3 Representation class hierarchy**

A subset of the Representation class hierarchy is shown in Figure 96.

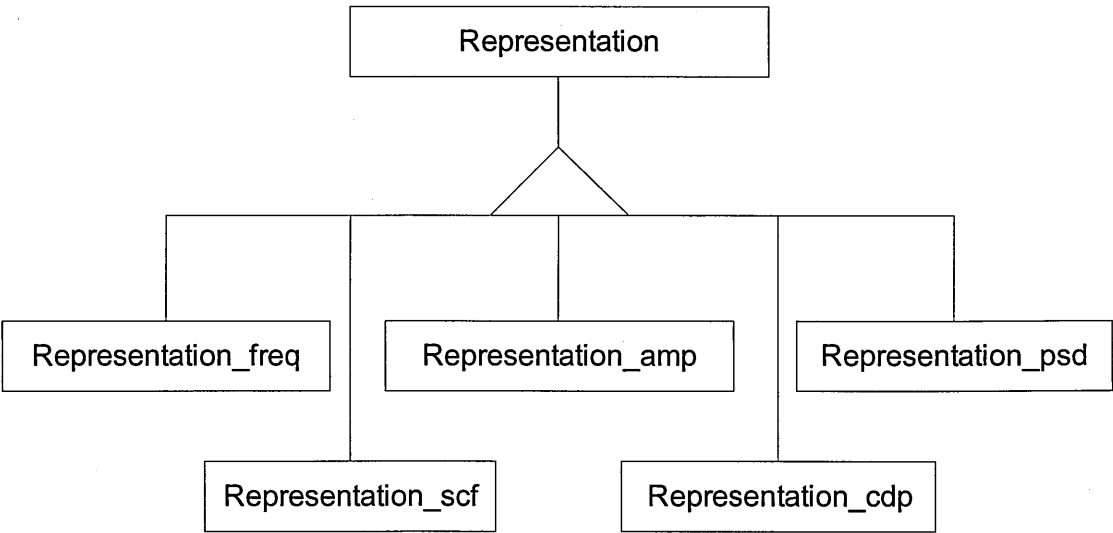


**Figure 96. Representation class hierarchy.**

There is an infinite variety of possible Representation classes, as it is possible to transform any given Segment object using any conceivable, valid mathematical function. Figure 96 shows only a handful of derived classes to illustrate the concept.

Table 9 lists examples of Representations that can be derived from the base Representation class.

Class	Description	Example
Representation_amp	Class for the storage of amplitude data	
Representation_a <sub>cn</sub>	Class for the storage of normalised-centred instantaneous amplitude, $a_{cn}$	4.3.6.2
Representation_cdp	Class for the storage of Cyclic frequency Domain Profile data	
Representation_constellation	Class for the storage of constellation data	4.3.6.3
Representation_freq	Class for the storage of instantaneous frequency	
Representation_ $\phi_{NL}$	Class for the storage of non-linear phase, $\phi_{NL}$ , data	4.3.6.2
Representation_psd	Class for the storage of power spectral density data	4.3.6.1, 4.3.6.2
Representation_scf	Class for the storage of SCF data	
Representaton_zci	Class for the storage of zci data	4.3.6.4
Representaton_zcid	Class for the storage of zcid data	4.3.6.4

**Table 9. Example Representation classes.**

#### 4.3.4.4 Feature class hierarchy

A subset of the Feature class hierarchy is shown in Figure 97.



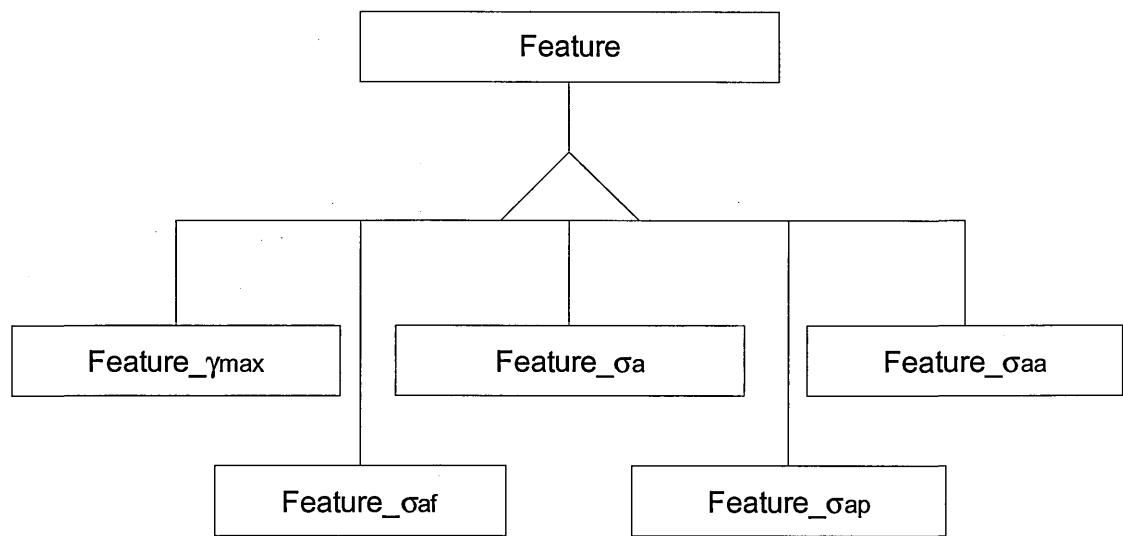


**Figure 97. Feature class hierarchy.**

There is an infinite set of possible Features and only a small number are shown in the diagram. The following classes are examples of those that can be derived from the base Feature class:

Class	Description	Example
Feature_G	Class for the storage of G data	4.3.6.4
Feature_Hellinger	Class for the storage of Hellinger distance data	4.3.6.3
Feature_J	Class for the storage of J data	4.3.6.4
Feature_N <sub>F</sub>	Class for the storage of N <sub>F</sub> data	4.3.6.4
Feature_P	Class for the storage of spectrum symmetry data, P	4.3.6.2
Feature_γ <sub>max</sub>	Class for the storage of γ <sub>max</sub> data	4.3.6.2
Feature_σ <sub>a</sub>	Class for the storage of σ <sub>a</sub> data	
Feature_σ <sub>aa</sub>	Class for the storage of σ <sub>aa</sub> data	
Feature_σ <sub>af</sub>	Class for the storage of σ <sub>af</sub> data	
Feature_σ <sub>ap</sub>	Class for the storage of σ <sub>ap</sub> data	4.3.6.2
Feature_σ <sub>dp</sub>	Class for the storage of σ <sub>dp</sub> data	4.3.6.2

**Table 10. Example Feature classes.**

4.3.4.5 Type class hierarchy

The Type class hierarchy has already been illustrated in Figure 92. For completeness, the following classes are derived from the Type class.

Class	Description	Example
Type_burst	Class for the storage of burst type descriptions	4.3.6.1, 4.3.6.2, 4.3.6.3, 4.3.6.4
Type_mode	Class for the storage of mode type descriptions	
Type_emitter	Class for the storage of emitter type descriptions	

Table 11. Example Type classes.

There is no consensus in the literature as to the list of Types that are obtained. Researchers tend to choose identifications that suit their own purposes, although all could be mapped to variants of the Type\_burst class. Examples might be called Type\_burst\_FM, Type\_burst\_AM, Type\_burst\_BPSK, etc.

No examples have been found that could be mapped to the Type\_mode or Type\_emitter class. This suggests to the author that ASR research has not yet engaged with the complexities of the modern radio environment.

4.3.5 Activities

The following sections address the analysis activities that could be used within each stage of processing. Each stage of the top-level activity diagram (Figure 93) is considered in turn.

#### 4.3.5.1 Pre-processing

Pre-processing is the set of processing activities that can be performed within the first activity of Figure 98. It comprises those functions that are needed in order to interface the data stream from the receiver into the recognition processing.

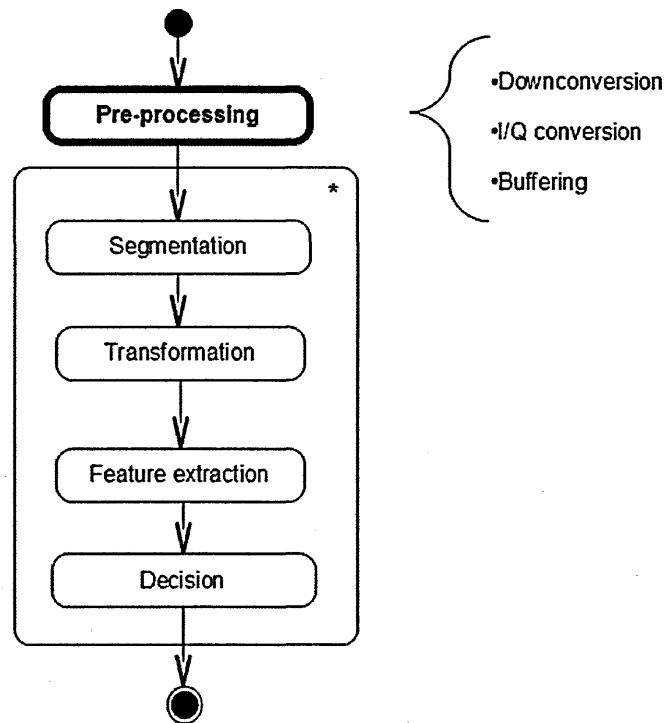


**Figure 98. Pre-processing activities.**

If it is assumed that the analogue output from the receiver has been digitised at an appropriate rate and fidelity, then there still remain some basic functions that need to be performed and these are grouped here under the heading of pre-processing activities.

The pre-processing includes activities such as:

1. Downconversion from Radio Frequency (RF) or Intermediate Frequency (IF) to real or complex baseband;

2. I/Q conversion, i.e. conversion to complex baseband from real baseband;
3. Buffering the data into memory windows that the hardware architecture can accommodate. It is important to note that these memory windows are unlikely to be time-aligned with the start and finish times of signals of interest. In this architecture recovering the time-alignment is the responsibility of the Segmentation activity and not the Pre-processing activity.

The Pre-processing activity will not be covered further here. It is assumed in this model that the Pre-processing activities are not dynamically configurable. Where changes are needed to, for example, sample rate, then these are to be accommodated via Segmentation or other activities. This assumption is not fundamental to the model, but reflects the implementations in current usage.

#### **4.3.5.2 Segmentation activities**

Segmentation (Figure 99) in this model is, potentially, the first intelligent step in all ASR systems. In the view of this thesis its primary objective is to deliver Segments, each of which contains samples of Signal from a single Source, to the activities that come after it.

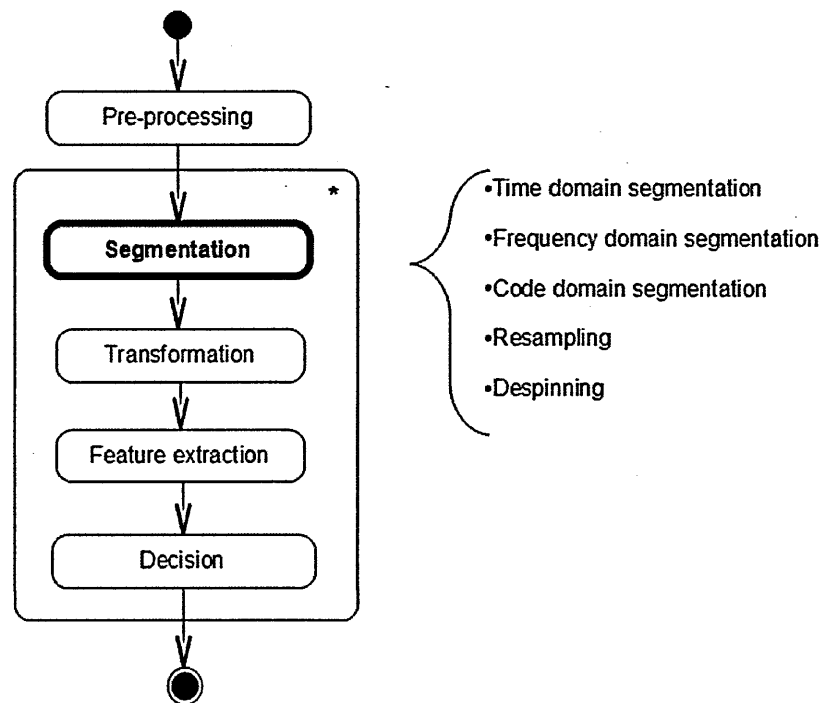


**Figure 99. Segmentation activities.**

Historically, the majority of systems investigated do not apply such intelligence at this stage and segment the incoming signal data by time and/or frequency in a simple manner. Some examples of algorithms that could be used in the Segmentation activity were given in section 2.4.1. Table 12 lists some examples of Segmentation activities, based on those found in the literature. Segmenting by time is by far the most common example of a Segmentation activity.

Activity	Description	Input	Output	Example
S_time	Splits a signal into segments of equal duration	Signal	Segment	4.3.6.2 4.3.6.4
S_frequency	Splits a signal into separate segments in the frequency domain	Signal	Segment	
S_code	Isolates a segment from a signal based on knowledge of the code space	Signal	Segment	
S_resample	Changes the bandwidth of the sample data to match that of the signal of interest	Signal	Segment	
S_despin	Remove the centre frequency offset of the sample data so that the signal of interest is centred	Signal	Segment	

**Table 12. Example Segmentation activities.**

#### 4.3.5.3 Transformation

The Transformation activity (Figure 100) has been introduced into the proposed processing model as it provides a clear differentiation between the typical operations performed on Segments and the detection of Features in the outputs of those operations. A Transformation is an activity that takes a Segment and uses it to create one or more Representations.

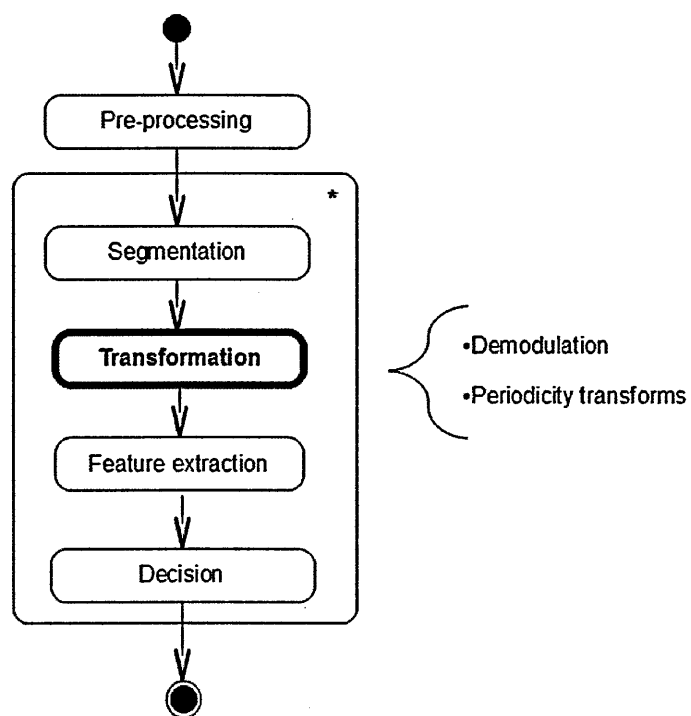


**Figure 100. Transformation activities.**

Examples of Transformation algorithms in the literature were given in section 2.4.2 and included a variety of demodulators and periodicity transforms. Table 13 lists a range of transformation activities, based on algorithms in the literature.

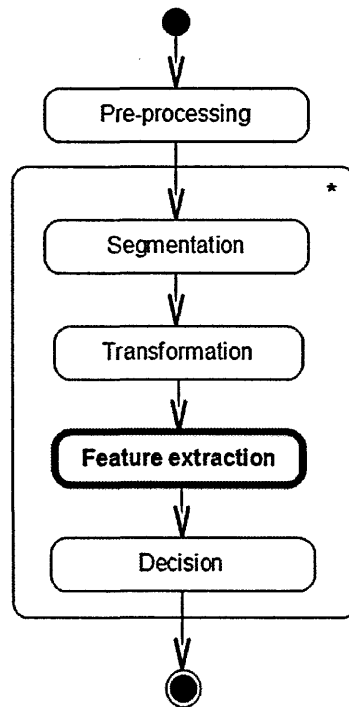
Activity	Description	Input	Output	Example
T_iq/a <sub>cn</sub>	Transforms I/Q data into $a_{cn}$ data	Segment_iq	Representation_can	4.3.6.2
T_iq/psd	Transforms I/Q data into power spectral density data	Segment_iq	Representation_psd	4.3.6.1, 4.3.6.2
T_iq/ $\phi_{NL}$	Transforms I/Q data into $\phi_{NL}$ data	Segment_iq	Representation_ $\phi_{NL}$	4.3.6.2
T_iq_coherent/constellation	Transforms I/Q data in symbol-coherent form into constellation data	Segment_iq	Representation_constellation	4.3.6.3
T_zc/zci	Transforms zc data into zci data	Segment_zc	Representation_zci	4.3.6.4
T_zc/zcid	Transforms zc data into zcid data	Segment_zc	Representation_zcid	4.3.6.4

Table 13. Example Transformation activities.



#### 4.3.5.4 Feature Extraction

The Feature extraction activities (Figure 101) take as input the Representations produced by the Transformation activities. They output Features, which are fed into the Decision activities.



**Figure 101. Feature extraction activities.**

The Feature extraction algorithms found in the literature were described in section 2.4.3. A range of example activities are listed in Table 14.

Activity	Description	Input	Output	Example
F $a_{cn}/\gamma_{max}$	Extracts the $\gamma_{max}$ feature from $a_{cn}$ data	Representation $a_{cn}$	Feature $\gamma_{max}$	4.3.6.2
F constellation/ Hellinger	Extracts the Hellinger distance from the constellation representation	Representation_constellation	Feature_Hellinger	4.3.6.3
F_psd/P	Extracts the feature, P, from PSD data	Representation_psd	Feature_P	4.3.6.2
F_zc/J	Extracts the J parameter from zc data	Representation_zc	Feature_J	4.3.6.4
F_zc/N <sub>F</sub>	Extracts the J parameter from zc data	Representation_zc	Feature_N <sub>F</sub>	4.3.6.4
F $\phi_{NL}/\sigma_{ap}$	Extracts the $\sigma_{ap}$ feature from $\phi_{NL}$ data	Representation $\phi_{NL}$	Feature $\sigma_{ap}$	4.3.6.2
F $\phi_{NL}/\sigma_{dp}$	Extracts the $\sigma_{dp}$ feature from $\phi_{NL}$ data	Representation $\phi_{NL}$	Feature $\sigma_{dp}$	4.3.6.2

Table 14. Example Feature extraction activities.

4.3.5.5 Decisions

At this stage it is assumed that the Segmentation activity has isolated the Segment of interest in time and frequency, the data has been transformed into the desired Representations and the required Features have been extracted. A decision is then made on the Type based on one or more Features.

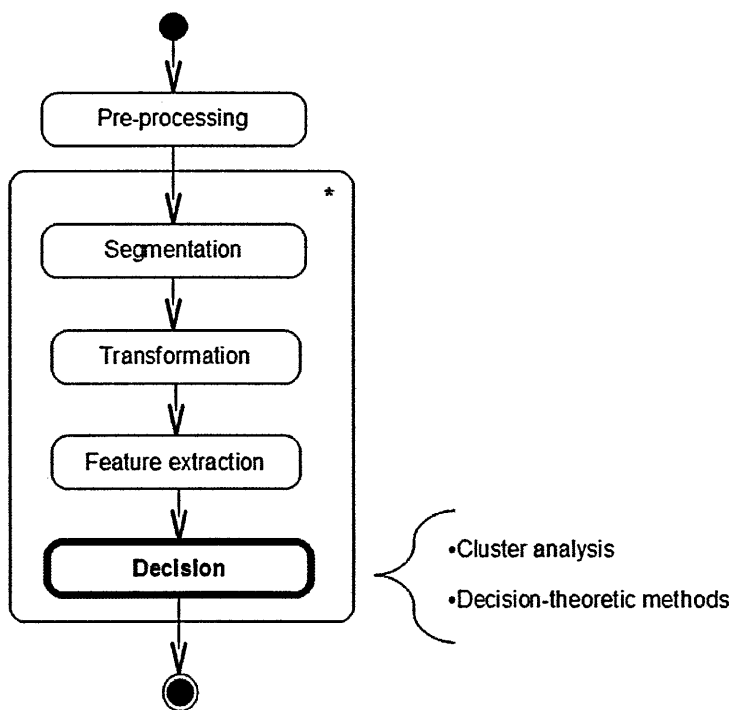


Figure 102. Decision activities.

Examples of Decision algorithms were given in section 2.4.4 and included a range of decision-theoretic and cluster analysis approaches. Table 15 lists some example Decision activities for use within this stage of the processing.

Activity name	Description	Example
D_Bayes	Uses the Bayes algorithm to make a decision-theoretic selection of the Type	
D_MAP	Selects the Type using the Maximum A Posteriori approach	
D_minimum	Makes a decision based on the minimum of a parameter	4.3.6.3
D_perceptron	Perceptron-type ANN which outputs a vector of probabilities following the input of a vector of parameters. It is assumed that the ANN will be trained prior to deployment in the recognition system	4.3.6.1
D_tree	Decision tree which provides a decision on the most likely signal type for a given input set of Features	4.3.6.2, 4.3.6.4

**Table 15. Example Decision activities.**

**4.3.6 Examples**

This section contains some examples of signal recognition algorithm architectures drawn using the notation introduced in this appendix. The aim is to demonstrate that the notation is capable of depicting the major facets of different architectures.

**4.3.6.1 PSD recognition by Artificial Neural Network ANN**

The first architecture to be considered is one of the simplest to implement and was constructed relatively early in the history of the subject. Ghani and Lamontagne (1993) compared the periodogram, Welch periodogram and bispectrum. They also compared the k-Nearest Neighbour and ANN methods for performing the classification. They decided that combining the Welch periodogram and a perceptron ANN gave the best performance of the configurations they tried.

This architecture is shown in Figure 103 and Figure 104. It is implemented using just two activities to perform transform and decision processing. Starting at the top of the activity diagram, it is assumed that I/Q data is available in a `Segment_iq` object. Ghani and Lamontagne (1993) used a simulation of 8192 samples at a sample rate of 75 kSamples/s, corresponding to a duration of 109.23ms. The segment is transformed, via a Welch periodogram, into a PSD estimate by the `T_iq/psd` activity. The resulting `Representation_psd` object is passed to a trained ANN, here shown as the `D_perceptron` activity. The decision processing creates a `Type_burst` object based on the outputs of the ANN. The `Type_burst` class supports the set {AM, FM, ASK, QPSK, SSB-USB, SSB-LSB, FSK1, FSK2, BPSK, CW}.

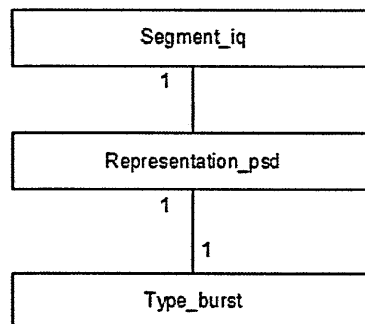


**Figure 103. Ghani and Lamontagne algorithm class diagram.**

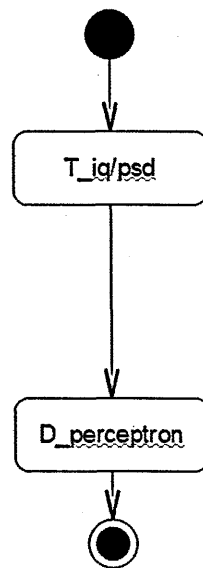


**Figure 104. Ghani and Lamontagne algorithm activity diagram.**

Notice how, in this architecture, there is no Feature extraction processing and the ANN operates directly on the power spectral density estimate. This is quite unusual in the literature. This means that the Feature class is missing and is the only example found where this is the case. Rather than modifying the main model, it was thought best to leave this as a special case and emphasise how it differs from all other ASR systems in the literature.

#### 4.3.6.2 AMRA 1

The example in this section is the first architecture described by Azzouz and Nandi (1996, pp. 45-76). This architecture is called the Analogue Modulated Signal Recognition Algorithm number 1 (AMRA 1) and is shown in Figure 105 as a class diagram and Figure 106 as an activity diagram.

This algorithm is inherently suited to parallel processing. Both diagrams show clearly how the calculation of the Features and Representations can be performed in parallel, with the Types being decided when all the Features are available.

AMRA 1 starts by segmenting I/Q data (Signal\_iq) into fixed duration Segments (Segment\_iq). Three Representations are then created and, from each of these a Feature is extracted. The decision on a Type is created using a decision tree (D\_tree). The decision tree outputs the probability of each of seven modulation types. As a binary decision tree is used, the probabilities will be all zero apart from the single modulation selected, which will have a probability of one.

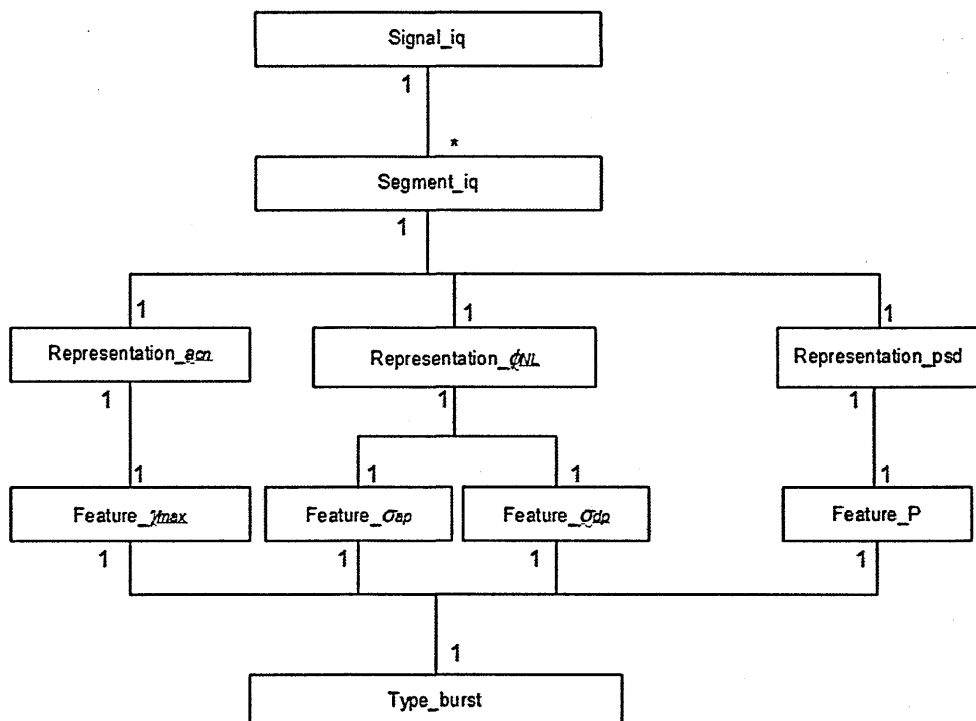


Figure 105. AMRA 1 class diagram.

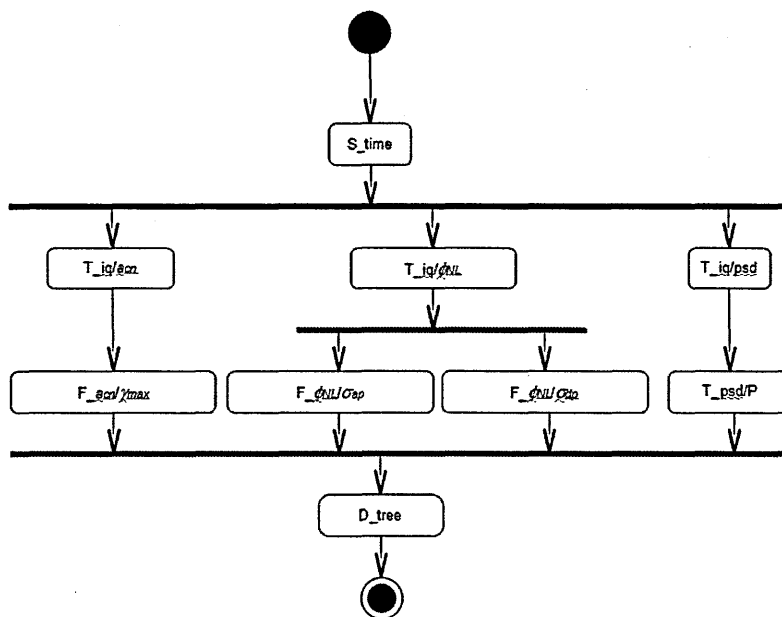


Figure 106. AMRA 1 activity diagram.

#### 4.3.6.3 Hellinger Distance

The Hellinger distance method (Donoho and Huo, 1997) is a form of probabilistic detection, similar to Bayes detection, applied to the constellation diagram. The processing is summarised in Figure 107 and Figure 108.

The first class in the recognition processing is Segment\_iq\_coherent. Not shown, but assumed to be present, is a Signal\_iq object. This could be converted to Segment\_iq\_coherent via any suitable route, e.g. via Signal\_iq\_coherent or via Segment\_iq. The route to achieving Segment\_iq\_coherent is not a significant part of the algorithm.

The modulation constellation is prepared using the T\_iq\_coherent/constellation Transform activity. This creates a Representation\_constellation object which is



then converted into a Feature\_Hellinger object. Finally the Type\_burst object is created based on the minimum Hellinger distance.

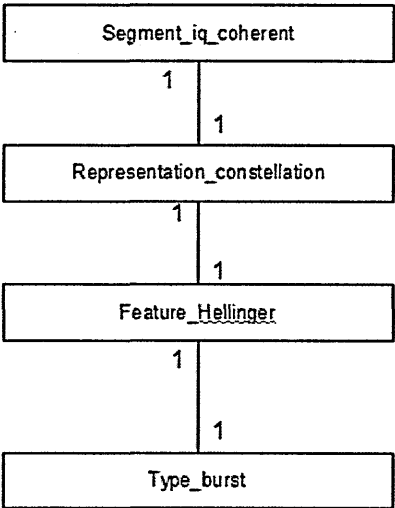


Figure 107. Hellinger distance method class diagram.

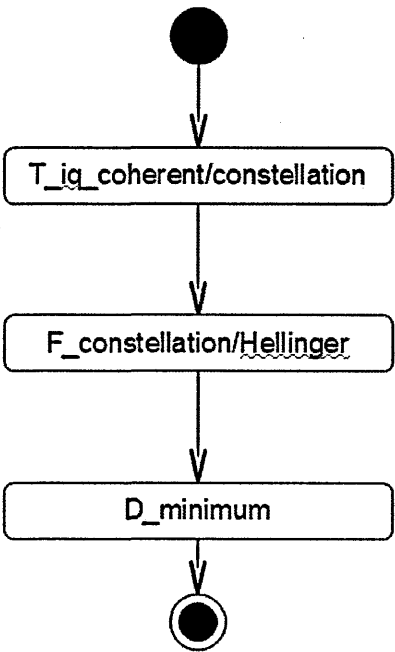


Figure 108. Hellinger distance method activity diagram.

#### 4.3.6.4 Recognition by zero crossing detection

Section 2.4.2 described the zero crossing modulation recognition scheme proposed by Hsue and Soliman (1989). The process is shown in more detail in Figure 109 and Figure 110.

As with AMRA1 the processing is inherently parallel. The Features and Representations can be calculated as three separate threads prior to deciding on the Type.

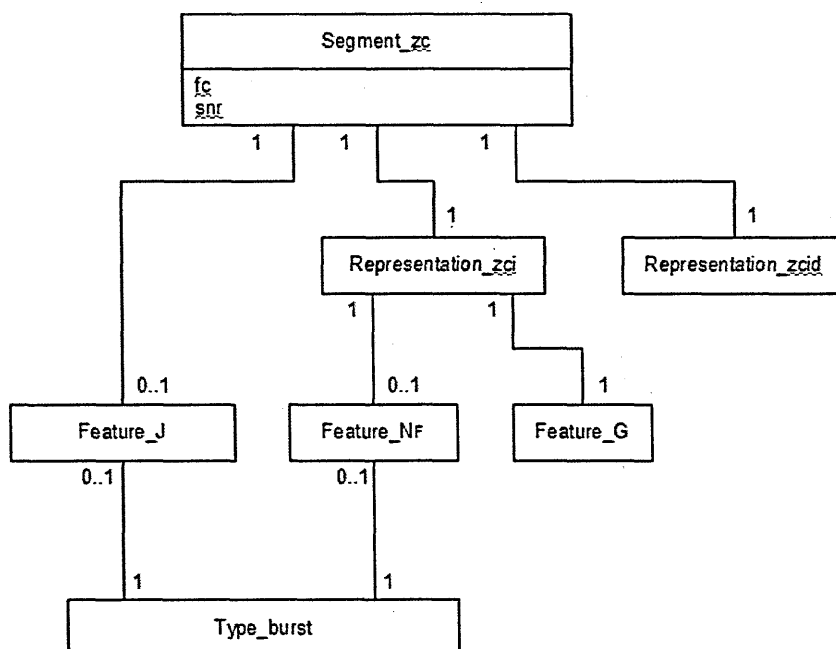
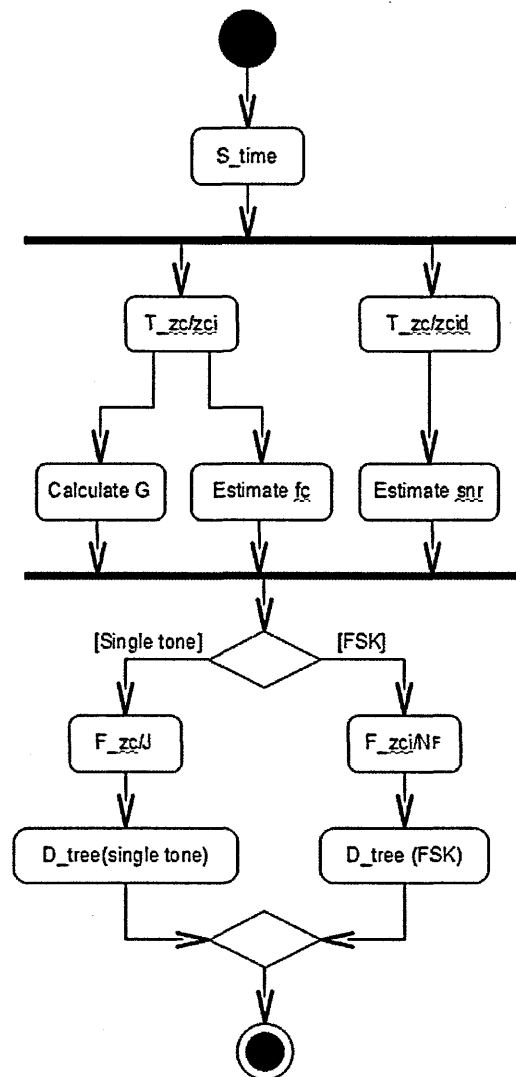


Figure 109. Zero crossing method class diagram.



**Figure 110. Zero crossing method activity diagram.**

Not shown here, but assumed to be present is a `Signal_zc` class with an unspecified relationship to the `Segment_zc` class. The main recognition process starts with zero crossing sampled data, `Segment_zc`, which comprises a list of the times at which the signal crosses the zero axis. The differences between these times are the zero crossing intervals, `Representation_zci`, which are calculated by `T_zc/zci`. Similarly, the second differences, `Representation_zcid`, are obtained via the `T_zc/zcid` activity.

Unlike previous examples there is a need for an explicit intermediate step. The parameter  $G$ , the centre frequency,  $f_c$ , and SNR are estimated from the available data. These are used to decide whether the segment contains a single tone (CW or PSK) or an FSK signal.

If a single tone is detected then the  $J$  parameter is calculated, but, if an FSK is detected, a different parameter,  $N_F$ , is calculated. A different decision tree is used depending on which parameter has been calculated.

Whilst this example has required an intermediate step, the class diagram adheres to the form of Figure 92 and the activity diagram is consistent with the architecture of Figure 93.

#### 4.3.7 Summary

The class and activity diagrams in the above paragraphs form a self-consistent model of a generic ASR system. It is canonical in the sense that it cannot be reduced to a simpler form, yet contains all the elements necessary to create a complete recognition system.

With this model in mind it is possible to consider the structure as a whole and consider to what extent it is suitable for giving accuracy identification estimates in a complex, interfering environment. Section 4.4, therefore, presents the results of considering the model from this point of view.

## 4.4 Feature performance in the presence of interference

In section 3.1 the following sub-question was posed:

**Given that it is possible to design algorithms with specific capabilities (e.g. modulation separation and logarithmic representation) it is reasonable to conclude that algorithms can be devised that possess one or more behaviours appropriate for recognising signals in the presence of interference. To what extent, then, can different algorithms be assessed in terms of their relative performance in the presence of interference?**

Section 4.3 started addressing this question by proposing a canonical architecture that can describe virtually all ASR systems at a high level. At this level it is possible to compare algorithms in terms of their relative performance in the presence of interference.

This section goes on to assert an approach whereby this comparison can be performed. It introduces novel concepts, which are the Ideal Feature and a metric called Interference Selectivity. It then applies these to a range of algorithms and signal types to show how the interference performance of different algorithms can be compared.

To start the discussion, the concept of Segmentation needs to be investigated in more detail, which is the subject of the next section.

#### 4.4.1 Segmentation

The problem of interference was introduced in section 2.3.5. Segmentation is the first stage in the recognition processing that has to deal with interference and is, therefore, particularly sensitive to it. Subsequent processing stages might assume that there is no interference if the Segmentation activity has isolated individual Sources. If the bulk of interference handling can be dealt with by a Segmentation activity, then the design of the following stages is considerably eased.

Seen from the point of view of interference rejection, Segmentation can be viewed as a search process in which the ASR system attempts to identify individual Sources for identification.

This section of the thesis considers the information available to the Segmentation activity and seeks to start answering the question of whether or not interference rejection is practical via a search process. The means of interference rejection is not specified here and could be by interference cancellation using multiple receivers, beam steering, time/frequency domain filtering or any other method.

Given that a received Signal may contain Bursts from more than one Source and that these may overlap in time and/or frequency, what is the best strategy for determining the Type of each of those Bursts?

Figure 111 illustrates a case of two Bursts interfering with each other. In this simple example with non-specific Types, Burst A is narrowband and long in duration, Burst B is relatively wide bandwidth and short duration. One example

of this situation would be where Burst A is a narrowband FM and Burst B is an impulsive noise event.

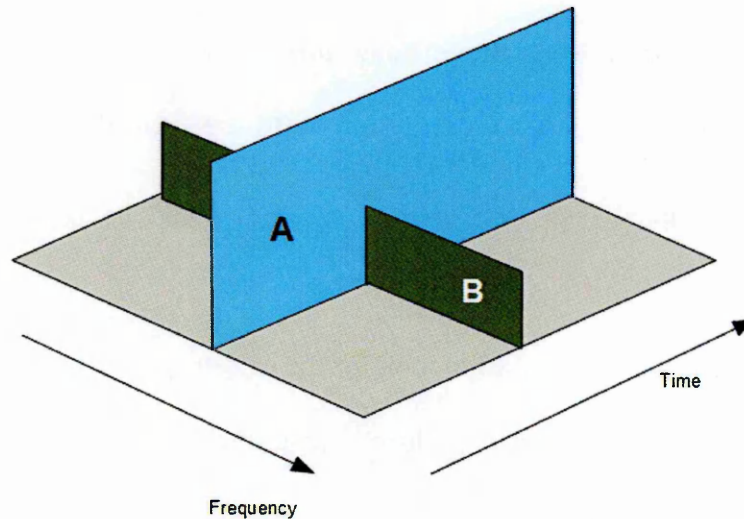


**Figure 111. Example of two interfering Bursts, one narrowband of long duration, the other wideband of short duration.**

One can readily envisage a search algorithm that searches through time and/ or frequency space to find regions in which it is believed that there is no interference. However, before constructing such an algorithm it is important to understand under what conditions such a search is beneficial.

The question that arises, when considering this line of enquiry, is, therefore, whether or not there is any advantage to be gained by trying to constrain each Segment to contain only Burst(s) from one Source.

Starting with a simple case, consider the scenario shown in Figure 112. A Burst from Source A exists on its own until it is interfered with by a Burst from Source B. Thereafter the received Signal comprises A and B in some combination.

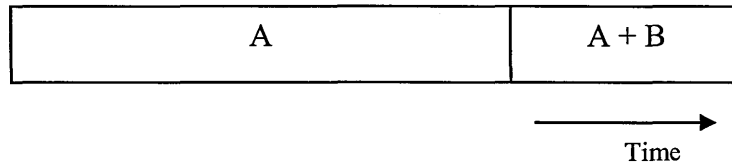


**Figure 112. Example of simple one-dimensional interference, in which a Burst from Source A is interfered with by a Burst from Source B for part of the observation time.**

The set of sampled data from such a scenario could be segmented in three different ways:

- All the data can be analysed to look for the existence of Source A;
- A search for the A region could eliminate the A+B region and only the A region data used for identification;
- The two regions could be analysed separately and the results combined.

It is not immediately apparent which Segmentation strategy would lead to the best results. One way of deciding on the best approach to take, would be to use the solution that gives the best detection probability.

#### 4.4.2 Detection probability

Bayes equation (Cooper and McGillem, 1999, p.26) for a set of  $N$  hypotheses and evidence,  $y_1$ , can be written in the following form, assuming that the probability density of  $y_1$  for hypothesis  $H_h$  is  $f(y_1|H_h)$ .

$$P(H_h | y_1) = \frac{f(y_1 | H_h)P(H_h)}{\sum_{i=1}^N f(y_1 | H_i).P(H_i)} \quad (43)$$

Using the above equation it would be possible to evaluate typical cases of interference and hence decide whether the data from an interfered region (A+B)



would be beneficial or not. In general terms, the data from any region,  $y_1$ , would be worth including in the recognition process if:

$$P(H_h | y_1) > P(H_h) \quad (44)$$

where  $H_h$  is the hypothesis that Source A is present.

Each of the terms in (43) can be evaluated *a priori*. The probability density functions  $f(\cdot)$ , in particular, can be estimated readily using simulations of the Sources to be recognised. They will not, however, be available to the Segmentation activity, which has no knowledge of the presence of either Source. This observation leads to the conclusion that feeding back the estimate of Type from the output of the ASR system to the segmentation process may lead to improvements in performance. This is an area for further research that has not been addressed by this thesis, because it would open up a major new line of enquiry and would depend heavily on the development of the concepts of the Ideal Feature and Interference Selectivity introduced in this thesis.

Equation (43) permits any probability density function  $f(\cdot)$  to be used and this would, ideally be a complete and accurate estimate of the observed Feature data. For the sake of improving compactness of representation one can use a standard distribution, providing such a distribution fits the observed Feature data. It has been found experimentally, as part of the analysis of many statistical Features during this project, that the lognormal distribution is a good fit in many cases for individual modulations.

The lognormal approximation is a pragmatic one. It is not suggested here that this approximation is always applicable and the reader is advised to ascertain for themselves the degree to which it is suitable for their own ASR system. Such an approximation must be made with caution (see Appendix E for more details). If no such approximation can be found, then numeric representations of the  $f(.)$  functions can be used instead.

It is important to note that  $f(.)$  represents the distribution for a combination of signal and interference. As the relative proportions of these two are not known in advance, the probability distribution must be estimated for a range of admixtures. Moreover, because noise will always be present to some degree, this adds a further dimension to the estimation.

By evaluating (43) for different interference scenarios, we can ascertain whether or not it is worth looking for a Segmentation algorithm. This answer does not, in itself, lead directly to an appropriate Segmentation search strategy. To do that, there has to be an indication of the presence of interference, which is a different problem.

#### **4.4.3 The Ideal Feature**

This section introduces and defines the concept of an *Ideal Feature* (IF), the purpose of which is to facilitate comparison of real Features in terms of their performance characteristics within a signal recognition system.

An Ideal Feature is defined to be one that, when the Segment being analysed contains two Sources, it only indicates the required characteristics of the dominant Source. This broad definition makes no assumption about the distribution of the two Sources or noise in the time domain, frequency domain or any other Representation of interest. Neither does it make any assumption about the meaning of the word 'dominant' in this context.

A corollary of the above definition is that, if a recognition system is constructed from a set of Ideal Features then only the dominant Source will be reported by each Feature extraction activity. The Decision activity will then be presented with an unambiguous set of Features on which to base its decision. In such a system there is no need for a Segmentation activity to isolate individual Sources.

Conversely, if a recognition system contains non-ideal Features, then there may be ambiguity in the identification. Such systems require intelligent processing within the Segmentation activity to handle the ambiguity caused by non-ideal Features. The ramifications of this would be additional complexity and an increased probability of erroneous identification, neither of which are desirable.

It follows then that, if a set of Features can be used that are ideal then the need for complex segmentation processing is removed. In practice it may also be possible to use Features that are very well-behaved under all expected interference conditions and approach the performance of an Ideal Feature such that the overall ASR performance is acceptable for the operational scenario.

Consider an additive mixture of two Sources within the received complex baseband signal,  $x(t)$ .

$$x(t) = \eta p(t) + (1 - \eta)q(t) + n(t) \quad (45)$$

Where  $p(t)$  is the Source of interest (i.e. that on which the receiver has been centred and is the Source to be recognised),  $q(t)$  is an interfering Source and  $n(t)$  is noise that is present in the receiver output. The amplitude ratio,  $\eta$ , defines the mix of the two Sources. In this model the amplitude ratio determines which Source is dominant and, in order to keep the reasoning simple, it is assumed that both Sources are continuous in the time domain over the duration of the Segment of interest.

The recognition system will convert  $x(t)$  into a number of Representations and then extract a set of  $L$  Features,  $y_i(t)$ ,  $1 \leq i \leq L$ .

The behaviour of an Ideal Feature is asserted here to be of the form shown in Figure 113 for the case of two, continuous Sources mixed in an amplitude ratio of  $\eta$ . Note that it is assumed that, without loss of generality, all Features (ideal or non-ideal) can be scaled such that they are -1 at  $\eta = 0$  and 1 at  $\eta = 1$ . When plotted in this form the graph is called the *interference selectivity curve*, which is a term introduced by this thesis as it has proved to be a practical concept for evaluating the behaviour of Feature estimation algorithms in the presence of interference.

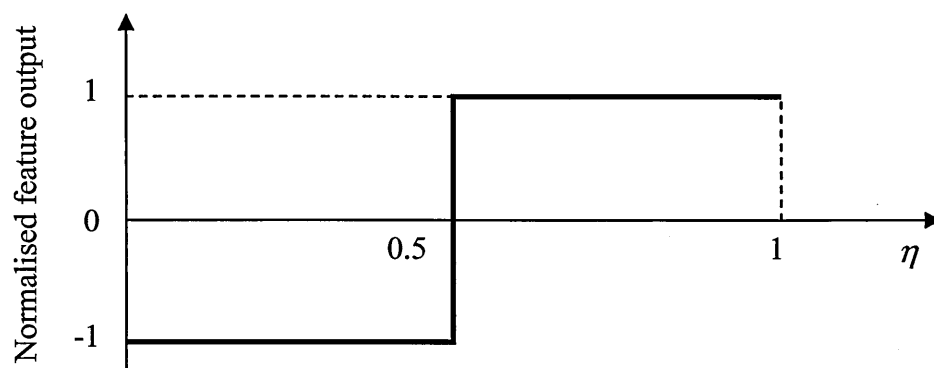


**Figure 113. Ideal Feature interference selectivity curve.**

An Ideal Feature for the model of equation (45) is defined by the relationship:

$$y(t) = \begin{cases} -1 & \eta \leq 0.5 \\ 1 & \eta > 0.5 \end{cases} \quad (46)$$

It is reasonable to ask whether an Ideal Feature can exist or is it only a theoretical concept? If the Segment is represented in a digital form then there are always a finite number of permutations of the bits in the sequence. In the absence of noise it is possible to conceive of an algorithm that assigns each possible bit permutation to an appropriate member of the set of Types that it supports. Hence, although this may not be a practical algorithm, it is possible to define an algorithm that implements the Ideal Feature when the signal representation is digital and there is interference but no noise.

A practical algorithm is unlikely to be straightforward and must be designed to trade off performance in interference selectivity against other requirements, such as speed of computation, memory limitations, ease of update, etc. A practical algorithm must also contend with noise. The addition of which will tend to lead to sequences of bits that cannot be assigned unambiguously to a single Type.

Equation (46) defines the IF for a single pair of Sources, but a practical ASR system must contend with many Sources. A *Globally Ideal Feature* (GIF) is defined here as one that satisfies equation (46) for all Sources. From a theoretical perspective there is an infinite set of possible Globally Ideal Features, as there are an unlimited number of wanted Sources,  $p(t)$ . Each wanted Source is a discrete entity defined by a set of discrete parameters (e.g. symbol rate, chip rate, frequency deviation). However, there is also an unlimited number of unwanted Sources,  $q(t)$ . The unwanted Sources are defined by infinite, continuous parameters, so there are more unwanted Sources than wanted Sources. Putting this argument another way, once a wanted Source has been selected as being of interest, there are an infinite number of unwanted Sources that could interfere with it. Therefore, whilst the set of Globally Ideal Features is infinite, the region of support of each is vanishingly small.

From a practical point of view, any given signal recognition system will be designed to handle a finite set of Types. For this reason (and despite the difficult theoretical concepts outlined above) the concept of the IF and GIF is meaningful in a practical system. Any given Feature can be designed to approach the behaviour of an Ideal Feature with respect to one, more than one or all undesired Types. The latter case would result in a Feature that can be considered to be an approximation to a GIF within the given recognition system. This is a useful concept, even if it is not proved that a Feature is a GIF for all possible Types. For this reason, a more relaxed term is defined and this is the *Complete Ideal Feature* (CIF). A CIF is a Feature that, in the limit, as SNR increases towards infinity, approaches the IF behaviour for all Types of interest for the application.

It is possible to conceive of an algorithm that implements CIF functionality in the same way as the theoretical IF algorithm conjectured above. Again, such an algorithm may not be practical, but the implication is that a practical algorithm may be designed to maximise interference selectivity. There is no similar argument for GIF functionality, however, as the number of Types is not constrained.

#### 4.4.4 Interference Selectivity of a Feature

Real Features, i.e. those that can be realised in a practical, real-world system, do not exhibit the properties of the Ideal Feature. Some may, however, approach this behaviour under certain circumstances and particularly as the SNR increases. It can be assumed that the presence of noise will introduce ambiguity that prevents true Ideal Feature behaviour from occurring in real Features.

The interference selectivity graph shows graphically how well a given Feature approaches the Ideal Feature. It is also useful to have a single metric that indicates 'how ideal' a Feature is. To address this a term is introduced called the *Interference Selectivity* of a Feature.

The Interference Selectivity is defined as follows and measures how closely a given Feature approaches the properties of the Ideal Feature for a single interfering Source.

$$\xi = \exp \left( - \sqrt{ \int_0^{0.5} \eta \left( \int_{-\infty}^{\infty} (y+1)^2 p(y) dy \right) d\eta + \int_{0.5}^1 \eta \left( \int_{-\infty}^{\infty} (y-1)^2 p(y) dy \right) d\eta } \right) \quad (47)$$

This definition has been scaled such that the value of  $\xi$  will be one if the Feature is ideal, but it will fall and approach zero the more that the Feature performance varies from that of the Ideal Feature.

The variance of the Feature,  $y$ , is averaged separately over each of the two ranges of  $\eta$ . The left hand term gives the average variance over the left hand region of the interference selectivity curve ( $0 \leq \eta \leq 0.5$ ) and assumes that the mean of  $y$  is -1. Similarly, the right hand term gives the average variance over the right hand region of the interference selectivity curve ( $0.5 \leq \eta < 1$ ) but assumes that the mean of  $y$  is 1 rather than -1. The more the measured performance of the Feature diverges from that of the Ideal Feature, the higher these variance terms will be.

The two variance terms are then scaled such that the Interference Selectivity,  $\xi$ , is one when the Feature exactly matches the behaviour of the Ideal Feature and approaches zero as the variance terms increase. There is no upper bound on the variance terms so the scaling has been based on an exponential decay, which means that the value of  $\xi$  will tend towards zero as either or both of the variance terms approach infinity.

Hence we now have a metric that allows the performance of any Feature to be measured and compared with that of any other Feature. The region of support of  $\xi$  has been scaled to be  $(0,1]$  and Features that have higher values of  $\xi$  will be better at rejecting interference than Features with lower values of  $\xi$ .



Before examining examples of the Interference Selectivity metric it is worth explaining the choice of the term Interference Selectivity, because the term is introduced by this thesis as a part of the original contribution to the subject. In radio engineering the term selectivity is applied to the ability of a receiver to tune into a desired station and reject unwanted signals (Krauss *et al*, 1980, p.267) which are normally considered to be close in frequency, but not overlapping. Selectivity is, from the point of view of this thesis, the ability of a receiver to separate closely spaced Sources (Ziemer and Tranter, 1995, p.163). The metric described in this section similarly describes the performance of a receiver system, but, in this case, the unwanted Sources are interferers that may overlap the wanted Source in time and/or frequency, so the term Interference Selectivity has been used to clarify the difference.

#### **4.4.5 Examples of Feature behaviour**

This section presents examples of Feature behaviour obtained by simulation of a single test scenario. It demonstrates that some Features have relatively good performance (i.e. they approach the performance of the Ideal Feature to some degree) and others have relatively poor performance (i.e. they deviate significantly from the desirable characteristics of the Ideal Feature).

Figure 114 shows a simulation of two types of Source at the same frequency. The Source of interest is IEEE 802.11 'WiFi' operating in its 2 Mbps mode, which uses DSSS and DQPSK. The interferer is a Bluetooth emitter operating in its DPSK8 mode. The plot is the power spectral density for one of the many cases included in the simulation. The receiver bandwidth has been set at 40 MHz to allow both

Signals to be captured correctly. Each simulation case comprises a Signal of interest (black trace), an interferer (red trace) and an additive combination of the two (blue trace) with varying amplitude ratios.

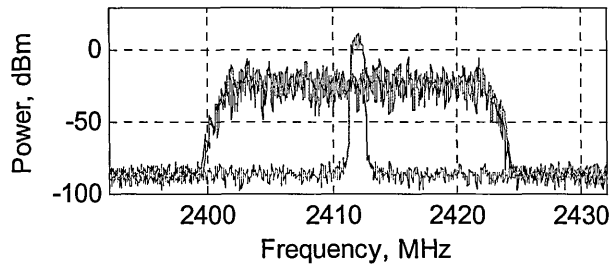


**Figure 114. Power spectral density for combination (blue) of DSSS+DQPSK 2Mbps WiFi (black) and DPSK8 Bluetooth (red), both at 2412 MHz.**

Figure 115 shows the results of simulating the above test case and estimating the  $\sigma_{ap}$  Feature (section 2.4.3). The left hand plot shows the estimate of the interference selectivity curve for a range of SNRs from -10 dB to +30 dB. On this plot the Ideal Feature characteristic is shown as a black dotted line for comparison with the actual results.

The right hand plot shows the interference selectivity,  $\xi$ , against the SNR. It will be seen that the Interference Selectivity settles down to a value of about 0.56 as the SNR is increased.

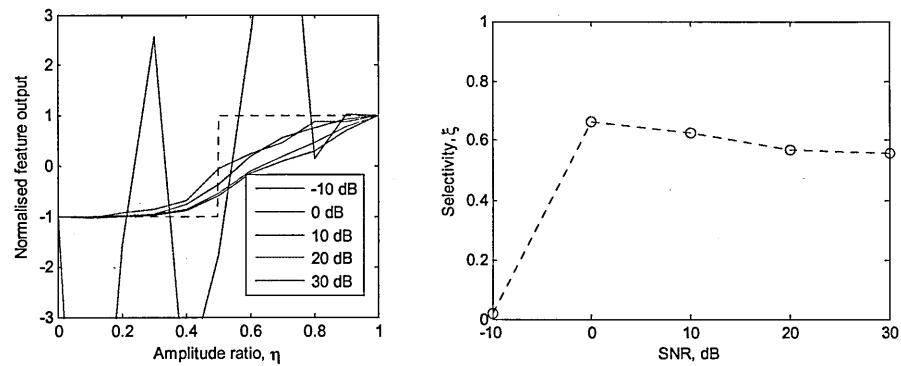


**Figure 115. Interference selectivity of  $\sigma_{ap}$  for DSSS+DQPSK 2Mbps WiFi and DPSK8 Bluetooth, both at 2412 MHz (500 runs per case).**

$\sigma_{ap}$  has an Interference Selectivity, for this scenario, of about 0.56. Whilst not ideal, its interference selectivity curve at high SNR is 'well-behaved' in that it tangentially approaches the lower and upper ends of the  $\eta$  range and does not diverge significantly from the  $\pm 1$  range between these extremes.

In contrast, consider the example shown in Figure 116 which gives the graphs for  $\sigma_{aa}$ , a Feature that has an Interference Selectivity approaching zero in this scenario and diverges significantly from the Ideal Feature. In this case the divergence appears to worsen as the SNR increases.

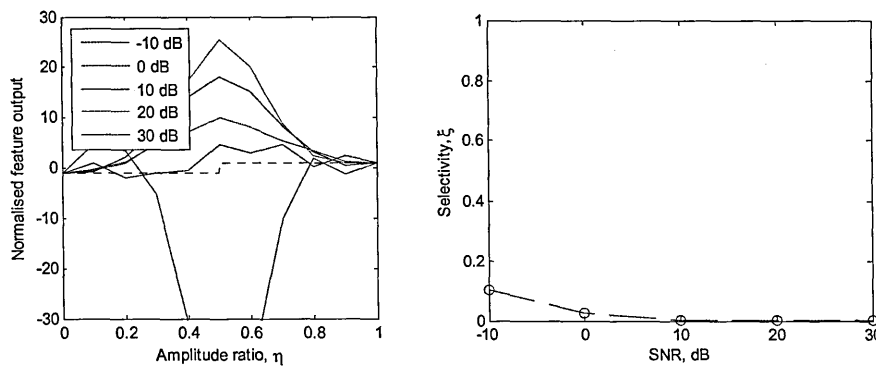


**Figure 116. Interference selectivity curves of  $\sigma_{aa}$  for DSSS+DQPSK 2Mbps WiFi and DPSK8 Bluetooth, both at 2412 MHz (50 runs per case).**

A similar example is  $\mu_{42}^a$  which has an Interference Selectivity of about 0.1 in this scenario and results in the graphs shown in Figure 117. Again the Interference Selectivity is approaching zero as the SNR increases. There is a small rise at 30 dB, but this does not represent a significant change in performance and can be considered to be noise in the results.

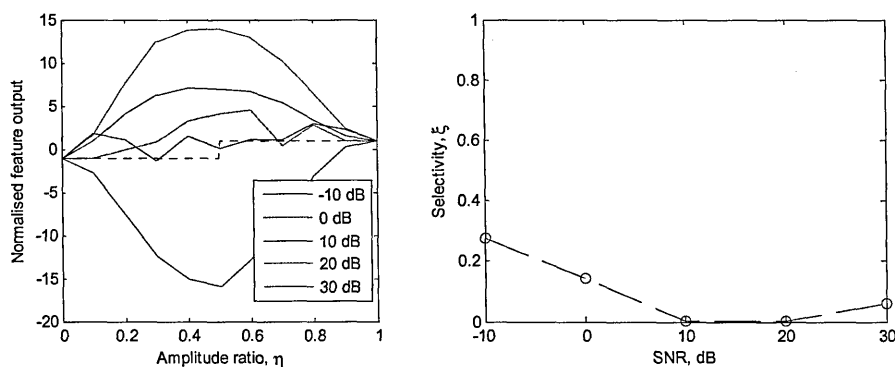


**Figure 117. Interference selectivity curves of  $\mu_{42}^a$  for DSSS+DQPSK 2Mbps WiFi and DPSK8 Bluetooth, both at 2412 MHz (50 runs per case)**

There are many examples such as these. In general it appears as though the probability distributions of the Features are being 'pulled away' from those of the Source of interest and the interferer. It is conjectured that all such cases of poor

Interference Selectivity are caused by artefacts generated by the additive combination of the two Sources. A simple example of such an artefact is the well-known phenomenon of the 'beat frequency' caused by the summation of two sinusoids that are closely spaced in frequency (Daintith and Nelson, 1989, pp. 30-31). Typically such artefacts are maximised when the two Sources are of similar amplitude. For Source recognition in the presence of interference, such artefacts are not desirable.

#### **4.4.6 Interference Selectivity statistics**

It is useful to have an understanding of how typical Features behave in the presence of interference. A simulation was constructed to obtain statistics of some Features based on those commonly used in the literature.

In this simulation the Interference Selectivity was calculated for each Feature over a wide range of interference scenarios. In total 1,000 scenarios were evaluated for 13 Features allowing the probability distribution of the Interference Selectivity to be estimated for each Feature. The SNR was 30 dB throughout. Further details on this simulation are given in Appendix B.

The first set of Features to be considered were those used by Azzouz and Nandi (1996). The results are shown in Figure 118 as a series of boxplots ordered by median values. Each boxplot shows the minimum, maximum, median and interquartile range.

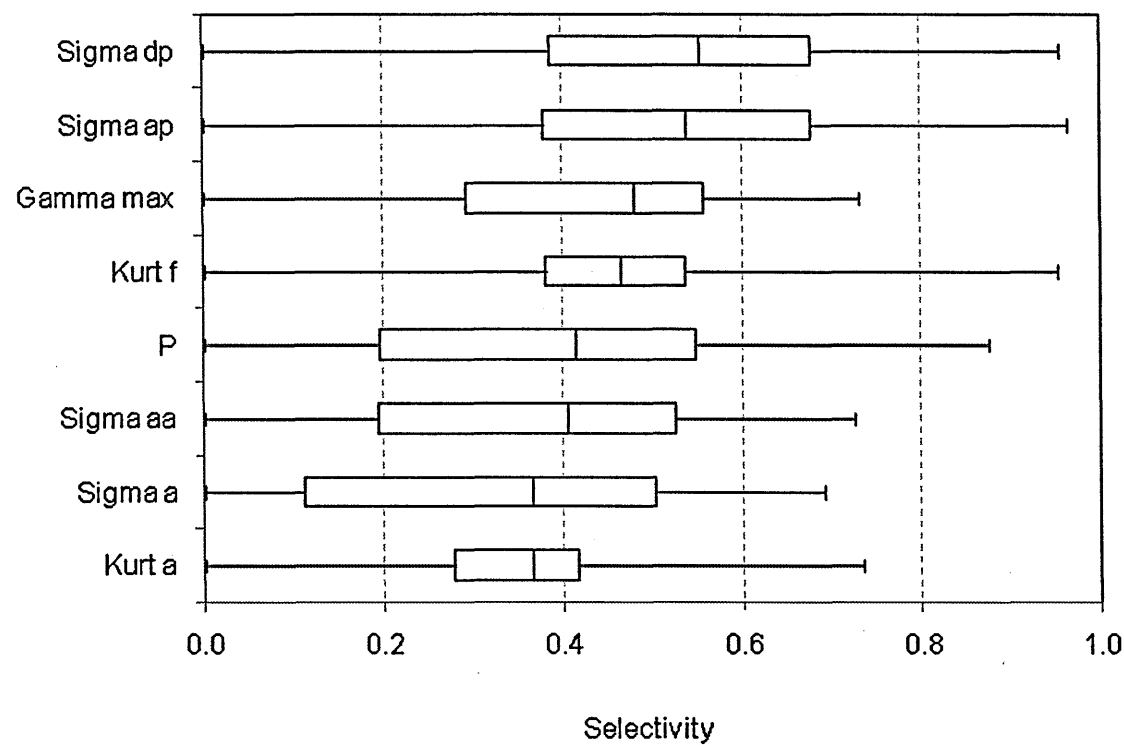


**Figure 118. Interference Selectivity distributions of Azzouz & Nandi Features.**

By way of comparison another set of Features was tested. These Features were based on the delay-multiply algorithm described in section 2.4.2 with delays set to the reciprocals of 100kHz, 200kHz, 250 kHz, 500kHz and 1MHz. The boxplots for these results are shown in Figure 119, again ordered by median values.

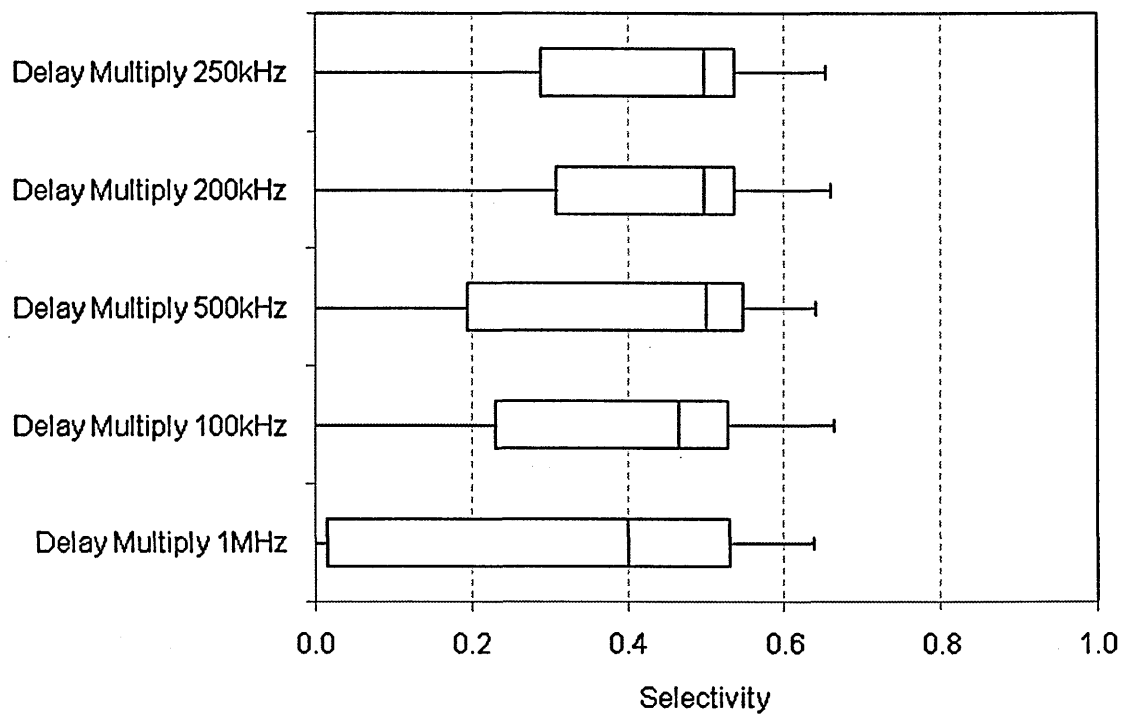


**Figure 119. Interference Selectivity distributions of delay-multiply features.**

Inspection of these two sets of boxplots leads to the following observations:

1. All the Features examined exhibit Interference Selectivities,  $\xi$ , very close to zero under some circumstances. The closer the value of  $\xi$  is to zero, the further its interference curve is from that of the Ideal Feature. All these Features, therefore, are potentially liable to perform very badly at times. With over 5 million interference events being simulated, it is not practical to examine them all and arrive at a definitive explanation of why the poor performance occurs. The key result is, however, that all the Features do perform badly in some cases;

2. None of the Features tested achieved an Interference Selectivity,  $\xi$ , of one. If  $\xi$  equals one then the feature performance matches that of the Ideal Feature.

In a few cases for the  $\sigma_{ap}$  and  $\sigma_{dp}$  Features, the Interference Selectivity

exceeded 0.9. It is therefore possible to produce a practical Feature that can have a performance near to that of the Ideal Feature in some cases;

3. The median values of  $\xi$  range from just below 0.4 to just above 0.6. These are not values that are close to one indicating significantly non-ideal performance with regards to Interference Selectivity in most cases. None of these Features were designed for good Interference Selectivity, but were taken from the literature and were originally used by their designers to make measurements in the presence of simple noise models but not interference. The implication is that, unless Interference Selectivity is used as one of the design criteria, good Interference Selectivity performance cannot be assumed;
4. The interquartile ranges of the two kurtosis parameters are narrow compared to the other parameters. The implication of this is that kurtosis has a more predictable response to interference than the lower order moments and therefore offers better performance. If one can use a higher order moment as a Feature and improve its median Interference Selectivity, then this is a better approach than trying to improve the median performance of a lower order moment. This is an interesting route for further research;
5. The medians of the delay-multiply Feature Interference Selectivities are close to each other and most are approximately 0.5. This is attributed to the structure of these algorithms, which are identical. Comparing these distributions to the statistical Features, which vary considerably more, leads towards the thought that Interference Selectivity might be related to the algorithm structure. The ability of an algorithm to reject interference is probably related to the way in which it looks for correlations in the input



Signal. Further research is required to determine the characteristics of an algorithm that lead to good Interference Selectivity;

6. The maximum values obtained for the delay-multiply features were all below 0.7. None of these Features, therefore, approached the Ideal Feature for any of the cases simulated. Some of the statistical Features did approach an Interference Selectivity of 1.0 in some cases, so there is an implication that the parametric Features may not be capable of achieving values as high as those of the statistical Features. This conjecture would need considerable research to confirm.

This section has shown that Interference Selectivity can be estimated and that it is different for different Feature extraction algorithms. The corollary of this is that it is possible to choose Feature extraction algorithms that have better Interference Selectivity. Selecting Features that have better Interference Selectivity will lead to improved robustness in the presence of interference and hence improved identification accuracy.

#### **4.4.7 Options for handling interference**

It was shown in section 4.4.5 that typical Features can be affected badly by interference. Furthermore it was shown in section 4.4.6 that, unless they have been designed to give acceptable Interference Selectivity, Features cannot be guaranteed to behave well in the presence of interference. A number of options can be considered for dealing with these problems:

### **1. Remove the interference by filtering**

Segmentation by filtering in the frequency and/or time domain is a practical option, provided the interference can be recognised and the Sources are not overlapping. If there is a human in the loop then an ASR system can depend to some degree on their input to guide the filtering process. In a fully automatic system the filtering will have to be automated. This is practical in cases where the interference can be clearly distinguished in some way. It does, however, add another layer of complexity to the system and may not handle all possible interference cases.

Option 1 requires an intelligent Segmentation activity that can identify and separate multiple signals. If any of the Features are non-ideal then this approach is preferred, as it means that minimal interference is introduced into the Decision activity.

### **2. Improve the Interference Selectivity of Features**

It was shown in section 4.4.6 that different Features have different Interference Selectivity characteristics. In many cases it can reasonably be expected that Features could be modified to make them more robust in the presence of interference. With the definition of Interference Selectivity in this thesis, it is now possible to quantify what is meant by robustness. A Feature with a higher Interference Selectivity than that of another Feature is more robust to interference. This is seen as a useful step forward, as designers can now consider robustness to interference as well as detection probability and thereby improve the Features they devise. Similarly, it is now possible to

conjecture new Features that are designed specifically for good Interference Selectivity.

Option 2 requires elimination of the susceptibility of a Feature to corruption by interference. This is a hard problem, but solving it implies easing the pressure on the Decision activity. Removing ambiguity from the inputs to the Decision activity will make the identification more accurate and it was accuracy that was determined to be the most important factor to users.

### **3. Multiple hypothesis techniques**

A refinement of the filtering approach is to use a multiple hypothesis approach. Here a search strategy is required that can look for the optimum set of hypothesised signals that match the observed data. This is a plausible approach, but the search must be guided by an appropriate metric.

One problem with the multiple hypothesis approach is that of overlapping Sources, which may not be amenable to separation by time or frequency domain filtering. Another problem, which is not expected to be trivial, is that of finding a suitable metric on which to base the search algorithm.

Option 3 is a strategy for dealing with Features that have been corrupted by interference, which the results to date suggest is likely to be the case. If one can avoid getting into the situation where this is the case, then this is an approach that would not be necessary.

#### **4. Pre-spreading the probability distributions**

The probability density functions of Features can be modified to incorporate some of the loss of confidence due to interference. This can be achieved by increasing the spread (i.e. standard deviation) of the probability density functions used in a Bayesian decision process. Doing this tells the decision process that one has less confidence in a Feature because one suspects that interference may have corrupted it. The net effect would be a lower confidence in the identification, so more observations would be needed to achieve higher confidence.

As with option 3, this option is a way of handling the fact that the Features may be corrupted by interference. If it can be avoided by using more robust Features then this would yield improved identification confidence.

#### **5. Do nothing.**

If interference is ignored in the design, the probability of successful recognition will be impaired when interference is encountered. There may be situations where it is arguable that recognition accuracy is only needed at high signal to interference ratios, in which case it may be acceptable to ignore the effects of interference. This cannot be assumed generally, however, so the do nothing option is not advisable.

A fully workable ASR system may have to include elements of more than one of the options above. A suggested approach is to start designing the ASR system with option 2 and aim to find Ideal Features, but recognise that this goal may not

be completely achievable. A practical system may, therefore, have to provide an intelligent Segmentation activity (i.e. option 1) and then use ideas from options 3 and 4 to deal with the residual interference effects.

## **4.5 Combining multiple decision-theoretic algorithms**

The previous sections have mainly considered individual Feature extraction algorithms. Section 4.1 looked at the PCRP method to show that an algorithm can be devised that emphasises modulation characteristics over information content. Section 4.2 introduced the LCDP as an algorithm that can handle a wide range of time scales to separate interferers with very different modulation characteristics. Section 4.4 proposed a means whereby the performance of different Feature extraction algorithms in the presence of interference could be compared. These are all elements of the problem of finding algorithms for use in ASR processing, but they do not, in themselves, lead to an overall processing architecture.

In an interfering environment the set of candidate modulations cannot be known in advance. There may be a single Feature extraction algorithm that works for all modulations, but such an algorithm has not been found during the literature search. The natural conclusion is, therefore, that an effective solution is most likely to require the combination of multiple algorithms.

This section considers the last sub-question in section 3.1, which was:

**Multiple algorithms can be applied to the ASR problem, each with its own strengths and weaknesses. To what extent can these be brought together to produce an accurate result?**

There is not a large body of extant research in this area and it will not be possible to completely solve the problem within a single thesis, so the approach is taken of asserting a method and using this to produce ideas for further work.

#### 4.5.1 Bayesian chaining

In this thesis it is proposed that a probabilistic approach to combining Features is preferred over both decision trees and artificial neural networks. The primary motivation for this comes from the experience gained in trying to train an artificial neural network for the ASR task. Subjectively it is relatively easy to train an artificial neural network to recognise signals that have high signal to noise ratios. It is not so easy, however, to train an artificial neural network on signals that have low signal to noise ratios. This problem has been known for some time (Yaqin *et al*, 2003). The ambiguities that arise because of noise tend to fragment the regions of parametric hyperspace assigned to each modulation. This can be overcome by increasing the complexity of the artificial neural network, but this leads to overtraining and a reduction in the effectiveness of the resultant artificial neural network when subjected to signals that it was not trained on. Similar arguments apply to the design of decision trees where the specification of decision thresholds poses problems analogous to those encountered in artificial neural network design.

A further issue with the existing techniques is that they do not provide a means of including *a priori* knowledge about the likely presence of different Sources in the environment.

The concept proposed is therefore to use Bayesian chaining, which promises to alleviate some of these problems. Figure 120 illustrates the concept.

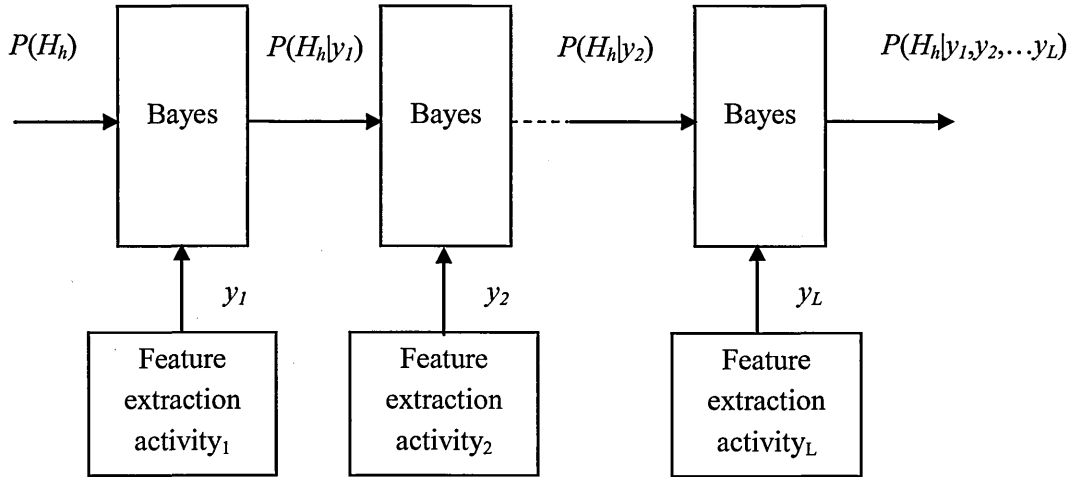


**Figure 120. Bayesian chaining of probabilities.**

Assume that the total number of Source types in the environment is known to be  $N$  and that the corresponding Types form a finite set. For practical expediency one of these can be elected to be the 'unknown' Type and another to represent a 'noise' Type. These allow us to include the situations where the Source is of a Type not seen before and no Source is present respectively.

$$H = \{H_1, H_2, \dots, H_N\} \quad (48)$$

For each Type,  $H_h$ , there is an *a priori* probability,  $p(H_h)$ . If no *a priori* information is available then all the probabilities can all be set equal to  $1/N$ . However these probabilities are assigned they must describe a marginal probability distribution and must therefore obey:

$$\sum_{h=1}^N P(H_h) = 1 \quad (49)$$

When a Segment of a Signal,  $x$ , is to be analysed, it is transformed and the Representations are applied to a set of Feature extraction activities. The resulting Features  $y_1, y_2, \dots, y_L$  are used to update the *a priori* probabilities using the chaining scheme shown in Figure 120 to produce a set of *a posteriori* probabilities,  $p(H_h | y_1, y_2, \dots, y_L)$ . These *a posteriori* probabilities can be interpreted by the client application as required.

At each stage in the chain the discrete form of Bayes rule (Cooper and McGillem, 1999, p26) is used to update the probabilities. If all the probabilities required were discrete, then the first stage in the chain would be:

$$P(H_h | y_1) = \frac{P(y_1 | H_h)P(H_h)}{\sum_{i=1}^N P(y_1 | H_i)P(H_i)} \quad (50)$$

However, in general the conditional probabilities,  $P(y_i | H)$ , are not available in discrete form. A Representation applied to a Feature extraction activity typically produces a continuous variable,  $y$ , so there is a mixture of continuous and discrete probabilities that must be taken into account when formulating the chaining algorithm. Equation (50) must therefore be modified to use the probability density function of the Feature rather than a discrete probability.



The modified chaining equation is then:

$$P(H_h | y_1) = \frac{f(y_1 | H_h) \cdot \Delta y \cdot P(H_h)}{\sum_{i=1}^N f(y_{1_i} | H_i) \cdot \Delta y \cdot P(H_i)} = \frac{f(y_1 | H_h) P(H_h)}{\sum_{i=1}^N f(y_{1_i} | H_i) \cdot P(H_i)} \quad (51)$$

where  $f(.)$  are the PDFs and  $\Delta y$  is the interval over which the probability is determined.

Figure 121 illustrates this concept for a Feature,  $y$ . It shows the joint probability density function for one Feature and three signal types,  $H_1$ ,  $H_2$  and  $H_3$ . Notice how the Feature axis is continuous, but the Type axis is discrete.

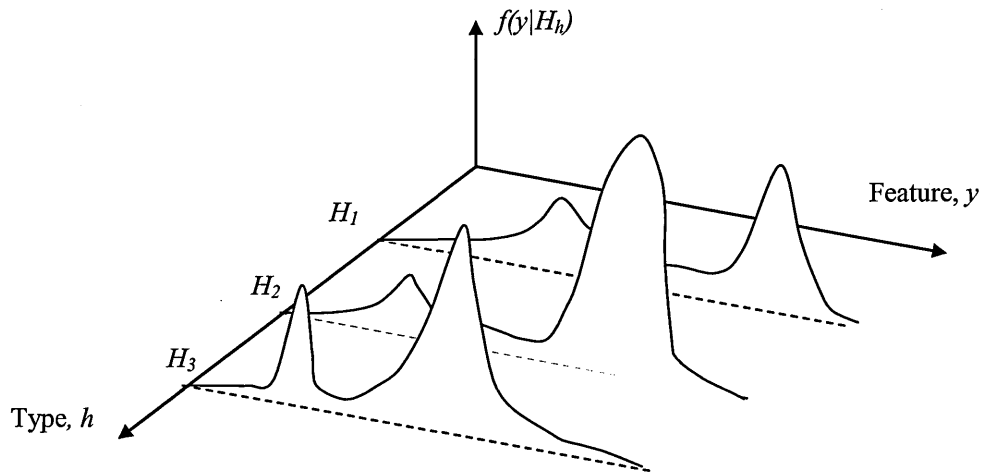


**Figure 121. Schematic illustration of joint probability density function for a single Feature,  $y$ , and three Types,  $H_1$ ,  $H_2$  and  $H_3$ .**

As this is a joint probability density function the total volume enclosed must be one, so the following relation must hold:

$$\sum_{h=1}^N \int_{-\infty}^{\infty} f(y|H_h) dy = 1 \quad (52)$$

The individual probability density functions,  $f(y_i|H_h)$ , can be found by testing each Feature for each of the Types in the set selected for recognition.

After the above calculation of the *a posteriori* probabilities has been carried out, a Decision must be made as to which hypothesis is the most likely. A straightforward way of doing this is to use the MAP approach (section 2.4.4). This gives the most likely hypothesis at the end of stage  $i$  as:

$$\hat{h} = \arg \max_{h \in [0, H]} (P(H_h | y_1, y_2, \dots, y_L)) \quad (53)$$

This process can be repeated for any number of Features and leads to a means of combining the results of different Feature extraction activities.

The process can also be repeated when further buffers of I/Q data are received. This leads to the concept of a 're-identification' function in which the *a posteriori* probabilities are updated each time a Feature extraction activity produces a result. Providing the receiver's parameters are not changed and, if the assumption is made that the Source characteristics have not changed, then it is possible to apply a re-identification function for as long as Signal data is made available. Such re-identification processing would enable the confidence in a Type to be increased as more Signal data is taken into account.

#### 4.5.2 Probability density function modelling approach

There are three different approaches to modelling the probability density functions for the purposes of calculating decision thresholds:

1. Assume that the received Signal has a high SNR and use a single probability distribution (e.g. lognormal) for each Feature. This is the approach used by Azzouz and Nandi (1996, p. 56);
2. Accept that the SNR is not known and that the actual PDF will be a combination of that for the Feature at high SNR and that produced when the Feature extraction activity processes noise only. There is a mixing region in which the two PDFs have to be combined;
3. Store the PDF obtained by experimentation across a wide variety of SNR conditions.

The table below summarises the advantages and disadvantages of these approaches.

	Advantages	Disadvantages
1. High SNR, single PDF	Readily amenable to decision-theoretic methods	Inherently weak at low SNR
2. Combined high and low SNR PDFs	Handle wider range of operational conditions	Multi-mode distributions not easily modelled as standard unimodal distributions
3. Stored PDFs	Most representative model	Cannot make extensive use of probability theory.

**Table 16. Advantages and disadvantages of different approaches to probability density function modelling.**

#### 4.5.2.1 High SNR, single PDF

Assume that a decision has to be made between two hypotheses,  $H_1$  and  $H_2$ . By way of example the Feature being used is  $\gamma_{\max}$  (section 2.4.3).

From Ziemer and Tranter (1995, pp.607-608) the Bayes detector is:

$$\Lambda(\gamma_{\max}) \underset{H_1}{\overset{H_2}{>}} \frac{p(H_1)(c_{21} - c_{11})}{p(H_2)(c_{12} - c_{22})} \quad (54)$$

where the likelihood ratio is:

$$\Lambda(\gamma_{\max}) = \frac{f_{\gamma_{\max}}(\gamma_{\max} | H_2)}{f_{\gamma_{\max}}(\gamma_{\max} | H_1)} \quad (55)$$

Assume that the Sources have high SNRs and that the Feature can be modelled as a random variable with a lognormal distribution (Cooper and McGillem, 1999, p86). Appendix E gives notes on the applicability of the lognormal distribution in this context. For  $\gamma_{\max}$  the conditional probabilities, depending on which hypothesis is correct, are:

$$F_{\gamma_{\max}}(\gamma_{\max} | H_1) = \Theta_{\mu_1, \sigma_1^2}(\ln(\gamma_{\max})) = \frac{1}{\sigma_1^2 \sqrt{2\pi}} \int_{-\infty}^{\ln(\gamma_{\max})} \exp\left(-\frac{(u - \mu_1)^2}{2\sigma_1^2}\right) du \quad (56)$$

$$f_{\gamma_{\max}}(\gamma_{\max} | H_1) = \frac{1}{\gamma_{\max} \sigma_1 \sqrt{2\pi}} \exp\left(-\frac{(\ln(\gamma_{\max}) - \mu_1)^2}{2\sigma_1^2}\right) \quad (57)$$

$$F_{\gamma_{\max}}(\gamma_{\max} | H_2) = \Theta_{\mu_2, \sigma_2^2}(\ln(\gamma_{\max})) = \frac{1}{\sigma_2^2 \sqrt{2\pi}} \int_{-\infty}^{\ln(\gamma_{\max})} \exp\left(-\frac{(u - \mu_2)^2}{2\sigma_2^2}\right) du \quad (58)$$

$$f_{\gamma_{\max}}(\gamma_{\max} | H_2) = \frac{1}{\gamma_{\max} \sigma_2 \sqrt{2\pi}} \exp\left(-\frac{(\ln(\gamma_{\max}) - \mu_2)^2}{2\sigma_2^2}\right) \quad (59)$$

If both distributions are assumed to be lognormal then the likelihood ratio becomes:

$$\Lambda(\gamma_{\max}) = \frac{\sigma_1}{\sigma_2} \frac{\exp\left(-\frac{(\ln(\gamma_{\max}) - \mu_2)^2}{2\sigma_2^2}\right)}{\exp\left(-\frac{(\ln(\gamma_{\max}) - \mu_1)^2}{2\sigma_1^2}\right)} \quad (60)$$

$$\therefore \Lambda(\gamma_{\max}) = \frac{\sigma_1}{\sigma_2} \exp\left(\frac{(\ln(\gamma_{\max}) - \mu_1)^2}{2\sigma_1^2} - \frac{(\ln(\gamma_{\max}) - \mu_2)^2}{2\sigma_2^2}\right) \quad (61)$$

Taking the natural logarithm of this gives:

$$\ln(\Lambda(\gamma_{\max})) = \ln(\sigma_1) - \ln(\sigma_2) + \frac{(\ln(\gamma_{\max}) - \mu_1)^2}{2\sigma_1^2} - \frac{(\ln(\gamma_{\max}) - \mu_2)^2}{2\sigma_2^2} \quad (62)$$

We could assume that the two hypotheses are equally probable and use the minimum probability of error criteria (Ziemer and Tranter, 1995, p.613), i.e.:

$$\begin{aligned} p(H_1) &= p(H_2) \\ c_{11} &= c_{22} = 0 \\ c_{12} &= c_{21} \end{aligned}$$

With these simplifications the Bayes' detector criterion becomes:

$$f_{\gamma_{\max}}(\gamma_{\max} | H_2) \underset{H_1}{\overset{H_2}{>}} f_{\gamma_{\max}}(\gamma_{\max} | H_1) \quad (63)$$

With a single lookup table to store a lognormal distribution this operation could be performed readily and efficiently. It is therefore attractive from a processing point of view.

The major problems with this approach are that:

- The lognormal distribution assumption may not always hold (see Appendix E) so the full *a priori* distribution may need to be used;
- The assumption of a high SNR may not be appropriate. Many Sources of interest will have low SNRs (section 2.3.3);
- The extension to three or more signal types requires further work. In the above form, this is not a practical Decision method.

#### 4.5.2.2 Combined high and low SNR PDFs

If, rather than being a single lognormal distribution, each Feature is assumed to approach the combination of two lognormals (one for the high SNR signal and one for a noise term), equation (58) becomes:

$$\Lambda(\gamma_{\max}) = \frac{\frac{w_{21}}{\gamma\sigma_2\sqrt{2\pi}} \exp\left(-\frac{(\ln(\gamma_{\max}) - \mu_2)^2}{2\sigma_2^2}\right) + \frac{w_{20}}{\gamma\sigma_0\sqrt{2\pi}} \exp\left(-\frac{(\ln(\gamma_{\max}) - \mu_0)^2}{2\sigma_0^2}\right)}{\frac{w_{11}}{\gamma\sigma_1\sqrt{2\pi}} \exp\left(-\frac{(\ln(\gamma_{\max}) - \mu_1)^2}{2\sigma_1^2}\right) + \frac{w_{10}}{\gamma\sigma_0\sqrt{2\pi}} \exp\left(-\frac{(\ln(\gamma_{\max}) - \mu_0)^2}{2\sigma_0^2}\right)} \quad (64)$$

where  $w_{10}$ ,  $w_{20}$ ,  $w_{21}$  and  $w_{22}$  are weighting factors that allow the pairs of distributions to be combined in different ratios.

The main advantage of (64) over (55) is the compactness of the representation. It allows the likelihood ratio to be expressed in terms of twelve parameters rather than requiring the full PDFs to be described in vector form.

Given that a representation such as (64) is desirable for compactness of description, it is reasonable to search for a better representation. Initial investigations suggest that one approach to this is to consider the means of the Feature PDFs to be sigmoidal. This is an area requiring further research, but the concept is illustrated in Figure 128 and Figure 129 in Appendix E.

#### **4.5.3 Conclusions on combining multiple algorithms**

A number of standard detectors were described in section 2.4.4. These form the basis for a decision-theoretic solution to the identification problem. If all the required *a priori* information is available, then a Bayes detector would give an optimal decision and allow the system designer to assign the relative costs of correct and incorrect decisions. In practice, some of the required information may be unavailable and a fast decision may be required, so it may be necessary to adopt the approach of one of the other detectors in section 2.4.4. Alternatively, a simplification may be possible by means of assuming a standard probability distribution that can be summarised with a limited number of parameters.

A Bayesian chain approach has been proposed that combines a discrete Type probability with a set of continuous Feature PDFs. It has been shown that regard must be given to the expected range of signal to noise ratios to be encountered. If it can be assumed that the SNR will always be high then the Bayesian chain can be simplified, as the probability density functions approximate to lognormal (see Appendix E for more details). If, on the other hand, the ASR system has to handle a wide range of SNRs, which is more likely, then the SNR variation must be taken into account when modelling the probability density functions of the Features.

This section has addressed the question of how multiple Feature extraction algorithms can be brought together to produce robust identification in the presence of interference. It has given one example of how this might be achieved, thereby showing that an appropriate method exists. There are, however, many more possible ways of fusing Features and it will only be by carrying out considerably more research in this area that the best architecture will be determined.

## **4.6 Summary**

This section has described the results of the research work carried out for this Ph.D. project.

Recurrence plots have been investigated and these promise to be an interesting area for further work in their own right. The method has been shown to be a novel method for visualising communication signals. It has also been shown to



yield quantitative measurements that relate directly to the features of interest to ASR processing. The particular examples given illustrated measurement of the symbol rate for basic digital modulation schemes. More importantly the recurrence plot approach was used to explain how the information content in a received signal can be suppressed in favour of the modulation type, which is felt to be a useful concept in constructing improved ASR algorithms. As an example of this, a novel variant of the recurrence plot, called the PCRP, was devised and shown to be effective at enhancing symbol rate detection.

A novel form of cyclostationarity transform, called the LCDP, was devised as a way of dealing with the wide range of bandwidths and time scales seen in the modern communications environment. Techniques such as this are seen to be important in allowing ASR systems to cope with the characterisation of radio signals in shared, interfering spectral bands.

A generic architecture was constructed based on examining the results of the literature search and organising the various techniques into a canonical form. Applying this rigour to the description of algorithms allows one to research high-level aspects of ASR system design and apply reasoning to whole classes of algorithms rather than individual algorithms.

The performance of Feature extraction algorithms in the presence of interference has been investigated. This required the development of a metric for measuring the relative performance of different algorithms and this metric was the Interference Selectivity. The Interference Selectivity was based on the concept of

deviation from an Ideal Feature, which is a feature that works perfectly in the presence of interference. This approach to handling the complex issue of performance in interference proved successful as it allowed a very complicated situation to be reduced to a quantitative comparison of a single metric that could be applied to any Feature extraction method.

Finally the investigation looked at how different algorithms could be assembled in a Bayesian reasoning chain. This is an area that will need considerable further work and linkage with the Segmentation processing, however the investigation here showed that multiple algorithms could be brought together in a way that can make use of well-developed probability theory.

## **5 CONCLUSIONS**

This section summarises the main conclusions of this research and identifies areas where further work is required.

The initial research question asked what strategies can be adopted for designing ASR algorithms that can deal with complex, interfering signal environments. The approach to answering this question was detailed in section 3 and involved breaking the main research question down into a series of five sub-questions that were more manageable. Section 4 then detailed the results of the investigations into each of these sub-questions. The general approach proved to be successful and productive. It resulted in useful, sometimes novel, outcomes. It also generated more questions that need further research to resolve.

### **5.1 Main conclusions**

The following conclusions have been arrived at from this research:

1. The review of the literature in section 2 showed that, despite the large amount of research carried out into signal recognition over the last few decades, there is still considerable need for innovation. All the evidence gathered suggests that the spectrum is becoming more complex and is likely to carry on doing so for the foreseeable future. Some parts of the radio spectrum, such as the 2.4 GHz ISM band, are Licence-Exempt and the interference in these bands can be considerable. To date, ASR systems have not been designed to handle such complex, interfering environments and research is needed to enable improvements in system performance;

2. Novel representations have been introduced as part of this work, as conventional representations were found to be inadequate for the modern radio environment. In particular the PCRP (section 4.1) and LCDP (section 4.2) have been proposed. Limited study has been performed in these areas, but they have shown that there is ample scope for innovation;
3. Addressing the problem of interference necessitated the introduction of a generic processing architecture that can represent a wide range of ASR systems (section 4.3). This model facilitates high-level discussions on the nature of the ASR process. Reasoning about the architecture resulted in the observation that Segmentation, which is a complex activity, is only necessary for removing interference if there is ambiguity in the Features used for recognition. This is an important result for the future study of ASR techniques;
4. An abstract concept called the Ideal Feature was introduced (section 4.4.3). It was argued that, if all Features were ideal then there would be, by definition, no need for Segmentation. The CIF and GIF were additional concepts that can be used when applying the IF concept to sets of signal types. A metric was devised, called Interference Selectivity (section 4.4.4), that allowed real Features to be compared to the Ideal Feature;
5. It was observed that none of the Features examined were ideal (section 4.4.6). The corollary of this is that there is a need for a strategy for dealing with non-ideal Features and options for this were proposed in section 4.4.7. One possible approach to combining Features was explained in section 4.5. The best route would be to use Ideal Features, but as this is not yet possible, the next best route is to filter out interference as the first stage in the processing

(i.e. intelligent Segmentation). This is a difficult problem to solve, especially when an interferer overlaps the Source of interest in time and/or frequency. There is then, a strong motivation for developing Features that have good Interference Selectivity and alleviate, as much as possible, the need for an intelligent Segmentation process.

This last point is the overall conclusion reached after investigating the research question in some detail. The goal of an Ideal Feature is a laudable one and is the first priority for research, but is probably not completely achievable in practice. Using non-ideal Features forces the ASR system designer to incorporate other interference mitigation measures in order to improve identification accuracy in the presence of interference.

## **5.2 Recommendations for further work**

1. Two novel representations have been introduced in this thesis, namely the PCRP (section 4.1) and LCDP (section 4.2). These have been investigated but more detail is required. Further experimentation and theoretical development are needed if these are to lead to practical representations from which useful Features can be extracted efficiently;
2. Section 4.4 compared the Interference Selectivity performance of a range of Features. It is not possible to examine every conceivable Feature within a single research programme. Extending the investigations to more kinds of Feature and more interference scenarios is expected to lead to further insights that will help to design ASR systems that operate in densely populated spectral bands. Techniques such as higher order spectra, higher order

- statistics, beamforming, etc. may all form part of future ASR systems. The relative performance of Features generated by such techniques can be compared with the concept of Interference Selectivity introduced in this thesis;
3. In section 4.4.2 it was noted that feeding back initial estimates of Type from the output of the ASR to the Segmentation activity may improve the quality of Segmentation and thereby result in an overall accuracy improvement. This improvement would be due to the enhanced interference rejection performance of the Segmentation activity once given an indication of the Source of interest. Whether such a feedback loop would be stable and the degree to which improvements would be possible have not been investigated here;
  4. It was observed in section 4.4.6 that different types of algorithm appear to have different Interference Selectivities. It is not yet possible to say what it is about the structure of a Feature extraction algorithm that gives it good Interference Selectivity. There was some suggestion that the statistical Features might be inherently capable of higher Interference Selectivities than parametric Features. By comparing the behaviour of a range of algorithms in the presence of different kinds of interference it is hoped that certain structural components can be identified that need to be present or absent in order to improve performance;
  5. The work to date has identified a number of tools and techniques, plus an overall framework for automatic radio signal recognition. There will be applications in other domains to which these concepts can be applied. These include audio and music analysis, radar signal analysis and any other domain in which a signal needs to be recognised in the presence of noise and

interference. In hindsight the work carried out has been important in terms of generating concepts for the holistic processing of signals in recognition applications. The concept of an Ideal Feature, in particular, appears to be a strong one that should be widely applicable to other areas.

This page intentionally blank



## 6 REFERENCES

Achatz, R.J., Lo, Y., Papazian, P.B., Dalke, R.A. and Hufford, G.A. (1998) *Man-Made Noise in the 136 to 138-MHz VHF Meteorological Satellite Band*, NTIA, Report 98-355.

Adlard, J.F. (2000) *Frequency shift filtering for cyclostationary signals* [online], PhD thesis, University of York,  
[http://www.yorkcomms.org/theses/adlard\\_thesis.pdf](http://www.yorkcomms.org/theses/adlard_thesis.pdf) (Accessed 27 June 2010).

Aegis (2006) *Spectrum Usage Rights. Final Report - Case Studies*, Aegis Spectrum Engineering, 1721/TNR/FR2/1 [online], <http://www.aegis-systems.co.uk/download/1721/casestudies.pdf> (Accessed 4 October 2011).

Agilent (2005). *Agilent N6820E-MR1 modulation recognition capability for E3238S/N6820E signal survey systems. Technical overview* [online],  
<http://cp.literature.agilent.com/litweb/pdf/5989-3081EN.pdf> (Accessed 4 October 2011).

Ahmad, S.A. and Chappell, P.H. (2008) 'Moving approximate entropy applied to surface electromyographic signals', *Biomedical Signal Processing and Control*, vol. 3, pp. 88-93.

Akmouche, W. (1999) 'Detection of multicarrier modulations using 4th-order cumulants', *IEEE Military Communications Conference Proceedings*, Atlantic City, New Jersey, USA, 31 October – 3 November 1999, vol.1, pp. 432-326.

Amindavar, H. and Moghaddam, P.P. (2000) 'Estimation of propeller shaft rate and vessel classification in multipath environment', *Proceedings of the 2000 IEEE Sensor Array and Multichannel Signal Processing Workshop*, Cambridge, Massachusetts, USA, 16-17 March 2000, pp. 125-128.

Andrews, J. (2008) 'The signal hunters', *Engineering & Technology*, 5 July - 18 July 2008, pp. 78-79.

Antoni, J., Bonnardot, F., Raad, A. and El Badaoui, M. (2004) 'Cyclostationary modelling of rotating machine vibration signals', *Mechanical Systems and Signal Processing*, vol. 18, no. 6, pp. 1285-1314.

Antoni, J. (2007) 'Cyclic spectral analysis in practice', *Mechanical Systems and Signal Processing*, vol. 21, no. 2, pp. 597-630.

Arulampalam, G., Ramakonar, V., Bouzerdoun, A. and Habibi, D. (1999). 'Classification of digital modulation schemes using neural networks', *Proceedings of the Fifth International Symposium on Signal Processing and its Applications*, Brisbane, Australia, 22-25 August 1999, vol. 2, pp. 649-652.

Asai, T., Benjebbour, A. and Yoshino, H. (2005) 'Recognition of CDMA signals with orthogonal codes using cyclostationarity', *IEEE 6th Workshop on Signal Processing Advances in Wireless Communications*, New York, USA, 5-8 June 1995, pp. 480-484.

Assaleh, K., Farrell, K. and Mammone, R.J. (1992) 'A new method of modulation classification for digitally modulated signals', *IEEE Military Communications Conference, Communications - Fusing Command, Control and Intelligence*, San Diego, California, USA, 11-14 October 1992, vol. 2, pp. 712-716.

Azzouz, E.E and Nandi, A.K. (1996) *Automatic modulation and recognition of communication signals*. The Netherlands, Kluwer Academic Publishers.

Bar-Shalom, Y. and Li, X-R. (1993) *Estimation and Tracking: Principles, Techniques and Software*, Norwood, Massachusetts, USA, Artech House Inc.

Beidas, B.F. and Weber, C.L. (1998) 'Asynchronous classification of MFSK signals using the higher order correlation domain', *IEEE Transactions on Communications*, vol. 46, no. 4, pp. 480-493.

Beran, R. (1977) 'Robust location estimates', *The Annals of Statistics*, vol. 5, no. 3, pp. 431-444.

Blackman, S.S. (2004) 'Multiple hypothesis tracking for multiple target tracking', *IEEE Aerospace and Electronic Systems Magazine*, vol. 19, no. 1, part 2, pp. 5-18.

Blankertz, B. (SA) *The constant  $Q$  transform* [online], Westfälische Wilhelms-Universität Münster, <http://wwwmath.uni-muenster.de/logik/Personen/blankertz/constQ/constQ.pdf> (Accessed 5 October 2011).

Bouder, C. and Burel, G. (2000) 'Spread spectrum codes identification by neural networks' *Systems and Control: Theory and Applications* [online], Université de Brest, <http://www.univ-brest.fr/lest/tst/publications/pdf/mastor00estim.pdf> (Accessed 5 October 2011).

Boudreau, D., Dubuc, C., Patenaude, F., Dufour, M., Lodge, J. and Inkoi, R. (2000) 'A fast automatic modulation recognition algorithm and its implementation in a spectrum monitoring application', *21st Century Military Communications Conference Proceedings*, Los Angeles, California, USA, 22-25 October 2000, vol. 2, no. 2, pp. 732-736.

Boutte, D. and Santhanam, B. (2008) 'ISI effects in a hybrid ICA-SVM modulation recognition algorithm', *42nd Asilomar Conference on Signals, Systems and Computers*, Pacific Grove, California, USA, 26-29 October, 2008, pp. 26-29.

Brown, J.C. (1991) 'Calculation of a constant Q spectral transform', *Journal of the Acoustical Society of America*, vol. 89, no. 1, pp. 425-434; also available online at <http://www.wellesley.edu/Physics/brown/pubs/cq1stPaper.pdf> (Accessed 5 October 2011).

Brown, J.C. and Puckette, M.S. (1992) 'An efficient algorithm for the calculation of a constant Q transform', *Journal of the Acoustical Society of America*, vol. 92, no. 5, pp. 2698-2701; also available online at <http://www.wellesley.edu/Physics/brown/pubs/effalgV92P2698-P2701.pdf> (Accessed 5 October 2011).

Brown, W.A. and Loomis, H.H (1993) 'Digital implementations of spectral correlation analyzers', *IEEE Transactions on Signal Processing*, vol. 41, no. 2, pp. 703-720.

Burr, A. (2001). *Modulation and coding for wireless communications*. Padstow, T.J. International.

Callan, R. (2003) *Artificial Intelligence*. Basingstoke, UK, Palgrave MacMillan.

Chacksfield, M. (2009) *Ofcom to turn TV white space into mobile broadband?* [online], <http://www.techradar.com/news/television/ofcom-to-turn-tv-white-space-into-mobile-broadband--652138> (Accessed 5 October 2011).

Chin Tan H., Sakaguchi, K., Takada, J. and Araki, K. (2001) 'DOA based signal combining aided automatic modulation recognition/demodulation for surveillance system', *Proceedings of the IEICE General Conference 2001*, pp. 541-542.

Cimponeriu, L. and Bezerianos, A. (1999) 'Simplified recurrence plots approach on heart rate variability data', *Computers in Cardiology 1999*, Hannover, Germany, 26-29 September 1999, pp. 595-598.

Cohen, L. (1993) 'Instantaneous "anything"', *IEEE International Conference on Acoustics, Speech and Signal Processing*, Minneapolis, Minnesota, USA, 27-30 April 1993, vol. 4, pp. 105-108.

Cooper, G.R. and McGillem, C.D. (1999) *Probabilistic methods of signal and system analysis*, New York, Oxford University Press.

Cormen, T.H., Leiserson, C.E. and Rivest, R.L. (1999) *Algorithms*, London, The MIT Press.

da Costa, E.L. (1996) *Detection and identification of cyclostationary signals* [online], MSc Thesis, Monterey, California, USA, Naval Postgraduate School, <http://www.dtic.mil/cgi-bin/GetTRDoc?AD=ADA311555&Location=U2&doc=GetTRDoc.pdf> (Accessed 5 October 2011).

Daintith, J. and Nelson, R.D. (1989) *Dictionary of Mathematics*, London, Penguin Books Ltd.

Dandawaté, A.V. and Giannakis, G.B. (1994) 'Statistical tests for presence of cyclostationarity', *IEEE Transactions on Signal Processing*, vol. 42, no. 9, pp. 2355-2369.

Davies, P. (2008) *Re: Spectrum Usage Rights – Licence verification approaches* [online], IET, <http://www.theiet.org/publicaffairs/submissions/sub795.pdf> (Accessed 5 October 2011).

Dianat, S.A and Raghuveer, M.R. (1990) 'Fast algorithms for bispectral reconstruction of two-dimensional signals', *International Conference on Acoustics, Speech, and Signal Processing*, Albuquerque, New Mexico, USA, 3-6 April 1990, vol. 5, pp. 2377-2379.

Doble, J. (1996) *Introduction to Radio Propagation for Fixed and Mobile Communications*, Norwood, Massachusetts, USA, Artech House.

Dobre, O.A., Abdi, A., Bar-Ness, Y. and Su, W. (2007) 'Survey of automatic modulation classification techniques: classical approaches and new trends', *IET Communications*, vol. 1, no. 2, pp. 137-156.

Donoho, D. and Huo, X. (1997) 'Large-sample modulation classification using Hellinger representation', *First IEEE Signal Processing Workshop on Advances in Wireless Communications*, Paris, France, 16-18 April 1997, pp. 133-136.

Druckmann, I., Plotkin, E.I. and Swamy, M.N.S. (1998) 'Automatic modulation type recognition', *IEEE Canadian Conference on Electrical and Computer Engineering*, Waterloo, Ontario, Canada, 24-28 May 1998, vol. 1, pp. 65-68.

Du, L., Liu, H., Bao, Z. and Xing, M. (2005) 'Radar HRRP target recognition based on higher order spectra', *IEEE Transactions on Signal Processing*, vol. 53, no. 7, pp. 2359-2368.

Dubuc, C., Boudreau, D., Patenaude, F. and Inkol, R. (1999) 'An automatic recognition algorithm for spectrum monitoring applications', *IEEE International Conference on Communications*, Vancouver, British Columbia, Canada, 6-10 June 1999, vol. 1, pp. 570-574.

Eckmann, J-P., Kamphorst, S.O. and Ruelle, D. (1987) 'Recurrence plots of dynamical systems', *Europhysics Letters*, vol. 4, no. 9, pp. 973-977.

Edinger, S., Gaida, M. and Fliege, N.J. (2007) 'Classification of QAM signals for multicarrier systems', *15<sup>th</sup> European Signal Processing Conference*, Poznan, Poland, 3-7 September 2007, pp. 464-468.



Evans, B.G. (1999) *Satellite Communication Systems*, 3<sup>rd</sup> edition, London, The Institution of Electrical Engineers.

Fedoseev, S.A. and Fedoseev, A.S. (2001) 'Tropical lightning stroke data collected and analyzed by computer based lightning detection system', *IEEE International Symposium on Electromagnetic Compatibility*, Montreal, Quebec, Canada, 13-17 August 2001, vol. 2, pp. 845-848.

Ferreira, R.R. (1996) *COMINT Analysis in a Littoral Environment* [online], MSc Thesis, Monterey, California, USA, Naval Postgraduate School, <http://www.dtic.mil/cgi-bin/GetTRDoc?AD=ADA321460&Location=U2&doc=GetTRDoc.pdf> (Accessed 5 October 2011).

Fitzgerald, D., Cranitch, M. and Cychowski, M.T. (2006) 'Towards an inverse constant Q transform' [online], *Audio Engineering Society Convention Paper. 120<sup>th</sup> Convention*, Paris, France, 20-23 May 2006, <http://homepage.eircom.net/~derryfitzgerald/AES120.pdf> (Accessed 5 October 2011).

Fowler, M. and Scott, K. (2000) *UML distilled*, 2<sup>nd</sup> edition, New Jersey, USA, Addison-Wesley.

Ganley, M. (2006) *Introduction to PSSTG*. ERA Report 2006-0552.

Gardner, W.A. (1986a) *Statistical Spectral Analysis: A Nonprobabilistic Theory*, Upper Saddle River, New Jersey, USA, Prentice Hall Inc.

Gardner, W.A. (1986b) 'The role of spectral correlation in design and performance analysis of synchronizers', *IEEE Transactions on Communications*, vol. 34, no. 11, pp. 1089-1095.

Gardner, W.A. (1986c) 'Measurement of spectral correlation', *IEEE Transactions on Acoustics, Speech and Signal Processing*, vol. 34, no. 5, pp. 1111-1123.

Gardner, W., Brown, W.A. and Chen C-K. (1987) 'Spectral Correlation of Modulated Signals', *IEEE Transactions on Communications*, 1987, vol. 35, no. 6, pp. 584-601.

Gardner, W.A. (1991) 'Exploitation of spectral redundancy in cyclostationary signals', *IEEE Signal Processing Magazine*, vol. 8, no. 2, pp. 14-36.

Gardner, W.A. and Spooner, C.M. (1992) 'Signal interception: performance advantages of cyclic-feature detectors', *IEEE Transactions on Communications*, vol. 40, no. 1, pp. 149-159.

Gardner, W.A. (1993) 'Cyclic Wiener filtering: theory and method', *IEEE Transactions on Communications*, vol. 41, no. 1, pp. 151-163.

Gardner, W.A., Napolitano, A. and Paura, L. (2006) 'Cyclostationarity: Half a century of research', *Signal Processing*, vol. 86, pp. 639-697.

Ghani, N. and Lamontagne, R. (1993) 'Neural networks applied to the classification of spectral features for automatic modulation recognition', *IEEE Military Communications Conference, 1993, Conference Record, 'Communications on the Move'*, Boston, Massachusetts, USA, 11-14 October 1993, vol. 1, pp. 111-115.

Ghasemi, A. and Sousa, E.S. (2008) 'Spectrum sensing in cognitive radio networks: requirements, challenges and design trade-offs', *IEEE Communications*, vol. 46, no. 4, pp.32-39.

Giannakis, G.B (1999) 'Cyclostationary Signal Analysis', in Madisetti, V.K. and Williams D.B. (Ed.): *Digital Signal Processing Handbook*, CRC Press LLC.

Gibbs, A.L. and Su, F.A. (2002) *On choosing and bounding probability metrics* [online], Harvey Mudd College Department of Mathematics, <http://www.math.hmc.edu/~su/papers.dir/metrics.pdf> (Accessed 5 October 2011).

Gini, F. and Greco, M. (2002) 'Texture modelling, estimation and validation using measured sea clutter data', *IEE Proceedings Radar, Sonar and Navigation*, vol. 149, iss. 3, pp. 115-124.

van Ginkel, M., Hendriks, C.L.L. and van Vliet, L.J. (2004) *A short introduction to the Radon and Hough transforms and how they relate to each other* [online], Delft University of Technology, Quantitative Imaging Group Technical Report QI-2004-01, <http://citeseerx.ist.psu.edu/viewdoc/download;jsessionid=4DC1670B0EFB747CD22D9C79C0E1D097?doi=10.1.1.2.9419&rep=rep1&type=pdf> (Accessed 5 October 2011).

Girault, J.-M., Biard, M., Kouame, D., Bleuzen, A. and Tranquart, F. (2006) 'Spectral Correlation of the embolic blood Doppler signal', *IEEE International Conference on Acoustics, Speech and Signal Processing*, Toulouse, France, 14-19 May 2006, vol. 2, pp. 1200-1203.

Gökmen, B. and Ertüzün, A. (1998) *A comparative study on higher order statistics and cyclostationarity in the context of identification and equalization*. [online], Boğaziçi University, Turkey, <http://www.busim.ee.boun.edu.tr/~ertuzun/publications/ICT98.pdf> (Accessed 5 October 2011).

Gold, R. (1967) 'Optimal binary sequences for spread spectrum multiplexing', *IEEE Transactions on Information Theory*, vol. 13, no. 4, pp. 619-621.

Grimaldi, D., Rapuano, S. and De Vito, L. (2007) 'An automatic digital modulation classifier for measurement on telecommunication networks', *IEEE Transactions on Instrumentation and Measurement*, vol. 56, no. 5, pp. 1711-1720.

Hachemani, R., Palicot, J. and Moy, C. (2007). 'A new standard recognition sensor for cognitive radio terminals', *15<sup>th</sup> European Signal Processing Conference*, Poznan, Poland, 3-7 September 2007, pp. 856-860.

Hall, M.P.M, Barclay, L.W. and Hewitt, M.T. (1996) *Propagation of radiowaves*, London, The Institution of Electrical Engineers.

Haykin, S. (2005) 'Cognitive radio: brain-empowered wireless communications', *IEEE Journal on Selected Areas in Communications*. vol. 23, no. 2, pp. 201-220.

Hero, A.O, O'Neill, J. and Williams, W.J. (1997) 'Moment matrices for recognition of spatial pattern in noise images', *Proceedings of the 1997 International Conference on Image Processing*, Santa Barbara, California, USA, 26-29 October 1997, vol. 2, pp. 378-381.

Hero III, A.O. and Hadinejad-Mahram, H. (1998) 'Digital modulation classification using power moment matrices', *Proceedings of the 1998 IEEE International Conference on Acoustics, Speech and Signal Processing*, Seattle, Washington, USA, 12-15 May 1998, vol. 6, pp. 3285-3288.

Hinich, M.J. (2000) 'Statistical theory of signal coherence', *IEEE Journal of Oceanic Engineering*, vol. 25, no. 2, pp. 256-261.

Hong, L. and Ho, K.C. (1999) 'Identification of digital modulation types using the wavelet transform' *Military Communications Conference Proceedings*, Atlantic City, New Jersey, USA, 31 October 31 – 3 November 1999, vol. 1, pp. 427-431.

Hsue, S-Z. and Soliman, S.S. (1989) 'Automatic modulation recognition of digitally modulated signals', *Military Communications Conference. Conference Record. Bridging the Gap. Interoperability, Survivability, Security*, Boston, Massachusetts, USA, 15-18 October 1989, vol. 3, pp. 645-649.

Huang, Z.-T. and Zhou Y.-Y. (2006) 'Multi-cycle estimator for time-difference-of-arrival (TDOA) and its performance', *IEE Proceedings - Radar, Sonar and Navigation*, vol. 153, no. 5, pp. 381-388.

Huo, X. and Donoho, D. (1998). 'A simple and robust modulation classification method via counting', *Proceedings of the 1998 IEEE International Conference on Acoustics, Speech and Signal Processing*, Seattle, Washington, USA, 12-15 May 1998, vol. 6, pp. 3289-3292.

Ifeachor, E.C. and Jervis, B.W. (2002) *Digital Signal Processing*, London, Prentice Hall.

ITU-R (1995) *Recommendation ITU-R SM.1138. Determination of necessary bandwidths including examples for their calculation and associated examples for the designation of emissions.*

ITU-R P.372-8. *Radio noise*.

Iversen, A. (2003) *The use of artificial neural networks for automatic modulation recognition*, Technical Report HW-MACS-TR-009 [online],

<http://www.macs.hw.ac.uk:8080/techreps/docs/files/HW-MACS-TR-0009.pdf>

(Accessed 3 February 2008).

Iversen, A. (2004) *Classification of digital modulation schemes using multi-layered perceptrons*, Technical Report HW-MACS-TR-0016 [online],

<http://www.macs.hw.ac.uk:8080/techreps/docs/files/HW-MACS-TR-0016.pdf>

(Accessed 3 February 2008).

Jeruchim, M.C, Balaban, P and Shanmugan, K.S. (1992) *Simulation of Communication Systems*. New York, Plenum Press.

Johnson, J. and Picton, P. (1995) *Designing Intelligent Machines. Volume 2. Concepts in artificial intelligence*, Oxford, Butterworth-Heinemann Ltd.

Kachenoura, A., Albera, L. and Senhadji, L. (2006) 'The PEP Approach: A New Family of Methods Solving the Phase Estimation Problem', *IEEE International Conference on Acoustics, Speech and Signal Processing*, Toulouse, France, 14-19 May 2006, vol. 3. pp. 628-631.

Kim, K., Akbar, I.A., Bae, K.K., Um, J-s., Spooner, C.M. and Reed, J.H. (2007)

'Cyclostationary approaches to signal detection and classification in cognitive radio', *2nd IEEE International Symposium on New Frontiers in Dynamic Spectrum Access*, Dublin, Ireland, 17-20 April 2007, pp. 212-215.

Kim, K., Min, J., Hwang, S., Lee, S., Kim, K, and Kim, H. (2008) 'A CR platform for applications in TV whitespace spectrum', *International Conference on Cognitive Radio Oriented Wireless Networks and Communications*, Singapore, 15-17 May 2008, pp.1-6.

Kim, K. and Polydoros, A. (1988) 'Digital modulation: The BPSK versus QPSK case', *IEEE Military Communications Conference. Conference Record, '21<sup>st</sup> Century Military Communications – What's Possible?* San Diego, California, USA, 23-26 October 1988, vol. 2. pp. 431-436.

Knaflitz, M. and Bonato, P. (1999) 'Time-frequency methods applied to muscle fatigue assessment during dynamic contractions', *Journal of Electromyography and Kinesiology*, vol. 9, no. 5, pp. 337-350.

Kozono, S. (1987) 'Co-channel interference measurement method for mobile communications', *IEEE Transactions on Vehicular Technology*, vol. 36, iss. 1, pp. 7-13.



Krauss, H.L., Bostian, C.W. and Raab, F.H. (1980) *Solid State Radio Engineering*, London, John Wiley & Sons Ltd.

Kremer, S.C. and Shiels, J. (1997) 'A testbed for automatic modulation recognition using artificial neural networks', *IEEE 1997 Canadian Conference on Electrical and Computer Engineering*, St. Johns, Newfoundland, Canada, 25-28 May 1997, vol. 1, pp. 67-70.

Kuehls, J.F. and Geraniotis, E. (1990) 'Presence detection of binary-phase-shift-keyed and direct-sequence spread-spectrum signals using a prefilter-delay-and-multiply device', *IEEE Journal on Selected Areas in Communications*, vol. 8, no. 5, pp. 915-933.

Lathi, B.P. (1983) *Modern Digital and Analog Communication Systems*, New York, USA. CBS College Publishing.

Lay, N.E. and Polydoros, A. (1995) 'Modulation classification of signals in unknown ISI environments', *IEEE Military Communications Conference*, San Diego, California, USA, 5-8 November 1995, vol. 1, pp. 170-174.

Le, B., Rondeau, T.W., Maldonado, D. and Bostian, C.W. (2005) 'Modulation identification using neural networks for cognitive radios', *SDR Forum Technical Conference*, Anaheim, California, USA, 14-18 November 2005 [online], <http://groups.winnforum.org/d/do/2662> (Accessed 6 October 2011)

Le, B., Rondeau, T.W., Maldonado, D., Scaperoth, D. and Bostian, C.W. (2006)

'Signal Recognition for cognitive radios', in *SDR Forum Technical Conference*,

Orlando, Florida, USA, 15 November 2006 [online],

<http://groups.winnforum.org/d/do/2076> (Accessed 6 October 2011).

Le Guen, D. and Mansour, A. (2002) 'Automatic recognition algorithm for

digitally modulated signals', *Proceedings of the IASTED International*

*Conference, Signal Processing, Pattern Recognition & Applications*, Crete, 25-28

June 2002, pp. 32-37.

Le Vine, D. and Krider, E.P. (1977) 'The temporal structure of HF and VHF

radiations during Florida lightning return strokes', *Geophysical Research Letters*,

vol. 4, no. 1, pp. 13-16.

Leung, H. and Wu, J. (2000) 'Bayesian and Dempster-Shafer target identification

for radar surveillance', *IEEE Transactions on Aerospace and Electronic Systems*,

vol. 36, no. 2, pp. 432-447.

Li, Y. (1992) 'Reforming the theory of invariant moments for pattern recognition',

*Pattern Recognition*, vol. 25, iss. 7, pp. 723-730

Lin, Y-C. and Kuo, C-C. J. (1996) 'Sequential modulation classification of

dependent samples', *IEEE International Conference on Acoustics, Speech and*

*Signal Processing*, vol. 5, pp. 2690-2693.

Lindsay, B.G. (1994) 'Efficiency versus robustness: the case for minimum Hellinger distance and related methods', *The Annals of Statistics*, vol. 22, no. 2, pp. 1081-1114.

Lopatka, J. and Pedzisz, M. (2000) 'Automatic modulation classification using statistical moments and a fuzzy classifier', *Proceedings 5th International Conference on Signal Processing*, Beijing, China, 21-25 August 2000, vol. 3, pp. 1500-1506.

Loughlin, P.J. and Davidson, K.L. (2000) 'Instantaneous spectral skew and kurtosis', *Proceedings of the Tenth IEEE Workshop on Statistical Signal and Array Processing*, Pocono Manor, Pennsylvania, USA, 14-16 August 2000, pp. 574-578.

Louis, C. and Sehier, P. (1994) 'Automatic modulation recognition with a hierarchical neural network', *IEEE Military Communications Conference*, Fort Monmouth, New Jersey, USA, 2-5 October 1994, vol. 3, pp. 713-717.

Lynn, P.A. (1984) *An Introduction to the Analysis and Processing of Signals*, London, Macmillan Publishers Ltd.

Maeda, K., Benjebbour, A., Asai, T., Furono, T. and Ohya, T. (2007) 'Recognition among OFDM-based systems utilizing cyclostationarity-inducing transmission', *2<sup>nd</sup> IEEE International Symposium on New Frontiers in Dynamic Spectrum Access Networks*, Dublin, Ireland, 17-20 April 2007, pp. 516-523.

Manetti, C., Ceruso, M-A, Giuliani, A., Webber Jr., C.L. and Zbilut J.P (1999) 'Recurrence quantification analysis as a tool for the characterization of molecular dynamics simulations', *Physical Review E*. vol. 59, iss. 1, pp. 992-998.

Martin, F.L., Correal, N.S., Ekl, R.L., Gorday, P. and O'Dea, R. (2008) 'Early opportunities for commercialization of TV whitespace in the US', 3<sup>rd</sup> *International Conference on Cognitive Radio Oriented Wireless Networks and Communications*, 2008. Singapore, 15-17 May 2008, pp. 1-5.

Marwan, N. and Meinke, A. (2002) *Extended Recurrence Plot Analysis and its Application to ERP Data* [online],  
[http://arxiv.org/PS\\_cache/physics/pdf/0212/0212082v1.pdf](http://arxiv.org/PS_cache/physics/pdf/0212/0212082v1.pdf) (Accessed 6 October 2011)

Marwan, N., Romano, M.C., Thiel, M. and Kurths, J. (2007) 'Recurrence plots for the analysis of complex systems', *Physics Reports*, vol. 438. iss. 5-6, pp. 237-329.

Masugi, M. (2006) 'Recurrence plot-based approach to the analysis of IP-network traffic in terms of assessing nonstationary transitions over time', *IEEE Transactions on Circuits and Systems-I: Regular Papers*, vol. 53, iss. 10, pp. 2318-2326.

Matassini, L., Kantz, H., Holyst, J. and Hegger, R. (2002) 'Optimizing of recurrence plots for noise reduction', *Physical Review Review E*, vol. 65, iss. 2.

Mathworks (2011) *Communications system toolbox* [online],  
<http://www.mathworks.co.uk/products/communications/demos.html?file=/products/demos/shipping/comm/scattereyedemo.html> (Accessed 6 October 2011)

Matsuzaki, E., Ichige, K. and Hiroyuki, A. (2003) 'An automatic recognition algorithm of analogue modulated signals for disturbance rejection', *Proceedings of the Seventh International Symposium on Signal Processing and its Applications*, Paris, France, 1-4 July 2003, vol. 1, pp. 165-168.

McGehee, J. (2008) 'Multi-site spatially diverse demodulation of HF propagated signals', *IEEE Military Communications Conference*, San Diego, California, 16-19 November 2008, pp. 1-6.

Mewett, D.T., Reynolds, K.J. and Nazeran, H. (1999) 'Recurrence plot features: an example using ECG', *Proceedings of the Fifth International Symposium on Signal Processing and its Applications*, Brisbane, Queensland, Australia, 22-25 August, 1999, vol. 1, pp. 175-178.

Middleton, D. (1973) 'Man-made noise in urban environments and transportation systems: Models and measurements', *IEEE Transactions on Vehicular Technology*, vol. 22, iss. 4, pp. 148-157.

Middleton, D. (1975) *Statistical-physical models of man-made and natural radio environments – Part I: First-order probability models of the instantaneous amplitude*, Office of Telecommunications Report OT 74-36.

Middleton, D. (1976) *Statistical-physical models of man-made and natural radio environments – Part II: First-order probability models of the envelope and phase*, Office of Telecommunications Report OT 76-86.

Middleton, D. (1978a) *Statistical-physical models of man-made and natural radio environments – Part III: First-order probability models of the instantaneous amplitude of class B interference*, NTIA Contractor Report 78-1.

Middleton, D. (1978b) *Statistical-physical models of man-made and natural radio environments – Part IV: Determination of the first-order parameters of class A and class B interference*, NTIA Contractor Report 78-2.

Mitola III, J. (2009) 'Cognitive radio architecture evolution', *Proceedings of the IEEE*, vol. 97, iss. 4, pp. 626-641.

Mitola III, J. and Maguire Jr, G.Q. (1999) 'Cognitive radio: making radios more personal', *IEEE Personal Communications*, vol. 6, no. 4, pp. 13-18.

Mobasser, B.G. (1999). 'Constellation shape as a robust signature for digital modulation recognition', *Proceedings of IEEE Military Communications Conference*, Atlantic City, New Jersey, USA, 31 October – 3 November 1999, vol. 1, pp. 442-446.

Oduncu, H. (2008) *Use of RFID in healthcare settings and electromagnetic interference of RFID devices with medical equipment: Review of current standards and case reports* [online], University of Glamorgan, [http://fat.glam.ac.uk/media/files/documents/2008-05-06/RFID\\_Healthcare\\_Report.pdf](http://fat.glam.ac.uk/media/files/documents/2008-05-06/RFID_Healthcare_Report.pdf) (Accessed 6 October 2011).

Ofcom (2005) *Ofcom Tackles Illegal Broadcasting* [online], <http://media.ofcom.org.uk/2005/11/03/ofcom-tackles-illegal-broadcasting/> (Accessed 6 October 2011).

Ofcom (2006) *Spectrum usage rights. Technology and usage neutral access to the radio spectrum* [online], <http://www.ofcom.org.uk/consult/condocs/sur/spur.pdf> (Accessed 6 October 2011).

Ofcom (2009) *Enforcement Report* [online], [http://www.ofcom.org.uk/enforcement/enforcement\\_report/enforcement\\_report.pdf](http://www.ofcom.org.uk/enforcement/enforcement_report/enforcement_report.pdf) (Accessed 27 February 2010).

Ofcom (2010a) *Outline of the role of Field Operations* [online], <http://www.ofcom.org.uk/radiocomms/ifi/enforcement/ops/> (Accessed 6 October 2011).

Ofcom (2010b) *Prosecution Statistics* [online], <http://www.ofcom.org.uk/radiocomms/ifi/enforcement/pstats/> (Accessed 6 October 2011).

Öner, M. and Jondral, F. (2003) 'Extracting the channel allocation information in a spectrum pooling system using a prefilter delay and multiply nonlinearity', *IEEE Workshop on Statistical Signal Processing*, St. Louis, Missouri, USA, 18 September - 1 October 2003, pp. 46-49.

Öner, M. and Jondral, F. (2004a) 'Cyclostationarity-based methods for the extraction of the channel allocation information in a spectrum pooling system', *IEEE Radio and Wireless Conference*, Atlanta, Georgia, USA, 19-22 September 2004, pp. 279-282.

Öner, M. and Jondral, F. (2004b) 'Cyclostationarity based air interface recognition for software radio systems', *IEEE Radio and Wireless Conference*, Atlanta, Georgia, USA, 19-22 September 2004, pp. 263 – 266.

Öner, M. and Jondral, F. (2007) 'Air interface identification for software radio systems', *International Journal of Electronics and Communications*, vol. 61, iss. 2, pp. 104-117.

Pace, P.E. (2004) *Detecting and classifying low probability of intercept radar*, Norwood, Massachusetts, USA, Artech House.

Parsons, D. (1992) *The Mobile Radio Propagation Channel*, London, Pentech Press Ltd.

Pätzold, M. (2002) *Mobile Fading Channels*, New York, USA, John Wiley & Sons Inc.



Poole, I. (2010) *Future of cognitive radio – an interview with Dr. Joseph Mitola* [online], <http://www.radio-electronics.com/analysis/receivers/2010-03/joe-joseph-mitola-cognitive-radio-future.php> (Accessed 7 October 2011).

Pourrostan, J., Zekavat, S.A. and Tong, H. (2007) 'Novel Direction-of-Arrival Estimation Techniques for Periodic-Sense Local Positioning Systems', *IEEE Radar Conference*, Waltham, Massachusetts, USA, 17-20 April 2007, pp. 568-573

Quinlan, J.R. (1986) 'Induction of decision trees', *Machine Learning*, vol., no. 1, pp. 81-106.

Radiocommunications Agency (2000) *RA 3G Auction* [online], [http://www.ofcom.org.uk/static/archive/spectrumauctions/auction/auction\\_index.htm](http://www.ofcom.org.uk/static/archive/spectrumauctions/auction/auction_index.htm) (Accessed 7 October 2011)

Rakov, V.A. and Rachidi, F. (2009) 'Overview of research progress in lightning research and lightning protection', *IEEE Transactions on Electromagnetic Compatibility*, vol. 51, iss. 3, pp. 428-442.

Ramakonar, V., Habibi, D. and Bouzerdoum, A. (1999) 'Automatic recognition of digitally modulated communications signals', *Proceedings of the Fifth International Symposium on Signal Processing and its Applications*, Brisbane, Australia, vol. 2, pp. 753-756.

Ranade, A. (1989) 'Local access radio interference due to building reflections', *IEEE Transactions on Communications*, vol. 37, iss. 1, pp. 70-74.

Reardon, M. (2008) *FCC opens free 'white space' spectrum* [online], [http://news.cnet.com/8301-1035\\_3-10082505-94.html](http://news.cnet.com/8301-1035_3-10082505-94.html) (Accessed 7 October 2011).

Richardson, D.C. and Dale, R. (2005) 'Looking to understand: The coupling between speakers' and listeners' eye movements and its relationship to discourse comprehension', *Cognitive Science*, vol. 29, iss. 6, pp. 1045-1060.

Richterova, M. (2005) 'Signal modulation recognizer based on method of artificial neural networks', *Progress in Electromagnetics Research Symposium*, Hangzhou, China, 22-26 August 2005, *PIERS Online*, vol. 1, no. 5, pp. 575-578..

Roberts, R.S., Brown, W.A. and Loomis, H.H., Jr. (1991) 'Computationally efficient algorithms for cyclic spectral analysis', *IEEE Signal Processing Magazine*, vol. 8, iss. 2, pp.38-49.

Rockwell, D.L. (2004) 'SIGINT: The New Electronic Warfare' [online], *Aerospace America*, June 2004, pp. 22-25, <http://www.aiaa.org/aerospace/images/articleimages/pdf/eyejune04.pdf> (Accessed 7 October 2011).

Sabri, K., El Badaoui, M., Guillet, F., Adib, A. and Aboutajdine, D. (2006) 'Gear Signal Separation by Exploiting the Spectral Diversity and Cyclostationarity', *IEEE International Conference on Acoustics, Speech and Signal Processing*, Toulouse, France, 14-19 May 2006, vol. 3, pp. 1200-1203.

dos Santos, C.N., Netto, S.L., Bescainho, L.W.P. and Graziosi, D.B. (2004) 'A modified constant-Q transform for audio signals.' *IEEE International Conference on Acoustics, Speech and Signal Processing*, Montreal, Quebec, Canada, 17-21 May 2004, vol. 2, pp. 469-472.

Samson, C.A. (1975) *Refractivity gradients in the northern hemisphere*, Institute for Telecommunications Services, Office of Telecommunications, OT Report 75-59.

Schreyögg, C., Kittel, K., Kressel, U. and Reichert, J. (1997) 'Robust classification of modulation types using spectral features applied to HMM', *MILCOM 97 Proceedings*, Monterey, California, USA, 2-5 November 1997, vol. 3, pp. 1377-1381.

Sengr, A. and Gldemir, H. (2005) 'An educational interface for automatic recognition of analog modulated signals', *Journal of Applied Sciences*, vol. 5, iss. 3, pp. 513-516.

Serpedin, E., Panduru, F., Sari, I. and Giannakis, G.B. (2005) 'Bibliography on cyclostationarity', *Signal Processing*, vol. 85, iss. 12, pp. 2233-2303.

Shao, X-M and Jacobson A.R. (2002) 'Polarization observations of lightning-produced VHF emissions by FORTE satellite', *Journal of Geophysical Research* vol. 107, no. D20, pp. 7-1 – 7-16.

Sheikh, A.U.H. and Parsons, J.D. (1983) 'The frequency dependence of urban man-made noise', *The Radio and Electronic Engineer*, vol. 53, no.3, pp. 92-98.

Sherman, M. (2009) *TV Whitespace Tutorial* [online],  
[http://www.ieee802.org/802\\_tutorials/2009-03/2009-03-10%20TV%20Whitespace%20Tutorial%20r0.pdf](http://www.ieee802.org/802_tutorials/2009-03/2009-03-10%20TV%20Whitespace%20Tutorial%20r0.pdf) (Accessed 7 October 2011).

Shi, Q. and Karasawa, Y. (2008) 'Maximum likelihood based modulation classification for unsynchronized QAMs', *IEEE Global Telecommunications Conference*, New Orleans, Louisiana, USA, 30 November - 4 December 2008, pp. 1-5.

Shukla (2001) *Feasibility Study Into the Measurement of Man-Made Noise*, DERA, Report DERA/KIS/COM/CR010470.

Simić, D.Č. and Simić, J.R. (1999) 'The strip spectral correlation algorithm for spectral correlation estimation of digitally modulated signals', *4<sup>th</sup> International Conference on Telecommunications in Modern Satellite, Cable and Broadcasting Services*, Nis, Yugoslavia, 13-15 October 1999, vol. 1, pp.277-280.

Singapore Technologies (2005) *HB 110 Microwave Sensor Module* [online], [http://www.agilsense.com/pdf/x-band%20sensor/DS\\_HB110\\_v102.pdf](http://www.agilsense.com/pdf/x-band%20sensor/DS_HB110_v102.pdf) (Accessed 7 October 2011).

Soliman, S.S. and Hsue, S-Z. (1992) 'Signal classification using statistical moments', *IEEE Transactions on Communications*, vol. 40, iss. 5, pp. 908-916.

Spaulding, A.D, Roubique, C.J. and Crichlow, W.Q. (1962) 'Conversion of the amplitude-probability distribution function for atmospheric radio noise from one bandwidth to another', *Journal of Research of the National Bureau of Standards - D. Radio Propagation*, vol. 66D, no. 6, pp. 713-720.

Stavroulakis, P. (2007) *Terrestrial trunked radio – TETRA: a global security tool*, New York, Springer-Verlag.

Steenkiste, P., Sicker, D., Minden, G. and Raychaudhuri, D. (2009) *Future directions in Cognitive Radio Research* [online], Carnegie Mellon School of Computer Science, [http://www.cs.cmu.edu/~prs/NSF\\_CRN\\_Report\\_Final.pdf](http://www.cs.cmu.edu/~prs/NSF_CRN_Report_Final.pdf) (Accessed 7 October 2011).

Sutton, P.D., Nolan, K.E. and Doyle, L.E. (2008) 'Cyclostationary signatures in practical cognitive radio applications', *IEEE Journal on Selected Areas in Communications*, vol. 26, iss. 1, pp.13-24.

Tadaion, A.A., Derakhtian, M., Gazor, S. and Aref, M.R. (2005) 'Likelihood ratio tests for PSK modulation classification in unknown noise environment', *Canadian Conference on Electrical and Computer Engineering*, Saskatoon, Saskatchewan, Canada, 1-4 May 2005, pp. 151-154.

Tadiran (2011) *HF & VHF/UHF signal classifiers* [online],  
<http://www.tadsys.com/images/Signal%20Classifiers.pdf> (Accessed 7 October 2011).

Thomas, R.J., Krehbiel, P.R., Rison, W., Hamlin, T., Harlin, J. and Shown, D. (2001) 'Observations of VHF source powers radiated by lightning', *Geophysical Research Letters*, vol. 28, no.1, pp. 143-146.

Tse, D. and Viswanath, P. (2005) *Fundamentals of Wireless Communication* [online], Cambridge University Press,  
<http://www.eecs.berkeley.edu/~dtse/book.html> (Accessed 7 October 2011).

Tugnait, J.K. and Zhou, Y. (2002) 'Identification of closed-loop MIMO systems from time-domain data using polyspectral analysis', *Proceedings of the American Control Conference*, Anchorage, Alaska, USA, 8-10 May 2002, vol. 4, pp. 3319-3324.

Tyler, D.W. and Schulze, K.J. (2004) 'Fast phase spectrum estimation using the parallel part-bispectrum algorithm', *The Publications of the Astronomical Society of the Pacific*, vol. 116, iss. 815, pp. 65-76.

Uman, M.A. (1994) 'Natural lightning', *IEEE Transactions on Industry Applications*, vol. 30, iss. 3, pp.785-790.

Wagstaff, A.J. (2003) *Automatic Music Transcription*, Unpublished MSc Thesis, Cranfield University.

Wagstaff, A.J. and Merricks, N.P. (2003) *Man-made noise measurement programme (AY4119). Final report* [online], Mass Consultants Ltd., MC/CC0251/REP012/2,

<http://www.mass.co.uk/technology/MMN%20Measurement%20Programme%20Final%20Report.pdf> (Accessed 7 October 2011).

Wagstaff, A.J. and Merricks, N.P. (2005) 'Man-made noise measurement programme', *IEE Proceedings - Communications*, vol. 152, iss. 3, pp. 371-377.

Wagstaff, A.J. and Merricks, N.P. (2006) *Autonomous Interference Monitoring System, Final Report* [online], Mass Consultants Ltd., MC/SC0526/REP020/2, <http://www.mass.co.uk/technology/spectrum.htm> (Accessed 7 October 2011).

Wagstaff, A.J. (2007) *Autonomous Interference Monitoring System. Phase 2, Final Report* [online], Mass Consultants Ltd., MC/SC0585/REP017/1, <http://www.mass.co.uk/technology/spectrum.htm> (Accessed 7 October 2011).

Wagstaff, A.J. (2008) 'Logarithmic cyclic frequency domain profile for automatic modulation recognition', *IET Communications*, vol. 2, iss. 8, pp. 1009-1015.

Wagstaff, A.J. (2009) *Estimating the utilisation of key licence-exempt spectrum bands. Final report* [online], Mass Consultants Ltd., MC/SC0710/REP003/3, <http://www.mass.co.uk/technology/Estimating%20the%20Utilisation%20of%20Key%20LE%20Spectrum%20Bands.pdf> (Accessed 7 October 2011).

Wang, C. and Tong, Y-C. (2004) 'An improved critical-band transform processor for speech applications', *Proceedings of the 2004 International Symposium on Circuits and Systems*, Vancouver, British Columbia, Canada, 23-26 May 2004, vol. 3, pp. 461-464.

Wang, J. and Gaddam, V. (2009) 'Feasibility Study of Sensing TV Whitespace with Local Quiet Zone', *IEEE International Conference on Systems, Man and Cybernetics*, San Antonio, Texas, USA, 11-14 October 2009, pp. 2287-2292.

Wang, X-g, Shen, H.C. and Qian, W-h (1998) 'A hypothesis testing method for multisensory data fusion', *Proceedings of the 1994 IEEE International Conference on Robotics and Automation*, Leuven, Belgium, 16-20 May 1998. vol. 4, pp. 3407-3412.

Ward, B.D. and Golley, M.G. (1991) 'Solar cycle variations in atmospheric noise at HF', *Fifth International Conference on HF Radio Systems and Techniques*. Edinburgh, Scotland, 22-25 July 1991, pp. 327-331.



Wavecom (2007). *Data decoder/analyser W61PC W61LAN W61BV W61 SAT W61 CL* [online],  
[http://www.phaisan.com/docs/products/W61\\_Family\\_Brochure.pdf](http://www.phaisan.com/docs/products/W61_Family_Brochure.pdf) (Accessed 7 October 2011).

Winder, S. and Carr, J. (2002) *Radio and RF Engineering Pocket Book*, Oxford, UK, Newnes.

Wood, S.L., Ready, M.J. and Treichler, J.R. (1988) 'Constellation identification using the Radon transform', *International Conference on Acoustics, Speech, and Signal Processing*, New York, USA, 11-14 April 1988, vol. 3, pp. 1878-1881.

Wood, S.L., Larimore, M.G. and Treichler, J.R. (1990) 'Modem constellation identification: A performance comparison of two methods', *International Conference on Acoustics, Speech and Signal Processing*, Albuquerque, New Mexico, USA, 3-6 April 1990, vol. 3, pp. 1651-1654.

Wood, S.L. and Treichler, J.R. (1994) 'Computational and performance analysis of Radon transform based constellation identification', *IEEE International Conference on Acoustics, Speech and Signal Processing*, Adelaide, South Ausatralia, 19-22 April 1994, vol. 3, pp. 241-244.

Yaqin, Z., Guanghui, R., Zhilu, W. and Xuemai, G. (2003). 'Automatic digital modulation recognition using artificial neural networks', *IEEE International Conference on Neural Networks & Signal Processing*, Nanjing, China, 14-17 December 2003, vol. 1, pp. 257-260.

Zaerin, M., Seyfe, B. and Nikoofar, H.R. (2009) *Multiuser Modulation Classification Based on Cumulants in AWGN Channel* [online], Cornell University Library, <http://arxiv.org/ftp/arxiv/papers/0908/0908.2117.pdf> (Accessed 7 October 2011).

Ziemer, R.E. and Tranter, W.H. (1995) *Principles of Communications*, New York, USA, John Wiley & Sons, Inc.

## 7 BIBLIOGRAPHY

Antoni, J. (2007). 'Cyclic spectral analysis in practice', *Mechanical Systems and Signal Processing*, vol. 21, iss. 2, pp. 597-630.

Beidas, B.F. and Weber, C.L. (1995) 'General framework for the higher-order correlation domain', *IEEE Military Communications Conference*, San Diego, California, USA, 5-8 November 1995, vol.1, pp. 180-185.

Beidas, B.F. and Weber, C.L. (1995) 'Modulation classification of MFSK signals using the higher-order correlation domain', *IEEE Military Communications Conference*, San Diego, California, USA, 5-8 November 1995, vol. 1, pp. 186-191.

Beidas, B.F. and Weber, C.L. (1995) 'Higher-order correlation-based approach to modulation classification of digitally frequency-modulated signals', *IEEE Journal on Selected Areas in Communications*, vol. 13, iss. 1, pp. 89-101.

Beidas, B.F. and Weber, C.L. (1996) 'Higher-order correlation-based classification of asynchronous MFSK signals', *IEEE Military Communications Conference*, MacLean, Virginia, USA, 21-24 October 1996, vol. 3, pp. 1003-1009.

Burel, G. and Boudier, C. (2000). Blind estimation of the pseudo-random sequence of a direct sequence spread spectrum signal, *21<sup>st</sup> Century Military Communications Conference Proceedings*, Los Angeles, California, USA, 22-25 October 2000, vol. 2, pp. 967-970.

Cullers, D.K., Linscott, I.R. and Oliver, B.M. (1985) 'Signal Processing in SETI', *Communications of the ACM*, vol. 28, iss. 11, pp. 1151-1163.

Davy, M., Doncarli, C. and Tournier, J-Y (2000) 'Supervised classification using MCMC methods', *IEEE International Conference on Acoustics, Speech and Signal Processing*, Istanbul, Turkey, 5-9 June 2000, vol. 1, pp. 33-36.

Eisner, R.F. (1982) 'Rusty bolt demonstrator', *IEEE Transactions on Electromagnetic Compatibility*, vol. EMC-24, iss. 4, pp. 420-421.

Fitzgerald, W.J., Godsill, S.J., Kokaram, A.C. and Stark, J.A. (1998) 'Bayesian methods in signal and image processing', *Bayesian Statistics 6*, Oxford University Press, pp. 239-254; also available online at <http://citeseerx.ist.psu.edu/viewdoc/summary?doi=10.1.1.30.8249> (Accessed 7 October 2011).

Gardner, W.A. (1987) 'Spectral Correlation of Modulated Signals', *IEEE Transactions on Communications*, vol. 35, iss. 6, pp. 584-601.

Horowitz, P., Matthews, B.S., Forster, J., Linscott, I., Teague, C.C., Chen, K. and Backus, P. (1986) 'Ultranarrowband searches for extraterrestrial intelligence with dedicated signal-processing hardware', *Icarus*, vol. 67, iss. 3, pp. 525-539.

ICS (2006) *Spectrum Explorer. Interactive automatic modulation recognition (AMR) software for sophisticated spectrum monitoring and analysis. The RF spectrum at your fingertips. AN-SR-8* [online],  
[http://www.radstone.com/uploads/Notes\\_862303.pdf](http://www.radstone.com/uploads/Notes_862303.pdf) (Accessed 30 December 2006)

Jeffrey, A. (2002) *Advanced Engineering Mathematics*, London, Harcourt/Academic Press.

Maritz, J.S. and Lwin, T. (1989) *Empirical Bayes methods*, 2<sup>nd</sup> edition, New York, Chapman and Hall.

Marwan, N. and Kurths, J. (2002) 'Nonlinear analysis of bivariate data with cross recurrence plots', *Physics Letters A*, vol. 302, iss. 5-6, pp. 299-307.

Marwan, N. and Kurths, J. (2005) 'Line structures in recurrence plots', *Physics Letters A*, vol. 336, iss. 4-5, pp. 349-357.

Marwan, N., Kurths, J. and Saparin, P. (2007) 'Generalised recurrence plot analysis for spatial data', *Physics Letters A*, vol. 360, iss. 4-5, pp.545-551.

Nolan, K.E., Doyle, L., O'Mahony, D. and Mackenzie, P. (2007) *Modulation scheme recognition techniques for software radio on a general purpose processor platform* [online], Scientific Commons, <http://citeseerx.ist.psu.edu/viewdoc/summary?doi=?doi=10.1.1.22.2786> (Accessed 7 October 2011).

Okunev, Y. (1997) *Phase and Phase-Difference Modulation in Digital Communications*, Norwood, Massachusetts, USA, Artech House.

Polydoros, A. and Kim, K. (1990). 'On the detection and classification of quadrature digital modulation in broad-band noise', *IEEE Transactions on Communications*, vol. 38, iss. 8, pp. 1199-1211.

Rai, S.S. and Pande, D.C. (2003) 'Prediction & modelling of EMI in communication systems due to non-linearities', *8<sup>th</sup> International Conference on Electromagnetic Interference and Compatibility*, Chennai, India, 18-19 December 2003, pp. 207-212.

Ramakonar, V., Habibi, D. and Bouzerdoum, A. (2001) 'Classification of band limited FSK4 and FSK8 signals', *Sixth International Symposium on Signal Processing and its Applications*, Kuala Lumpur, Malaysia, 13-16 August 2001, pp. 398-401.

Reichert, J (1992) 'Automatic classification of communication signals using higher order statistics', *IEEE International Conference on Acoustics, Speech, and Signal Processing*, San Francisco, California, USA, 23-26 March 1992, vol. 5, pp. 221-224.

Sapiano, P.C. and Martin, J.D. (1996) 'Maximum likelihood PSK classifier', *IEEE Military Communications Conference*, MacLean, Virginia, USA, 21-24 October 1996, vol. 3, pp. 1010-1014.

Schreyögg, C. and Reichert, J. (1997) 'Modulation classification of QAM schemes using the DFT of phase histogram combined with modulus information', *MILCOM 97 Proceedings*, Monterey, California, USA, 2-5 November 1997, vol. 3, pp. 1372-1376.

Sills, J.A. (1999) 'Maximum-likelihood modulation classification for PSK/QAM', *Military Communications Conference*, Atlantic City, New Jersey, USA, 31 October – 3 November 1999, vol. 1, pp. 217-220.

Swami, A. and Sadler, B.A. (2000) 'Hierarchical digital modulation classification using cumulants', *IEEE Transactions on Communications*, vol. 48, iss. 3, pp. 416-429.

Taira, S. and Murakami, E. (1999) 'Automatic classification of analogue modulation signals by statistical parameters', *IEEE Military Communications Conference*, Atlantic City, New Jersey, USA, 10-11 March 1999, vol.1, pp. 202-207.

Thiel, M., Romano, M.C. and Kurths, J. (2004) 'How much information is contained in a recurrence plot', *Physics Letters A*, vol. 330, iss. 5, pp. 343-349.

Tkachenko, A., Cabric, D. and Brodersen, R.W. (2007) 'Cyclostationary feature detector experiments using reconfigurable BEE2', *2nd IEEE International Symposium on New Frontiers in Dynamic Spectrum Access Networks*, Dublin, Ireland, 17-20 April 2007, pp. 216-219.

Wang, X-g. and Shen, H.C. (1999) 'Multiple hypothesis testing method for decision making', *IEEE International Conference on Robotics and Automation*, Detroit, Michigan, USA, 10-15 May 1999, vol. 3, pp. 2090-2095.

Webb (2007) 'Viewpoint - Steady as she goes', *IET Engineering & Technology*, vol. 2, iss. 1, p. 35.

Wong, M.L.D. and Nandi, A.K. (2001) 'Automatic digital modulation recognition using spectral and statistical features with multi-layer perceptrons', *Sixth International Symposium on Signal Processing and its Applications*, Kuala Lumpur, Malaysia, 13-16 August 2001, pp. 390-393.



Zeng, Y. and Liang, Y-C. (2007) 'Covariance based signal detections for cognitive radio', *2nd IEEE International Symposium on New Frontiers in Dynamic Spectrum Access Networks*, Dublin, Ireland, 17-20 April 2007, pp. 202-207.

This page intentionally blank

## **APPENDIX A USER SURVEY**

### **A.1 Introduction**

This appendix details the findings of an investigation carried out as part of the author's Ph.D. project. The aim of the investigation was to try to test some of the assumptions that the author had about the needs of users with regards to signal recognition problems.

In February 2008 a questionnaire was sent by email to 62 people that had been identified as potentially knowledgeable in the area of signal recognition. Some of the people were very well known to the author and others were not. The aim here was to try to cover a wide range of organisations likely to have interests in signal recognition tools. Of the people targeted, 16 returned the questionnaire and this report presents the analysis of those responses. Four of these worked for government organisations, eleven for industry and one in academia.

A mixture of open and closed questions was used in order to try to let people express themselves as well as obtaining material that could be statistically analysed (although it must be noted that the sample size was small). This report therefore presents the statistical results and also includes direct quotes from some of the questionnaires received. Names of individuals have been deliberately excluded in order to maintain confidentiality. Similarly, whilst some products were mentioned in the replies, these have not been disclosed.

The following sections present the results of analysing each of the questions in turn. Section A.7 contains the conclusions from this investigation.

## A.2 Question 1

"Which RF bands do you believe are the most difficult for a human operator to analyse?"

This question was posed in order to see whether any particular part of the spectrum is perceived as more difficult to deal with than others. Any one person will normally have more experience working in certain bands. By canvassing opinions from other people, this bias may be alleviated to some degree. The questionnaire gave options for:

- Licensed Bands;
- Licence-Exempt bands;
- Specific bands;
- Don't know;
- Prefer not to disclose.

The specific bands option allowed the respondents to indicate whether they have concerns over any particular frequency bands. A number of different bands were mentioned and the answers have been grouped as:

- Below 30 MHz (HF);
- 30 MHz - 1 GHz (VHF/UHF);
- Above 1 GHz (UHF/SHF);
- UWB.

UWB could, arguably, be incorporated into the above 1 GHz band, but this would not affect the results significantly.

Figure 122 shows the results from question 1. The LE bands and those above 1 GHz are seen as those giving more concern. This can be explained by the growth in licence-exempt wide bandwidth services, typified by the 2.4 GHz ISM band, in which a very wide range of signal types can be seen ("WiFi", "Bluetooth", microwave ovens, video senders, presentation controllers, etc.).

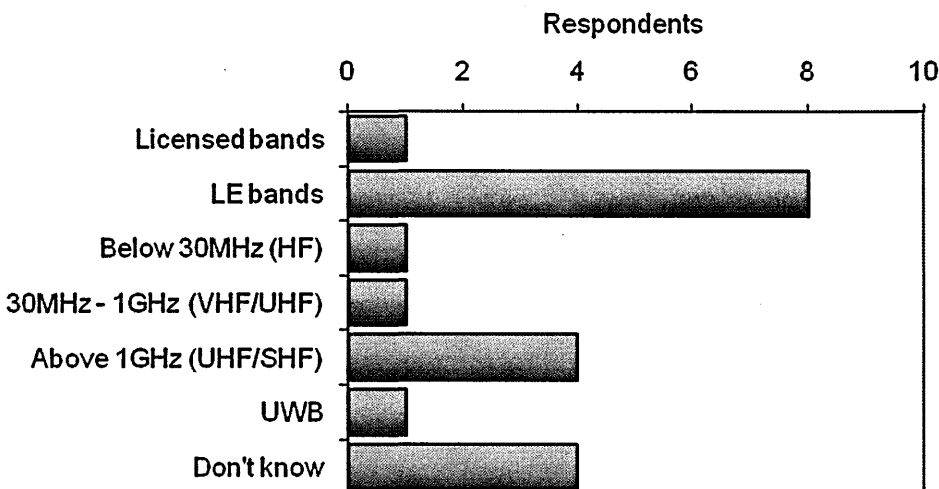


Figure 122. Summary of responses to question 1.

Specific replies:

- "I would have thought it depended on what you were looking for, but the higher you go in frequency, the more difficult it must be because the potential data carrying rate increases."
- "Licence exemption by definition requires that usage, standards and licensing information is difficult to ascertain."

- "Proliferation of users and uses in unlicensed bands makes signal identification difficulty grow exponentially."
- [Licence-exempt] "Because it's very difficult to identify the source of the emission and the localisation of the unlicensed station."
- [2.4 GHz ISM] "Variety of modulation and coding schemes permitted."
- [108 MHz - 136 MHz] "Because of strong RF carriers in the commercial FM band (88 MHz - 108 MHz)."
- "Difficult to monitor over-air above 1 GHz and often encounter proprietary or multiplexed modulation not exactly matching anticipated theoretical spectral appearance."
- "The unlicensed bands such as the ISM bands operate a free-for all policy with unregulated use of modulation schemes. At the moment everyone is flooding into the 2.4 GHz band (e.g. radio control transmitters are the latest to move there). There is potential for a true interference nightmare in these bands."
- [HF] "Proprietary waveforms, sun spots, other ionospheric impact, co-channel interferences."
- [Don't know] "It is difficult in any of the above cases. Higher frequencies have wider bandwidth but more local coverage. The human operator needs tools (antennas, receivers, spectrum analysers, etc.) appropriate to the band."
- [Most microwave bands] "Most emissions in this band are machine-generated and intended for machine reception, i.e. fixed links, radar and point-to-multipoint. This tends to make them all look and sound similar. They're also most removed from anything that a human operator may have encountered in the past."

### A.3 Question 2

"Which automated signal recognition systems do you use?"

This question was posed in order to see whether people were actually using such systems. It was felt, following the preliminary literature search, that automated signal recognition systems are not widely used in the context of interference recognition and location, but there was no evidence to support this.

As well as giving space for people to list the systems they used, the questionnaire also gave options for:

- Do not use;
- Don't know;
- Prefer not to disclose.

Twelve of the respondents did not use any kind of automated system in their work and relied on spectrum analysers for signal recognition.

The remaining four respondents reported a variety of systems ranging from free products to high-end SIGINT systems.

## A.4 Question 3

"Do you think that, as more services move towards digital communications, signal recognition will become easier or harder for the human operator?"

After performing a reasonably extensive literature search, the perception had been formed that the signal recognition problem will get harder in the future, as new and varied digital modulation schemes are introduced and as spectrum bands are liberalised. This view needed to be challenged, however, as it was important not to bias the research at an early stage.

The questionnaire gave options for:

- Easier;
- Harder;
- Don't know;
- Prefer not to disclose.

Sixteen of the replies said that the problem would get harder and only one that it would get easier. Three of the replies were "don't know".

Most of the explanations given were for the case of the task becoming harder. The first two quotes in the list below were notable however, because they made cases for the task becoming easier in one way but harder in another.



- "Easier: DSP/FPGA technology becomes low cost and widely available...  
Harder: complex waveforms are selected for new digital communication technologies."
- "I assume signal recognition techniques can advance at the same pace as services increase."
- [Harder] "With analogue or quasi-analogue systems, a skilled operator can recognise the characteristic sounds (e.g. fax set up tones, GSM phone registration pulses, dial-up modem training sequence, etc.)."
- "As the number of possible transmission standards increases, the ability to discern between them will obviously become more difficult. There is a trend (in terms of "liberalising" spectrum management) towards more "unlicensed bands" in these bands very little is known of the usage and this lack of knowledge leads to an increase in difficulty."
- "I think signal i.d. is going to get more difficult because of the increase in the number of unlicensed devices not because they are likely to use digital modulation as opposed to analogue."
- [Harder] "Mainly because there are many kinds of modulation, codifications and services operating in the same band."
- "Most digital modulation approximates to noise-like spectrum: much less structure than analogue. You have to "guess" the basic modulation mode and configure the receiver to do a correlation over time. Requires a lot of algorithm development."
- "Digital transmissions are effectively coded using a universal modulation technique that can be easily encrypted. Can be detected but not 'recognised'

easily by humans. Digital techniques also lend themselves to complex coding / wide spectrum use."

- "Discontinuous digital emissions are the hardest when using swept-tuned spectrum analysers because signal probability of intercept is very low."
- [Harder] "Because of the large number of different systems in use."
- [Harder] "Operator can't hear the raw channel."
- "The advanced digital modulation schemes that are in operation, or proposed, may well use LPI techniques to aid their assimilation into an unlicensed band (e.g. the use of direct sequence transmissions or burst mode transmissions in the unlicensed band allow overlaid bandsharing) These methods require extremely advanced detection methods to de-interleave the various digital signals."
- [Harder] "Analogue can be demodulated and processed by ear/ eye, but digital signals appear just as a stream of digits."
- [Harder] "One anonymous lump of QPSK-derived mush sounds very much like another. The more there is the more we're going to have to use diagnostic tools to identify the modulation scheme, possible source and use being made of it."

Overall, the results of this question supported the author's view that signal recognition will become more difficult in future. There is a need for signal recognition technology to be developed to meet the problems arising from the increasing complexity and density of emitters.

### A.5 Question 4

Question 4 provided a list of thirteen features that are desirable in a signal recognition system. The respondents were asked to grade their importance for their needs on a scale of 1 (most important) to 5 (least important).

Figure 123 shows a set of box plots, one for each feature listed. These have been sorted by the medians.

Each box plot shows the extent of the lower and upper quartiles using a rectangular box. Also shown are the minimum and maximum values as 'whiskers' and the medians, which are shown as vertical lines inside the boxes.

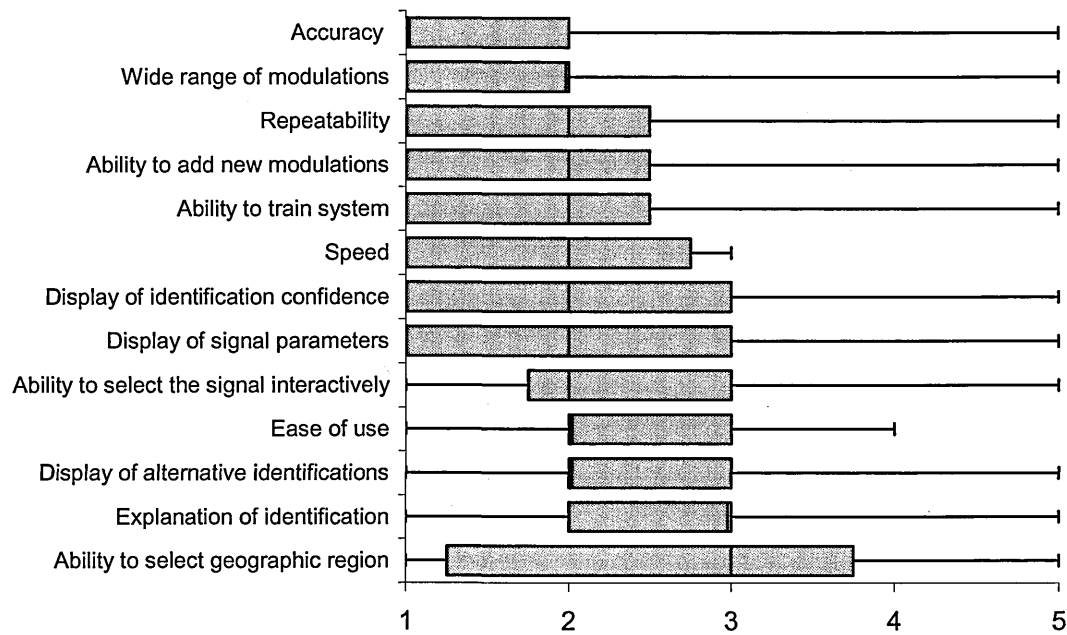


Figure 123. Histogram summarising responses to question 4.

The following observations are made concerning these results:

1. For every feature, apart from speed, opinions from 1 to 5 were expressed, so there was a wide variety of perceived importance;
2. Accuracy was seen as the most important feature, with a median of 1. This was not surprising and could have been predicted. What was surprising was that one of the respondents scored this feature with a 5;
3. The least important feature was that of being able to select the geographic region and this is understandable. This particular feature is arguably more of importance to developers than users. Typically users work in one geographic region so just need a system that works in their area. Developers need to ensure that their products will work in any region.

## A.6 Question 5

Question 5 simply asked people to express any other comments they had. The following comments are representative of those received, but exclude references to specific organisations, people's roles or particular products.

- "The problem for commercial organisations is cost justifying any form of complex analysis tools when the need and opportunity to use them is very limited."
- "Automated signal detection is a necessary pre-cursor to the advent of advanced radio technologies such as cognitive radio and much work is being done in this field."
- "Signal recognition and its localisation is a big problem for the human operator."
- "In my experience the radio and TV broadcast bands suffer predominantly from man-made sources of interference."
- "The widespread use of digital wireless technology is certainly putting severe strains on the RF spectrum. The increasing use of advanced modulation schemes in the unlicensed bands could soon create havoc. The proposed answer is self-regulating systems and cognitive radio. If this happens the control of the spectrum could reduce to a free-for-all where the largest power wins. However, there would appear to be little other alternative since the pressure on the spectrum is so great."
- [A tool should] "list all active frequencies the exact waveform/waveforms (simultaneously) are currently on, requires detection of the signal energy and identification of the waveform parameters, e.g. modulation, baudrate,

interleaving settings, data terminal modes (for serial port, number of start/stop bit, data bits), special data preamble, tone sets (in case of OFDM-like signal), etc."

## A.7 Conclusions

The following conclusions have been drawn from the responses received:

1. The questionnaire produced a wider range of responses than expected, but generally supported the belief that improved signal recognition algorithms, software and tools will be needed to deal with an increasingly complex and densely populated spectrum. This complexity is seen as inevitable and is being driven by the increasing demand for spectrum. The human operator can no longer identify all signals with a spectrum analyser and needs other tools to resolve interferers and wanted signals.
2. The current research in cognitive radio is expected to produce some of the algorithms required and ongoing progress in signal processing hardware will allow ever more advanced techniques to be used in real-time. The expectation is that signal recognition tools will continually evolve to meet the complexities of the radio environment.
3. Most respondents were concerned with the higher frequencies and the Licence-Exempt bands, with expressions such as 'free for all' indicating the general mood.
4. Only 25% of the respondents indicated that they used signal recognition products. The cost of these was the one factor that was explicitly mentioned for not using them.

5. Above all, people want such tools to be accurate. They are aware that such systems can never be 100% accurate and so need to be presented with the detailed parameters that were used for the automatic decision.

All the respondents were very supportive of the survey and the author is extremely grateful to all concerned.

This page intentionally blank



## APPENDIX B SIMULATION DETAILS

This appendix describes the simulations used to explore the concepts introduced in this thesis.

The results presented in sections 4.4.5 and 4.4.6 are based on a simulation created in Matlab. This simulation was based on the UML model of section 4.3 and used the object-oriented features of Matlab to implement the major class structures.

It was decided that a good example of a shared spectrum band is the 2.4 GHz ISM band, which is one of the LE bands in the UK. Interference in this band is widespread and increases in urban areas (Wagstaff, 2009), so there is a motivation for concentrating on this region of the spectrum for the purposes of simulation.

A total of 63 signal types were modelled, as listed in Table 17 and Table 18. Parameters for each of the first 23 types were taken from the open literature for devices that might be encountered in the 2.4 GHz ISM band. The remaining signal types are based on the standard modulations available in the MATLAB Communications Toolbox.

Index	Signal type
1	CW
2	DPSK8 (Bluetooth)
3	DSSS+DBPSK (WiFi 1Mbps)
4	DSSS+DQPSK (WiFi 2Mbps)
5	DSSS+OQPSK (ZigBee)
6	FM video
7	FSK2 (AMIC A7301 4.8kbps)
8	FSK2 (AMIC A7301 9.6kbps)
9	FSK2 (AMIC A7301 19.2kbps)
10	FSK2 (AMIC A7301 64kbps)
11	FSK2 (ML2724 1.536Mbps)
12	FSK2 (Motorola Canopy)
13	GFSK (Bluetooth)
14	GFSK (TRF-2.4G 250kbps)
15	GFSK (TRF-2.4G 1Mbps)
16	GFSK (nRF24L01 2Mbps)
17	Microwave (inverter type I)
18	Microwave (inverter type II)
19	Microwave (transformer type)
20	OFDM+BPSK (WiFi 6Mbps)
21	OFDM+QPSK (WiFi 12Mbps)
22	OFDM+QAM16 (WiFi 24Mbps)
23	OFDM+QAM64 (WiFi 48Mbps)

**Table 17. Simulated signal types – 2.4 GHz ISM band specific types.**

Index	Signal type
24	BPSK (100kBaud)
25	BPSK (250kBaud)
26	BPSK (500kBaud)
27	BPSK (1MBaud)
28	DBPSK (100kBaud)
29	DBPSK (250kBaud)
30	DBPSK (500kBaud)
31	DBPSK (1MBaud)
32	QPSK (100kBaud)
33	QPSK (250kBaud)
34	QPSK (500kBaud)
35	QPSK (1MBaud)
36	DQPSK (100kBaud)
37	DQPSK (250kBaud)
38	DQPSK (500kBaud)
39	DQPSK (1MBaud)
40	PSK8 (100kBaud)
41	PSK8 (250kBaud)
42	PSK8 (500kBaud)
43	PSK8 (1MBaud)
44	DPSK8 (100kBaud)
45	DPSK8 (250kBaud)
46	DPSK8 (500kBaud)
47	DPSK8 (1MBaud)
48	OQPSK (100kBaud)
49	OQPSK (250kBaud)
50	OQPSK (500kBaud)
51	OQPSK (1MBaud)
52	PAM4 (100kBaud)
53	PAM4 (250kBaud)
54	PAM4 (500kBaud)
55	PAM4 (1MBaud)
56	QAM16 (100kBaud)
57	QAM16 (250kBaud)
58	QAM16 (500kBaud)
59	QAM16 (1MBaud)
60	QAM64 (100kBaud)
61	QAM64 (250kBaud)
62	QAM64 (500kBaud)
63	QAM64 (1MBaud)

Table 18. Simulated signal types – generic types.

The simulation works on one pair of signal types at a time, adding them in varying amplitude ratios, using equation (45) and using WGN for the noise component at 30 dB SNR. At each amplitude ratio thirty runs are performed and the mean feature output is calculated. This enables the interference selectivity curve to be drawn and, from that, the Interference Selectivity is estimated.

This estimation was carried out for different combinations of signal types and for each of the features studied. It allowed the statistics of each feature's Interference Selectivity to be visualised using the box plots in Figure 118 and Figure 119.

A total of 1,339 signal pairings were used in the simulations. This required 5,827,250 simulation events to be run over a period of approximately three months.

## APPENDIX C NEURAL NETWORK PRUNING

This section introduces a specific technique for reducing the amount of processing required in an artificial neural network of the multilayer perceptron type. As discussed in section 2.4.4, Le *et al* (2005) were interested in optimising the performance of their OCON architecture by minimising the number of statistical features needed to recognise each modulation. The pruning technique described in this section achieves this for any general perceptron and is therefore applicable in other domains in which perceptrons are applied.

Consider the diagram of a perceptron with a single hidden layer shown in Figure 124. This shows a hidden node and an output node, the output of each of which is influenced by the outputs of the preceding layers. The final output is assumed to be shaped using a sigmoid function of the logistic curve type (Johnson and Picton, 1995, p. 116).

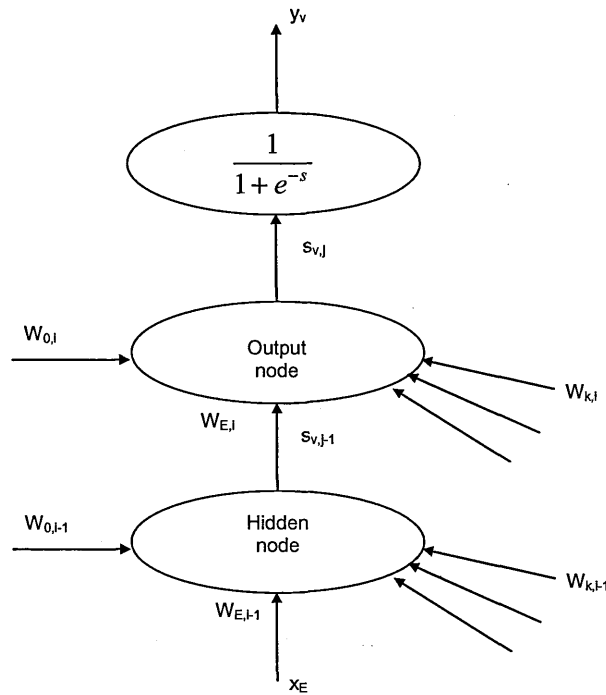


**Figure 124. Perceptron influence diagram.**

The output element,  $y_v$ , is produced by the sigmoid function and influenced by the two preceding layers,  $i$  and  $i-1$  with respect to the input element  $x_E$ . At each of the nodes a set of weights,  $W$ , is applied and these weights dictate the sensitivity of the output to the selected input.

Define the sensitivity of the output by its partial derivative with respect to variations in the selected input element.

$$\text{Sensitivity} = \frac{\delta y_v}{\delta x_E} \quad (65)$$

Now consider the outputs of the two layers,  $S_{i-1}$  and  $S_i$ .

$$S_{v,i-1} = W_{0,i-1} + W_{E,i-1}x_E + \sum_{m \neq E} W_{m,i-1}x_m \quad (66)$$

$$S_{v,i} = W_{0,i} + W_{E,i}S_{v,i-1} + \sum_{n \neq v} W_{n,i}S_{n,i-1} \quad (67)$$

The final output is:

$$y_v = \frac{1}{1 + e^{-S_{v,i}}} \quad (68)$$

Now, by the chain rule the sensitivity defined in (65) is given by:

$$\frac{\delta y_v}{\delta x_E} = \frac{\delta y_v}{\delta S_{v,i}} \frac{\delta S_{v,i}}{\delta S_{v,i-1}} \frac{\delta S_{v,i-1}}{\delta x_E} \quad (69)$$

Which leads to the result that the sensitivity is:

$$\frac{\delta y_v}{\delta x_E} = y_v(1 - y_v)W_{E,i}W_{E,i-1} \quad (70)$$

The sensitivity of the perceptron output is therefore proportional to the product of the weights along the path from the input element concerned. It is also, however, a non-linear function and depends on the current value of the output,  $y_v$ . This result makes it less useful than it might otherwise be if it were only dependent on the weights.

It is proposed that a more useful measure of sensitivity can be based on the output stage prior to the sigmoid function, which simplifies the analysis considerably.

This simpler measure is:

$$\text{Sensitivity} = \frac{\delta S_{v,i}}{\delta x_E} = W_{E,i}W_{E,i-1} \quad (71)$$

Using this definition the sensitivity is simply the product of the weights between the output node and the input. This result can be generalised for a perceptron of any number of hidden layers. For a single output node this definition generalises, then to:

$$Sensitivity = \frac{\delta S_{v,i}}{\delta x_E} = \prod_i W_{E,i} \quad (72)$$

The final step in this analysis is to define the sensitivity across all output vector elements for a single input node as the squared sum of the weights across all output elements. The squaring operation allows negative and positive weights to be handled.

$$Sensitivity = \sum_E \left( \prod_i W_{E,i} \right)^2 \quad (73)$$

where  $E$  is the input vector element and  $i$  is the layer number.

Either (72) or (73) can be used as part of an adaptive algorithm. The form of (72) lends itself to application in the OCON architecture proposed by Le *et al* (2005) as described in section 2.4.4.

Experiments to date have used the sensitivity in form given by (73). This form is appropriate for perceptrons with multiple outputs, such as that shown in Figure 25. The approach taken has been to run the training sequence once and then plot the value of the sensitivity parameter versus the statistical features. The sensitivity can then be thresholded and all input vectors falling below the



threshold removed from the training sequence. In this way, the amount of processing required by the real-time perceptron is reduced. The saving is in the order of the number of statistical features removed.

This pruning technique has some similarities to the Optimal Brain Damage (OBD) algorithm described by Ghani and Lamontagne (1993). Further work is needed to determine if the OBD method would give any significant advantage over the algorithm presented here.

This section has introduced a practical method for estimating the sensitivity of a perceptron to its inputs. This parameter can be used as part of the training sequence to remove less relevant inputs from the calculation and thereby reduce the real-time processing requirements.

This page intentionally blank

## APPENDIX D MODULATION TIME SCALES

In section 2.3.1 it is stated that ASR systems have to deal with a wide range of signal bandwidths and time scales. This can be seen by looking at the characteristics of typical modulations.

This appendix lists 200 time domain characteristics compiled from public domain literature for a variety of modulation types in the HF, VHF and UHF bands. The object of this is to show that there is a very wide range of time scales in use.

Modulation	Parameter	Rate (Hz)	Duration (s)	Log <sub>10</sub> (Duration/s)
GSM	Hyperframe rate	3.07E-07	3.26E+06	6.51
UMTS	Superframe rate	1.39E-06	7.20E+05	5.86
GSM	Superframe rate	6.28E-04	1.59E+03	3.20
TETRA	Hyperframe rate	1.63E-02	6.12E+01	1.79
GSM	Multiframe rate	1.92E-02	5.20E+01	1.72
GSM	Multiframe rate	3.77E-02	2.65E+01	1.42
TETRA	Multiframe rate	9.80E-01	1.02E+00	0.01
Microwave - Inverter	Duty cycle	1.00E+00	1.00E+00	0.00
Emergency beacon	Chirp period	3.00E+00	3.33E-01	-0.48
EV-DO	Data rate	3.10E+00	3.23E-01	-0.49
DVB-T	Superframe rate	3.28E+00	3.05E-01	-0.52
DVB-T	Superframe rate	3.65E+00	2.74E-01	-0.56
DVB-T	Superframe rate	3.86E+00	2.59E-01	-0.59
DVB-T	Superframe rate	3.98E+00	2.51E-01	-0.60
DAB	Frame rate	1.04E+01	9.60E-02	-1.02
DVB-T	Frame rate	1.31E+01	7.62E-02	-1.12
DVB-T	Superframe	1.31E+01	7.62E-02	-1.12
DVB-T	Frame rate	1.46E+01	6.85E-02	-1.16
DVB-T	Superframe	1.46E+01	6.85E-02	-1.16
DVB-T	Frame rate	1.54E+01	6.47E-02	-1.19
DVB-T	Superframe	1.54E+01	6.47E-02	-1.19
DVB-T	Frame rate	1.59E+01	6.28E-02	-1.20
DVB-T	Superframe	1.59E+01	6.28E-02	-1.20
TETRA	Frame rate	1.76E+01	5.67E-02	-1.25
DAB	Frame rate	2.08E+01	4.80E-02	-1.32
PAL-I	Vertical rate	2.50E+01	4.00E-02	-1.40
DAB	Frame rate	4.17E+01	2.40E-02	-1.62
MDM Q9604	Data rate	4.80E+01	2.08E-02	-1.68
Microwave - Transformer	Duty cycle	5.00E+01	2.00E-02	-1.70
MDM Q9604	Data rate	5.00E+01	2.00E-02	-1.70
DVB-T	Frame rate	5.25E+01	1.90E-02	-1.72

Modulation	Parameter	Rate (Hz)	Duration (s)	Log <sub>10</sub> (Duration/s)
DVB-T	Frame rate	5.84E+01	1.71E-02	-1.77
DVB-T	Frame rate	6.18E+01	1.62E-02	-1.79
Clover-2000 DSP4100 2K	Symbol rate	6.25E+01	1.60E-02	-1.80
DVB-T	Frame rate	6.37E+01	1.57E-02	-1.80
MDM Q9604	Data rate	6.40E+01	1.56E-02	-1.81
TETRA	Slot rate	7.06E+01	1.42E-02	-1.85
MDM Q9604	Data rate	7.50E+01	1.33E-02	-1.88
RTTY	Symbol rate	7.50E+01	1.33E-02	-1.88
DECT	Frame rate	1.00E+02	1.00E-02	-2.00
UMTS	Frame rate	1.00E+02	1.00E-02	-2.00
ART	Symbol rate	1.50E+02	6.67E-03	-2.18
MDM Q9604	Data rate	1.50E+02	6.67E-03	-2.18
GSM	Frame rate	2.17E+02	4.61E-03	-2.34
Link 1	Data rate	2.40E+02	4.17E-03	-2.38
WRM2	Symbol rate	3.00E+02	3.33E-03	-2.48
MDM Q9604	Data rate	3.00E+02	3.33E-03	-2.48
AX.25	Symbol rate	3.00E+02	3.33E-03	-2.48
POCSAG	Symbol rate	5.12E+02	1.95E-03	-2.71
Link 11B	Data rate	6.00E+02	1.67E-03	-2.78
MDM Q9604	Data rate	6.00E+02	1.67E-03	-2.78
MBDL	Data rate	7.50E+02	1.33E-03	-2.88
DAB	Symbol rate	8.03E+02	1.25E-03	-2.90
DVB-T	Symbol rate	8.93E+02	1.12E-03	-2.95
DVB-T	Symbol rate	9.92E+02	1.01E-03	-3.00
DVB-T	Symbol rate	1.05E+03	9.52E-04	-3.02
DVB-T	Symbol rate	1.08E+03	9.24E-04	-3.03
POCSAG	Symbol rate	1.20E+03	8.33E-04	-3.08
Link 1	Data rate	1.20E+03	8.33E-04	-3.08
MDM Q9604	Data rate	1.20E+03	8.33E-04	-3.08
AX.25	Symbol rate	1.20E+03	8.33E-04	-3.08
D-Star	Data rate	1.20E+03	8.33E-04	-3.08
Xstream	Symbol rate	1.28E+03	7.81E-04	-3.11
Link 11	Data rate	1.36E+03	7.33E-04	-3.13
Bluetooth	Slot rate	1.60E+03	6.25E-04	-3.20
FLEX	Symbol rate	1.60E+03	6.25E-04	-3.20
DAB	Symbol rate	1.61E+03	6.23E-04	-3.21
GSM	Slot rate	1.73E+03	5.77E-04	-3.24
Link 11	Data rate	1.80E+03	5.56E-04	-3.26
Link 11	Data rate	2.25E+03	4.44E-04	-3.35
POCSAG	Symbol rate	2.40E+03	4.17E-04	-3.38
Link 11B	Data rate	2.40E+03	4.17E-04	-3.38
MDM Q9604	Data rate	2.40E+03	4.17E-04	-3.38
FLEX	Symbol rate	3.20E+03	3.13E-04	-3.51
MDM Q9604	Data rate	3.20E+03	3.13E-04	-3.51
DAB	Symbol rate	3.21E+03	3.12E-04	-3.51
DVB-T	Symbol rate	3.57E+03	2.80E-04	-3.55
Link 11B	Data rate	3.60E+03	2.78E-04	-3.56
DVB-T	Symbol rate	3.97E+03	2.52E-04	-3.60
DVB-T	Symbol rate	4.20E+03	2.38E-04	-3.62

Modulation	Parameter	Rate (Hz)	Duration (s)	Log <sub>10</sub> (Duration/s)
DVB-T	Symbol rate	4.33E+03	2.31E-04	-3.64
ARF29	Symbol rate	4.80E+03	2.08E-04	-3.68
A7301	Symbol rate	4.80E+03	2.08E-04	-3.68
AS3977	Symbol rate	4.80E+03	2.08E-04	-3.68
WRM2	Symbol rate	4.80E+03	2.08E-04	-3.68
Link 11B	Data rate	4.80E+03	2.08E-04	-3.68
MDM Q9604	Data rate	4.80E+03	2.08E-04	-3.68
AMIC A7301	Symbol rate	4.80E+03	2.08E-04	-3.68
D-Star	Data rate	4.80E+03	2.08E-04	-3.68
MDM Q9604	Data rate	6.40E+03	1.56E-04	-3.81
DAB	Symbol rate	6.41E+03	1.56E-04	-3.81
MDM Q9604	Data rate	7.68E+03	1.30E-04	-3.89
MDM Q9604	Data rate	8.00E+03	1.25E-04	-3.90
WRM2	Symbol rate	9.20E+03	1.09E-04	-3.96
LonWorks	Symbol rate	9.60E+03	1.04E-04	-3.98
Z-Wave	Symbol rate	9.60E+03	1.04E-04	-3.98
ART/ZRT	Symbol rate	9.60E+03	1.04E-04	-3.98
MDM Q9604	Data rate	9.60E+03	1.04E-04	-3.98
AMIC A7301	Symbol rate	9.60E+03	1.04E-04	-3.98
AX.25	Symbol rate	9.60E+03	1.04E-04	-3.98
ISO 18000-6	Symbol rate	1.00E+04	1.00E-04	-4.00
Xstream	Symbol rate	1.00E+04	1.00E-04	-4.00
MDM Q9604	Data rate	1.28E+04	7.81E-05	-4.11
WRM2	Symbol rate	1.52E+04	6.58E-05	-4.18
PAL-I	Horizontal rate	1.56E+04	6.40E-05	-4.19
MDM Q9604	Data rate	1.60E+04	6.25E-05	-4.20
TETRA	Symbol rate	1.80E+04	5.56E-05	-4.26
LonWorks	Symbol rate	1.92E+04	5.21E-05	-4.28
ARF29	Symbol rate	1.92E+04	5.21E-05	-4.28
WRM2	Symbol rate	1.92E+04	5.21E-05	-4.28
MDM Q9604	Data rate	1.92E+04	5.21E-05	-4.28
AMIC A7301	Symbol rate	1.92E+04	5.21E-05	-4.28
ZigBee	Symbol rate	2.00E+04	5.00E-05	-4.30
Xstream	Symbol rate	2.00E+04	5.00E-05	-4.30
NADC	Symbol rate	2.40E+04	4.17E-05	-4.38
IS-54	Symbol rate	2.40E+04	4.17E-05	-4.38
ISO 18000-6	Symbol rate	2.67E+04	3.75E-05	-4.43
ISO 18000-4	Symbol rate	3.00E+04	3.33E-05	-4.48
PADIL	Data rate	3.20E+04	3.13E-05	-4.51
ISO 18000-6	Symbol rate	3.30E+04	3.03E-05	-4.52
One-Net	Symbol rate	3.84E+04	2.60E-05	-4.58
ARF29	Symbol rate	3.84E+04	2.60E-05	-4.58
ZigBee	Symbol rate	4.00E+04	2.50E-05	-4.60
ISO 18000-6	Symbol rate	4.00E+04	2.50E-05	-4.60
Z-Wave	Symbol rate	4.00E+04	2.50E-05	-4.60
ISO 18000-7	Symbol rate	5.56E+04	1.80E-05	-4.74
WE2408	Symbol rate	5.76E+04	1.74E-05	-4.76
ZigBee	Symbol rate	6.25E+04	1.60E-05	-4.80
A7301	Symbol rate	6.40E+04	1.56E-05	-4.81
AMIC A7301	Symbol rate	6.40E+04	1.56E-05	-4.81

Modulation	Parameter	Rate (Hz)	Duration (s)	Log <sub>10</sub> (Duration/s)
Insteon	Symbol rate	7.68E+04	1.30E-05	-4.89
AC4486	Symbol rate	7.68E+04	1.30E-05	-4.89
Link 16	Hop rate	7.78E+04	1.29E-05	-4.89
AS3977	Symbol rate	1.00E+05	1.00E-05	-5.00
HIDL	Data rate	1.00E+05	1.00E-05	-5.00
EnOcean	Symbol rate	1.20E+05	8.33E-06	-5.08
ISO 18000-6	Symbol rate	1.28E+05	7.81E-06	-5.11
1xRTT	Data rate	1.44E+05	6.94E-06	-5.16
EV-DO	Data rate	1.50E+05	6.67E-06	-5.18
Common Data Link	Data rate	2.00E+05	5.00E-06	-5.30
One-Net	Symbol rate	2.30E+05	4.35E-06	-5.36
Link 16	Data rate	2.38E+05	4.20E-06	-5.38
ANT	Symbol rate	2.50E+05	4.00E-06	-5.40
TRF-2.4G	Symbol rate	2.50E+05	4.00E-06	-5.40
GSM	Symbol rate	2.71E+05	3.69E-06	-5.43
ZigBee	Chip rate	3.00E+05	3.33E-06	-5.48
NICAM	Symbol rate	3.64E+05	2.75E-06	-5.56
ZigBee	Chip rate	6.00E+05	1.67E-06	-5.78
EDGE	Data rate	9.00E+05	1.11E-06	-5.95
Bluetooth	Symbol rate	1.00E+06	1.00E-06	-6.00
WiFi	Symbol rate	1.00E+06	1.00E-06	-6.00
ANT	Symbol rate	1.00E+06	1.00E-06	-6.00
TRF-2.4G	Symbol rate	1.00E+06	1.00E-06	-6.00
DECT	Symbol rate	1.15E+06	8.68E-07	-6.06
IS95	Chip rate	1.23E+06	8.14E-07	-6.09
ML2724	Symbol rate	1.54E+06	6.51E-07	-6.19
Tactical Common Data Link	Data rate	1.54E+06	6.48E-07	-6.19
Flash-OFDM	Data rate	1.80E+06	5.56E-07	-6.26
EV-DO	Data rate	1.80E+06	5.56E-07	-6.26
EDGE	Data rate	1.90E+06	5.26E-07	-6.28
ZigBee	Chip rate	2.00E+06	5.00E-07	-6.30
ANT	Symbol rate	2.00E+06	5.00E-07	-6.30
Go-Link	Symbol rate	2.00E+06	5.00E-07	-6.30
Link 16	Data rate	2.00E+06	5.00E-07	-6.30
nRF24L01	Symbol rate	2.00E+06	5.00E-07	-6.30
EV-DO	Data rate	2.45E+06	4.08E-07	-6.39
EV-DO	Data rate	3.10E+06	3.23E-07	-6.49
UWB	Symbol rate	3.20E+06	3.13E-07	-6.51
Flash-OFDM	Data rate	3.60E+06	2.78E-07	-6.56
UMTS	Chip rate	3.84E+06	2.60E-07	-6.58
WiFi	Symbol rate	4.00E+06	2.50E-07	-6.60
UMTS	Chip rate	4.10E+06	2.44E-07	-6.61
WM450	Symbol rate	5.30E+06	1.89E-07	-6.72
Flash-OFDM	Data rate	5.30E+06	1.89E-07	-6.72
Flash-OFDM	Data rate	5.40E+06	1.85E-07	-6.73
WiFi	Chip rate	5.50E+06	1.82E-07	-6.74
GNS-1142	Symbol rate	7.50E+06	1.33E-07	-6.88
PTP 24100	Symbol rate	1.00E+07	1.00E-07	-7.00
Canopy	Symbol rate	1.00E+07	1.00E-07	-7.00

Modulation	Parameter	Rate (Hz)	Duration (s)	Log <sub>10</sub> (Duration/s)
Flash-OFDM	Data rate	1.06E+07	9.43E-08	-7.03
Tactical Common Data Link	Data rate	1.07E+07	9.35E-08	-7.03
Common Data Link	Data rate	1.07E+07	9.34E-08	-7.03
WiFi	Chip rate	1.10E+07	9.09E-08	-7.04
Flash-OFDM	Data rate	1.59E+07	6.29E-08	-7.20
WiMAX	Data rate	3.50E+07	2.86E-08	-7.54
iBurst	Data rate	3.60E+07	2.78E-08	-7.56
Tactical Common Data Link	Data rate	4.50E+07	2.22E-08	-7.65
UWB	Data rate	5.50E+07	1.82E-08	-7.74
HIPERMAN	Data rate	5.69E+07	1.76E-08	-7.76
LTE	Data rate	8.00E+07	1.25E-08	-7.90
iBurst	Data rate	9.50E+07	1.05E-08	-7.98
UWB	Data rate	1.10E+08	9.09E-09	-8.04
Tactical Common Data Link	Data rate	1.27E+08	7.87E-09	-8.10
Common Data Link	Data rate	1.37E+08	7.30E-09	-8.14
WiMAX	Data rate	1.44E+08	6.94E-09	-8.16
UWB	Data rate	2.00E+08	5.00E-09	-8.30
Common Data Link	Data rate	2.74E+08	3.65E-09	-8.44
Tactical Common Data Link	Data rate	2.74E+08	3.65E-09	-8.44
LTE	Data rate	3.60E+08	2.78E-09	-8.56
UWB	Data rate	4.80E+08	2.08E-09	-8.68

Note that symbol rates have been used, where available, but data rates have been used otherwise. As the main interest here is in the order of magnitude the difference does not affect the conclusions significantly.

These data are summarised in Figure 125 in the form of a histogram. It will be seen that the bulk of the parameters are spread over approximately six orders of magnitude but that the total range is sixteen orders of magnitude.

To some extent these data are biased by the fact that the easiest parameters to glean from the open literature is usually the symbol rate provided by a particular chip set. There are frequently longer time scale structures, such as frame times, but these tend to be more proprietary and decided by the application designers.

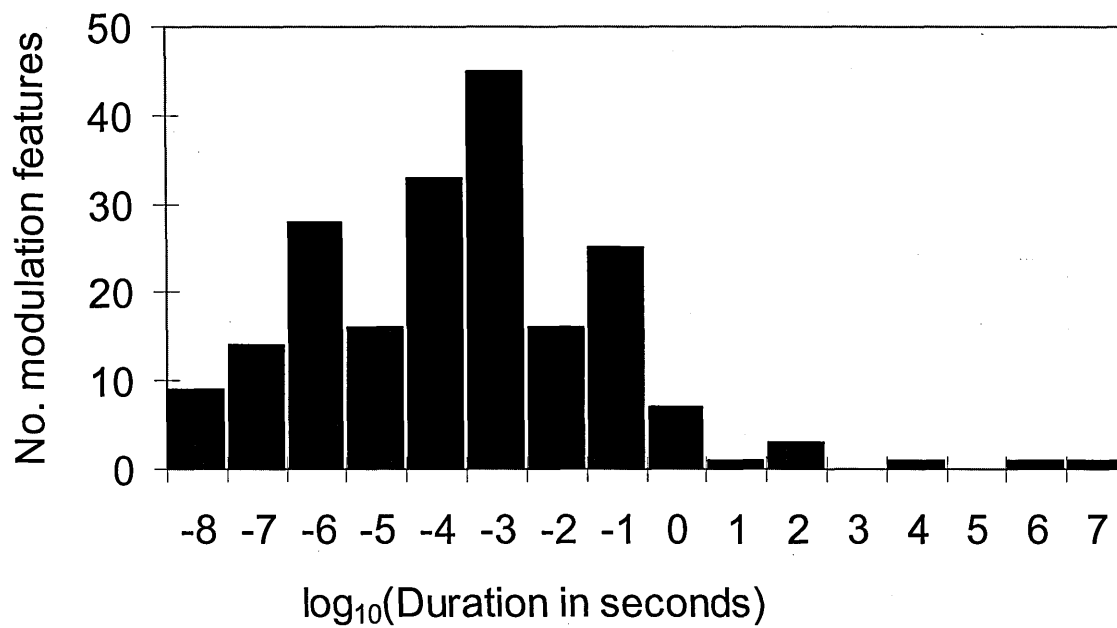


Figure 125. Histogram of time feature lengths in common modulations.



## APPENDIX E LOGNORMAL APPROXIMATION TO A STATISTICAL FEATURE

The output of a Feature may be sometimes approximated by a lognormal distribution. It should be emphasised, however, that different features will have different characteristics and, if an approximation is used, then the type of approximation must be selected for the individual feature concerned. It is important to be able to justify when this approximation can be made and to look out for conditions where it is not valid.

The lognormal distribution arises in the case of random variables that are defined as the logarithms of other random variables (Cooper and McGillem, 1999, p.85-86). It has a probability density function given by:

$$f_x(x) = \begin{cases} \frac{1}{\sqrt{2\pi}\sigma x} \exp\left(-\frac{(\ln x - \mu)^2}{2\sigma^2}\right) & x \geq 0 \\ 0 & x < 0 \end{cases} \quad (74)$$

where the values of  $\mu$  and  $\sigma$  are the parameters that define the distribution's shape.

This appendix examines the applicability of this particular distribution to statistical features when presented with WGN and FM. Other features and signals have been found to exhibit similar behaviours and the conclusions are generally applicable, i.e. that the researcher should be cautious when assuming standard

probability distributions. In ASR work it is safer to assume that a standard distribution will not work unless evidence can be produced to show otherwise.

## E.1 White Gaussian Noise

Azzouz and Nandi (1996) proposed a series of statistical Features, one of which was called  $\gamma_{\max}$  (see section 2.4.3). The output of the  $\gamma_{\max}$  Feature when WGN is applied is shown in Figure 126 in the form of a probability plot.

The probability plot is a standard function provided by Matlab for evaluating the fit of measured data to a probability distribution. It will be seen that the output of this Feature approaches the lognormal over the probability range 0.1 to 0.9, but diverges from it outside that region.

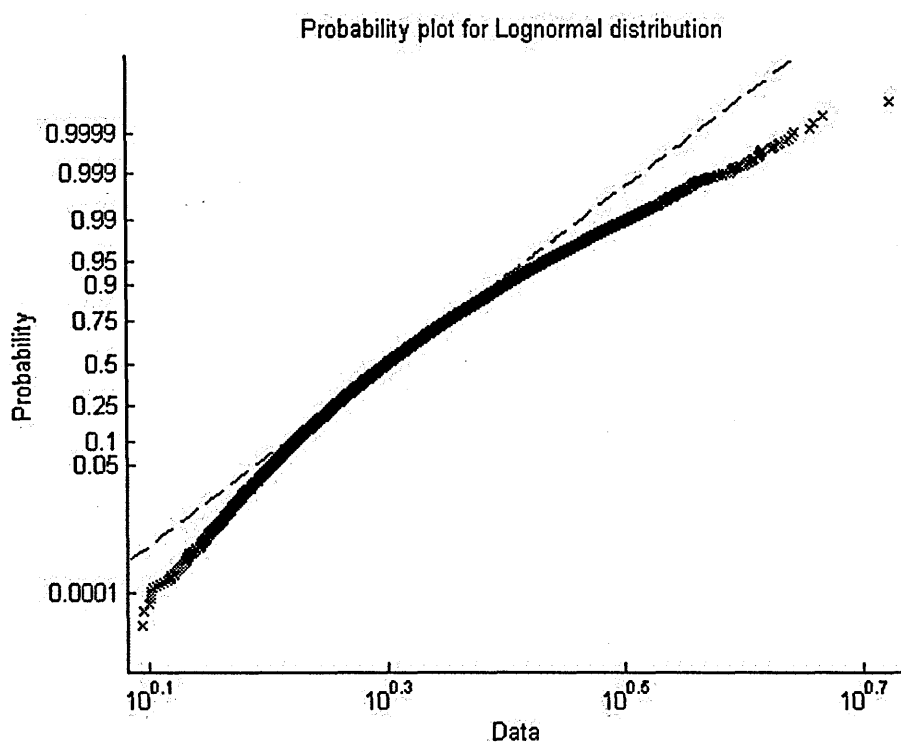
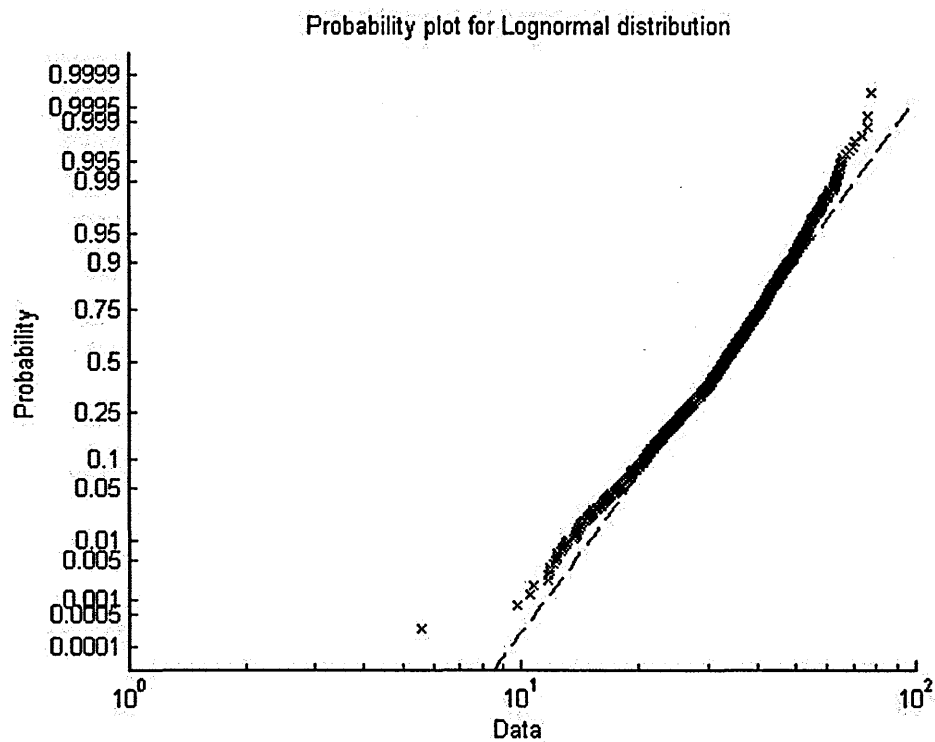


Figure 126. Probability plot of  $\gamma_{\max}$  with WGN as an input.

Gardner developed the theory of cyclostationarity, which explains the function of the DMD, in which a signal is multiplied by a time delayed version of itself (see section 2.4.2). This is a non-linear operation which produces spectral lines in its output and these lines facilitate the detection of a signal with a cyclostationary feature corresponding to the time delay.

If WGN is presented to a DMD feature then the resulting probability plot is shown in Figure 127. Comparing this with Figure 126 we see that the divergence from lognormal is somewhat less at the extreme probabilities but that the region of fit is again between 0.1 and 0.9.



**Figure 127. Probability plot of DMD feature with WGN as an input.**

This is the general finding with statistical features, i.e. that their outputs can be reasonably well described by a lognormal distribution for WGN input. Other

distributions, such as the normal or Weibull are expected to be suitable when the lognormal is inappropriate. One example is the spectrum symmetry statistic,  $P$ , (see section 2.4.3) which can take negative values as well as positive values and the normal distribution is a reasonable fit in that case.

## E.2 Frequency Modulation

FM is simulated using the following definition (Ziemer and Tranter, 1995, p. 167).

$$y(t) = a \cos \left[ 2\pi f_c t + 2\pi f_d \int_0^t m(\alpha) d\alpha \right] \quad (75)$$

where  $y$  is the modulated signal,  $a$  is the amplitude,  $f_c$  is the carrier frequency,  $f_d$  is the frequency deviation constant,  $t$  is time and  $m$  is the modulating (or message) signal. After simulating as a real signal, the resulting samples,  $y(t)$ , were then moved to complex baseband representation via a Hilbert transform.

A number of simulations were run with different value of  $f_d$  and SNR. The carrier frequency was kept constant at  $f_c = 0.1$  and the number of samples was also kept the same throughout the tests.

When the  $\gamma_{\max}$  feature was evaluated for FM with a relatively high frequency deviation constant,  $f_d = 0.05$ , the following observations were made:

1. At very low SNR the distribution of  $\gamma_{\max}$  tends towards that of WGN, as expected.
2. At high values of SNR the mean value of  $\gamma_{\max}$  decreases but the distribution still resembles a lognormal, as it did with WGN alone.

3. Figure 128 and Figure 129 show how the mean and standard deviation of  $\gamma_{\max}$  change with the SNR. It will be seen that both parameters start to drop once the SNR increases above approximately -5 dB. There is a region between about -5 dB and 20 dB where the mean and standard deviation are changing and neither the WGN nor the FM dominates the distribution. In this intermediate region it is not safe to assume that the lognormal approximation can be used overall, but the mean and standard deviation change with a sigmoidal characteristic between two values.

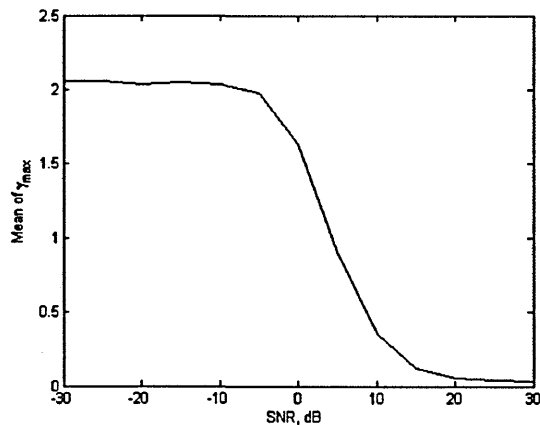


**Figure 128. Mean of  $\gamma_{\max}$  with FM as input.**

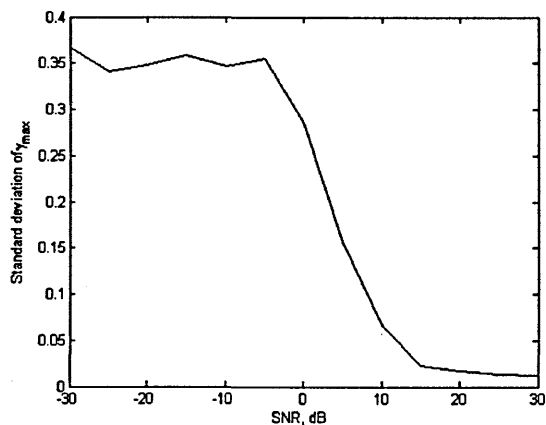


**Figure 129. Standard deviation of  $\gamma_{\max}$  with FM as input.**

4. It is found that a lognormal distribution approximation can be used for some values of the frequency deviation, but not all. To demonstrate the way in which the probability distribution changes, Figure 130, Figure 131 and Figure 132 show how the assumption of a lognormal distribution breaks down at certain values of  $f_d$  but not others.

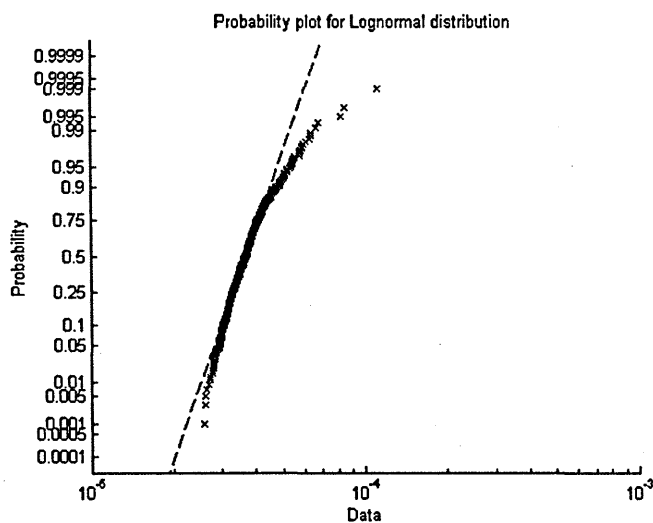


Figure 130. Lognormal plot, SNR = 50 dB,  $f_d = 0.0001$ .

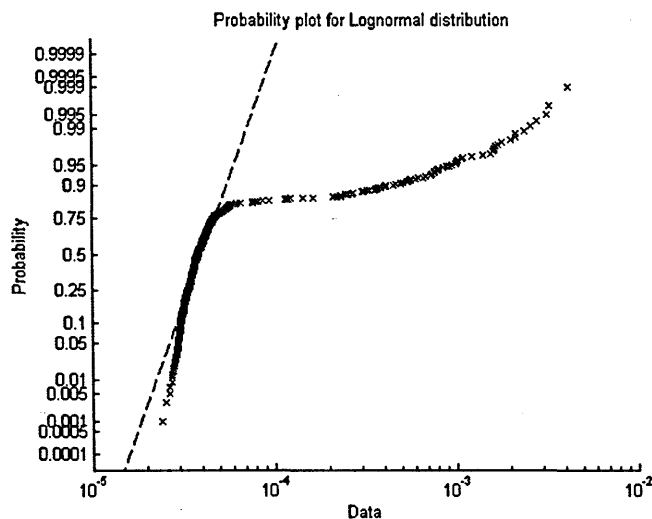


Figure 131. Lognormal plot, SNR = 50 dB,  $f_d = 0.001$ .

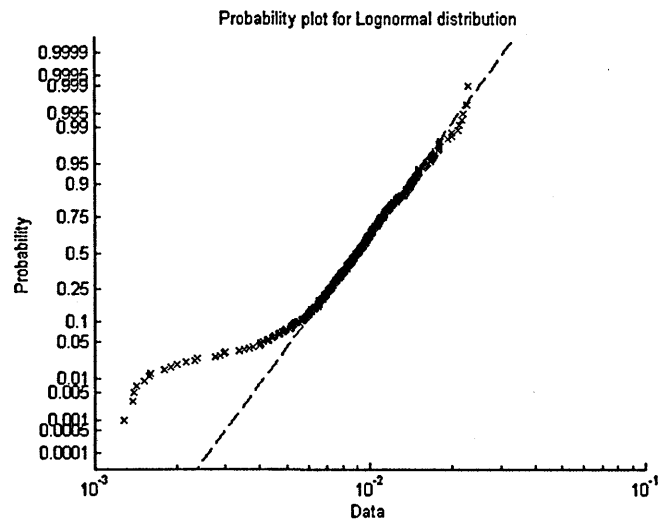


Figure 132. Lognormal plot, SNR = 50 dB,  $f_d = 0.05$ .

5. Such effects have been observed with experiments on other features and signal types and should be expected to arise in any ASR system.

### E.3 Conclusions

In general it is found that the assumption of a lognormal distribution can sometimes be made and is a useful simplification when it is valid. The assumption does, however, break down because of:

- the mixing of a signal with noise, as shown in the WGN example above, or
- the sensitivities of particular Features to certain signal parameters, as in the case of FM frequency deviation above, or
- the mixing of a signal with an interferer.

It was this last observation that led to the work on Interference Selectivity in this thesis. A statistical Feature can sometimes be modelled as a single lognormal distribution, but the effects of interference typically have an adverse effect on any such assumption.

In the cases where the lognormal assumption breaks down, it can be possible to produce a fit to the combination two or more standard distributions, but this must be done carefully and on a case by case.